

# Improved Strategies towards Conjugated Oligo Phenylene Ethynylenes

Zur Erlangung des akademischen Grades eines

DOKTORS DER NATURWISSENSCHAFTEN

(Dr. rer. nat.)

von der KIT-Fakultät für Chemie und Biowissenschaften  
des Karlsruher Instituts für Technologie (KIT)

genehmigte  
DISSERTATION

von

M. Sc. Daniel Hahn  
aus Bühl

Dekan: Prof. Dr. Hans-Achim Wagenknecht

1. Referent: Prof. Dr. Michael A. R. Meier

2. Referent: Prof. Dr. Stefan Bräse

Tag der mündlichen Prüfung: 15.12.2021



“There are more things in heaven and earth, Horatio,  
than are dreamt of in your philosophy.”

William Shakespeare in Hamlet



## Danksagung

Eine aufregende und turbulente Zeit geht zu Ende. An dieser Stelle möchte ich mich zunächst bei allen Personen bedanken, die mich auf dem langen Weg des Studiums und der Promotion begleitet haben.

Zuerst möchte ich Mike danken für die Aufnahme in den Arbeitskreis. Vielen Dank für das entgegengebrachte Vertrauen und die Freiheit bei der Bearbeitung des Themas. Deine Tür stand stets offen für Fragen, Probleme aber auch private Themen, selbst wenn der Wind sie mal wieder zugeweht hatte. Ich bin froh ein Teil des AK Meiers zu sein.

Als nächstes möchte ich dem gesamten Arbeitskreis danken für eine unvergessliche Zeit mit vielen lustigen, aber auch ernsten Momenten. Die gegenseitige Unterstützung und der Gruppenzusammenhalt waren für mich sehr wichtig, um eine angenehme Arbeitsatmosphäre zu schaffen. Thanks to the whole group for being more than just colleagues, for being friends. Vielen Dank auch an Becci für zahlreiche Bestellungen, Nachfragen bei Lieferanten, alles Organisatorische und die Hilfe im Labor. Der AK Meier wird dich vermissen. Danke Philipp und Anja für eure positive Art und den ganzen Spaß während und außerhalb der Arbeit. Ihr habt jeden Tag zu einem besonderen für mich gemacht. Danke Jonas für den NMR Finder und zahlreiche Stromberg Zitate. Danke Clara für viele hitzige Diskussion zum Gendern der Sprache und anderen kontroversen Themen. Danke auch an alle anderen, die mich in der langen Zeit im Arbeitskreis begleitet haben: Dafni, Roman, Michi, Juli, Luca, Federico, Eren, Dennis, Kevin, Caitlyn, Francesca, Andreas.

Ein großes Dankeschön geht auch an die Alumni des AK Meier: Yasmin, Pia, Marc, Kenny. Danke Rebekka, dass ich dein Thema fortführen durfte und du mir zahlreiche Tipps gegeben hast. Bis heute bin ich beeindruckt, wie lange du teilweise gesäult hast. Danke Katharina, ein Stück Bühler Heimat in Karlsruhe. Für technischen Support stehe ich dir gerne weiter zur Verfügung. Danke Bierbesteller Ben Bitterer für die schöne Zeit gemeinsam im Labor mit guter deutscher Blasmusik.

Herzlichen Dank auch an alle Korrekturleser: Julian, Kevin, Roman, Clara, Philipp, Anja, Katharina, Rebekka und Maxi. Danke für eure Hilfe und dass ihr meine Arbeit, teilweise in eurer Freizeit, Korrektur gelesen habt.

Vielen Dank an meine beiden Studenten, Lars und Till, für eure Hilfe und säulenreiche Zeit im Labor. Danke auch an Elena für die zahlreichen Synthesen und die Unterstützung im Labor. Vielen Dank Maya für Hilfe in letzter Minute.

Der Deutschen Forschungsgesellschaft danke ich für das Projekt im Rahmen des Sonderforschungsbereichs 1176 „Strukturierung weicher Materie“ (Projekt A4). Durch die Vernetzung der verschiedenen Arbeitskreise und den Austausch auf zahlreichen Workshops entstanden viele Ideen, die in die Arbeit eingeflossen sind.

Herzlichen Dank an die Analytische Abteilung des Instituts für das Messen zahlreicher Masse- und NMR Proben sowie an die Glasbläserei für das Reparieren vieler Säulen. Besonderen Dank an Christoph Götz, für die Lösungsmittel und Chemikalienausgabe.

Vielen Dank an meine Studienfreunde Ted, Mareen, Felix, Sebastian, Fabian, Kevin und Maxi. Auch wenn ich bis heute nicht weiß, wie ich euch alle kennen gelernt habe, bin ich froh, dass ihr mich während des gesamten Studiums begleitet habt. Danke Ted, dass du bei fast jedem Spaß dabei warst. Danke Mareen fürs Korrekturlesen meiner (gesamten) Masterarbeit, dein kreatives Chaos und die Deeptalks. Danke Fabi, der rasende Reporter von KA-News, dass du uns ständig mit wichtigen Fakten und den aktuellen Topdeals auf MyDealz versorgt hast. Danke Felix und Sebastian für eine unvergessliche Zeit in der WG, bei Game of Thrones Abenden oder beim Zocken, auch wenn ihr mir ein Jahr lang eine wichtige Information vorenthalten habt. Und ein Riesendankeschön an Maxi. Seit dem ersten Tag sind wir den Weg gemeinsam durch viele Praktika gegangen. Haben zusammen gelacht und geweint und haben stets zueinander gehalten. Ohne dich wäre die Zeit nur halb so schön gewesen. Ich bin froh eine so gute Freundin zu haben und freue mich schon auf die nächsten 10 Jahre. Zum Schluss bleibt nur noch eine Frage: Wo ist eigentlich Jan?

Der größte Dank gilt meiner Familie, ganz besonders meinen Eltern. Danke, dass ihr mich in all den Jahren immer unterstützt habt und ich mich immer auf euch verlassen kann. Danke auch an meine Schwiegereltern für zahlreiche (Action)Urlaube, bei denen ich „entspannen“ konnte. Mein letzter großer Dank geht an meine Frau, Julia für ununterbrochene Unterstützung, Motivation und Liebe, auch in stressigen Phasen des Studiums und der Promotion. Vielen Dank!

## Declaration of Authorship

Die vorliegende Arbeit wurde von September 2018 bis November 2021 unter Anleitung von Prof. Dr. Michael A. R. Meier am Institut für Organische Chemie (IOC) des Karlsruher Instituts für Technologie (KIT) angefertigt.

### Erklärung

Hiermit versichere ich, dass ich die Arbeit selbstständig angefertigt, nur die angegebenen Quellen und Hilfsmittel benutzt und mich keiner unzulässigen Hilfe Dritter bedient habe. Insbesondere habe ich wörtlich oder sinngemäß aus anderen Werken übernommene Inhalte als solche kenntlich gemacht. Die Satzung des Karlsruher Instituts für Technologie (KIT) zur Sicherung wissenschaftlicher Praxis habe ich beachtet. Des Weiteren erkläre ich, dass ich mich derzeit in keinem laufenden Promotionsverfahren befinde, und auch keine vorausgegangenen Promotionsversuche unternommen habe. Die elektronische Version der Arbeit stimmt mit der schriftlichen Version überein und die Primärdaten sind gemäß Abs. A (6) der Regeln zur Sicherung guter wissenschaftlicher Praxis des KIT beim Institut abgegeben und archiviert.

Karlsruhe, den 23. Februar 2022

---

Daniel Hahn



## Abstract

Conjugated rod-like oligomers, like oligo(1,4-phenylene ethynylene)s (OPEs), represent a unique class of macromolecules. Due to their extended  $\pi$ -conjugated backbone, they are discussed in terms of electronic applications, and thus, investigated regarding structure-property-relationships. Several procedures for the synthesis of uniform OPEs were reported, but only a few focus on sequence-definition. The established iterative synthesis concept is based on Sonogashira coupling followed by deprotection of a triple bond. Purification is challenging, also due to practically unavoidable side reactions.

In this work, an improved approach towards highly defined OPEs is developed comprising the decarboxylative coupling and subsequent saponification. Therefore, a building unit, which exhibits a bromine moiety and an ethyl ester protected alkynyl carboxylic acid as well as solubilizing propoxy side chains, was synthesized in four steps with 54% overall yield.

The rod-like oligomers were build-up in a linear iterative fashion by successive decarboxylative coupling and saponification steps. A uniform pentamer was obtained after ten reaction steps in a scale of 73 mg and 14% overall yield. The copper-free conditions prevent homocoupling until the trimer stage, thus purification is facilitated. Homocoupling is observed for the tetramer and pentamer, but a simple variation of the work-up procedure yielded the respective pure oligomers. All final products and intermediates were completely characterized by proton and carbon nuclear magnetic resonance (NMR) spectroscopy, infrared (IR) spectroscopy, high-resolution mass spectrometry (HRMS), and size exclusion chromatography (SEC). These analytical methods were investigated regarding the detection threshold of impurities. Combination of different analytical methods is demanded to assure the successful synthesis and high purity as well as uniformity of the obtained oligomers.

The observed results are compared to the established Sonogashira coupling approach towards OPEs. With the herein presented synthesis strategy, OPEs can be build-up in comparable overall yield, but with simpler purification and in a third of the time.



## Kurzzusammenfassung

Konjugierte Stäbchenmoleküle stellen eine besondere Klasse von Makromolekülen dar. Aufgrund ihres konjugierten Rückgrats werden sie bezüglich elektronischer Anwendungen diskutiert und ihre Struktur-Eigenschafts-Beziehungen werden untersucht. Mehrere Syntheseverfahren zu derartigen uniformen Oligomeren wurden bereits publiziert, aber nur wenige konzentrieren sich dabei auf Sequenzdefinition. Das etablierte iterative Synthesekonzept basiert auf der Sonogashira Kupplung und anschließender Entschützung einer Dreifachbindung, jedoch ist die Aufreinigung wegen unvermeidbarer Nebenreaktionen erschwert.

In dieser Arbeit wurde eine neue, verbesserte Synthesestrategie entwickelt, die sich aus einer decarboxylierenden Kupplung mit anschließender Verseifung zusammensetzt. Dafür wurde zunächst ein Bausteinmolekül, mit einem Bromrest und einer als Ethylester geschützten Alkynylcarbonsäure, synthetisiert. Um die Löslichkeit zu verbessern, wurden zudem Propoxy Seitenketten verwendet.

Die Stäbchenmoleküle wurden anschließend über die lineare, iterative Synthesestrategie bestehend aus decarboxylierender Kupplung und Verseifung aufgebaut. Nach zehn Reaktionsschritten wurde ein uniformes Pentamer mit einer Ausbeute von 14% und 73 mg erhalten. Die kupferfreien Bedingungen verhinderten Homokupplung bis zum Trimer und vereinfachten daher die Aufreinigung der Oligomere. Alle finalen Produkte sowie die entsprechenden Intermediate wurden vollständig mit Protonen und Kohlenstoff NMR Spektroskopie, Infrarot Spektroskopie, Massenspektrometrie und Größenausschluss Chromatographie charakterisiert. Außerdem wurden die analytischen Methoden hinsichtlich ihrer Nachweisgrenzen von Verunreinigungen untersucht. Nur eine Kombination verschiedener analytischer Methoden kann die erfolgreiche Synthese sowie eine hohe Reinheit und Uniformität der hier erhaltenen Produkte garantieren.

Die Ergebnisse wurden mit der etablierten Strategie basierend auf der Sonogashira Kupplung eingehend verglichen. Mit der neu entwickelten Synthesestrategie können OPEs mit ähnlicher Ausbeute, vereinfachter Aufreinigung und in einem Drittel der Zeit erhalten werden.



---

## Table of Content

Danksagung .....	I
Declaration of Authorship .....	III
Abstract .....	V
Kurzzusammenfassung .....	VII
1 Introduction .....	1
2 Theoretical Background .....	3
2.1 Cross-Coupling Reactions .....	3
2.1.1 Sonogashira Reaction .....	14
2.1.2 Decarboxylative Coupling Reaction .....	22
2.2 Sequence-Definition in Chemistry .....	29
2.2.1 Non-conjugated sequence-defined macromolecules .....	34
2.2.2 Conjugated sequence-defined macromolecules .....	43
3 Motivation .....	51
4 Results and Discussion.....	53
4.1 Analyzing uniform Macromolecules .....	53
4.1.1 Synthesis .....	54
4.1.2 Impurity study.....	57
4.1.3 Conclusion .....	63
4.2 Development of a new synthesis strategy .....	65
4.2.1 Synthesis of building units.....	70
4.2.2 Synthesis concept for uniform OPEs.....	74
4.2.3 Synthesis of uniform rod-like oligomers .....	76
4.2.4 Synthesis of new building units for sequence-defined OPEs .....	87
4.2.5 Conclusion .....	92
4.3 Sonogashira versus decarboxylative coupling – a comparison .....	93
4.4 Application of uniform stiff-oligomers in Multicomponent Reactions .....	99

## Table of Content

---

5	Conclusion and Outlook.....	105
6	Experimental Section.....	109
6.1	Materials.....	109
6.2	Instrumentation .....	110
6.3	Experimental Procedures .....	112
6.3.1	Analyzing Macromolecules .....	112
6.3.2	Synthesis of the Building Units.....	116
6.3.3	Synthesis of uniform OPEs .....	130
6.3.4	Synthesis of the double building unit.....	147
6.3.5	Synthesis of new building units.....	152
6.3.6	Applications of OPEs in MCRs.....	163
7	Abbreviations.....	173
7.1	List of abbreviation .....	173
7.2	List of symbols .....	175
8	List of Figures, Schemes and Tables.....	177
8.1	List of Figures.....	177
8.2	List of Supporting Figures .....	179
8.3	List of Schemes.....	180
8.4	List of Tables.....	183
9	Publication List .....	185
10	References .....	187

## 1 Introduction

### Why synthesize uniform conjugated sequence-defined Oligomers?

Uniform conjugated sequence-defined oligomers, such as oligo(1,4-phenylene ethynylene)s (OPEs), are a unique class of macromolecules. The extended  $\pi$ -conjugation through their rigid backbone exhibits interesting properties for optical and electronic applications, including biosensors,<sup>[1]</sup> organic solar cells,<sup>[2]</sup> light-emitting diodes,<sup>[3]</sup> and molecular wires.<sup>[4–6]</sup> The high degree of rigidity in the stiff, linear backbone enables high photoluminescence efficiencies as well as maximum orientation.<sup>[7,8]</sup> However, since these features are also observed in the polymeric equivalent, the question arises: Why to synthesize uniform conjugated sequence-defined oligomers?

Highly defined oligomers, which are uniform in size and sequence, can serve as excellent model compounds for their polydisperse counterparts.<sup>[9,10]</sup> They often provide specific information about solubility, electronic, photonic, thermal, and morphological properties of the corresponding polymers.<sup>[11,12]</sup> The field of precise oligomeric materials is suggested to be termed “macro-organic chemistry”, as it is inspired from both, the precision of organic chemistry and the properties of traditional polymer science.<sup>[13]</sup> Oligomers are closing the gap between discrete small molecules and high molecular weight polymers. There is no clear point at which degree of polymerization an oligomer becomes a polymer, however, the international union of pure and applied chemistry (IUPAC) defines an oligomer as a molecule that “has properties which do vary significantly with the removal of one or a few units”, making it a property related rather than a structural related definition.<sup>[14]</sup> Furthermore, the precise positioning of monomers within an oligomer of defined length allows for direct correlation of the physical properties with the chemical structure, since no structural defects or dispersity are present.<sup>[9]</sup> These structure-property-relationships can give new insights and understanding in how the structure on a molecular level affects the macromolecular properties.<sup>[15,16]</sup> Sequence-defined macromolecules with a precise positioning of each monomer unit and of defined length are also referred to as uniform molecules ( $\mathcal{D}=1.00$ ).<sup>[17–19]</sup>

Apart from serving as model compounds for their polymeric homologous, uniform conjugated oligomers are also used for molecular electronics, like molecular wires.<sup>[4-6,20]</sup> Uniformity is essential to exhibit consistent properties in nanoelectronic or nanophotonic processes.<sup>[11]</sup> Moreover, controlling the sequence of the molecular junctions enables tailoring of the properties.<sup>[21,22]</sup> Hence, focusing on the synthesis of uniform conjugated sequence-defined oligomers is important due to the valuable insight of structure-property-relationships and the use in molecular electronics.<sup>[23]</sup> In the present work, an improved synthesis concept towards OPEs is developed. The availability of such an alternative system allows faster synthesis of OPEs with constant yield and purity.

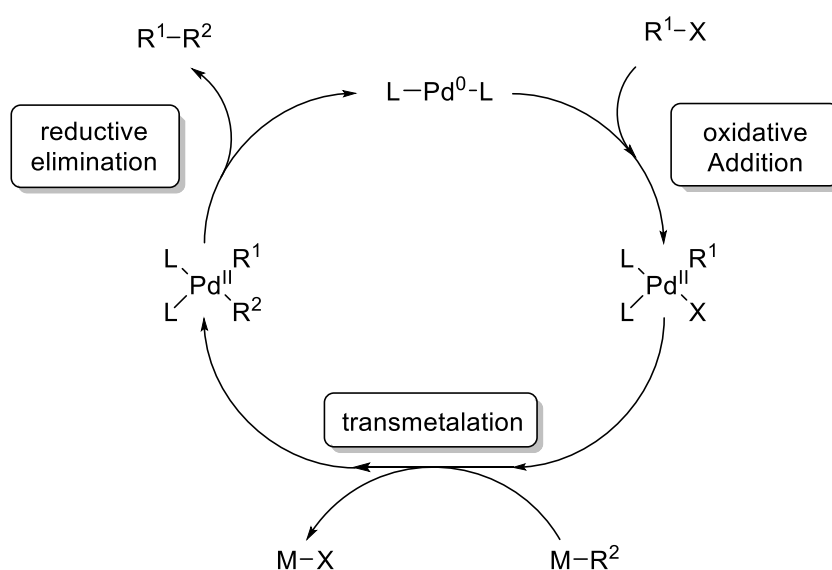
## 2 Theoretical Background

### 2.1 Cross-Coupling Reactions

Cross-coupling reactions are known since the end of the 19<sup>th</sup> century and are a versatile tool for forming new carbon-carbon bonds. Nowadays, many different variations exist and are used for the synthesis of complex molecules.<sup>[24]</sup> The impact of cross-coupling reactions was acknowledged in 2010, when Richard F. Heck, Ei-ichi Negishi and Akira Suzuki were awarded the Nobel Prize in Chemistry for their work on palladium catalyzed cross-coupling reactions.<sup>[25]</sup>

In the following sections, cross-coupling reactions in general and their application in the synthesis of sequence-defined molecules are described. First, a historic overview of the development of coupling and cross-coupling reactions is presented. A special focus is set on the Sonogashira reaction and the decarboxylative cross-coupling reaction, since both reactions were used and compared with each other regarding the synthesis of sequence-defined oligomers within this thesis.

In general, a cross-coupling reaction is defined as the substitution of an aryl, vinyl, or alkyl halide or pseudohalide by an organometallic nucleophile *via* metal catalysis, forming a new carbon-carbon bond.<sup>[26]</sup> It comprises three elementary steps: oxidative addition, transmetalation and reductive elimination.<sup>[27]</sup> In Scheme 1, the generally accepted reaction mechanism is depicted.<sup>[28]</sup>



Scheme 1: Generally accepted catalytic cycle for cross-couplings.<sup>[28]</sup>

The reaction starts with an active catalyst species, e.g. different transition metals. The mechanism depicted is based on a palladium catalyst, which is the most prominent and often used type of catalyst for this reaction type. The catalytic active  $\text{Pd}^0$  species can be directly introduced or is generated from precursors. Typically,  $\text{Pd}(\text{PPh}_3)_4$  is used to introduce zero-valent palladium as catalyst, but also precursors like  $\text{Pd}(\text{OAc})_2$  or  $\text{Pd}(\text{PPh}_3)_2\text{Cl}_2$  are often employed together with triphenylphosphine, which reduces the palladium *in situ*. In the first step of the catalytic cycle, an organohalide is added to the palladium complex in an oxidative addition. The resulting  $\text{Pd}^{\text{II}}$  complex is then reacted in a so-called transmetalation step with an organometallic reagent, which transfers an organic moiety to the active palladium complex. Upon reductive elimination, the coupling product is released from the catalytic cycle and the active  $\text{Pd}^0$  species is restored. Most cross-coupling reactions follow this mechanism, however, with the Mizoroki-Heck coupling, there is an exception which is discussed later.

Historically, the development of metal catalyzed cross-coupling reactions began with stoichiometric metal-promoted homocouplings, establishing the foundation for later discoveries in this field. One of the first published coupling reactions forming a new carbon-carbon bond was the Wurtz reaction (*cf.* Figure 1a). In 1855, Charles Adolphe Wurtz described the homocoupling of alkyl halides in the presence of metallic sodium.<sup>[29]</sup> This work was extended by Rudolph Fittig, who reported the homodimerization of aryl halides in 1862 and further broadened the application to the coupling of alkyl halides with aryl halides, also known as the Wurtz-Fittig reaction (*cf.* Figure 1b).<sup>[30,31]</sup> However, the reaction was not very applicable, since stoichiometric amounts of metallic sodium were used. The high reactivity of sodium reagents led to various side reactions, like rearrangements or eliminations, thus limiting the scope of the reaction, but promoting the development of milder organometallic nucleophiles.<sup>[32]</sup>

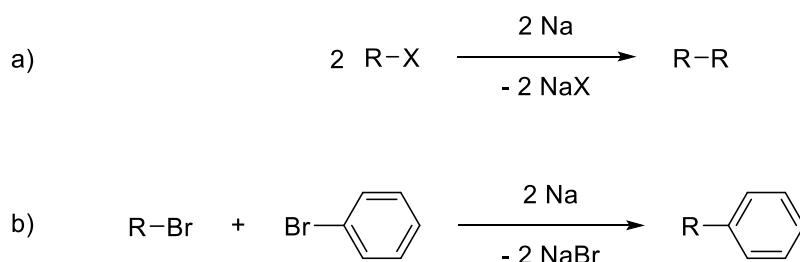


Figure 1: a) Wurtz reaction.<sup>[29]</sup> b) Wurtz-Fittig reaction.

In 1869, Glaser reported on the homocoupling of copper and silver phenyl acetylides with stoichiometric amounts of copper under oxidative conditions.<sup>[33,34]</sup> The benefits of this reaction, namely forming a new carbon-carbon bond between two sp carbon centers, were exploited, for example, in the synthesis of indigo by Baeyer in 1882 and led to the synthesis of various acetylenic compounds.<sup>[35]</sup> The scope of copper mediated homocoupling was then extended to bond formation between two sp<sup>2</sup> carbon centers in 1901. The Ullmann reaction described the dimerization of 2-bromonitrobenzene promoted by an excess of a copper source.<sup>[36]</sup> In this reaction, however, the homocoupling occurs between carbons bearing halides, like in the Wurtz<sup>[29]</sup> or Fittig<sup>[30]</sup> reaction, contrary to the unfunctionalized alkynes in the Glaser coupling. Regarding milder nucleophiles, Grignard reagents were investigated and the dimerization of phenylmagnesium bromide with stoichiometric amounts of chromium (III) chloride was first reported by Bennett and Turner in 1914.<sup>[37]</sup> The coupling reactions at this time, however, suffered from the use of stoichiometric metal reagents, which were poorly soluble, and the low selectivity, since the reactions were limited to homocoupling. Investigations in terms of transition metal catalyzed coupling of sp<sup>2</sup> carbon centers were performed by Kharasch in 1941 based on the observations of Job, who had made progress in introducing catalysis in the field of organometallics in the 1920s.<sup>[38]</sup> In 1943, Kharasch extended his work to the coupling of aryl organomagnesium reagents with vinyl bromides, which is considered to be the first cross-coupling reaction, as two different coupling partners are connected *via* metal catalysis. However, these reactions were not broadly applicable in synthesis due to limitation in substrate scope and functional group tolerance. The ratio of homocoupling and cross-coupling product was substrate dependent thus also leading to a problem in selectivity. Nevertheless, the demonstration that catalytic amounts of transition metals are sufficient in coupling reactions, set a starting point for further investigations.

In 1955, the first selective cross-coupling reaction was published by Cadiot and Chodkiewicz.<sup>[39,40]</sup> In this copper catalyzed coupling, two sp carbon centers of a bromoalkyne and an alkyne are connected (*cf.* Figure 2a). In 1963, the scope of selective cross-couplings was further extended by the Castro-Stephens reaction, in which a copper acetylide reacts with an aryl halide connecting a sp- and a sp<sup>2</sup>-carbon center (*cf.* Figure 2b).<sup>[41]</sup> Although the reaction still required elevated

temperatures and the use of poorly soluble and potentially explosive copper acetylides in stoichiometric amounts, it solved the selectivity problem.

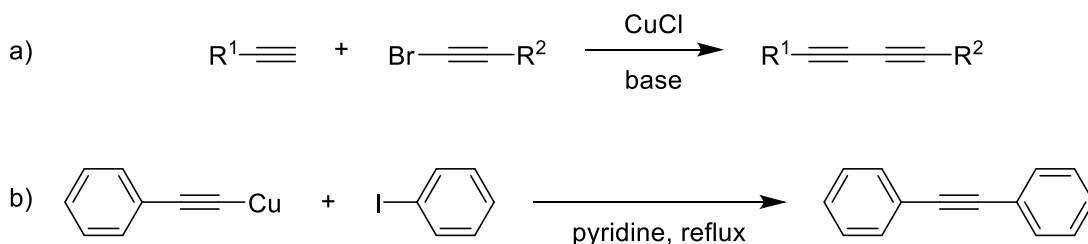
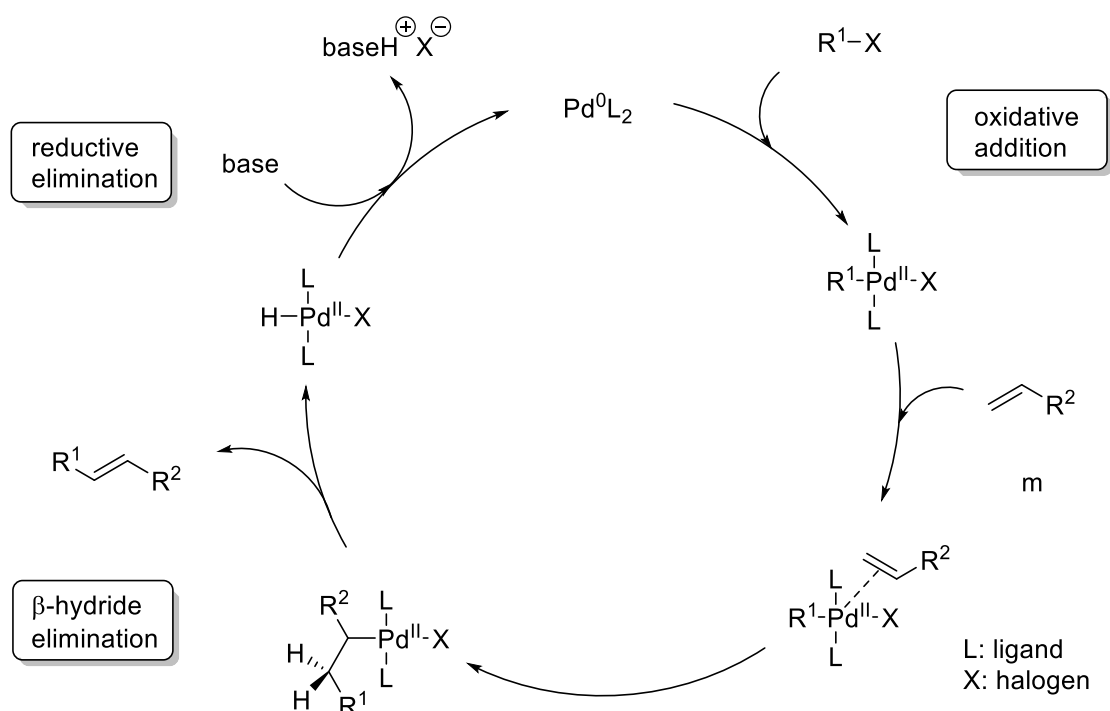


Figure 2: a) Cadiot-Chodkiewicz reaction.<sup>[39,40]</sup> b) Castro-Stephens reaction.<sup>[41]</sup>

With these early cross-couplings, three standard requirements towards a selective cross-coupling were observed: 1) an organohalide, mainly aryl or alkynyl is coupled with 2) stoichiometric amounts of an organometallic partner under 3) the use of catalytic amounts of a transition metal.<sup>[42]</sup> These principles proved to be fundamental in the investigation and publication of many cross-coupling reactions during the 1970s and following decades.

In 1972, the nickel-catalyzed coupling of Grignard reagents with aryl and alkenyl halides was reported by Kumada and Corriu, respectively.<sup>[43]</sup> The use of a nickel catalyst resolved the selectivity problem, which was predominant in the Kharasch coupling.<sup>[38]</sup> Almost simultaneously to Kumada and Corriu, Mizoroki and Heck independently reported on the coupling of aryl and benzyl halides and alkenes with a palladium catalyst.<sup>[44]</sup> Their findings were based on the emerging palladium chemistry after World War II and observations made at Wacker Chemie.<sup>[45]</sup> Mechanistically, the Mizoroki-Heck reaction differs from the previously presented coupling reactions, since no organometallic reagent is used and therefore transmetalation does not take place.

The catalytic cycle of the Mizoroki-Heck coupling is depicted in Scheme 2. Similar to the general catalytic cycle, which was described before, oxidative addition of an organohalide occurs first. Subsequently, the palladium forms a  $\pi$ -complex with the alkene followed by insertion of the alkene into the Pd-R<sup>1</sup> bond. The respective coupling product is obtained by  $\beta$ -hydride elimination and the catalytically active palladium species is restored by reductive elimination promoted by a base.<sup>[46]</sup>



Scheme 2: Catalytic cycle of the Mizoroki-Heck coupling consisting oxidative addition, migratory insertion,  $\beta$ -hydride elimination and reductive elimination.<sup>[46]</sup>

However, many variations of the reaction have been published and the employment of palladium opened a wide field of palladium catalyzed cross-couplings.

Acetylene coupling, for instance, was dominated using a copper catalyst as described above. But in 1975, the groups of Sonogashira,<sup>[47]</sup> Cassar<sup>[48]</sup> and Heck<sup>[49]</sup> independently reported coupling of acetylenes with aryl or vinyl halides under palladium catalysis. The approaches from Cassar and Heck still needed rather high temperatures, whereas Sonogashira used copper as a co-catalyst resulting in very mild reaction conditions. Since the Sonogashira reaction is used for the synthesis of sequence-defined stiff oligomers, it is described in more detail in the following chapter.

In 1976, Negishi used organoaluminum reagents in cross-coupling reactions first with a nickel catalyst, which was later substituted by palladium due to problems of stereospecificity.<sup>[50]</sup> One year later, Negishi, Fauvarque and Jutand introduced organozinc reagent to cross-couplings.<sup>[51]</sup> By this substitution of the organomagnesium reagent, which was used mainly in cross-couplings before, with a organozinc reagent, Negishi demonstrated that other metals are also capable of transferring organic moieties in the proposed transmetalation step.<sup>[52]</sup> In 1987, Stille reported the coupling of organostannanes with aryl chlorides.<sup>[53]</sup> Mild reaction

conditions and a broad compatibility of functional groups are advantageous but the toxicity of organostannanes is a major drawback. However, the Stille coupling is still frequently used. A cross-coupling, which produces less toxic byproducts was published in 1979. Heck already stated in 1975 that boronic acids are valid cross-coupling partners in the presence of stoichiometric amounts of palladium. Suzuki then demonstrated that the palladium can be reduced to catalytic amounts by the reaction of 1-alkenylboranes and aryl halides, a reaction now known as the Suzuki-Miyaura coupling.<sup>[54]</sup> An even more environment friendly reaction is based on the palladium catalyzed coupling of organosilanes with aryl halides, published by Hiyama in 1988.<sup>[55]</sup> In the 1990s, carbon heteroatom couplings got into focus. In 1995, Buchwald and Hartwig reported on the palladium catalyzed formation of a carbon-nitrogen bond.<sup>[56]</sup> Free amides are cross coupled to aryl halides in the presence of a strong base and with a palladium catalyst. This was further extended to the development of cross-couplings forming carbon-oxygen, carbon-sulfur and carbon-phosphor bonds

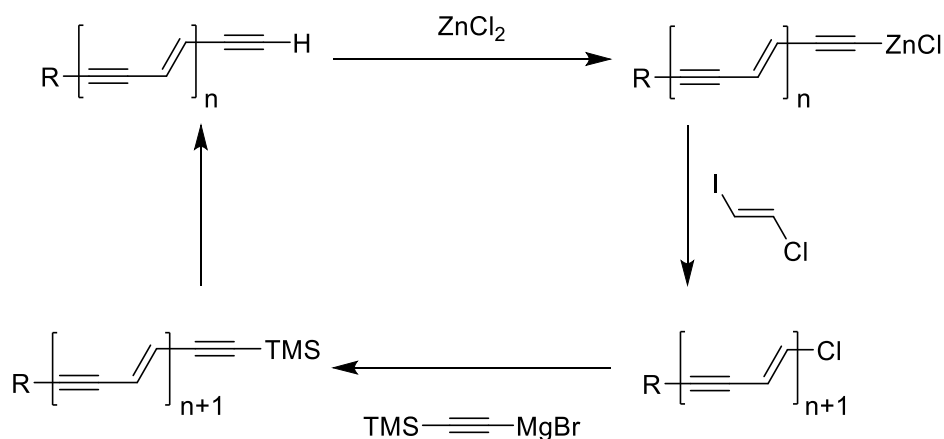
The cross-couplings presented so far proceed in the generally accepted catalytic cycle of oxidative addition, transmetalation and reductive elimination (*cf.* Scheme 1). They feature the three main principles of cross-couplings of an organohalide coupled to an organometallic reagent with transitionmetal catalysis. The historical development is summed up in Table 1.

Table 1: Overview of coupling and cross-coupling reactions.

	Reaction	Year	Reactant A	Reactant B	Catalyst/ Reagent
homocoupling	Wurtz	1855	Alkyl-X	-	Na
	Fittig	1862	Aryl-X	-	Na
	Wurtz-Fittig	1864	Alkyl-X	Aryl-X	Na
	Glaser	1869	alkyne	-	Cu
	Ullmann	1901	Ar-X	-	Cu
	Bennett	1914	Ar-MgBr	-	CrCl <sub>3</sub>
cross-coupling	Kharasch	1943	Ar-MgBr	vinyl-Br	CoCl <sub>2</sub>
	Cadiot-Chodkiewicz	1955	alkyne	Alkyne-Br	Cu
	Castro-Stephens	1963	alkyne-Cu	Ar-X	Cu
	Mizoroki-Heck	1972	alkene	Ar-X	Pd or Ni
	Kumada	1972	Ar-MgBr	R-X	Pd or Ni
	Sonogashira	1975	alkyne	R-X	Pd and Cu
	Negishi	1977	R-ZnX	R-X	Pd or Ni
	Stille	1978	R-SnR <sub>3</sub>	R-X	Pd or Ni
	Suzuki	1979	R-B(OR) <sub>2</sub>	R-X	Pd or Ni
	Hiyama	1988	R-SiR <sub>3</sub>	R-X	Pd
Buchwald-Hartwig	1995	R <sub>2</sub> NH	Ar-X	Pd	

This overview clearly demonstrates the vast variety of cross-coupling reactions, chemists can rely on. However, development of cross-coupling has not stopped and also cross-coupling reactions, which do not exhibit the general features, have been developed. The decarboxylative coupling, for instance, does not require an organometallic reagent. Instead, aryl carboxylic acids are used and coupled to aryl halides or alkenes. In 2008, Lee extended the scope to alkynyl carboxylic acids.<sup>[57]</sup> Since the decarboxylative coupling can be seen as an alternative to the Sonogashira reaction and is used in this work for the synthesis of sequence-defined stiff oligomers, it is described in more detail later. Still, especially in the synthesis of conjugated molecules, cross coupling reactions are often employed to form new carbon-carbon bonds. In the following sections, three examples of the application of cross-couplings for three different classes of conjugated molecules are described.

An elegant way for synthesizing conjugated oligomers based on an ene-yne scaffold, which employed two different cross-couplings, was published by Wudl and Bitler in 1986.<sup>[58]</sup> The unsaturated and conjugated backbone makes these materials interesting for optical and electronic applications. The iterative four-step synthesis is depicted in Scheme 3.

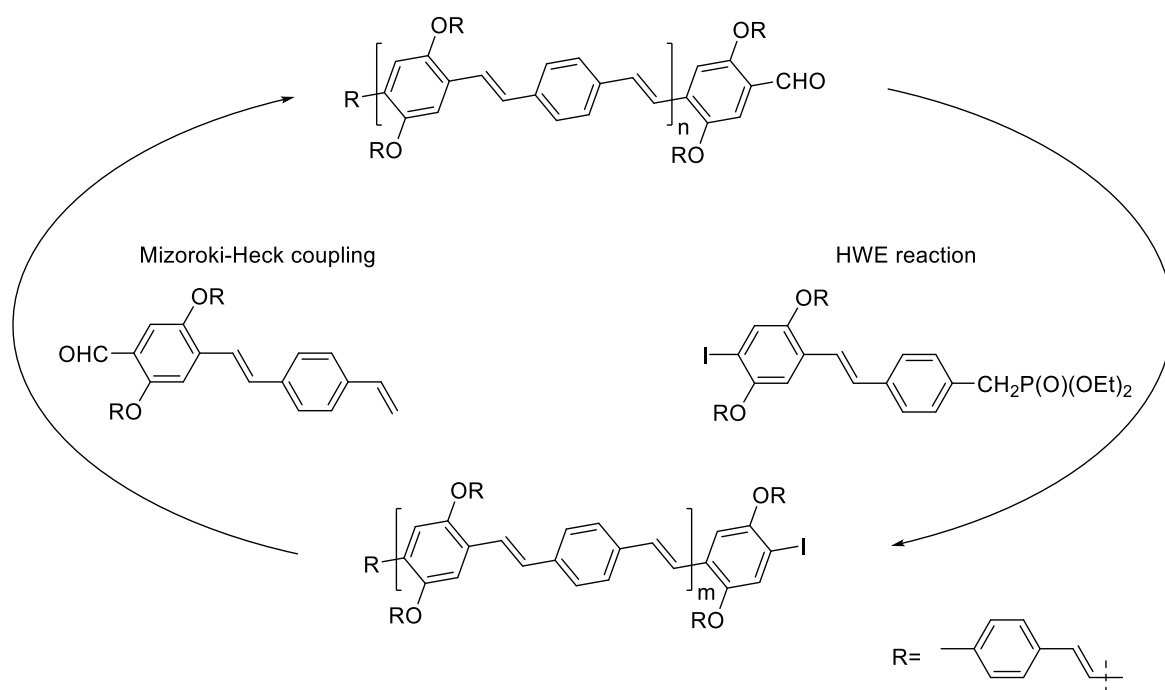


Scheme 3: Four-step approach towards oligo(diacetylene)s by Wudl and Bitler. Two cross-couplings, the Negishi and the Kumada coupling are employed.<sup>[58]</sup>

Initially, a triple bond is converted with zinc chloride to the corresponding alkynyl zinc compound. Organozinc compounds serve as the organometallic species in the Negishi coupling, thus the alkynyl zinc reagent is reacted with an organo halide under palladium catalysis. In order to retain the ene-yne backbone (*E*)-1-chloro-2-iodoethylene was used. Subsequently, another cross-coupling, the Kumada coupling, was performed which requires an organomagnesium reagent.

Wudl and Bitler used trimethylsilyl protected ethynyl magnesium bromide to reintroduce a triple bond into the molecule. After deprotection of the TMS group, the four-step procedure is repeated. Following this iterative procedure, a monomer, dimer and trimer with 6, 10 and 14 conjugated carbon atoms were obtained after one, two or three cycles, respectively. Furthermore, the dimer was coupled with 1,2-diiodoethylene after activation with zinc chloride to form a pentamer with 22 conjugated carbons. The same procedure was applied to the trimer, which resulted in formation of a heptamer with 30 conjugated carbon atoms. However, their goal of 50 conjugated carbon atoms was unachievable due to solubility issues. All oligomers were analyzed by proton and carbon NMR spectroscopy, mass spectrometry, UV/VIS spectroscopy and elemental analysis and compared with each other. The heptamer was not soluble enough, thus, NMR spectroscopy was problematic, but the respective mass was found. No experimental data is provided, which complicates comparison to other approaches, however, the employed of the Negishi and Kumada coupling demonstrates the versatile applications of cross-coupling reactions.

Also, the Mizoroki-Heck reaction was used for the synthesis of conjugated oligomers since it connects two organic moieties *via* a carbon-carbon double bond.

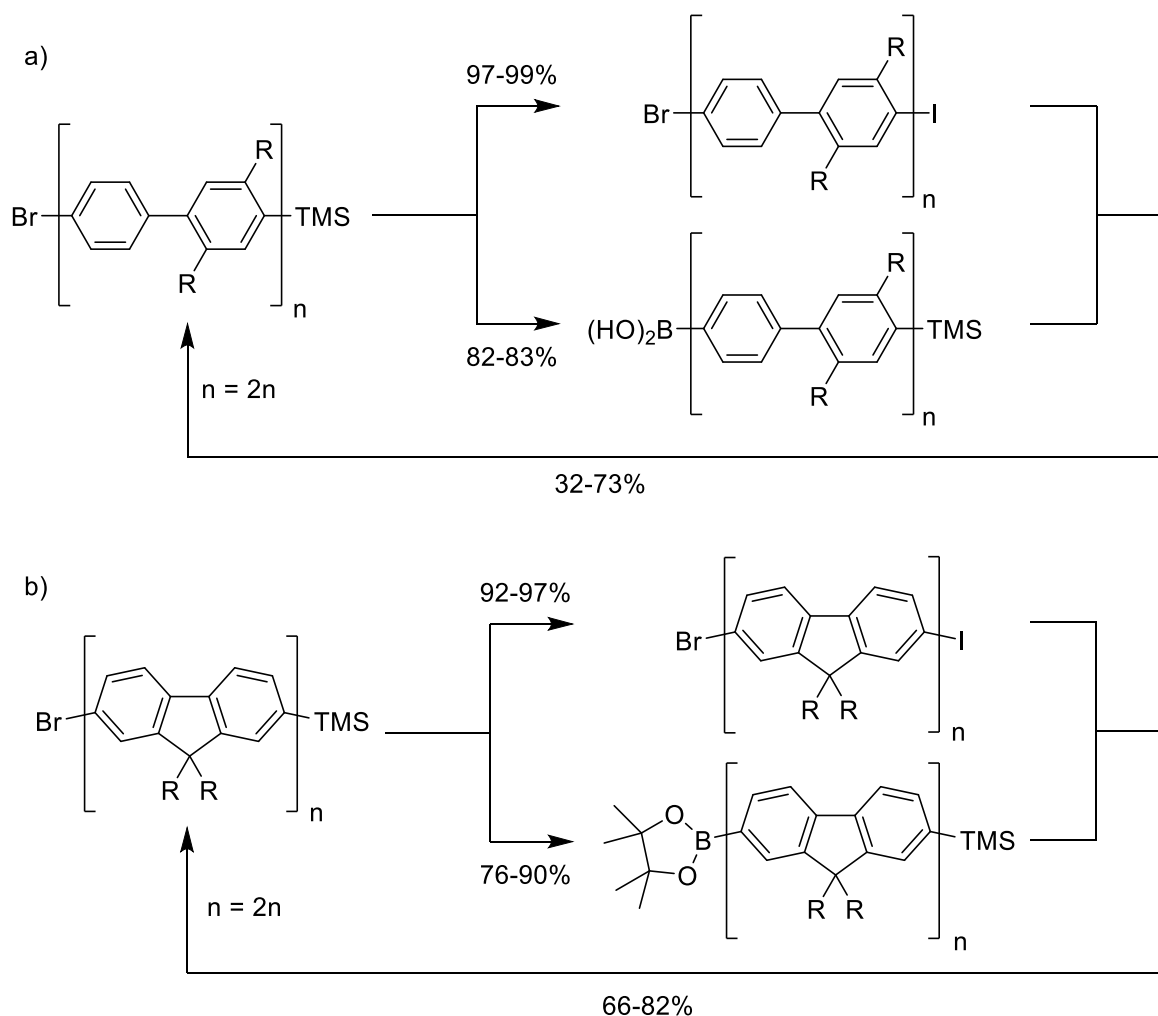


Scheme 4: Orthogonal approach from Yu et al. towards OPVs.<sup>[59]</sup>

In 1997, Yu and co-workers published an orthogonal synthesis of substituted oligo(phenylene vinylene)s (OPVs) involving the Mizoroki-Heck reaction and the Horner-Wadsworth-Emmons (HWE) reaction (*cf.* Scheme 4).<sup>[59]</sup> One starting compound and two building blocks were required. Styrylbenzene with an iodine moiety served as the starting compound. One building block is a vinyl styryl benzaldehyde bearing both an aldehyde and a vinyl group. As second building block, an iodo styryl benzylphosphonate exhibiting an iodine and a phosphonate group was employed. Octyloxy side chains were used on both building blocks as well as the starting compound to improve their solubility. The key to the stepwise synthesis of OPVs was the implementation of the complementary functional groups. The iodine group of the starting compound or the second building block can couple with the vinyl group of the first building block in a Mizoroki-Heck reaction. Subsequently, the aldehyde group of the coupled first building block is reacted with the phosphonate group of the second building block resulting in a dimer with an iodine group, which can then couple again with the vinyl group of the first building block. After five steps, a pentamer with twelve aromatic rings connected *via* double bonds was obtained. For the series of aldehyde terminated OPVs, the absorption and emission spectra were presented. It was found that the maximal absorption wavelength converges to that of poly(phenylene vinylene)s already at relatively short conjugation length, since no further red shift was noticed at the pentamer compared to the trimer. Defined OPVs are therefore ideal model compounds to study and understand the optoelectronic properties of PPV materials.

Two other classes of conjugated molecules, which are often synthesized by a cross-coupling reaction and investigated due to their optical and electrical properties, are oligo(*p*-phenylene)s and oligo(flourene)s. Schlüter *et al.* reported an approach towards oligo(*para* phenylene)s based on the Suzuki coupling (*cf.* Scheme 5a).<sup>[60]</sup> This approach required an orthogonally protected biphenyl with a TMS group on one side and a bromine group on the other side. The activation step is split into two parts. In one part, the bromine end group is converted to a boronic acid and in the other part, the TMS group is converted into an iodine group. Subsequently, a Suzuki coupling is performed combining the two parts. Repeating the two steps of activation/deprotection and Suzuki coupling leads to an exponential growth of the respective oligomer. After six steps, an oligomer with 16 connected

aromatic rings was obtained. Analysis of these rigid oligomers *via* SEC revealed high purity with only minor impurities.



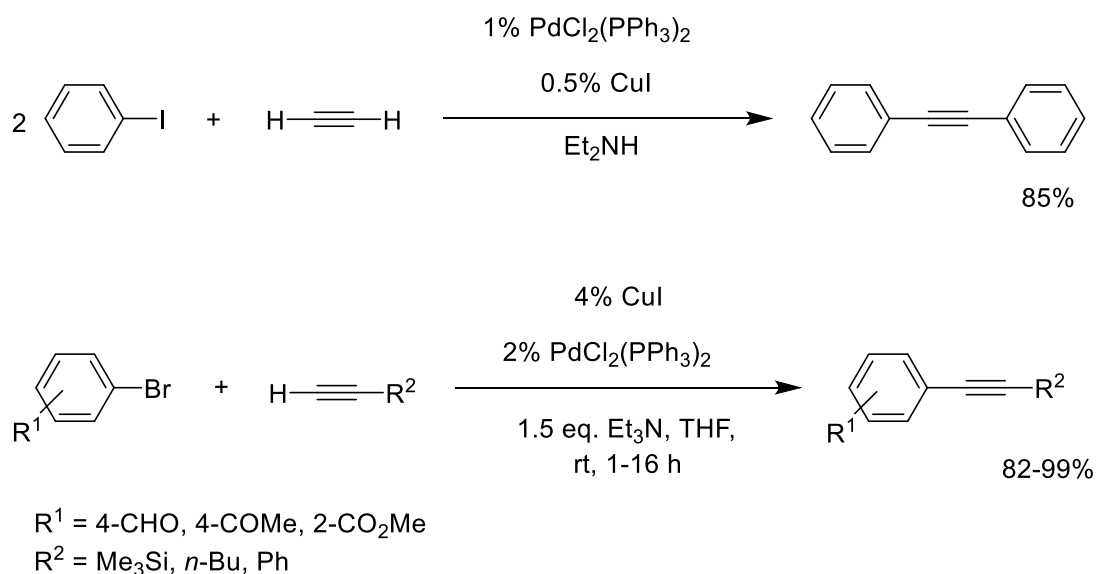
Scheme 5: a) Synthesis of oligo(paraphenylene)s based on Schlüter et al.<sup>[60]</sup> b) Synthesis of oligo(flourene)s based on Geng et al.<sup>[61]</sup>

Regarding oligo(flourene)s, Geng and co-workers published a similar approach (*cf.* Scheme 5b) in 2011.<sup>[61]</sup> As described before, an orthogonally protected building block with a TMS group and a bromine group was utilized. The building block was synthesized by a Suzuki coupling from 2-bromo-7-iodofluorene and TMS-protected fluorene bearing a boronic acid. Separate activation of one side, respectively, and subsequent Suzuki reaction produced a 32-mer after 9 steps, which was then homocoupled to a 64-mer. Column chromatography was essential to obtain the final product, however, the shown SEC traces are slightly broadened and dispersities  $\bar{D}$  as high as  $\bar{D}=1.06-1.09$  are reported. This observation indicates the presence of impurities, like higher and lower molecular weight species, yet still the term “monodisperse” is used to describe the obtained molecules.

Less than 100 years have passed since the first selective cross-coupling was published, but the large scope of application shows the importance of carbon-carbon bond forming reactions and confirms the award with the Nobel price back in 2010. Apart from conjugated molecules, cross-couplings are often found in total synthesis or the synthesis of pharmaceuticals due to their easy set up and high functional group tolerance.<sup>[62]</sup>

### 2.1.1 Sonogashira Reaction

In this chapter, the Sonogashira cross-coupling is described in more detail. The Sonogashira reaction (also referred to as Sonogashira-Hagihara reaction) was first published by Kenkichi Sonogashira in 1975.<sup>[47]</sup> It describes the coupling of a terminal alkyne with an aryl or vinyl halide (*cf.* Scheme 6). In contrast to other cross-coupling reactions,  $sp$ -hybridized substrates are coupled with  $sp^2$ -hybridized substrates introducing a triple bond to the resulting coupling product.



Scheme 6: First reported Sonogashira coupling (top) and a typical Sonogashira reaction (bottom).<sup>[47,63]</sup>

Development in catalyst design gave access to  $sp^3$ -hybridized alkyl iodides and alkyl bromides, which can be applied in the Sonogashira reaction further enlarging the scope of the reaction. However, mainly vinyl and aryl halides are used due to the reactivity of the reagents, as described in the following (*cf.* Figure 3). In general, vinyl substrates exhibit better reactivity than aryl substrates. Alkyl substrates, however, are rather unreactive and thus are rarely seen in Sonogashira reactions.

Among the halide species, iodides show the best reactivity followed by bromides and chlorides.<sup>[64]</sup> A variation is the Cacchi cross-coupling reaction, in which aryl triflates are coupled with acetylenes.<sup>[65]</sup> Regarding the reactivity, the triflates are ranked between the iodides and the bromides, but the reaction is hypothesized to proceed *via* a slightly different mechanism.

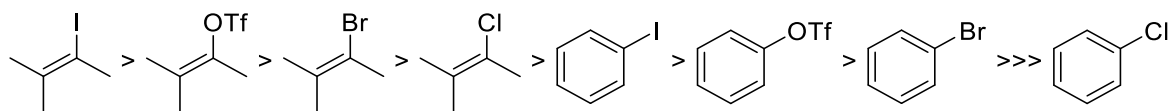
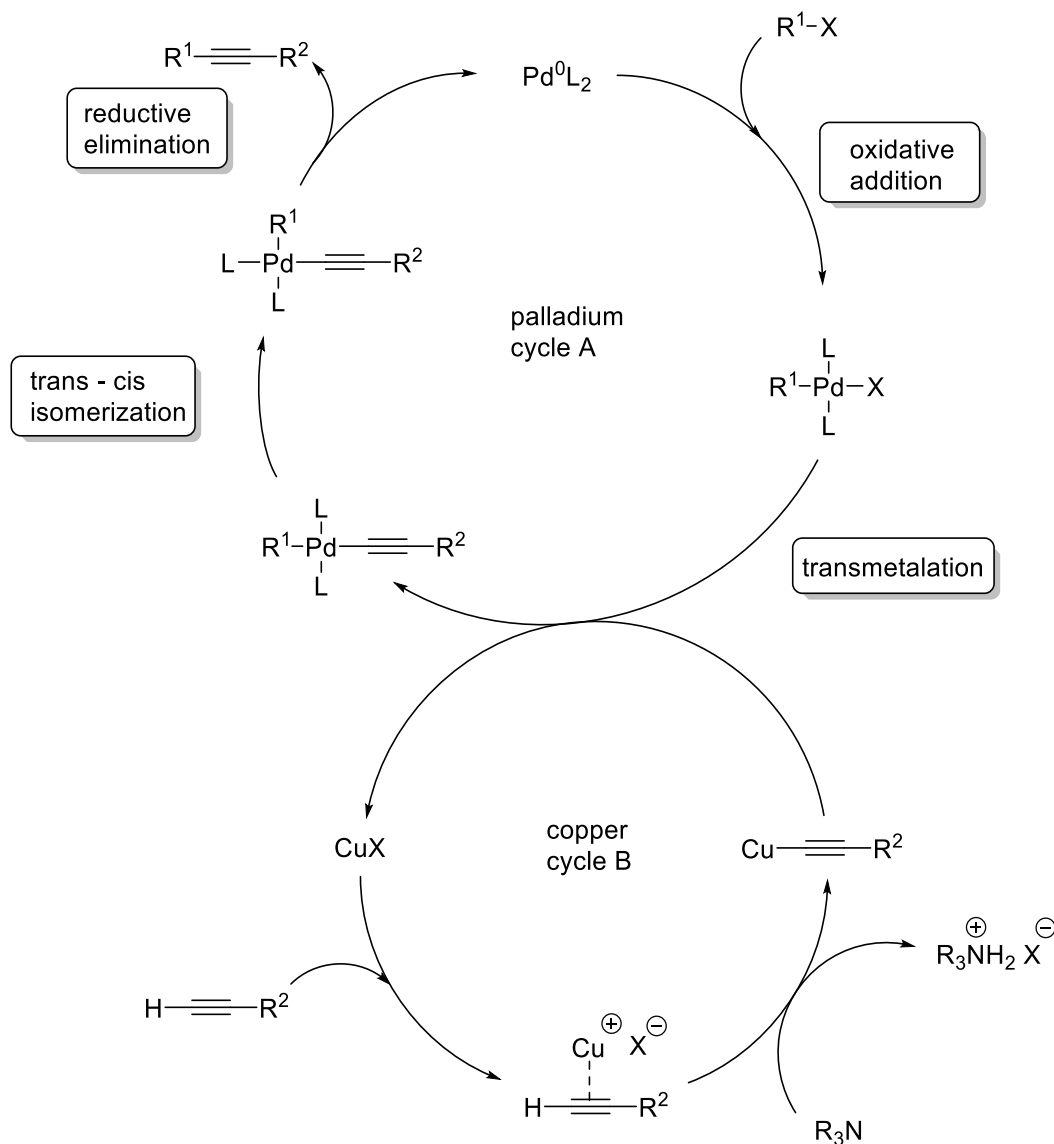


Figure 3: Reactivity of different vinyl and aryl halides and triflates in the Sonogashira coupling, respectively.<sup>[64]</sup>

Due to the enormous scope of possible substrates that can be employed, the Sonogashira reaction is widely used in the synthesis of a wide variety of molecules, e.g. pharmaceuticals, natural products, optoelectronics materials or nanomaterials.<sup>[63]</sup> Although the reaction is known for more than 45 years, the mechanism is not completely understood yet.<sup>[66]</sup> Compared to other cross coupling reactions, the mechanism of the Sonogashira reaction (*cf.* Scheme 7) is more complex, since two catalytic cycles are involved: a palladium cycle (A) and a copper cycle (B). In chapter 2.2, the general mechanism for palladium catalysed cross-coupling reactions was discussed. However, the Sonogashira reactions uses copper as a co-catalyst. The addition of the co-catalyst provides the opportunity to run the reaction at mild conditions and good yields are obtained already at ambient temperature. Previously, in the related Cadiot-Chodkiewicz and the Castro-Stephens reactions, high temperatures were essential. Multiple investigations regarding the mechanism have been published to date and there is an ongoing debate about the presence of possible intermediates. The catalytic active palladium species  $(\text{PPh}_3)_2\text{Pd}^0$  for example, does not exist in solution when generated in the presence of halide anions. Instead, the halide coordinates to the palladium forming an anionic  $[(\text{PPh}_3)_2\text{PdX}]^-$  complex.<sup>[67]</sup> Still,  $(\text{PPh}_3)_2\text{Pd}^0$  is mainly used in the generally accepted reaction mechanism.

As a palladium catalyzed cross-coupling, the Sonogashira reaction requires a catalytic active  $\text{Pd}^0$  species. There are two possible types of catalysts. The first type already consists of the active  $\text{Pd}^0$  species and is ligated, e.g. by four triphenylphosphines. The second type is a catalytic inactive  $\text{Pd}^{\text{II}}$  pre-catalyst, which is reduced *in situ* to the active  $\text{Pd}^0$  species. In general, these  $\text{Pd}^{\text{II}}$  pre-catalysts are more stable and can be stored under laboratory conditions. A common palladium

derivative used for the Sonogashira reaction is  $\text{Pd}(\text{PPh}_3)_2\text{Cl}_2$ . This inactive  $\text{Pd}^{\text{II}}$  pre-catalyst forms an intermediate with two alkynes with the aid of an amine base. Subsequently, the active  $\text{Pd}^0$  catalyst species is obtained by reductive elimination of a dialkyne. This step is usually not depicted and the mechanism in Scheme 7 already starts with the active palladium species.



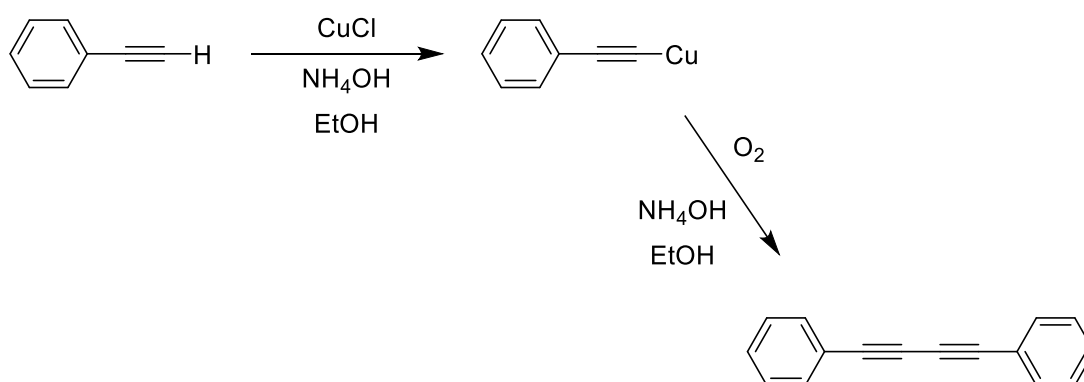
Scheme 7: Proposed catalytic cycles of the Sonogashira coupling.<sup>[66]</sup>

First, the aryl halide forms a  $\pi$  complex with the active palladium species, followed by oxidative addition, which is considered to be the rate limiting step.<sup>[68]</sup> Transmetalation of the resulting  $\text{Pd}^{\text{II}}$  complex with the copper acetylide transfers the organic moiety to the palladium. In this step, the palladium cycle A and the copper cycle B overlap. *Trans-cis* isomerization of the formed  $\text{Pd}^{\text{II}}$  complex brings the organic moieties in proximity. In a last step, the coupled alkyne is released from the

catalytic cycle by reductive elimination and the restored active  $\text{Pd}^0$  species enters another catalytic cycle. The steps in the palladium cycle A follow the general catalytic cycle for cross-coupling reactions (cf. Scheme 1).

The required copper acetylide is generated *in situ* in the copper cycle B. It is suggested that the copper halide forms a  $\pi$ -alkyne complex in the presence of an amine base. Upon complexation, the acidity of the acetylenic proton is increased. Thus, the mild amine base deprotonates the alkyne forming a highly reactive copper acetylide, which enters the palladium cycle A in the transmetalation step. The organic moiety is transferred from the copper to the palladium complex restoring the copper halide.<sup>[66]</sup>

The reaction of copper acetylides and aryl halides is also known as the Castro-Stephens reaction, which was described before. In contrast to the Sonogashira coupling, the Castro-Stephens reaction requires stoichiometric amounts of explosive copper acetylides and harsh reaction conditions are necessary for the reaction to proceed.<sup>[41]</sup> In contrast, the Sonogashira coupling only requires simple addition of catalytic amounts of copper to generate the copper acetylide *in situ* and thus handling of hazardous acetylides becomes unnecessary, since they are readily consumed. However, the application of copper salts also exhibits disadvantages since they also catalyze the Glaser coupling (cf. Scheme 8), which often occurs as homocoupling side reaction of two terminal alkynes.<sup>[33]</sup>

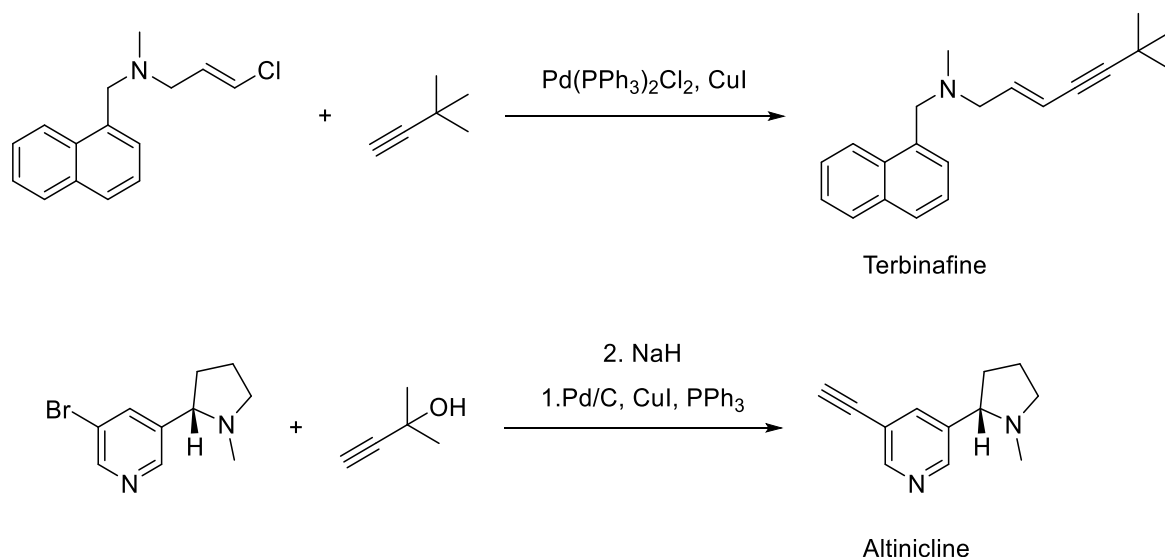


Scheme 8: A common side reaction in the Sonogashira coupling: the copper catalysed Glaser coupling.<sup>[33,34]</sup>

The Glaser coupling was first published by Carl Andreas Glaser in 1869. First, a copper acetylide is formed similar to the copper cycle B in the Sonogashira reaction. Originally, ammonia in water or an alcohol was used as a base. The copper acetylide then couples with itself under oxidative conditions forming the homocoupling product. The Glaser coupling is the main side reaction in the Sonogashira reaction,

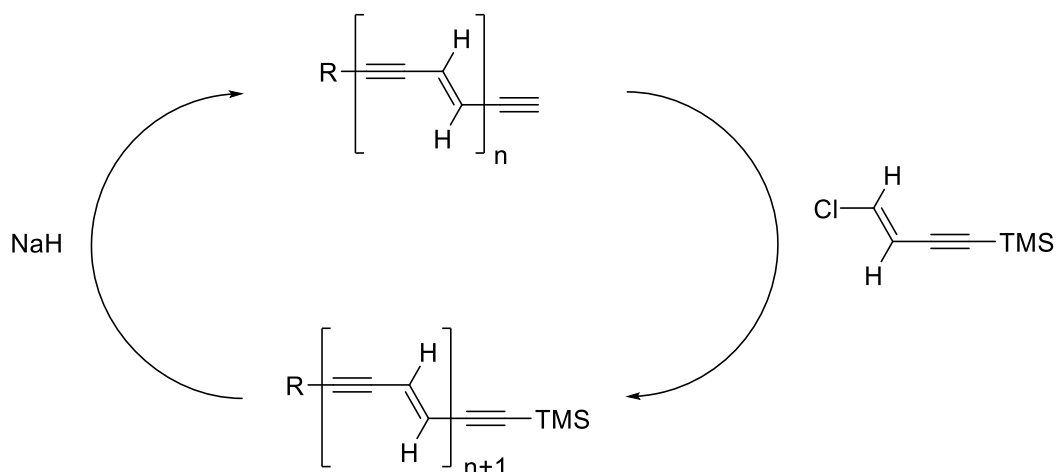
and several methods have been developed to suppress the homocoupling. Replacing the reaction atmosphere with inert gases, like nitrogen or argon, is beneficial since the Glaser coupling requires an oxidant, typically oxygen. Addition of reducing gases like hydrogen further suppress Glaser coupling, however, requires a more complicated reaction setup. Homocoupling is inevitable under typical reaction conditions, since the activation of the Pd<sup>II</sup> pre-catalyst always produces minimal amounts of diacetylenes. A lot of effort has been made developing a copper-free Sonogashira reaction and several examples have been published to date.<sup>[69]</sup> Since copper-free conditions avoid Glaser coupling as a side reaction and eliminate the need of costly processes to remove copper traces, it would be advantageous regarding the synthesis of pharmaceuticals. Furthermore, the cost of palladium limits the application in large scale synthesis, however, the Sonogashira coupling found its way into pharmaceutical synthesis, as it allows for a rather simple introduction of a triple bond.<sup>[63]</sup>

As an example, in the synthesis of Terbinafine, an antifungal agent, the Sonogashira reaction is applied in a large scale, coupling a vinyl chloride with *tert*-butylacetylene.<sup>[70]</sup> Another example is Altinicline, a nicotinic acetylcholine receptor, which shows potential application in treatment of Parkinson's disease, Alzheimer's disease, attention deficit hyperactivity disorder, Tourette's syndrome, and schizophrenia.<sup>[71]</sup> The structure is based on nicotine, but a triple bond is introduced *via* Sonogashira coupling of 2-methyl-3-butyn-2-ol and subsequent deprotection (cf. Scheme 9).



Scheme 9: Application of the Sonogashira reaction in the synthesis of pharmaceuticals Terbinafine (top) and Altinicline (bottom).<sup>[70,71]</sup>

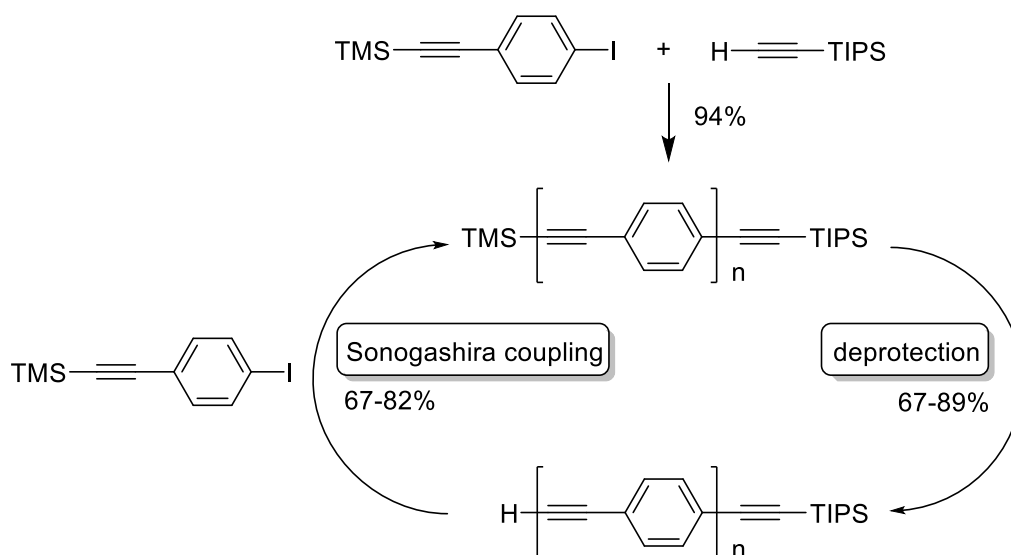
Apart from pharmaceuticals, the Sonogashira coupling is used for the synthesis of conjugated oligomers and polymers. Consistent with the section before, oligo(diacetylene)s are prepared exploiting the Sonogashira coupling (*cf.* Scheme 10). In 2003, Zuilhof and Sudhölter reported on the synthesis of oligomeric diacetylenes.<sup>[72]</sup> In an initial step, a terminal acetylene bearing an alkyl chain was reacted with *trans*-1,2-dichloroethene. After further Sonogashira reaction with TMS acetylene, the monomer was obtained. The required building block was prepared in the same manner, however, TMS acetylene was used in the initial step. Deprotection of the monomer and Sonogashira coupling with the building block yielded the TMS protected dimer. Repeating the procedure once more, a trimer was obtained in an overall yield of 4%. The oligomers were purified using column chromatography since also Glaser coupling of the terminal alkynes was observed during the reaction.



Scheme 10: Two-step approach for the synthesis of oligo(diacetylene)s based on the Sonogashira coupling and subsequent deprotection by Zuilhof and Sudhölter.<sup>[72]</sup>

Due to its mild reaction conditions, the Sonogashira coupling was used in various approaches not only towards *trans* oligo(diacetylene)s but also *cis* oligo(diacetylene)s<sup>[73]</sup> and even *trans* oligo(triacetylene)s.<sup>[74]</sup>

Another group of conjugated molecules are OPEs. Since the late 20<sup>th</sup> century, this class of molecules has been investigated and several approaches towards uniform macromolecules are described in the literature.<sup>[75]</sup> Mainly, OPEs are built up by Sonogashira coupling. An example of a strategy, which is frequently used for such syntheses, is depicted in Scheme 11.

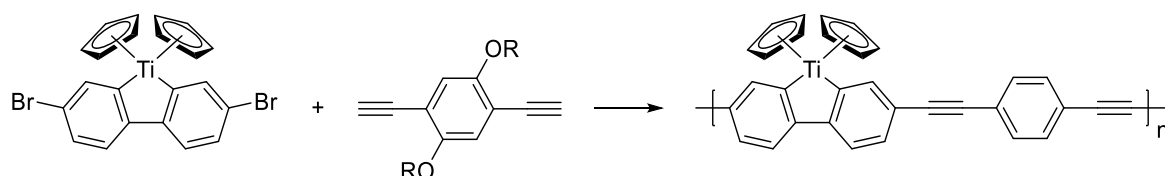


Scheme 11: Commonly used two-step strategy for the synthesis of OPEs from Dixneuf et al.<sup>[76]</sup>

In 1996, Dixneuf and co-workers published an approach towards OPEs involving a Sonogashira coupling and a deprotection step.<sup>[76]</sup> This two-step cycle is commonly

employed for the synthesis of OPEs and only a few other strategies have been published. In the approach from Dixneuf, a tri-isopropylsilyl protected acetylene was reacted with the building block, a TMS-protected 4-iodophenylacetylene, in a first step. Subsequently, the TMS group was deprotected and the resulting terminal acetylene used in a further Sonogashira coupling with the building block. Repeating this two-step cycle, a trimer was obtained after six steps. Unfortunately, analytical data was only reported briefly. The strategy described was then exploited by other scientists, e.g. the group of Tour, who demonstrated to synthesis of a OPE up to a 16-mer and is discussed in more detail in chapter 2.2.2.

In contrast to this stepwise procedure, the Sonogashira reaction was also applied in polymerization reaction to obtain poly(phenylene ethynylene)s or poly(arylene ethynylene)s.



Scheme 12: Application of the Sonogashira coupling in polymerization by Tomita *et al.*<sup>[77]</sup>

Recently, Tomita *et al.* used the Sonogashira coupling for the synthesis of a polymer containing titanocene moieties (*cf.* Scheme 12).<sup>[77]</sup> The incorporation of versatile elements into a conjugated polymer is often discussed in terms of their optoelectronic properties. The alternating polymer was synthesized from two monomers: one monomer being a titanocene derivative with two bromine moieties, the other monomer being a phenyl derivative with two solubilizing octyloxy side chains and two terminal acetylenes. The obtained air-stable polymer was fully characterized by proton and carbon NMR spectroscopy, IR spectroscopy and SEC. The optical properties were analyzed *via* UV/VIS spectroscopy. Two absorption maxima were observed. The absorption was red shifted compared to a model compound, a 2,7-bis(phenylethynyl) titanocene, and is consistent with the presence of an extended conjugated polymer backbone.

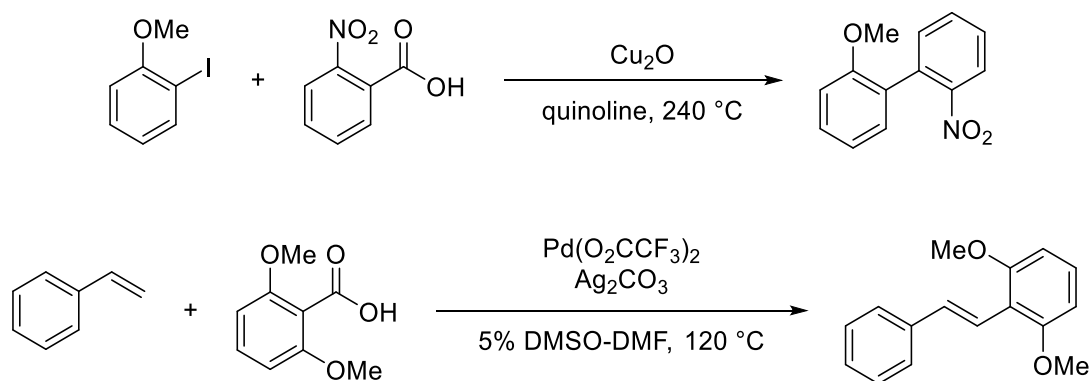
### 2.1.2 Decarboxylative Coupling Reaction

In this chapter, the decarboxylative cross-coupling and its application in synthesis are described. Since no organometallic reagents are used, the general reaction mechanism for cross coupling reaction is not applicable anymore and another reaction mechanism is discussed. The focus is then set on decarboxylative coupling of alkynyl carboxylic acids.

So far, traditional cross coupling reactions have been described, in which organometallic reagents are coupled with organohalides. Research in the field of cross-coupling reactions led to the development of highly efficient reactions in terms of functional group tolerance, selectivity, and yield. However, in most cross-coupling reactions, the organometallic reagent must be generated in stoichiometric amounts which produces equal amounts of metal waste. In contrast, decarboxylative cross-couplings release less toxic carbon dioxide. Moreover, the employment of carboxylic acids confers specific benefits as they are readily available and stable in storage and handling, thus making the decarboxylative cross coupling an alternative to traditional cross coupling reactions.

Likewise, to other cross coupling reactions, a new carbon-carbon bond is formed, but without the utilization of organometallic reagents. Instead, a carboxylic acid is reacted with an organohalide, and carbon dioxide is cleaved.

The first decarboxylative coupling was already published by Nilsson *et al.* in 1966.<sup>[78]</sup> They assumed a relation between the Ullmann reaction and the copper catalyzed decarboxylation of aromatic acids. Indeed, copper-catalyzed decarboxylation in the presence of an excess aryl iodide produced symmetric as well as unsymmetric biaryls, which indicated that both reactions proceed *via* a common intermediate. However, it was not practicable due to the drastic conditions and the low yields combined with a limited scope and was therefore not further pursued. Almost 40 years later, in 2002, Myers *et al.* reported on a decarboxylative Heck-type reaction.<sup>[79]</sup> In a first step, the arene carboxylic acid is converted to an arylpalladium species with the loss of carbon dioxide, which then reacts with an olefinic reagent comparable to the Heck coupling reaction to form vinylarenes. Good yields were reported for carboxylic acid substrates with electron-donating as well as electron-withdrawing substituents. However, ortho substitution was suggested essential for the decarboxylative palladation to happen.



Scheme 13: Top: First decarboxylative coupling reported by Nilsson.<sup>[78]</sup> Bottom: Decarboxylative Heck-type coupling from Myers.<sup>[79]</sup>

Four years later, in 2006, Gooßens *et al.* presented a cross-coupling strategy for the synthesis of biaryls based on the decarboxylative coupling of arylcarboxylic acid salts with arylhalides.<sup>[80]</sup> The synthesis of 26 different biaryls demonstrated the large scope of the decarboxylative coupling. Biaryls are often found in biologically active and functional materials, such as pharmaceuticals, agrochemicals, or liquid crystals. Gooßens *et al.* showed that these highly valuable compounds are easily accessible via a decarboxylative coupling. Since 2006, the decarboxylative coupling reaction has been developed further and exists nowadays in many different variations (*cf.* Figure 4).<sup>[81]</sup> Not only biaryls can be synthesized but also ketones,<sup>[82]</sup> arenecarboxylate esters,<sup>[83]</sup> olefines,<sup>[84]</sup> benzofuranes<sup>[85]</sup> or diarylalkynes.<sup>[57,86]</sup> Furthermore, decarboxylative coupling with amines,<sup>[87]</sup> thiols,<sup>[88]</sup> and secondary phosphines<sup>[89]</sup> was demonstrated generating carbon-heteroatom bonds.

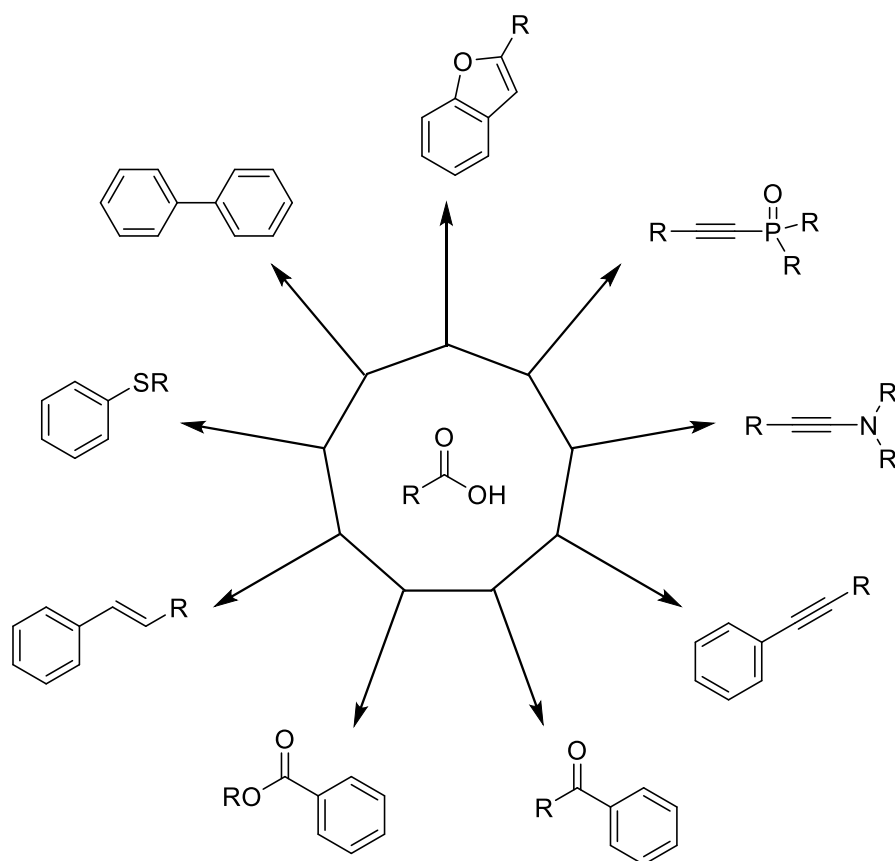
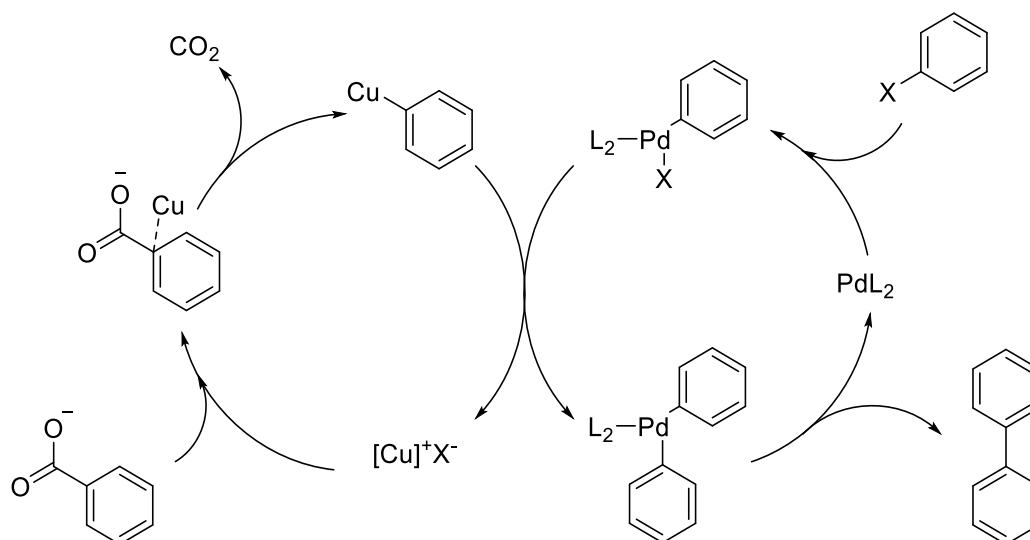


Figure 4: Possibilities of the decarboxylative coupling.

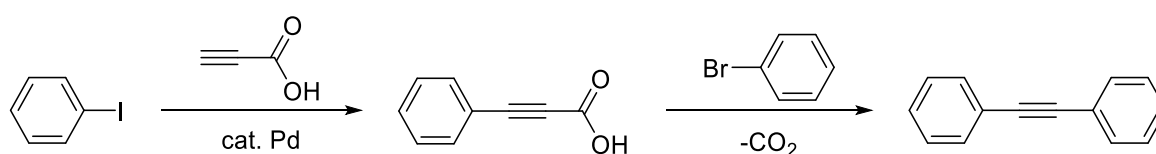
Gooßens *et al.* used a bimetallic catalyst system for their decarboxylative coupling and proposed a mechanism for their biaryl synthesis.<sup>[80]</sup> Similar to the Sonogashira coupling, copper and palladium are used, and the catalytic cycle is divided into two parts. One part describes the cleavage of carbon dioxide from the arylcarboxylic acid. In the initial step, the copper species coordinates to the carboxylate oxygen before shifting to the aryl  $\pi$ -system. Subsequently, carbon dioxide is released, and a stable copper intermediate is formed. The second part is similar to the general cross coupling reaction mechanism. Initially, palladium inserts into the halide carbon bond of an aryl halide in an oxidative addition. The previously formed copper intermediate then transfers its aryl group to the resulting arylpalladium species. The formed palladium complex, bearing both aryl moiety undergoes reductive elimination, releasing the biaryl from the catalytic cycle, and restoring the catalytic active palladium(0) species.



Scheme 14: Proposed bimetallic catalytic cycle for the decarboxylative coupling towards biaryls.<sup>[80]</sup>

In the beginning, copper carbonate was used as the copper source. In combination with potassium fluoride, mixed aryl copper fluoride salts were generated, which decarboxylated at lower temperature. However, stoichiometric amounts of copper were still required although the proposed mechanism suggest catalytic amounts are already sufficient. Development of another catalyst system using copper (I) iodide as copper source was as effective as the initial catalyst system, but with substoichiometric amount of copper and palladium.

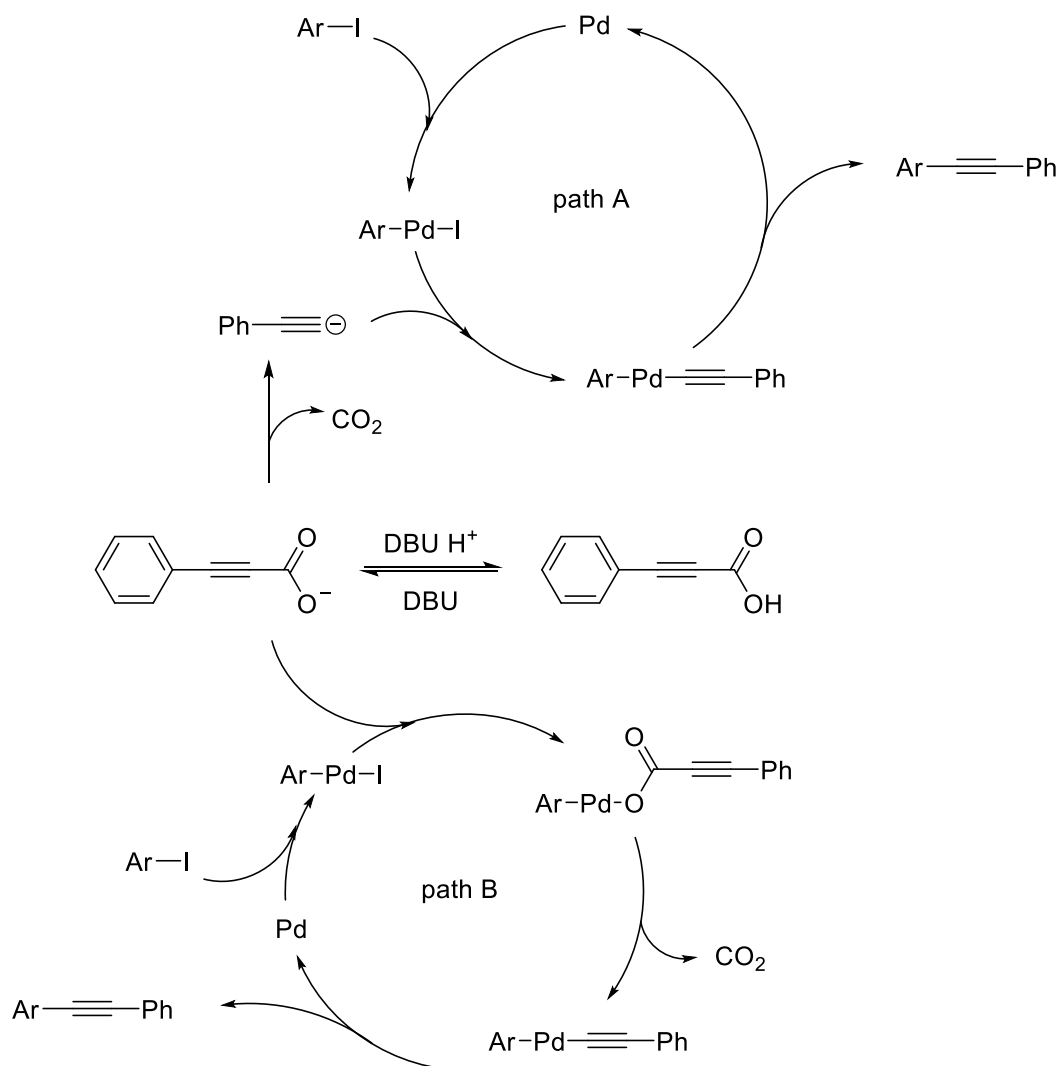
In 2008, Lee and co-workers reported on decarboxylative coupling of alkynyl carboxylic acids and aryl halides using a monometallic palladium catalyst system.<sup>[57]</sup> Propiolic acid was reacted in a Sonogashira coupling with an aryl halide and the resulting alkynyl carboxylic acid was immediately further converted with another aryl halide in a decarboxylative coupling. Both reactions were conducted successively in one pot and symmetric as well as unsymmetric substituted diaryl alkynes were obtained.



Scheme 15: One-pot synthesis of biaryls reported by Lee *et al.* consisting of a Sonogashira coupling and a subsequent decarboxylative coupling.<sup>[57]</sup>

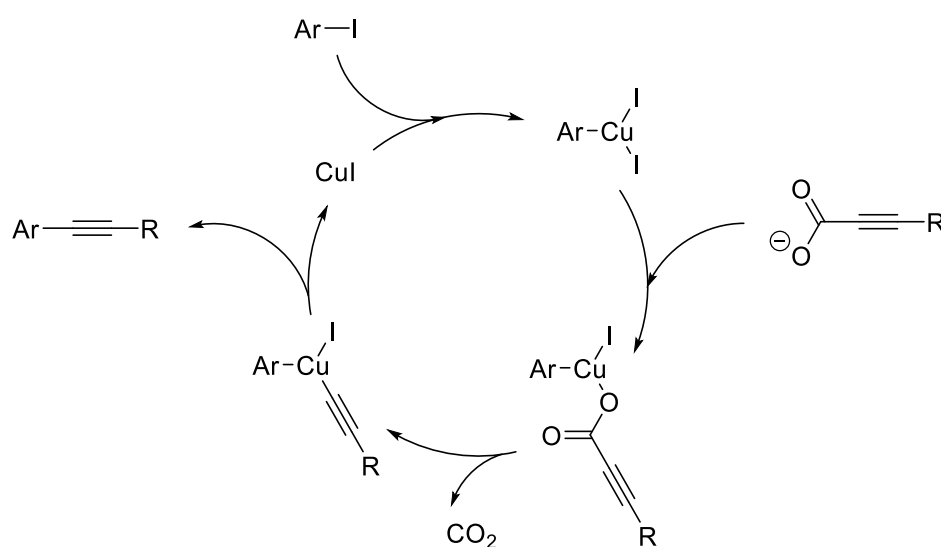
In 2012, also Lee *et al.* studied the mechanism of the decarboxylative coupling of alkynyl carboxylic acids with aryl halides.<sup>[90]</sup> They used gas chromatography and

FT-IR spectroscopy to investigate the reaction of phenyl propiolic acid with methyl-4-iodobenzoate. They found that phenyl propiolic acid releases carbon dioxide in the presence of a base, here 1,8-diazabicyclo[5.4.0]undec-7-en (DBU), at 80 °C without any metal. Two possible pathways A and B for the coupling were proposed. In pathway A, decarboxylation occurs first and then the decarboxylated alkyne reacts with the arylpalladium complex. In pathway B, phenyl propiolic acid reacts first with the arylpalladium complex and decarboxylation then proceeds in the phenyl propiolate palladium complex. The thermal decarboxylation in the presence of a base suggests pathway A. However, it was found that the yield of the coupling product was higher than the yield of the decarboxylation. Thus, they proposed that the decarboxylative coupling proceeds through both pathways A and B, but additional experimental data suggests that pathway B is predominant.



Scheme 16: Two possible reaction pathways of the decarboxylative coupling of alkynyl carboxylic acids.<sup>[90]</sup>

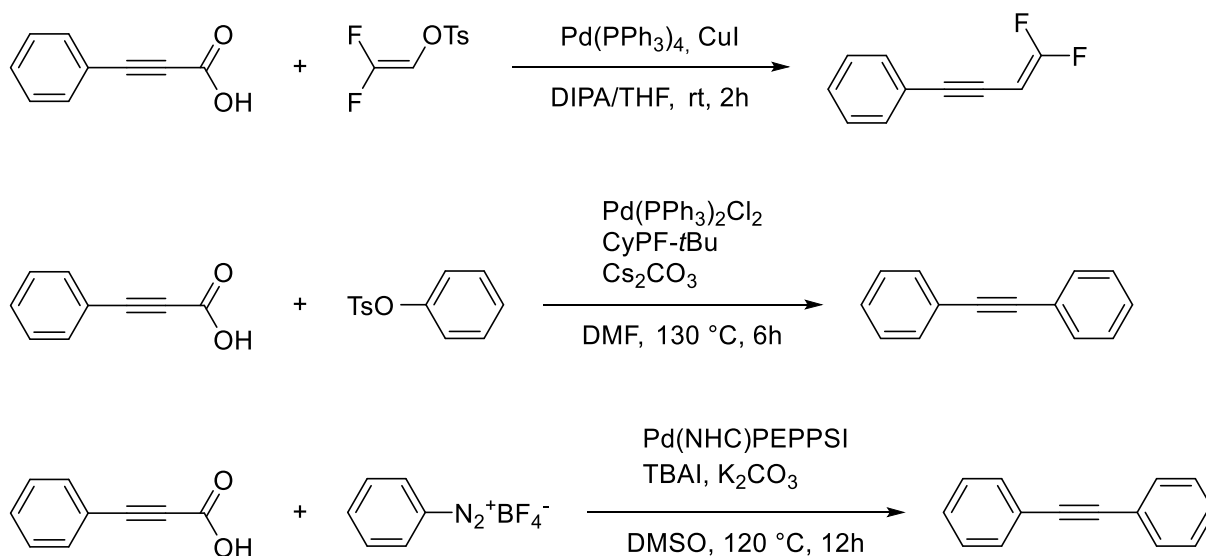
Similar to the development of a monometallic palladium catalyst, an approach using only copper as a catalyst was investigated. It was the group of Xue who first reported on the copper catalyzed decarboxylative coupling of aryl alkynyl carboxylic acids with aryl halides by the use of a copper(I) iodide and phenanthroline catalytic system.<sup>[85]</sup> Although the required temperature was rather high, good functional group tolerance was maintained. Their computational study of the mechanism suggests that the oxidative addition of the aryl halide to the copper(I) occurs first. The formed copper(III) complex then reacts with the alkynyl carboxylic acid. Upon decarboxylation and reductive elimination, the coupled product is obtained.



Scheme 17: Proposed catalytic cycle for the monometallic copper catalyzed decarboxylative coupling.<sup>[85]</sup>

The development of catalysts has still not stopped, and Nolan et al. reported the use of palladium catalyst carrying a *N*-heterocyclic (NHC) ligand in 2019.<sup>[91]</sup> The decarboxylative coupling of aryl bromides with aryl alkynyl carboxylic acids proceeded under mild reaction conditions and even in the presence of water. By use of a ferrocene-based palladacycle, the scope of the possible reagents can be extended to alkynoic acids and aryl chlorides.<sup>[92]</sup>

The scope was even further extended to the use of aryl and vinyl tosylates instead of aryl and vinyl halides. In 2016, Satoh *et al.* reported the decarboxylative coupling of phenylpropionic acid with 2,2-difluoroethenyl tosylate with palladium and copper bimetallic catalytic system.<sup>[93]</sup> One year later, the group of Lee published the decarboxylative coupling of aryl and alkyl alkynyl carboxylic acids with aryl tosylates to give diarylacetylenes.<sup>[94]</sup> Besides tosylates, arenediazonium salts have been applied as well.<sup>[95]</sup>



Scheme 18: Decarboxylative coupling with tosylates and arene diazonium salts. PEPPSI<sup>TM</sup> stands for Pyridine-Enhanced Precatalyst Preparation Stabilization and Initiation.<sup>[93–95]</sup>

Since the first report of the decarboxylative coupling of alkynyl carboxylic acids with aryl halides, a variety of possible coupling partners ranging from aryl and alkyl halides to tosylates and diazonium salts have been applied. Various catalytic systems have been established and recent investigations also focus on metal-free conditions for decarboxylative reactions.<sup>[96]</sup> Most examples of decarboxylative couplings show similar results compared to their Sonogashira coupling counterparts.

## 2.2 Sequence-Definition in Chemistry

Over the last decades, the preparation of defined oligomeric and polymeric materials has attracted a lot of attention in organic chemistry as well as polymer science.<sup>[17,97]</sup> The field of defined macromolecules is inspired by highly defined biomacromolecules, like deoxyribonucleic acid (DNA) and ribonucleic acid (RNA) or peptides. The exact molecular weight in combination with precise positioning of monomeric units (sequence) determines the function of the molecule.<sup>[98]</sup> The term sequence is not used for biomacromolecules exclusively, but found its way into the synthesis of non-natural macromolecules.<sup>[99,100]</sup>

A first definition of sequence-controlled polymers was given by Lutz, Ouchi and Sawamoto in 2013.<sup>[97]</sup> The definition describes sequence-controlled polymers as “*macromolecules in which monomer units of different chemical nature are arranged in an ordered fashion.*”<sup>[97]</sup> This general definition comprises all kinds of controlled polymers, ranging from absolutely defined macromolecules with a dispersity index  $\bar{D}=1.00$ , like the mentioned biomacromolecules, to less defined polymers ( $\bar{D}>1.00$ ), like block copolymers, alternating polymers, and periodic polymers (cf. Figure 5).<sup>[101]</sup> As a result, more precise terms were necessary to determine the different degrees of control in copolymers.

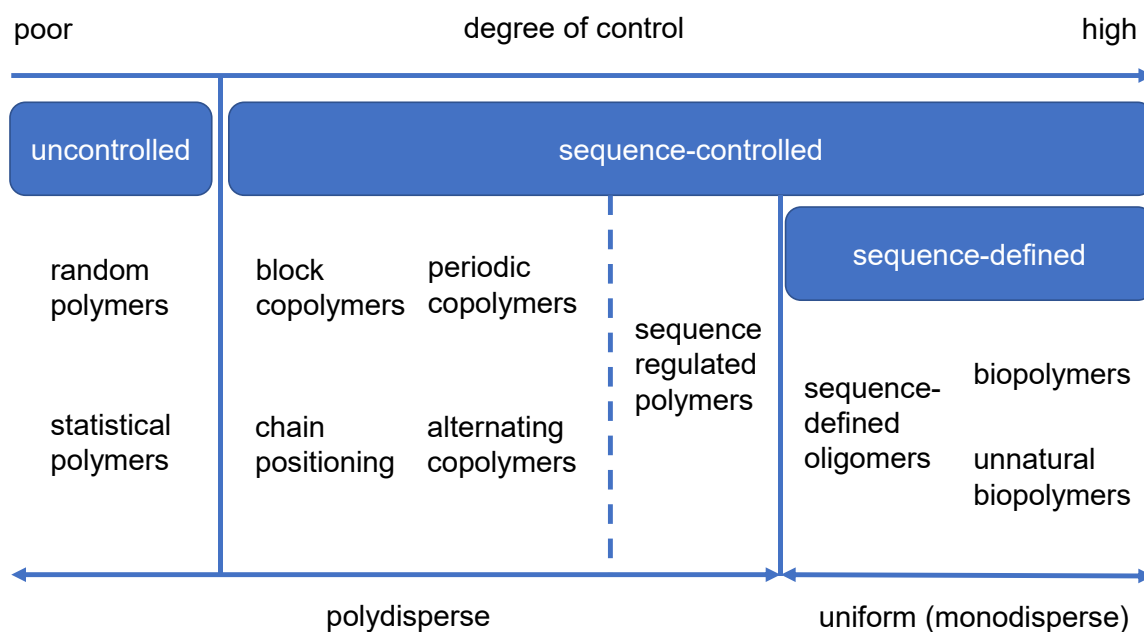
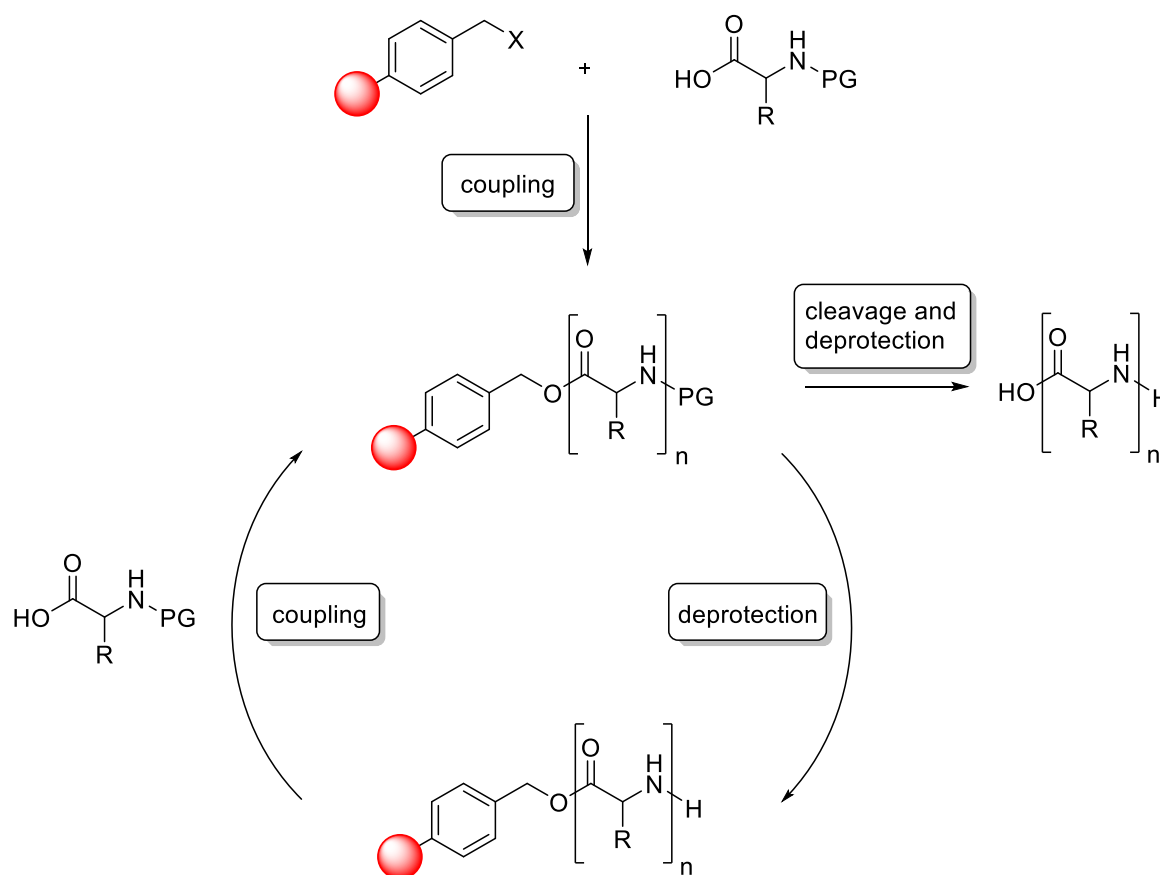


Figure 5: Classification of polymers regarding different degrees of control.<sup>[101]</sup>

According to Figure 5, the terms sequence-controlled and sequence-defined occur to have different meanings.<sup>[101]</sup> For example, alternating copolymers obtained from free radical polymerization are referred to as sequence-controlled, but not sequence-defined. Still, sequence-controlled copolymers exhibit a disperse chain-length distribution ( $\mathcal{D} > 1.00$ ). Polymers with a higher degree of control and dispersities close to  $\mathcal{D} = 1.00$  can be referred to as sequence-regulated. Sequence-defined macromolecules, however, are of uniform size and monomer composition, exhibiting the highest degree of control ( $\mathcal{D} = 1.00$ ).<sup>[102]</sup> Per definition from the IUPAC, a polymer is described as “*a substance composed of macromolecules.*”<sup>[14]</sup> Since all chains are the exact same length and each monomer unit is precisely placed within the chain in sequence-defined polymers, the definition as a polymer is not valid anymore. Also, terms like sequence-ordered or uniform polymers are used to describe uniformity and might lead to confusion.<sup>[103]</sup> Within this work, strictly defined molecules, in which the (different) monomers are precisely placed in the chain and all chains exhibit the same length, are referred to as sequence-defined or uniform macromolecules.

As mentioned in the beginning of this chapter, the field of sequence-definition is inspired by nature.<sup>[98,104]</sup> DNA, for example, is a sequence-defined polynucleotide with a defined molecular weight, storing the code of life. DNA consists the four nucleobases adenine, guanine, thymine, and cytosine which form complementary base pairs.<sup>[105]</sup> Hydrogen bonding between the base pairs enables the double-helical structure of DNA, which was described in 1953 by Watson and Crick, demonstrating that DNA is one of the longest naturally occurring sequence-defined macromolecules.<sup>[105]</sup> While biology uses enzymes to synthesize sequence-defined biomacromolecules, chemists have developed approaches based on solid phase supports. In 1963, Merrifield reported the first approach towards sequence-defined peptides, today known as the solid phase peptide synthesis (SPPS).<sup>[106]</sup> The iterative two-step synthesis strategy is outlined in Scheme 19. In 1984, Merrifield was awarded with the Nobel prize for this work which allowed the facile synthesis of sequence-defined oligopeptides, and later oligopeptoids as well as oligonucleotides.<sup>[106,107,108]</sup> In 1966, the process was automated allowing the fast synthesis of longer sequences.<sup>[109]</sup> SPPS generally follows an iterative cycle of coupling and deprotection. Initially, the first amino acid is coupled to an insoluble resin which exhibits a linker group. The use of monoprotected amino acids in excess

guaranteed quantitative conversion and decreased side-products.<sup>[110]</sup> Purification is performed by simple filtration and washing. Deprotection enables further coupling with another monoprotected amino acid. Following the iterative cycle, sequence-defined peptides are obtained after cleavage from the resin in a final step. The efficiency of SPPS was demonstrated by Merrifield and co-workers, for instance, when they reported on the synthesis of bovine insulin with a sequence of 52 amino acids.<sup>[111]</sup> However, peptides with more than 30 to 50 amino acids are generally difficult to obtain.<sup>[112]</sup>



Scheme 19: Iterative cycle for the SPPS by Merrifield.<sup>[106]</sup>

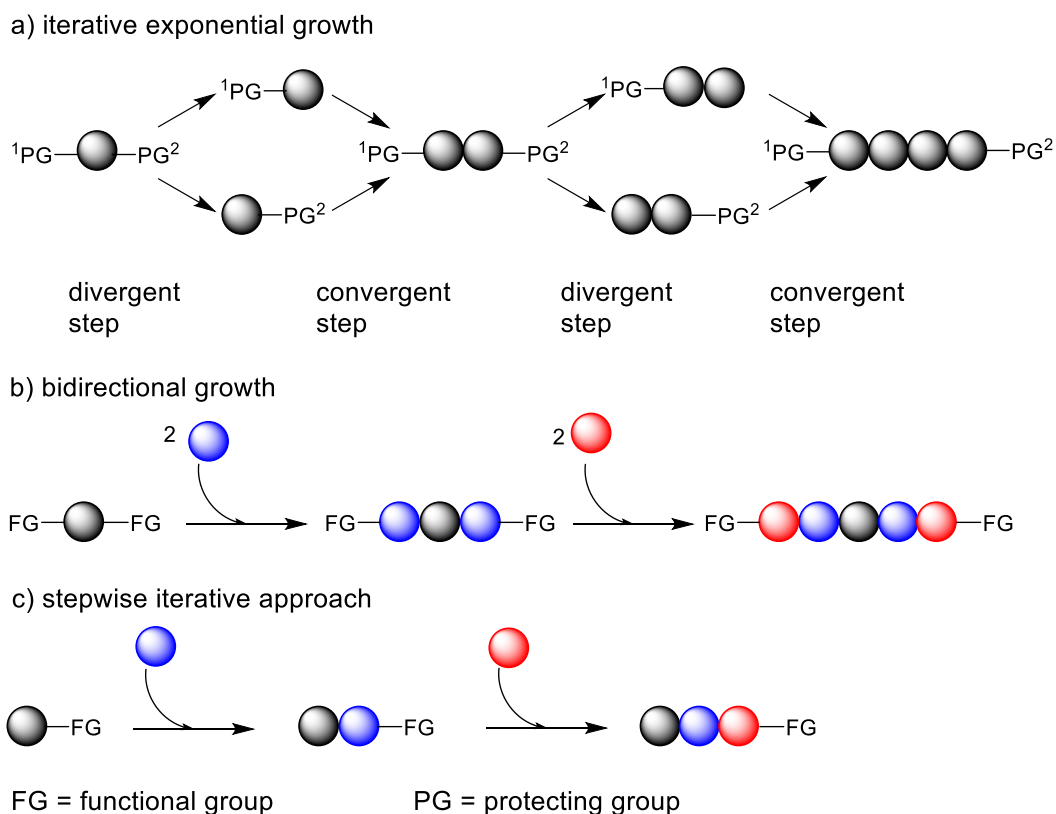
Besides oligopeptides and oligonucleotides, oligopeptoids have been synthesized using a solid phase support. Peptoids are non-naturally occurring macromolecules with a similar structure to peptides but different backbone substitution. Peptides are typically substituted on the carbon atom, whereas peptoids exhibit nitrogen substitution.<sup>[113]</sup> However, this small change in the backbone substitution shows a large impact on the properties of the respective macromolecule. Biological activity or improved resistance against enzymatic degradation compared to their peptide analogues make peptoids an important class of biomacromolecules.<sup>[108,113,114]</sup> Since

the coupling steps in peptoid synthesis are much slower, the synthesis was adapted with a sub monomer strategy by Zuckermann *et al.*<sup>[113]</sup> Similar to the peptide synthesis, the peptoid synthesis was automated and polypeptoids with up to 50 glycine units were obtained.<sup>[115]</sup>

The great success in the solid phase supported synthesis of sequence-defined biomacromolecules was then translated to organic synthesis.<sup>[116]</sup> The solid phase organic synthesis (SPOS) has become a valuable tool for iterative synthesis procedures.<sup>[117,118]</sup> However, besides solid phase synthesis, the approaches towards sequence-defined macromolecules are divided into liquid phase synthesis, fluorous phase synthesis and polymer tethered synthesis.<sup>[18]</sup> Concerning the synthesis strategy, sequence-defined macromolecules can be obtained from continuous iterative synthesis routes or non-iterative strategies. However, to achieve sequence-definition, continuous iterative strategies are the method of choice. Therefore, mainly three iterative approaches are used for the synthesis of sequence-defined macromolecules: iterative exponential growth (IEG), bidirectional growth and liner stepwise approach.<sup>[119]</sup> Scheme 20 depicts the three approaches.

Large macromolecules can be rapidly synthesized by applying the IEG strategy. Monomers with orthogonally protecting or activating groups are required, which are divided into two parts. The two parts are separately and orthogonally deprotected or activated and subsequently re-combined in a coupling reaction. Since monomers form dimers, dimers form tetramers, tetramers form octamers, and so on, the number of building units, which are incorporated in the macromolecule rises exponentially. However, due to this nature of the strategy, it is limited to repetitive sequences. In the field of conjugated uniform macromolecules, it is also referred to as divergent/convergent approach, since it features a divergent step for the orthogonal deprotection/activation and a convergent step for the coupling.<sup>[18,120]</sup> Due to the exponential character of the strategy, higher DP macromolecules are obtained in only a few steps. In the bidirectional growth strategy, symmetric macromolecules can be obtained. In this strategy, a bifunctional starting compound is reacted with two building units simultaneously. In this way, two monomers are incorporated in each cycle. However, this strategy is limited to symmetric sequences. The highest control over the sequence is provided by an iterative stepwise approach, whereby one building is added after the other. Compared with the other strategies, the

stepwise approach requires more steps for obtaining large molecules, since only one building unit is added during each cycle. However, macromolecules built up with the iterative stepwise strategy are not limited to symmetric sequences, rather high control in side chain substitution is guaranteed.



Scheme 20: Three frequently used approaches towards sequence-defined macromolecules.<sup>[18]</sup>

All three approaches have been used for the synthesis of highly defined macromolecules.<sup>[18]</sup> Different examples of the approaches are described in the following chapters (chapters 2.2.1 and 2.2.2). First, the focus is set on non-conjugated macromolecules. Afterwards, examples for conjugated sequence-defined macromolecules, which are also used in this thesis, are described.

### 2.2.1 Non-conjugated sequence-defined macromolecules

One class of non-conjugated macromolecules, which have been uniformly synthesized by the above mentioned three approaches, is poly(ethylene glycol)s (PEGs). Hereinafter, only selected examples of the relevant synthesis strategies are presented. In 1992, for example, Jenneskens *et al.* reported the synthesis of PEGs by a bidirectional growth strategy.<sup>[121]</sup> Two monoprotected building units were prepared by reaction of di(ethylene glycol) or tetra(ethylene glycol) with trityl chloride, respectively. After activation of the starting block *via* tosylation, a coupling with one of the building units can be performed. Subsequent cleavage of the trityl protecting group and further activation enables the coupling with another building unit. Following the three step iterative cycle, a dodeca(ethylene glycol) was synthesized. Several similar approaches have been published and uniform PEGs with up to 44 ethylene glycol units were obtained. Besides the bidirectional growth, many synthesis strategies towards uniform PEGs are based on IEG. In 1999, Burns *et al.* published an approach using tetrahydropyrane (THP) and benzyl (Bn) protecting groups combined with leaving groups, like tosylates or halides. Orthogonal deprotection of the THP and Bn group and subsequent coupling yielded an undeca(ethylene glycol). Hill *et al.* reported the synthesis of a 24-mer PEG similar to the approach of Burns.<sup>[122]</sup> They also used THP and Bn protecting groups and tosylation for activation of the hydroxyl groups. A final coupling of two dodeca(ethylene glycol)s yielded the 24-mer PEG in high purity, which was verified by elemental analysis and mass spectrometry. Davis and co-workers published another approach based on IEG towards uniform PEGs, which were then analyzed by SEC, another highly precise strategy to prove uniformity.<sup>[123]</sup> Initially, tetra(ethylene glycol) was split into two parts. One part was monoprotected with a Bn protecting group and subsequently tosylated. The other part was monoprotected with a trityl protecting group. Coupling of the two parts in an ether synthesis yielded an orthogonally protected octa(ethylene glycol). The steps of trityl deprotection and tosylation of one part and Bn deprotection of the other part followed by recombination of the two parts were repeated to obtain a 32-mer. As mentioned before, the oligo(ethylene glycol)s were analyzed by SEC which verified the high purity. Furthermore, PEGs have also been synthesized using an iterative approach by Livingston in 2014.<sup>[124]</sup> The oligomers were synthesized as separate arms of a

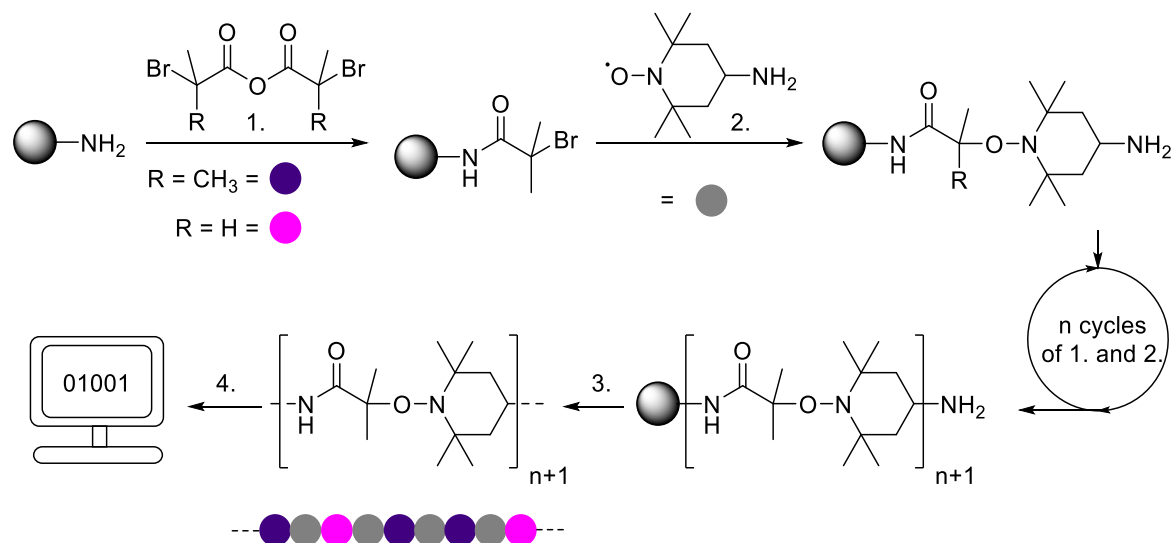
three-arm benzylic star, which was used as core. Decoupling from the benzylic star core yielded a 24-mer PEG. In 2019, this approach was extended and molecular sieving was used for purification instead of column chromatography.<sup>[125]</sup>

A comparative study of the different strategies towards uniform oligo(ethylene glycol)s was published in 2019.<sup>[126]</sup> It revealed that only analysis by SEC provides sufficient information to confirm uniformity. Nevertheless, comparing a 15-mer with a 16-mer was difficult due to their small difference in hydrodynamic radius which clearly demonstrated the limits of the characterization method in this case with a rather small repeating unit.

To this point, the synthesis of uniform PEGs *via* the three main strategies was described. Despite the same building unit was used in every step leading to a rather simple and repetitive structure, it can be considered as sequence-definition since the building units were carefully introduced at specific positions *via* one of the iterative strategies discussed above (chapter 2.2). In contrast, in the following examples, different building units are introduced into macromolecules *via* the same iterative strategies to form actual sequences that can be precisely adjusted.

A large field for the application of sequence-defined macromolecules was opened by Lutz *et al.* who proposed that data could be stored in synthetic macromolecules.<sup>[97]</sup> This was inspired by nature, as the sequence of four different nucleotides in DNA stores the information of life. In the same way, a sequence in a synthetic macromolecule can store any kind of data. To implement a sequence into a molecule, iterative build-up of oligomeric structures is crucial. Furthermore, read-out of the implemented information is essential and often achieved *via* tandem MS. One possibility is the introduction of a binary code into a sequence-defined macromolecule. For this system, only two building units are necessary. One building unit is defined as “1” in the binary code and the other one as “0”. By an iterative stepwise approach, any code can be transferred to a macromolecule on a molecular level. In 2015, Lutz *et al.* established a solid phase supported iterative procedure towards an information-containing macromolecule which is depicted in Scheme 21.<sup>[127]</sup> They used anhydrides with different side chains as building units, which were connected by amino functionalized 2,2,6,6-tetramethylpiperidinyloxy (TEMPO). Read-out of the stored information was performed after cleavage of the oligomer from the solid support, using tandem MS. Later, the approach was extended to

poly(alkoxyamine phosphodiester)s since the read-out of poly(alkoxyamine amide)s was only possible for small chains.<sup>[128,129,130]</sup>

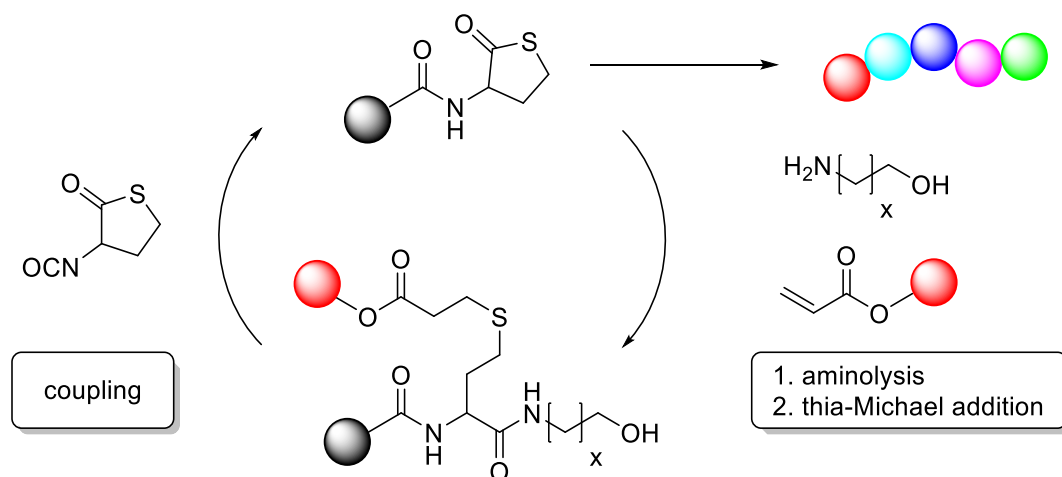


Scheme 21: Iterative solid-supported synthesis of an information containing macromolecule.<sup>[127]</sup> The binary code is introduced by different sidechains. Cleavage from the solid support (3.) enabled sequential read-out via tandem MS (4.).

It is noted that a lot of effort has been put into the synthesis of sequence-defined macromolecules for the application in the field of data storage. Advances in data storage capacity and the sequential read-out are frequently reported by the groups of Lutz,<sup>[17,97,100,127,129,130,131]</sup> Meier<sup>[132–139]</sup> and Du Prez.<sup>[140,141,142]</sup> However, it is not further discussed in here.

In 2013, Du Prez *et al.* reported the synthesis of a multifunctionalized sequence-defined oligomer from a single building block on solid support.<sup>[117]</sup> The protecting group free approach is based on thiolactone chemistry, hence, a thiolactone acrylamide served as building block. Aminolysis with a primary amine ring-opens the thiolactone forming a thiol, which is then reacted in a thia-Michael addition with the thiolactone-acrylamide building block to extend the chain. Ring-opening with different commercially available primary amines yielded sequence-defined oligomers up to tetramers. In 2016, the same group extended the approach with a slightly different, but improved system (*cf.* Scheme 22).<sup>[143]</sup> Again, thiolactone chemistry was applied, but this time with an isocyanate functionalized thiolactone. Synthesis on solid phase was maintained and a thiolactone was reacted with a 2-chlorotriylchloride resin in an initial step. Subsequently, the thiolactone is ring-opened by an amino alcohol forming a thiol and a hydroxyl function. By thia-Michael

reaction of the thiol with an acrylamide or an acrylate, different side chains were introduced. Variation in the backbone was achieved by using amino alcohols of different lengths. The chain was then extended by reaction of the hydroxy group with the isocyanate group of the thiolactone building block. Following this two-step cycle, different sequence-defined decamers were obtained in an iterative fashion. Automation of the process with a synthesizer decreased the reaction time for a decamer significantly from 3-5 days to 33 hours.

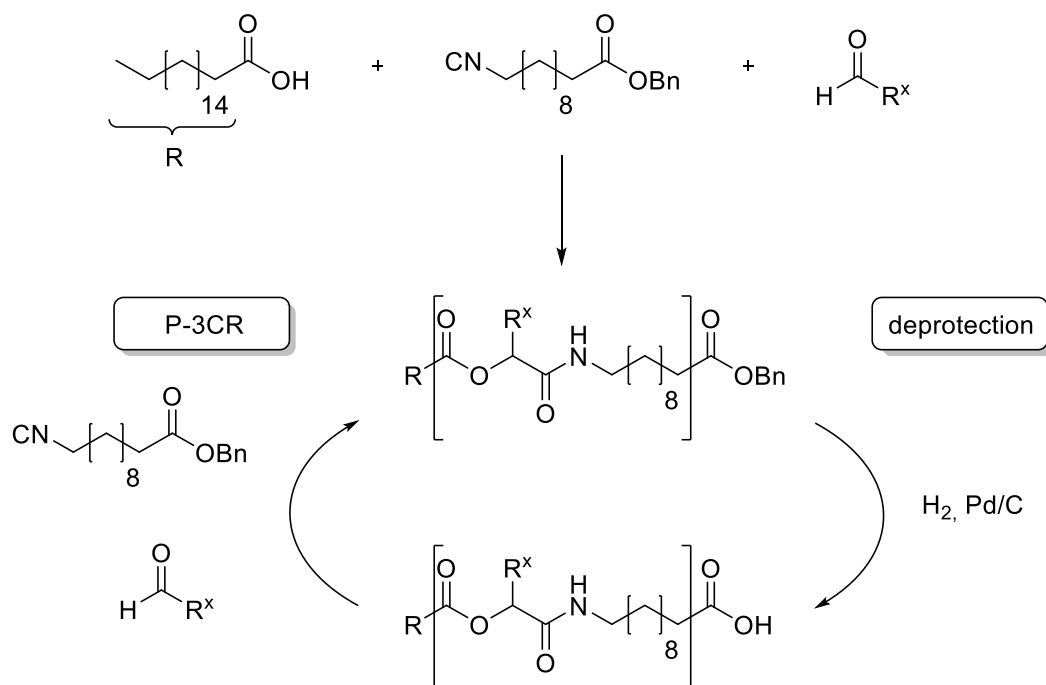


Scheme 22: Iterative two-step reaction cycle to build up sequence-defined oligomers on solid phase using thiolactone chemistry.<sup>[143]</sup>

Furthermore, Barner-Kowollik *et al.* demonstrated the use of photochemistry for the synthesis of sequence-defined macromolecules in a bidirectional growth.<sup>[144]</sup> In 2019, they reported on a protecting group free approach based on orthogonal photochemistry.<sup>[145]</sup> The strategy is based on a nitrile imine-carboxylic acid ligation (NICAL) of a visible light responsive pyrene-functionalized tetrazole upon irradiation at 410 nm, and a Diels-Alder [4+2] cycloaddition of a diene with a fumarate at 365 nm. A symmetric core with two carboxylic acids and two building units was used. One building unit bears the pyrene-functionalized tetrazole and a  $\alpha$ -methyl benzaldehyde, which exhibits a photo-caged diene, while the other building unit is functionalized with a carboxylic acid and a fumarate. Sequential irradiation at 410 and 365 nm and switching between the two building units yielded a sequence-defined decamer. High purity was confirmed by SEC and demonstrated the efficiency of this protecting group free approach based on selective orthogonal photochemistry.

Another important approach towards sequence-defined macromolecules is based on multicomponent reactions (MCRs). In general, MCRs offer a wide range of application and several groups have reported solid or solution phase approaches towards sequence-defined macromolecules *via* MCRs.<sup>[132,139,141,142,146]</sup> In 2014, Meier *et al.* used the Passerini three component reaction (P-3CR) in order to synthesize sequence-defined macromolecules in an iterative fashion.<sup>[132]</sup> The approach combines the P-3CR with the thiol-ene reaction. Stearic acid was used in a first P-3CR together with 10-undecenal and an isocyanide. The introduced double bond was subsequently reacted with 3-mercaptopropionic acid in a thiol-ene addition restoring a free carboxylic acid which was reacted in another P-3CR. The sequence was introduced by variation of the isocyanide in every P-3CR. This way, a sequence-defined tetramer was obtained with 26% overall yield. One year later, the approach was extended by substitution of the P-3CR with the Ugi four component reaction (U-4CR).<sup>[133]</sup> In the U-4CR, a carboxylic acid reacts with an aldehyde, an amine, and an isocyanide. Compared to the previous approach, the amine component is added, which enabled not only variation of the isocyanide, but also the amine at the same time leading to dual side chain definition. Following the previously described two-step iterative reaction cycle of MCR and subsequent thiol-ene reaction, a pentamer with variation of the isocyanide and amine component was obtained in 15% overall yield. Careful selection of the components was mentioned to assure high yields, which is a key element for synthesizing long sequences. In 2016, another approach using the P-3CR was reported by the same group.<sup>[134]</sup> In this improved approach, the P-3CR was not combined with the thiol-ene addition anymore, but the basic concept of a coupling step and a deprotection step was introduced. Therefore, a monoprotected building unit exhibiting an isocyanide functionality and a benzyl ester was synthesized in three steps. Again, stearic acid was used in a first P-3CR with the building unit and an aldehyde. Subsequently, the benzyl ester of the resulting Passerini product was deprotected using palladium on carbon and hydrogen gas. The obtained free carboxylic acid was then reacted with the building unit and a different aldehyde. Variation of the aldehyde component is beneficial compared to variation of the isocyanide component, since far more aldehydes are commercially available. Following the two-step iterative cycle, which is depicted in Scheme 23, a sequence-defined decamer with 9 different side chains was obtained in an overall yield of 44%. Introduction of a *cis* double bond in the side

chain in a final P-3CR allowed further modifications. A sequence-defined 20-mer was obtained after self-metathesis of two decamers. The macromolecules were completely characterized by NMR spectroscopy, mass spectrometry and SEC confirming their high purity.

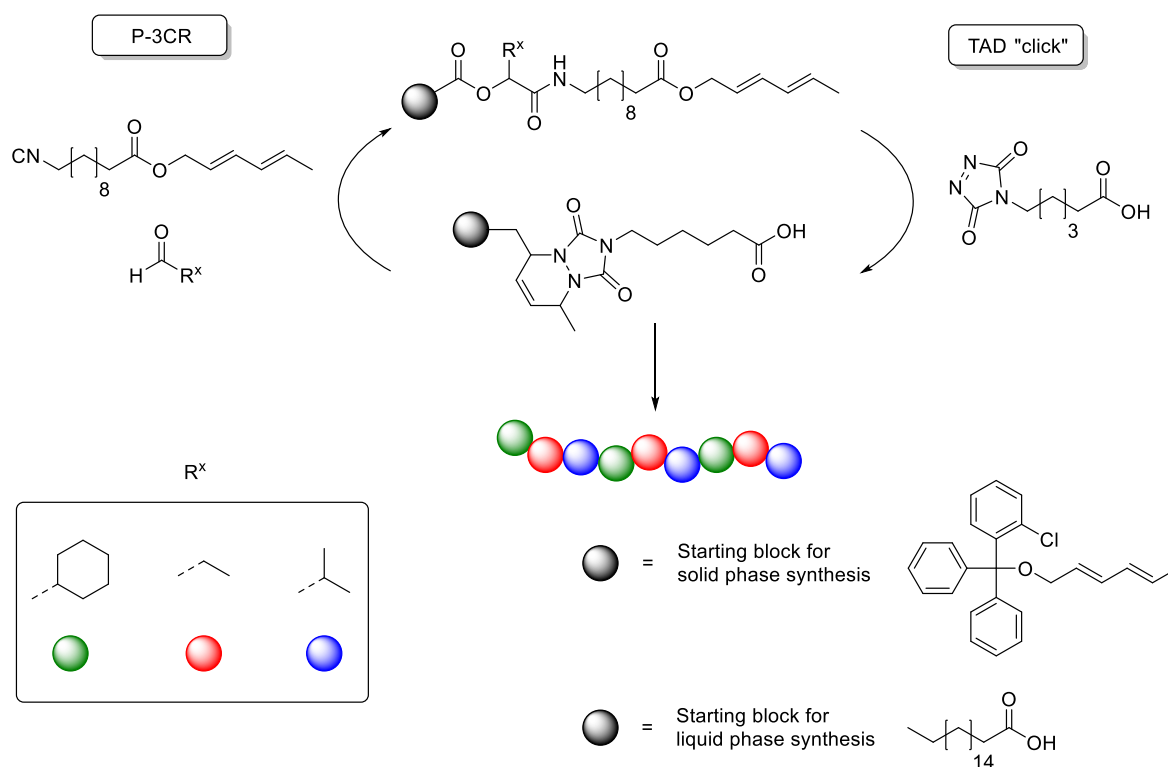


*Scheme 23: Iterative two-step reaction cycle comprising the P-3CR and a deprotection step. A monoprotected isocyanide is used as an AB monomer and aldehydes are varied which introduces a sequence.<sup>[134]</sup>*

This approach has been exploited in the last decade for the synthesis of various sequence-defined macromolecules especially for data storage, but also combinations of MCR with thiolactone chemistry, click chemistry or photochemistry have been investigated.<sup>[135,141,147]</sup>

In 2017, Meier and Du Prez reported on an approach which combined the P-3CR and thiol-ene addition with the aminolysis of a thiolactone and thia-Michael addition.<sup>[135]</sup> For the first time two different approaches of sequence-definition were combined and macromolecules with up to 15 individually selectable side chains were obtained in gram scale. In another joined project of the two groups, the synthesis of sequence-defined oligomers on solid phase and in solution were compared.<sup>[141]</sup> For the approach, the P-3CR was combined with 1,2,4-triazoline-3,5-dione (TAD) “click” reaction (*cf.* Scheme 24). Two linker molecules were synthesized, one bearing an isocyanide and a diene and the other with a TAD and a carboxylic acid moiety. The synthesis in solution started with

stearic acid, which was reacted in a P-3CR with the first linker molecule and an aldehyde. Subsequently, the diene of the Passerini product reacted with the TAD functionality of the second linker molecule in a Diels-Alder click reaction. Following the iterative cycle, a sequence-defined nonamer was synthesized. The obtained oligomers were purified *via* column chromatography after each P-3CR and thoroughly analyzed. The synthesis on solid phase proceeded in the same way, however, started with the reaction of the second linker molecule with a functionalized resin, introducing a free carboxylic acid which was then used in the P-3CR. Sequence-defined-oligomers up to a dodecamer were obtained, but only the trimer, nonamer and dodecamer were cleaved from the resin and thoroughly analyzed. In a comparative study, the two approaches on solid phase and in solution were evaluated regarding various parameters. The synthesis in solution offered high purity ( $\geq 99\%$  instead of 84%), on a larger scale (200 mg instead of 50 mg) with a higher overall yield (18% compared to 5%). Synthesis on solid phase was advantageous concerning purification (simple washing steps instead of column chromatography), shorter reaction times for the P-3CR (30-120 min instead of 8-48 h) and as a result shorter overall time (2 days instead of 3 weeks). The successful combination of the P-3CR with the TAD- "click" reaction was demonstrated and the comparison of the syntheses in solution and on solid phase marked several advantages and disadvantages of each method.

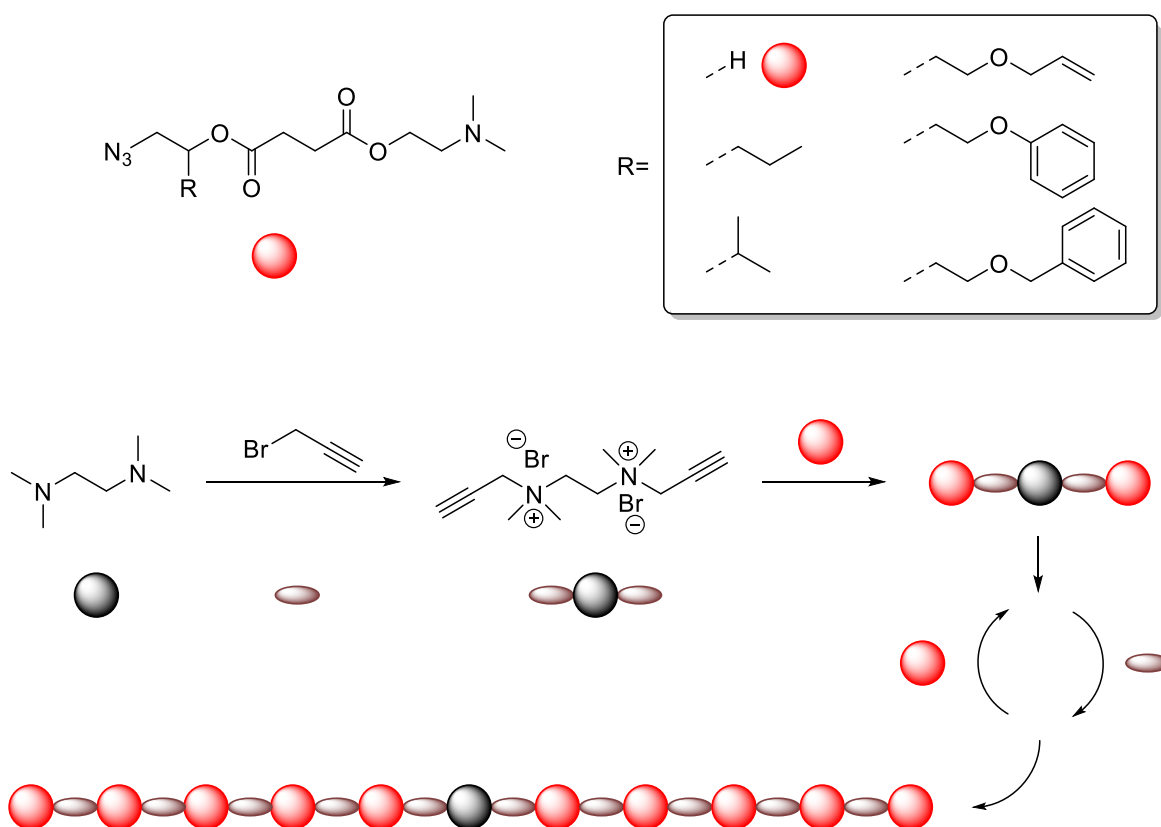


Scheme 24: Iterative two-step reaction cycle which combines the P-3CR and the TAD "click" reaction. Three different aldehydes were used to build up a sequence. The reaction was performed in solution as well as on solid phase and the results were compared.<sup>[141]</sup>

Moreover, the P-3CR was combined with a Diels-Alder reaction of photocaged dienes for the synthesis of sequence-defined macromolecules in a bidirectional approach.<sup>[147]</sup> Therefore, a linker molecule with an isocyanide and a maleimide was synthesized which was reacted in a P-3CR with sebacic acid as a bidirectional starting block and an aldehyde. Subsequently, the maleimide function reacted with a second linker, which exhibits a photocaged diene ( $\alpha$ -methyl benzaldehyde) and a carboxylic acid moiety, in a Diels-Alder reaction. Introduction of the free carboxylic acids enabled further P-3CR.

However, most of the described approaches rely on column chromatography for purification. Despite this purification method being highly time consuming, column chromatography is often necessary to obtain pure sequence-defined macromolecules. In 2019, Gao reported the scalable synthesis of positively charged sequence-defined functional polymers (*cf.* Scheme 25).<sup>[148]</sup> The bidirectional approach was carried out in solution and features a much simpler purification protocol of precipitation and centrifugation. The applied two-step iterative cycle consists of a Menshutkin reaction, which introduces a positive charge to the

backbone, and the copper catalyzed azide alkyne cycloaddition (CuAAC). Repeating the two steps, uniform and sequence-defined macromolecules were obtained. The yields remained high over all steps and excellent purity was confirmed *via* NMR spectroscopy, SEC, and matrix-assisted laser desorption ionization-time of flight (MALDI-ToF) experiments. Six linker molecules with different side chain substitutions were synthesized and used to build up sequence-defined macromolecules in a bidirectional as well as linear fashion. Due to the positively charged backbone, the sequence-defined macromolecules are water soluble and can interact with negatively charged DNA, enabling a controllable effect in bioapplications, like gene transfection or drug delivery.<sup>[149]</sup>

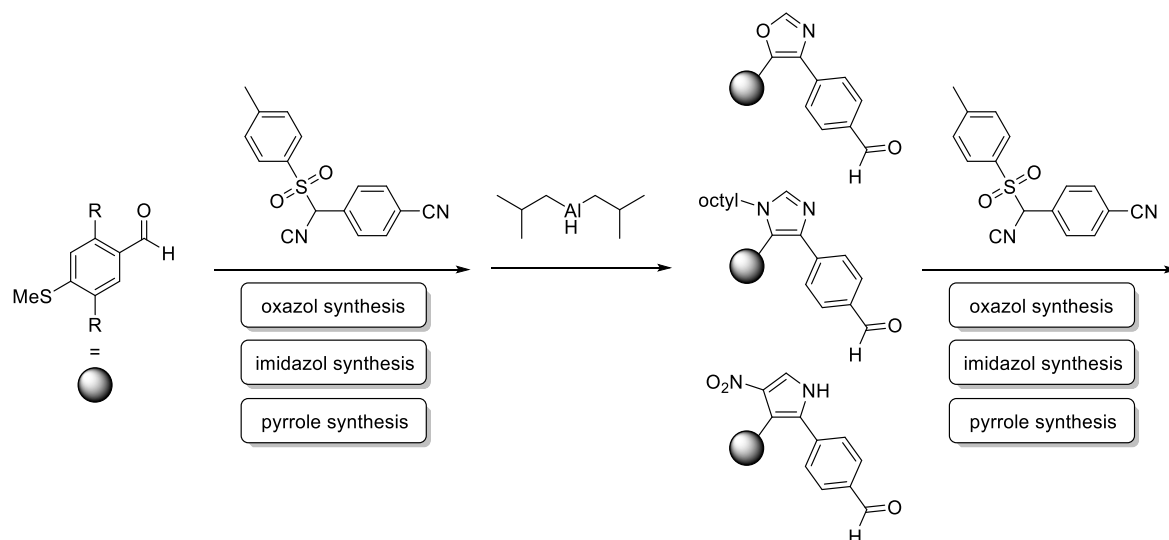


*Scheme 25: Bidirectional synthesis towards positively charged sequence-defined oligomers. The positively charged quaternary ammonium group in the backbone enables purification by precipitation and centrifugation.*<sup>[148]</sup>

### 2.2.2 Conjugated sequence-defined macromolecules

While non-conjugated sequence-defined macromolecules are mainly investigated for application in data storage, the field of conjugated sequence-defined macromolecules focuses on the investigation of structure-property-relationships, i.e. how the structure affects the properties of the macromolecule, and the transfer of the gained knowledge to their polymeric analogous. However, conjugated macromolecules are limited to certain structures to maintain a  $\pi$ -conjugated backbone. As already discussed in chapters 2.1 and 2.2, conjugated oligomers, like oligo(diacetylene)s, oligo(para phenylene)s and oligo(fluorene)s, OPVs, and OPEs are often synthesized using cross-coupling reactions.

However, also other reactions are employed in the synthesis of sequence-defined oligomers. A recent example was published by Schroeder *et al.* who studied the charge transport in sequence-defined oligomers.<sup>[21]</sup> They prepared a series of sequence-defined oligomers in an iterative approach using the van Leusen reaction and reduction of a nitrile with diisobutylaluminium hydride (DIBAL-H). Therefore, a monomer equipped with an isocyanide, a tosyl and a nitrile group, and a nitrile group was prepared. This monomer reacts with an aldehyde in a van Leusen reaction generating a heterocycle (oxazole, imidazole or nitro substituted pyrrole), which connects two phenyl rings. Subsequently, DIBAL-H is used to reduce the nitrile group to an aldehyde, which enables further coupling. Following the two-step reaction procedure, sequence-defined oligomers ranging from dimers to heptamers were prepared. Analysis of their molecular conductance revealed that the charge transport depends on the primary sequence of monomers. Molecular geometry and steric interaction, which are influenced by the choice of sequence, are important factors when it comes to sequence-depending properties.

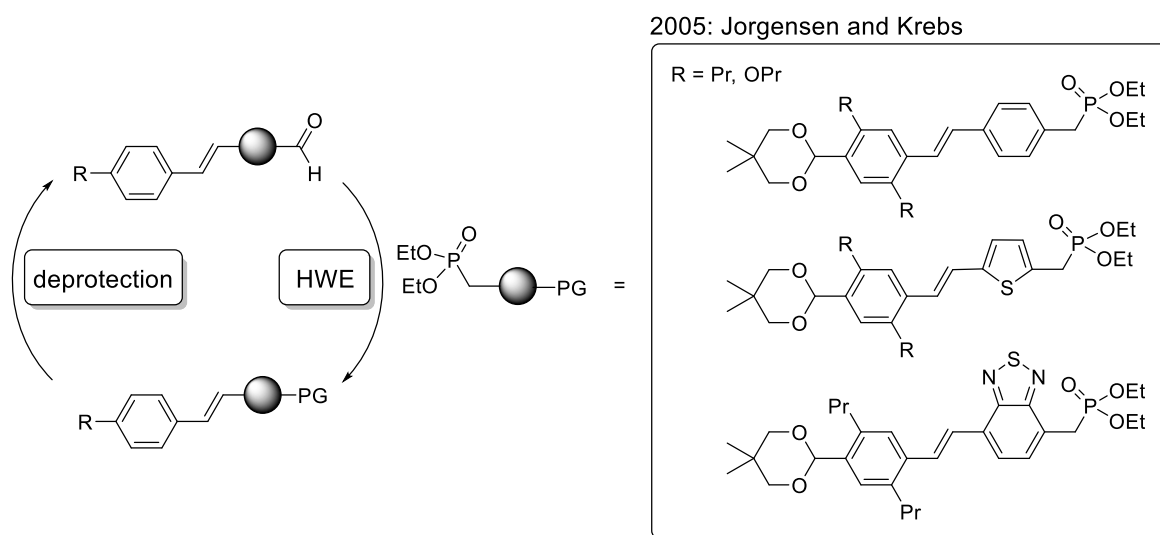


Scheme 26: Iterative synthesis concept towards sequence-defined oligomers. Three different heterocycles are generated by varying the reaction conditions in each cycle to achieve sequence-definition.<sup>[21]</sup>

Furthermore, sequence-defined macromolecules were synthesized *via* cross-metathesis. In 2010, Meyer *et al.* published an iterative stepwise approach towards OPVs based on cross-metathesis followed by a Wittig olefination.<sup>[150]</sup> Initially, 2,5-bis(hexyloxy)-4-iodostyrene, which served as starting molecule, was reacted with 4-vinylbenzaldehyde. Subsequent Wittig olefination using the aldehyde group restored the vinyl group. Then, 2,5-(hexyloxy)-4-vinyl benzaldehyde was used in a further cross-metathesis reaction. Alternation of the substituted and the unsubstituted vinyl benzaldehydes was beneficial to avoid self-metathesis. Repeating the two-step iterative cycle, an alternating pentamer was obtained with an overall yield of 21%. The oligomer was then attached to a chromophore in a Suzuki coupling and, after a final Wittig olefination, used in an acyclic diene metathesis polymerization (ADMET).

Another approach towards sequence-defined OPVs was published by Jørgensen and Krebs in 2004.<sup>[151]</sup> They combined the HWE reaction with subsequent acetal deprotection (*cf.* Scheme 27). A monomer with a methyl phosphonate ester group on one end and an acetal protected aldehyde on the other end of a stilbene core was prepared. The two-step iterative cycle then proceeds *via* reaction of the aldehyde terminated OPV with the monomer and subsequent deprotection of the acetal. A series of OPVs ranging from three to seven phenylene vinylene units was obtained. After end-group functionalization with electron-donating and electron-accepting substituent the OPVs were used in photovoltaic cells. In 2005, Jørgensen

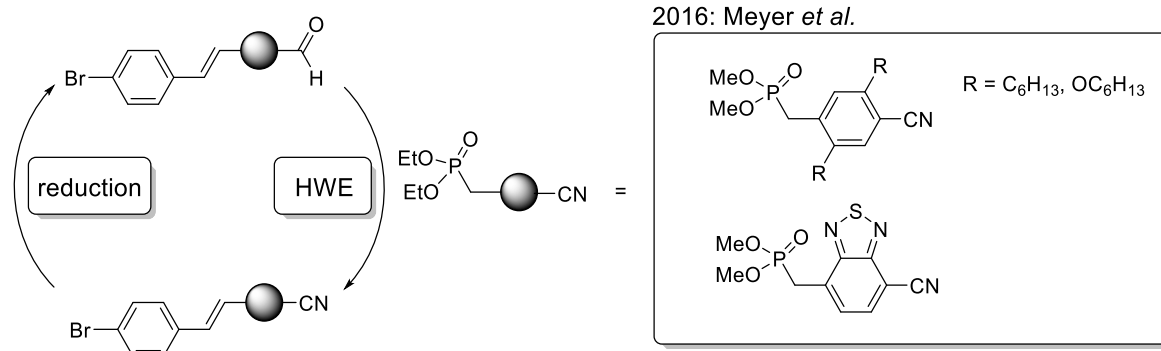
and Krebs extended the scope of their approach by the introduction of four new monomers.<sup>[152]</sup> Two monomers were still based on stilbene, but with propyl or propoxy side chain substitution. The other two monomers were styrylthiophene and styrylbenzothiadiazole with propyl side chains on the phenyl ring. All monomers were used to synthesize the first reported sequence-defined OPV. The obtained materials were again used in photovoltaic cells.



Scheme 27: Left: Iterative two-step reaction cycle towards sequence-defined OPVs. The HWE reaction is combined with a deprotection. Right: monomers based on stilbene core which were used to synthesize the first sequence-defined OPV.<sup>[151,152]</sup>

A similar approach was reported by Meyer *et al.* in 2013.<sup>[153]</sup> They applied the HWE reaction as well, however, used a nitrile group instead of an acetal to improve *E:Z* selectivity in the HWE reaction of an electron poor unsubstituted phenylene vinylene with an electron-rich dialkoxy substituted phenylene vinylene (*cf.* Scheme 28). The nitrile was then reduced with DIBAL-H to an aldehyde, which enabled further coupling. Several OPVs with different sequences were prepared and characterized, indicating that optical, thermal, and electronical properties are modulated by the sequence. In 2016, a benzothiadiazole monomer was introduced by the same group. Two dimers were synthesized, one with the benzothiadiazole in the center and one with the benzothiadiazole at the end of the oligomer.<sup>[154]</sup> The two dimers were compared with their polydisperse polymer analogous. It was found that the electrochemical properties of the dimers are similar to the polymer counterparts suggesting that oligomers can be used as model compounds. Further investigation in this field was published by Meyer *et al.* in 2017.<sup>[155]</sup> This time, four sequence-

defined tetramers were prepared from phenylene and benzothiadiazole monomers by the above-mentioned approach of HWE reaction and reduction of a nitrile group with DIBAL-H to the respective aldehyde. Again, it was demonstrated that the properties are sequence dependent and tuning of optoelectronic properties and photovoltaic performance can be achieved by sequence-definition.

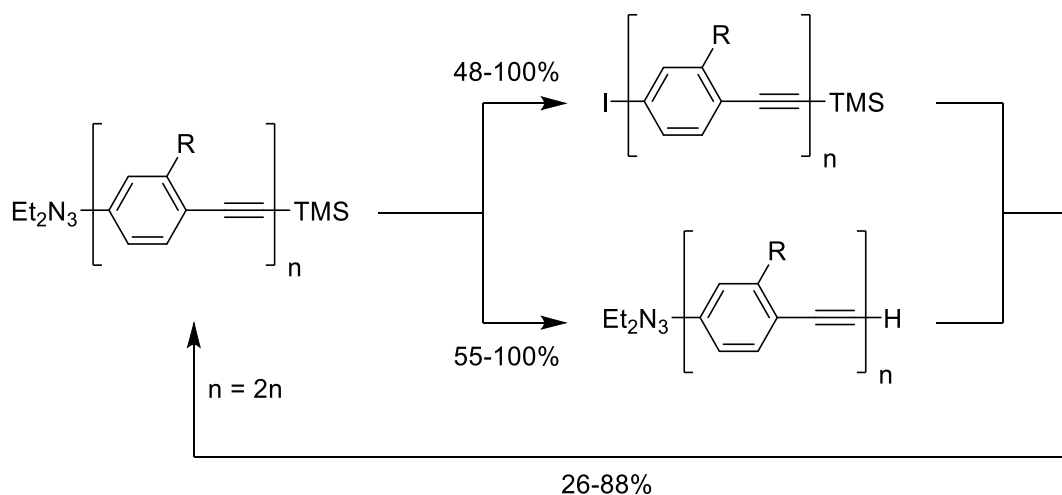


Scheme 28: Left: Iterative two-step reaction cycle towards sequence-defined OPVs using the HWE reaction and subsequent reduction of a nitrile. Right: monomers which were used for the synthesis of sequence-defined OPVs by Meyer *et al.*<sup>[153–155]</sup>

Two other unique classes of conjugated sequence-defined macromolecules are OPEs and oligo(arylene ethynylene)s (OAEs). They are discussed in terms of molecular electronics, due to the stiff and conjugated backbone. As already mentioned in chapter 2.1.1, OPEs are mainly synthesized *via* Sonogashira coupling.

One of the first IEG approaches towards OPEs was published by the group of Tour in 1994 and is depicted in Scheme 29.<sup>[156]</sup> The starting compound is based on phenylacetylene with a diethyltriazene moiety and a TMS protected triple bond. Two starting compounds with different side chains (ethyl and 3-ethylheptyl) were synthesized. For the IEG of the OPEs, the starting compound is split into two parts. In one part, the diethyltriazene is converted with methyl iodide to the respective iodine moiety. In the other part, the TMS protecting group is cleaved forming a terminal triple bond. Combination of the two parts in a Sonogashira coupling yielded the respective orthogonal protected oligomer. Following the steps of splitting up, activation or deprotection and Sonogashira, coupling results in a fast-growing oligomer since the degree of polymerization is doubled in each step. After twelve steps, an oligomer with 16 phenyl rings connected by triple bonds and carrying 3-ethylheptyl side chains was obtained. Due to solubility issues, the corresponding oligomer with ethyl side chains was only synthesized until the octamer stage. Three

years later, the same approach was published, but with improved results.<sup>[7]</sup> Another starting compound with better solubilizing dodecyl side chains was synthesized. The oligomers were purified by column chromatography, however, difficulties for the separation of a 16-mer from an 8-mer were mentioned. Furthermore, the procedure was transferred to solid phase synthesis.

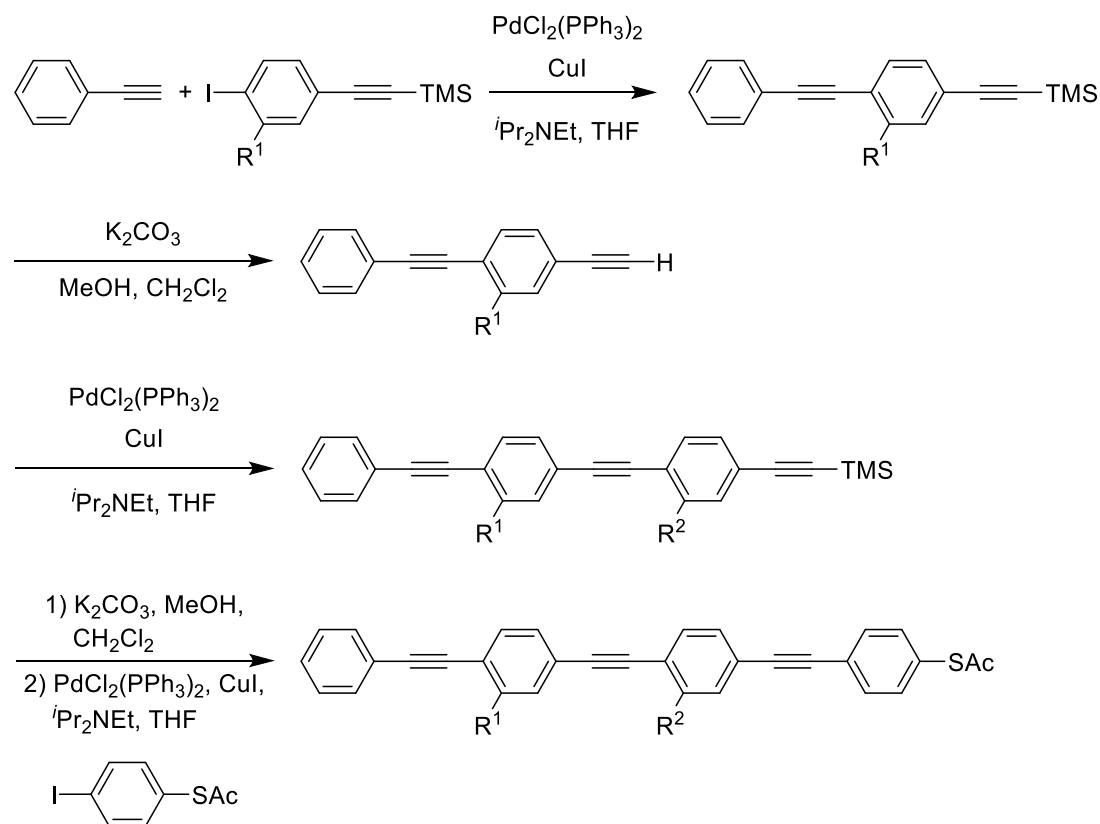


Scheme 29: IEG approach towards OPEs. Orthogonal deprotection and subsequent combination yielded a fast growing OPE.<sup>[156]</sup>

In 1999, the same group reported on a rapid bidirectional synthesis of OPEs.<sup>[157]</sup> They used 1,4-didodecyl-2,5-diiodobenzene as a bifunctional core molecule. In a first step of the iterative cycle, the core molecule was reacted with TMS acetylene. The TMS group was cleaved, and the terminal alkyne used in a Sonogashira coupling with two equivalents of 1-bromo-4-iodobenzene. By repeating the cycle, an oligomer with seven aromatic rings was obtained. Solubility problems were mentioned, since only the core molecule exhibits solubilizing side chains.

After publishing the synthesis of OPEs via IEG and bidirectional growth, Tour *et al.* reported also a linear approach towards OPEs in 2002.<sup>[75]</sup> For their combinatorial synthesis an iterative procedure was applied. Five building units bearing both an iodine moiety and a TMS protected triple bond with different electron-donating or electron-accepting side chains were prepared and used to build-up sequence-defined trimers for the first time. An initial Sonogashira coupling of a building unit with phenyl acetylene yielded the protected monomer. Subsequent deprotection of the TMS group enabled further Sonogashira coupling with another building unit. Since one building unit is added after the other, this stepwise procedure offers high control over the sequence. Following the iterative cycle, 24 different sequence-

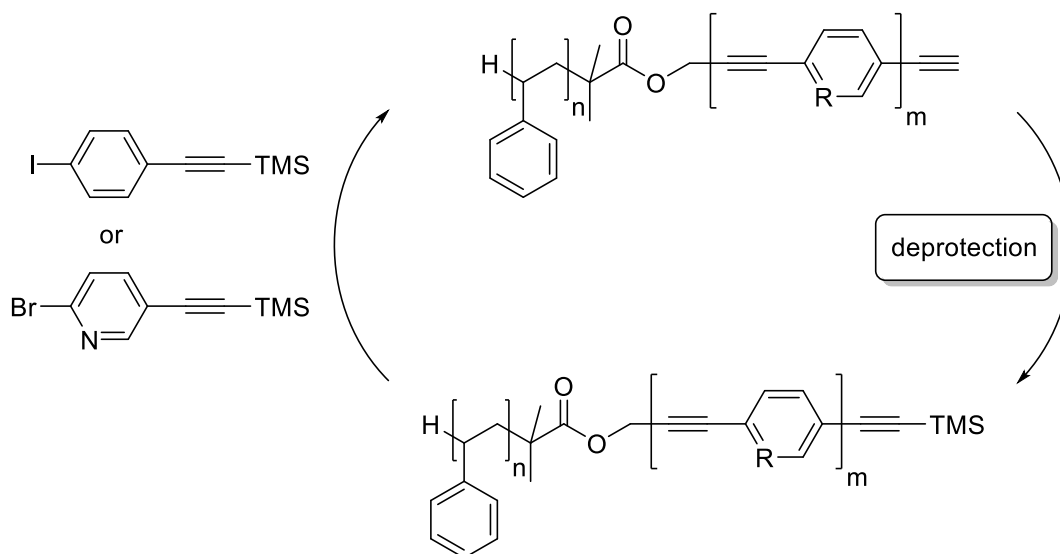
defined trimers were obtained. Similar to the IEG approach of Tour *et al.*, the linear procedure was transferred to synthesis on solid phase which facilitated purification.



Scheme 30: Top: two-step synthesis of the building unit bearing an iodine moiety and a TMS protected triple bond. Bottom: Iterative synthesis towards a sequence-defined OPE based on Sonogashira coupling and subsequent deprotection.<sup>[75]</sup>

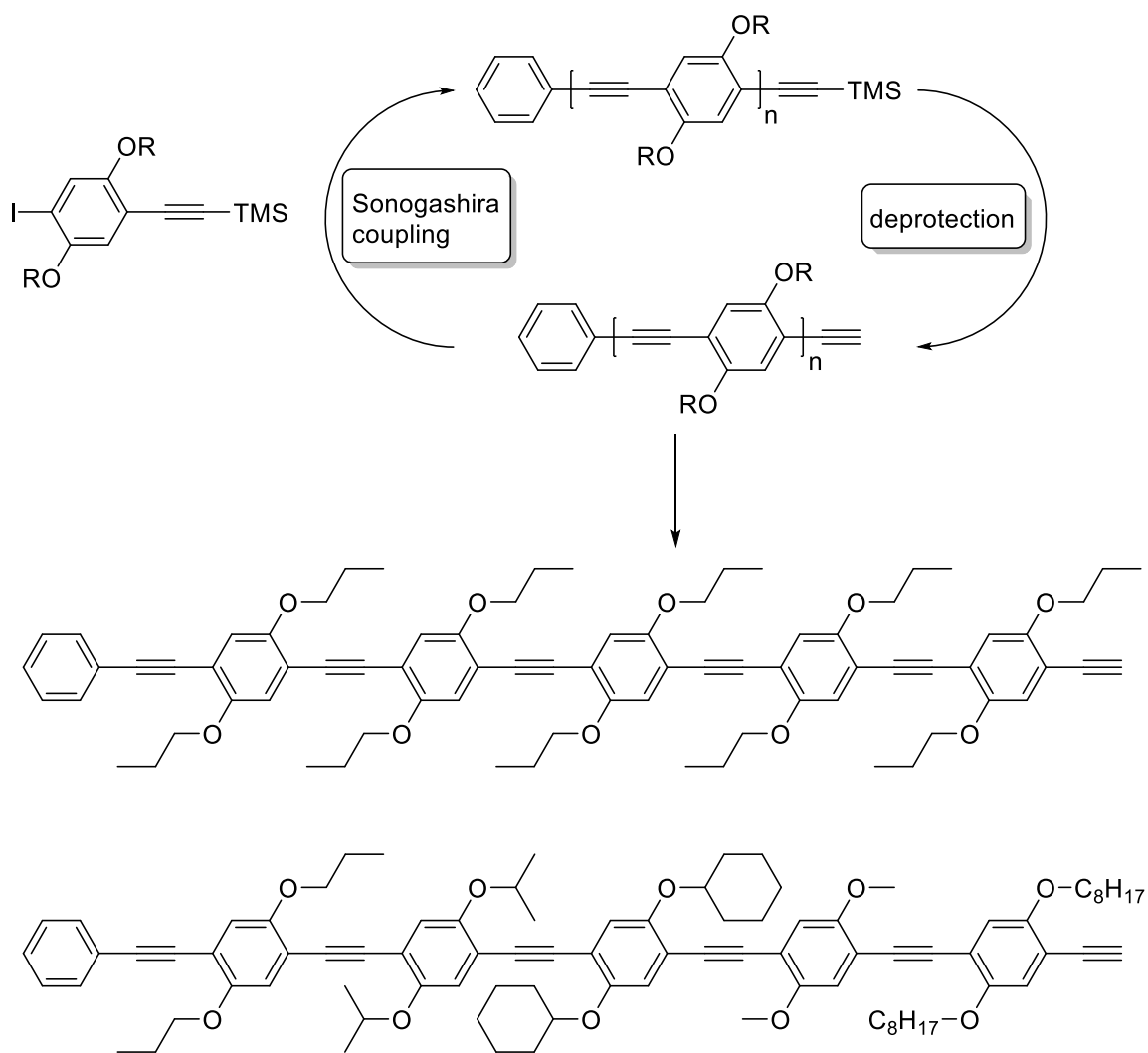
The approach of Tour *et al.* which combined the Sonogashira reaction and subsequent deprotection, was not only used for the synthesis of sequence-defined OPEs, but also for OAEs. However, a common problem when synthesizing rod-like macromolecules is the solubility. Especially the strong tendency of self-aggregation of unfunctionalized OAEs makes the synthesis difficult. In 2017, Lutz *et al.* reported on the synthesis of OAEs using a soluble polymer support.<sup>[158]</sup> A tailored polystyrene soluble support was synthesized first using atom transfer radical polymerization (ATRP) and post-polymerization modification. The polymer support was functionalized with a terminal acetylene enabling the first Sonogashira coupling of a building unit to the soluble polystyrene support. Two building units with either a phenyl or a pyridine core were used. As in the approach from Tour *et al.* the building units exhibit an iodine moiety and a TMS protected triple bond. Alternating reactions of Sonogashira coupling and deprotection of the TMS protected triple bond yielded

sequence-defined oligomers up to tetramers which were still soluble in a variety of organic solvents, thus enabling characterization by NMR spectroscopy, SEC, IR spectroscopy, UV/VIS and fluorescence spectroscopy.



Scheme 31: Iterative two-step reaction cycle towards sequence-defined OAEs. The synthesis was performed on a soluble polymer support.<sup>[158]</sup>

Another approach towards sequence-defined OPEs in solution was published by Meier *et al.* in 2018.<sup>[16]</sup> The synthesis is based on the approach of Tour *et al.* and involves a Sonogashira coupling and a deprotection step. First, a pentamer with only propoxy side chains was synthesized and served as role model. Then, the procedure was extended and a sequence-defined pentamer with five different side chains was prepared. The building units were based on TMS-protected 4-iodoacetylenes bearing different side chains (propoxy, isopropoxy, cyclohexyloxy, methoxy, and octyloxy). Besides the synthesis of a sequence-defined pentamer, three trimers with a 9H-fluorene building unit at predefined positions were synthesized. All intermediates were purified *via* column chromatography and completely characterized. Narrow distribution in the depicted SEC traces confirmed the high purity of each sequence-defined oligomer. The trimers with predefined positions of a fluorene unit exhibit only small differences in their photophysical properties, however, the sequence had an impact on the thermal properties. It is further suggested that iterative synthesis procedures could be used to obtain further sequence-defined macromolecules to investigate and understand structure-property-relationships.



*Scheme 32: Iterative two-step synthesis based on Sonogashira coupling and subsequent deprotection. The strategy was established using the same building unit. Then, five different building units were used to synthesise a sequence-defined pentamer.<sup>[16, 159]</sup>*

### 3 Motivation

This thesis started within the Cooperative Research Centre 1176 “Molecular Structuring of Soft Matter” as a part of project A4 “Tailor-made sequence-controlled polymer-dye conjugates for controlling exciton dynamics”. The main objective of this subproject was the synthesis of sequence-defined oligomers with precisely positioned units with electron accepting and electron donating properties. The oligomers were subsequently connected to dyes with thermally activated delayed fluorescence (TADF) function and investigated in terms of exciton dynamics and structure-property relationships.<sup>[16,160]</sup>

The sequence-defined oligomers in this project are based on OPEs. To achieve the sequence definition, an iterative linear synthesis strategy is applied. There were only a few examples for sequence-defined conjugated oligomers and most of them used the same building units and synthesis approach. Although these molecules exhibit uniform size, they are not sequence-defined in the sense of exhibiting different side chains. The established two-step synthesis strategy for the rod-like oligomers consists of a Sonogashira coupling followed by deprotection of a TMS protected triple bond.<sup>[16,75]</sup> The resulting terminal triple bond can then proceed further in the iterative cycle.

However, a major problem, which occurred during the synthesis of the sequence-defined oligomers, was the formation of a homocoupling product *via* Glaser coupling. This is unfavorable in two ways: on the one hand, the yield decreases since two terminal triple bonds couple with each other and are therefore not available for the Sonogashira coupling anymore. On the other hand, purification complicates since the homocoupling product, and the sequence-defined oligomer exhibit a similar polarity. Thus, carefully performed column chromatography is inevitable for the isolation of the sequence-defined oligomers.<sup>[159]</sup>

The aim of this thesis is therefore to improve the synthesis of these sequence-defined oligomers. The main focus is set on the suppression of a homocoupling product, which would facilitate purification consequently. However, to obtain uniform oligomers, column chromatography is unavoidable. The improved strategy should still feature a synthesis in solution to give the opportunity for large scales. Additionally, the oligomers should be built up in an iterative stepwise fashion

to enable sequence-definition. The reactions chosen for the iterative cycle are meant to have high yields. During the stepwise synthesis, suitable characterization methods need to be applied to ensure the successful formation of the oligomers. Adjustment of the building units might be necessary. However, precursors with electron donating, such as dialkoxybenzenes, or electron accepting properties, such as benzothiadiazole derivatives, are still preferable to investigate structure-property-relationships.

## 4 Results and Discussion

In the following chapters, the results of this thesis are presented and discussed. The first section focuses on characterization of uniform macromolecules and shows advantages as well as limits of three different analyzing methods (NMR spectroscopy, SEC and mass spectrometry). The second section presents the development of an alternative synthesis strategy towards sequence-defined uniform OPEs based on a decarboxylative coupling reaction. The developed synthesis strategy is then compared to the established Sonogashira approach in the next section. In the last section, the application of the obtained OPEs in MCRs is discussed.

### 4.1 Analyzing uniform Macromolecules

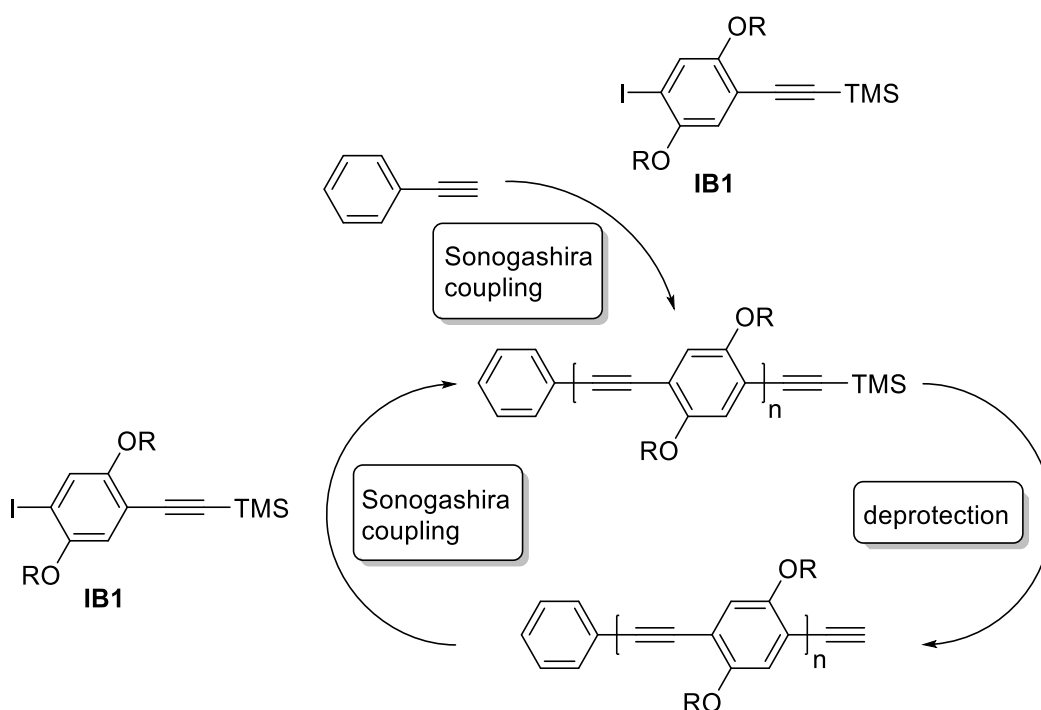
*Abstract:*

*Determination of the uniformity of macromolecules is challenging. To demonstrate the necessity of a combination of different analyzing methods, an impurity study was performed. For this purpose, a sequence-defined tetramer was contaminated with different wt% amounts of the corresponding sequence-defined trimer. The sequence-defined tetramer and the respective trimer were synthesized via an established iterative stepwise approach consisting of a Sonogashira coupling and a subsequent deprotection of a trimethylsilyl protected triple bond. After full characterization of the tetramer and the trimer, respectively, the trimer was added in different wt% amounts to the tetramer and the mixtures were analyzed by  $^1\text{H}$  NMR spectroscopy, MS, and SEC. Detection of the impurity via  $^1\text{H}$  NMR was not possible, since the signals overlapped, and the integrals did not change. If the impurity is known, 1 wt% impurity is detectable via MS. In SEC impurities of 1 wt% were also detected.*

## 4.1.1 Synthesis

The molecules used for this study were synthesized by Dr. Rebekka Schneider during her PhD studies in our group.<sup>[159]</sup> Preparation of the samples and interpretation of the received data was performed by Daniel Hahn in a collaboration with Dr. Maximiliane Frölich and Philipp Bohn.

For this study, sequence-defined OPEs, which were synthesized *via* an well-established iterative stepwise approach, were used.<sup>[16,75,157]</sup> The iterative two-step cycle, consisting of a Sonogashira coupling followed by a deprotection of a TMS protected triple bond, is depicted in Scheme 33.



Scheme 33: Iterative two-step approach consisting of Sonogashira coupling and subsequent deprotection of a TMS protected triple bond.<sup>[16]</sup>

The synthesis of the oligomers was reported before and not carried out by the author of this thesis but is described in here for a better understanding.<sup>[16]</sup>

The respective building block **IB1**, bearing an iodine moiety and a TMS protected triple bond, was synthesized in three-step synthesis from hydroquinone with an overall yield of 29% in a 4.26 g scale.

For the synthesis of the tetramer **IO4**, phenyl acetylene was initially reacted with **IB1** to the protected monomer **IO1** in a Sonogashira coupling reaction. After purification *via* column chromatography, **IO1** was obtained with a yield of 99% and high purity.

Cleavage of the TMS protection group proceeded with two equivalents potassium carbonate in a mixture of methanol and dichloromethane. The deprotected monomer **IOD1** was obtained with a yield of 97% after column chromatography and used for the next iterative cycle. After seven steps, the tetramer **IO4** was synthesized with an overall yield of 35%. After each step, the molecules were purified *via* column chromatography and fully characterized by proton and carbon NMR spectroscopy, SEC, IR spectroscopy and MS. In Figure 6, the chemical structure of the tetramer **IO4**, the SEC traces of **IO4** and **IO3** and the high-resolution isotopic pattern obtained by ESI-MS compared to the calculated isotopic pattern of **IO4** are depicted.

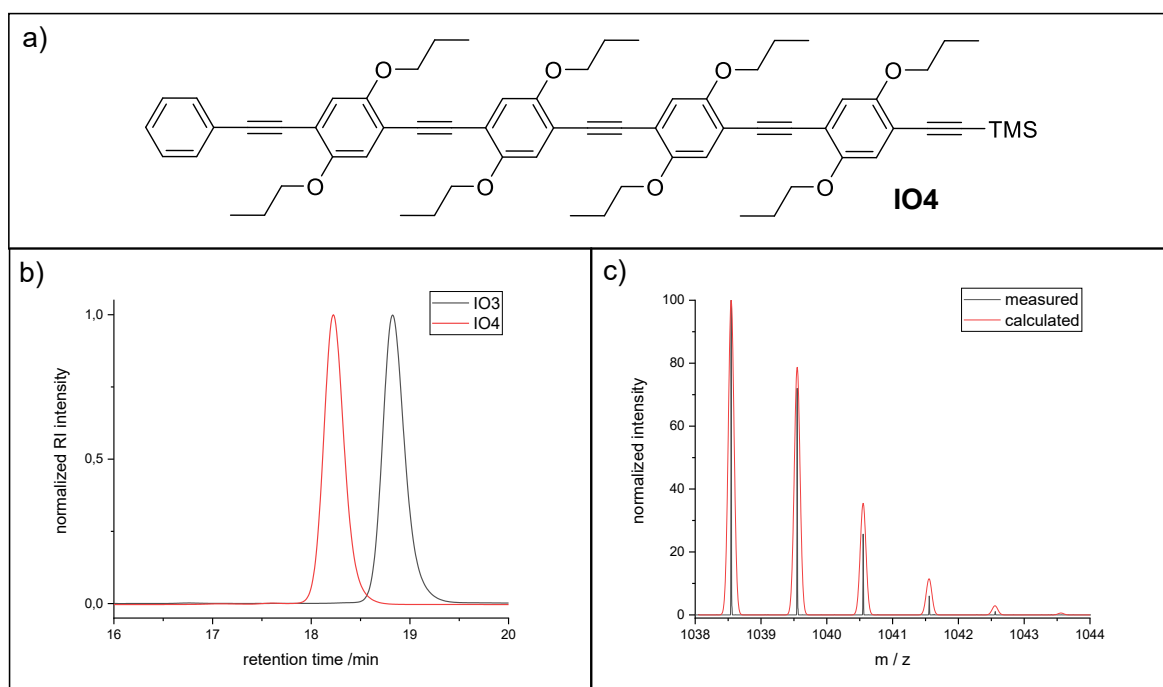


**Figure 6:** Characterization of the sequence-defined tetramer **IO4**. a) chemical structure of the sequence-defined tetramer **IO4**. b) SEC traces of the pure trimer **IO3** (black) and tetramer **IO4** (red). c) Overlay of the calculated isotopic pattern (red) and the measured isotopic pattern (black) obtained from ESI-MS measurement of **IO4**.

In Figure 7, the <sup>1</sup>H NMR spectra of **IO3** and **IO4** are depicted. All signals can be assigned and confirm the successful synthesis. The aromatic signals at 7.53 ppm (a) and 7.34 ppm (b) arise from the phenyl end group and serve as reference, since it remains the same through the whole synthesis. The resonance signal of the aromatic protons of the oligomeric chain is observed at 7.03 ppm (c). The signals at 4.00 ppm (d), 1.87 ppm (e) and 1.08 ppm (f) arise from the solubilizing propoxy side chains. The singlet at 0.26 ppm (g), originating from the TMS protecting group, further indicates the successful synthesis of the respective oligomer.

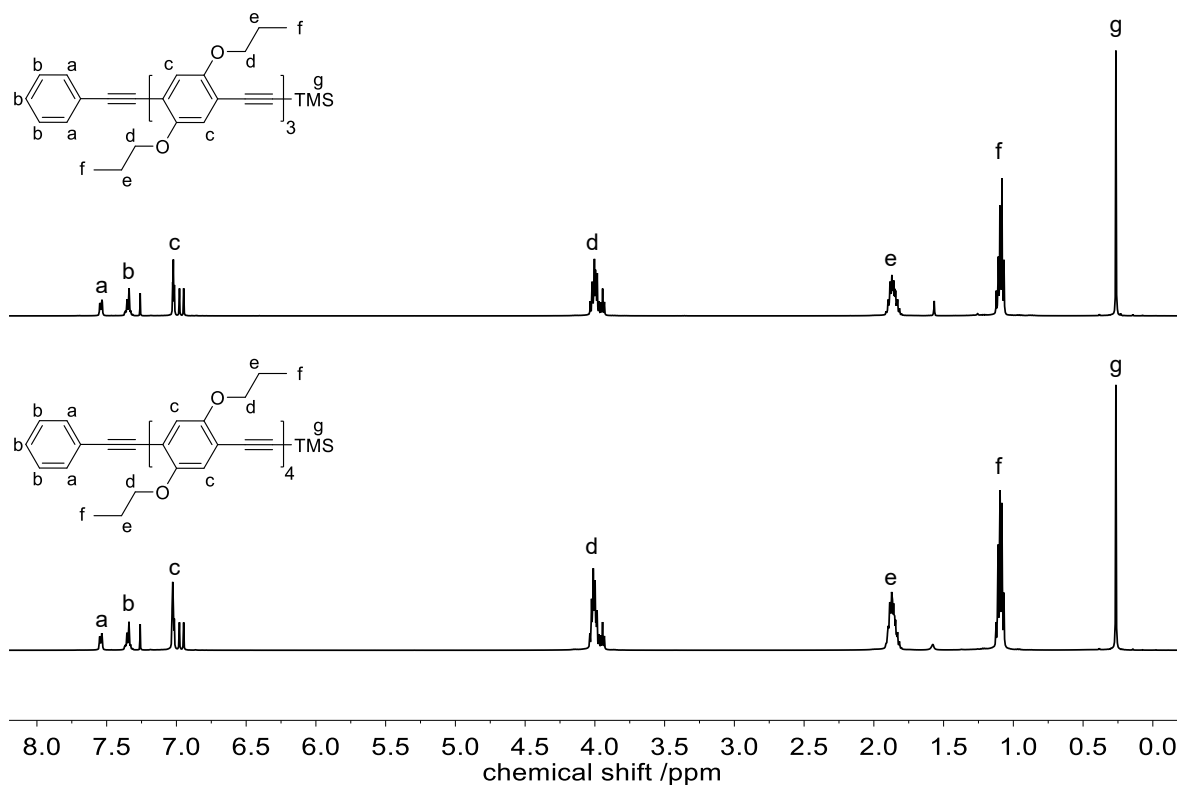


Figure 7: Comparison of the  $^1\text{H}$  NMR spectra of **IO3** (top) and **IO4** (bottom).

Comparison of the  $^1\text{H}$  spectra of **IO3** and **IO4** shows no significant differences in terms of chemical shifts. Although the oligomer is growing by one unit per cycle, the chemical environment changes only marginally and all signals remain in the same ppm range. The integrals of the signals c, d, e, and f increase relative to the signals a and b from the phenyl end group which confirms the growing of the oligomer.

#### 4.1.2 Impurity study

The purity of these highly defined oligomers was analyzed by NMR spectroscopy, SEC, and MS. To demonstrate the necessity of all three methods combined, an impurity study was performed. Chapter 4.1.1 focused on the structure determination *via* NMR spectroscopy. Especially regarding purity, NMR spectroscopy is often not sufficient and other characterization methods become necessary. In particular, the combination of different characterization methods is essential. Furthermore, the importance of liquid chromatography to determine the purity of highly defined macromolecules is highlighted in this chapter.

For the impurity study, a known impurity, here the trimer **IO3**, was added to the tetramer **IO4**. Initially, the pure tetramer **IO4** and the pure trimer **IO3** were individually completely characterized by  $^1\text{H}$  and  $^{13}\text{C}$  NMR spectroscopy, SEC, IR spectroscopy and mass spectrometry. Subsequently, the tetramer **IO4** was contaminated with different amounts of the respective trimer **IO3**. In total, ten different samples with impurities ranging from 1-15 wt% were prepared. The samples were separately analyzed by NMR spectroscopy, SEC and ESI-MS. For NMR spectroscopy, the samples were prepared in a concentration of 20 mg/mL and measured on a 500 MHz spectrometer from Bruker. SEC was measured on a THF-SEC from Shimadzu with oligo columns at 30 °C in a concentration of 2 mg/mL. All samples used for the impurity study and the corresponding results from NMR spectroscopy, MS, and SEC are displayed in Table 2.

Table 2: Summary of the results of the impurity study.

Impurity	Tetramer IO4	Trimer IO3	Detectable in NMR	Detectable in ESI-MS	Detectable in SEC
<b>0 wt%</b>	100%	0%			
<b>1 wt%</b>	99%	1%	✘	✘	✔
<b>2 wt%</b>	98%	2%	✘	✘	✔
<b>3 wt%</b>	97%	3%	✘	✘	✔
<b>4 wt%</b>	96%	4%	✘	✔	✔
<b>5 wt%</b>	95%	5%	✘	✔	✔
<b>7 wt%</b>	93%	7%	✘	✔	✔
<b>9 wt%</b>	91%	9%	✘	✔	✔
<b>11 wt%</b>	89%	11%	✘	✔	✔
<b>13 wt%</b>	87%	13%	✘	✔	✔
<b>15 wt%</b>	85%	15%	✘	✔	✔
<b>100 wt%</b>	0%	100%			

Analysis by <sup>1</sup>H NMR spectroscopy proved to be challenging. As mentioned before, no significant difference regarding the chemical shifts of the respective oligomers was observed. For structure determination of the oligomers, NMR spectroscopy is a strong and valuable analyzing method, however, evaluation of the oligomer purity is difficult, as discussed. However, the detection of other impurities, like residues of solvents and by-products, remains easy with NMR spectroscopy, if they do not overlap with the oligomer signals. Regarding sequence-defined macromolecules in particular, the main impurities are oligomers of different length originating from

previous stages of the synthesis procedure. Therefore, it was decided to contaminate the tetramer with the trimer so simulate the situation in a certain way. In Figure 8, the NMR spectra of the pure tetramer (0% impurity) and the sample containing 15 wt% impurity of trimer are depicted.

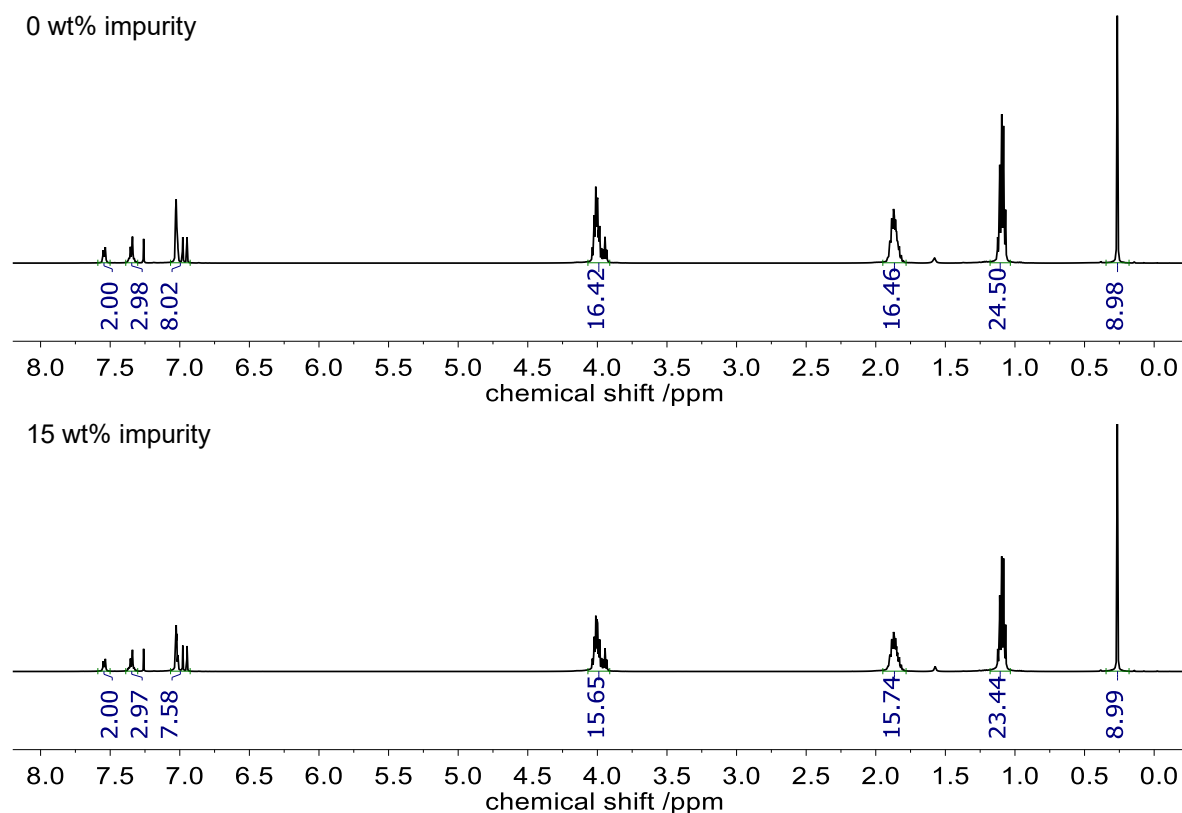


Figure 8: Comparison of the  $^1\text{H}$  NMR spectra of the pure IO4 (top) and the sample with 15% impurity (bottom). All signals arise in the same ppm range and the integrals are not changing.

Even with the highest impurity of 15 wt% in this series, the integrals fit to the structure of the tetramer within the error ranges of NMR spectroscopy. Since no signals are shifting or new signals are arising and the integrals are not significantly changing, determination of the purity is impossible using routine proton NMR spectroscopy. Furthermore, NMR spectroscopy offers a lot of additional two-dimensional measurements, like diffusion ordered NMR spectroscopy (DOSY), which could be used to determine purity. However, in this work, the focus is primary set on standard NMR spectroscopy, as typically performed by synthetic chemists.

Another essential analyzing method is MS. All samples of the impurity series, including the pure tetramer and the pure trimer, were measured by ESI-MS. Analysis of the mass spectra was still challenging for the low wt% samples, since baseline

noises were hindering detection to some extent. In Figure 9, the mass spectra of the 1 wt% impurity sample and a zoom-in from 822-826 m/z are displayed.

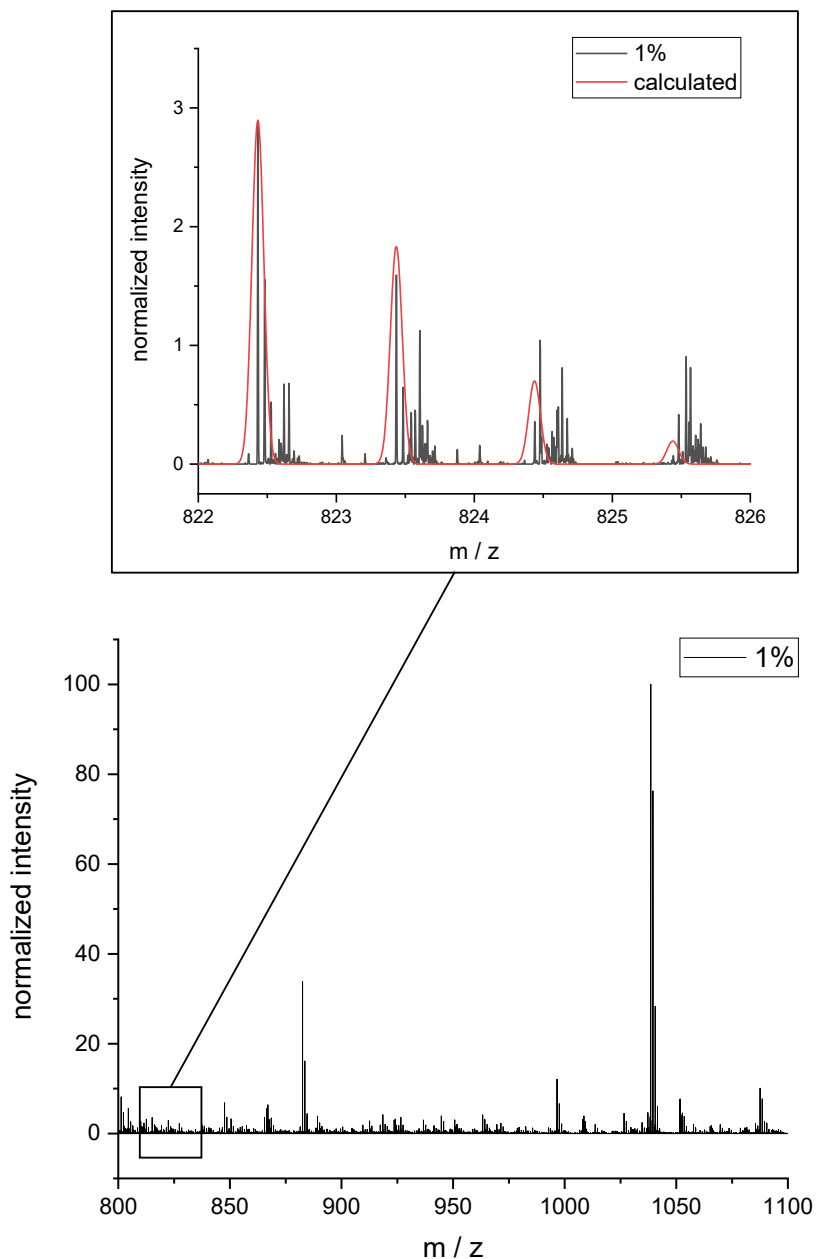


Figure 9: Mass spectrum of the sample with 1 wt% impurity. Subjectively, no impurity is detected. Zoom-in on the respective area reveals the presence of the impurity (IO3) with the respective mass of 822.4317 m/z.

In the sample with 1 wt% sample, the respective mass of the trimer (822.4317 m/z) was observed, however the signals are overlapping with the baseline noise of the measurement. In comparison with the spectra of the pure tetramer, no mass signals of the trimer were present. From an objective point of view, it is only possible to detect 1 wt% impurity in ESI-MS by comparing the two spectra, if the impurity is known and searched for. An even more objective approach would be to determine

a certain threshold, which separates reliable signals from the baseline. This could, for instance, be based on requiring a signal intensity of five times the standard deviation of the baseline signals. From a subjective point of view, 1 wt% impurity is considered not detectable in ESI-MS, since the signal is not clearly distinguishable from the baseline noise (Figure 10, left). Following the subjective approach, only peaks with an intensity of 10% of the main peak were considered, thus, the impurity was observed from 4 wt% and higher in the mass spectrum (Figure 10, right). This example demonstrates that analysis by mass spectrometry is another useful method to investigate the purity of the samples. However, if the impurity is unknown, it remains very challenging to distinguish an impurity signal from the baseline noise. In this case, additional analytical methods are necessary.

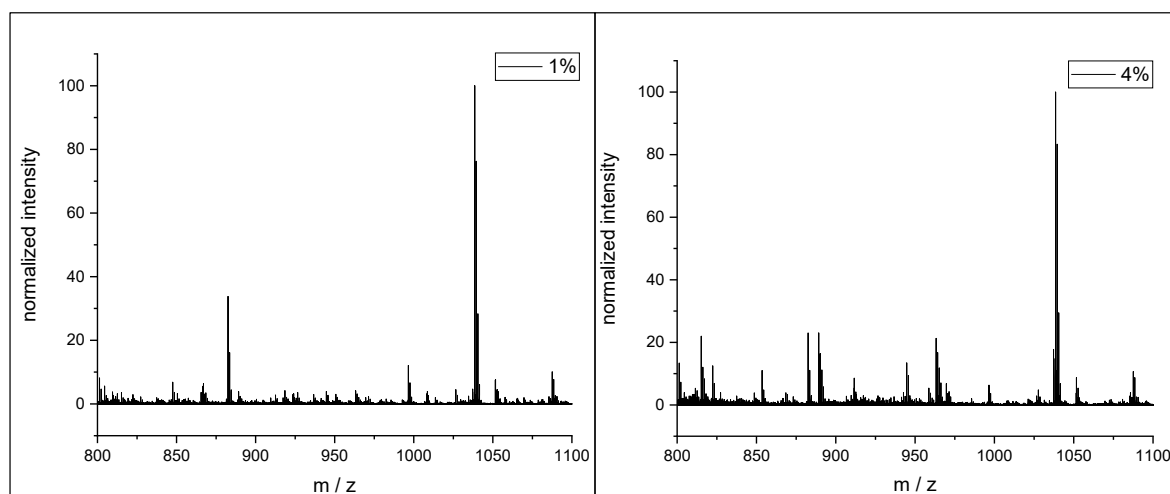


Figure 10: Comparison of the mass spectra of the sample with 1 wt% (left) and 4 wt% (right) impurity.

Furthermore, the samples of the impurity series were analyzed by SEC. In SEC, the molecules are separated depending on their hydrodynamic radius. In general, larger molecules elute faster than smaller molecules. In Figure 6, the SEC traces of the pure tetramer and trimer are depicted. Both show a narrow distribution, which confirms their high purity and uniformity. The SEC traces of the respective mixtures from 1-15 wt% impurity are displayed in Figure 11.

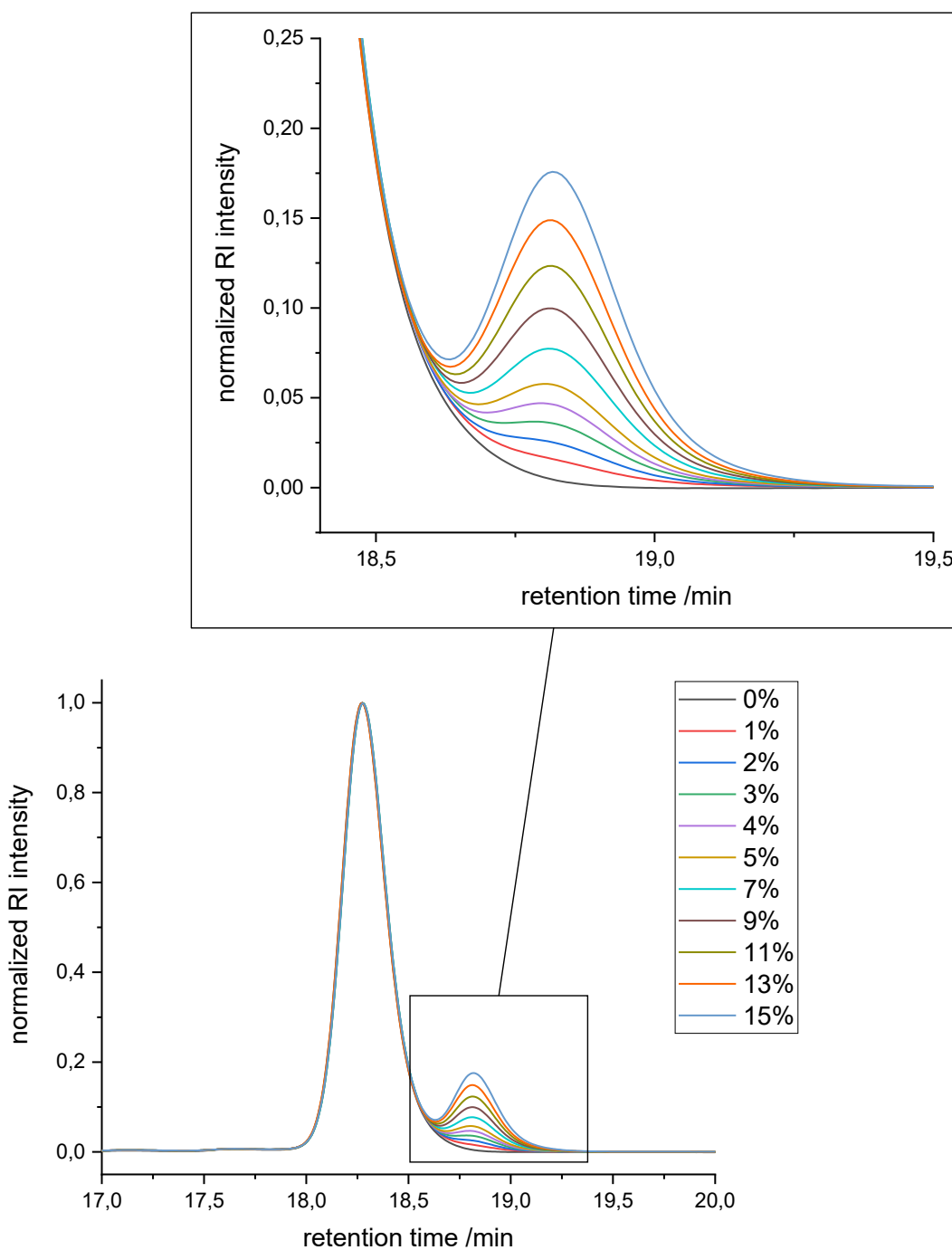


Figure 11: Comparison of the SEC traces of the tetramer **IO4** containing different wt% amounts of impurity.

Detection of the impurity is possible starting from 1 wt% impurity (red curve). Since the molecular weight difference between the tetramer and the trimer is rather big and the molecule is based on a rigid rod-like structure, the hydrodynamic radius increases significantly, hence, the retention times are well separated. For the 1 wt% impurity, a clear shoulder is observed. The intensity of this signal rises for the higher impurities of the series and from the 3 wt% impurity sample onwards, a separated

signal is observed. Hence, SEC is a valuable method to determine the purity and this measurement series demonstrates that SEC is capable to identify an impurity of as low as  $\geq 1$  wt%. Compared to NMR spectroscopy and MS spectrometry, SEC offers the opportunity to detect minimal impurities and is essential when it comes to uniform macromolecules.

#### 4.1.3 Conclusion

In this impurity study, three standard analysis methods, NMR spectroscopy, MS and SEC, were used to evaluate the purity of a uniform OPE tetramer, which was contaminated with different wt% amounts of a known impurity. The respective trimer served as impurity and was added to the tetramer ranging from 1-15 wt%. In a first step, the pure tetramer and trimer were fully characterized, followed by the measurement of the impurity series. Detection of an impurity *via* NMR spectroscopy was not possible, since the signals are in the same ppm range and the integrals do not change. However, NMR spectroscopy is an important analyzing method for structure determination and a first indication of the purity since solvent residues can be detected. Additionally, MS was performed. Impurities from 7 wt% on were clearly visible. Lower wt% impurities were challenging, since they overlapped with the baseline noise. By comparison of the pure tetramer spectrum, impurities of as low as 1 wt% can be detected, if the impurity is known. Analysis *via* SEC proved to be a valuable method for evaluating uniformity. Impurities of as low as 1 wt% were easily observed, and it might be possible to detect even lower impurities in the case of OPEs. In conclusion, the results demonstrate that a complete characterization by different analyzing methods is essential. The combination from NMR spectroscopy, MS, and SEC provides the information to confirm a successful synthesis and a high purity.



## 4.2 Development of a new synthesis strategy

Parts of this chapter and the associated parts in the experimental part have been published before:

D. Hahn, R. V. Schneider, E. Foitzik, M. A. R. Meier, *Macromol. Rapid Commun.* **2021**, 2000735.

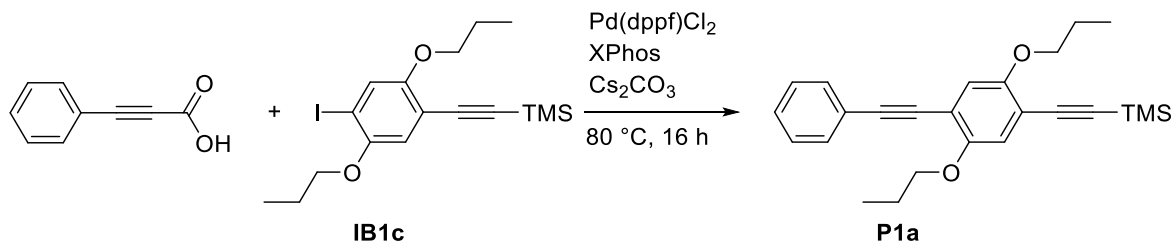
### *Abstract*

*In this chapter, a more practical and efficient synthesis protocol for the preparation of uniform OPEs is presented. The developed iterative reaction cycle features a decarboxylative coupling of an alkynyl carboxylic acid and subsequent saponification of an alkynyl carboxylic ester. To establish the reaction protocol, the same building unit with propoxy side chains is used in every coupling step. A uniform pentamer is obtained after ten steps with 14% overall yield. The copper-free conditions prevent homocoupling until the trimer stage. In case of homocoupling for the syntheses of the tetramer and the pentamer, a simple variation of the work-up procedure yields the uniform oligomers. Furthermore, three different building units and one double building unit are synthesized.*

The decarboxylative coupling is a versatile reaction with a broad substrate scope, as described in chapter 2.1.2. In 2008, Lee *et al.* demonstrated that also alkynyl carboxylic acids can be used in the decarboxylative coupling, giving access to diphenylacetylenes.<sup>[57]</sup> The similarity to the Sonogashira coupling makes the decarboxylative coupling a promising alternative, also for the synthesis of OPEs. Thus, in this thesis, the decarboxylative coupling was evaluated in a first test reaction.

For this test reaction, phenyl propiolic acid, as a starting compound, was coupled with a building unit **IB1c**. The building unit **IB1c** exhibits an iodine moiety as well as a TMS protected triple bond and is typically used in the Sonogashira approach. Propoxy side chains, attached to the benzene core, increased the solubility of the building unit **IB1c**. It was synthesized in three steps from hydroquinone

(cf. Scheme 35) in a previous PhD thesis in our group by Rebekka Schneider.<sup>[159]</sup> In Scheme 34, the test reaction is depicted.



Scheme 34: First test reaction towards OPEs. The commonly used building unit **IB1c** is reacted with phenyl propiolic acid in a decarboxylative coupling to obtain the monomer **P1a**.

The reaction conditions were adopted from Li *et al.* using palladium acetate as catalyst, XPhos as ligand and cesium carbonate as base.<sup>[161]</sup> However, minor changes were applied, for instance, the palladium source was changed from palladium acetate to 1,1'-bis(diphenylphosphino)ferrocene-palladium(II)dichloride (Pd(dppf)Cl<sub>2</sub>). The remaining conditions were adopted, namely XPhos as ligand, cesium carbonate as base and THF as solvent. Phenyl propiolic acid was used in excess of 1.5 equivalents to assure full conversion of the building unit **IB1c**. Thin layer chromatography (TLC) was used to monitor the reaction. After 16 hours, TLC indicated full conversion of the building unit **IB1c** showing one major spot, which was fluorescent under irradiation at 254 nm. The monomer **P1a** was obtained after purification *via* column chromatography with cyclohexane/ethyl acetate in a scale of 490 mg and 93% yield. In Figure 12, the corresponding <sup>1</sup>H NMR spectrum is depicted.

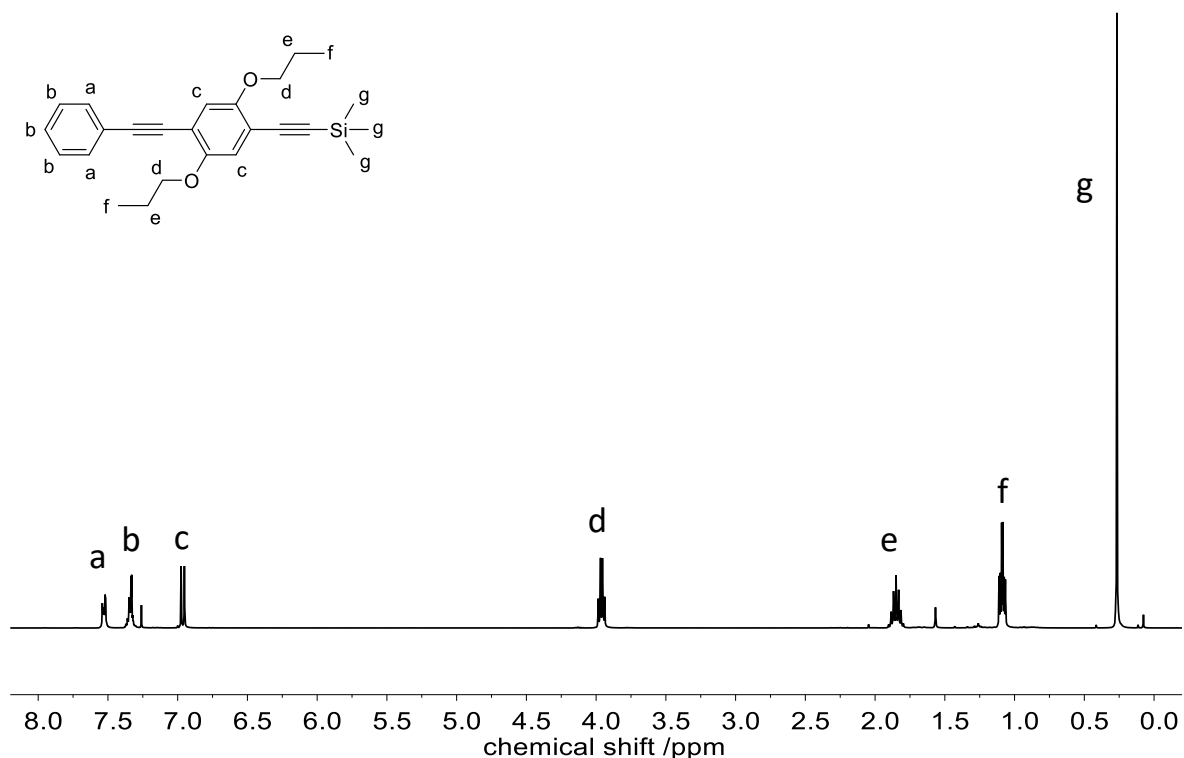


Figure 12:  $^1\text{H}$  NMR spectrum of the monomer **P1a**. The observed chemical shifts are in accordance with the literature.<sup>[16]</sup>

The  $^1\text{H}$  NMR spectrum of **P1a** confirms the successful formation of the coupling product. The respective integrals of the signals are in accordance with the chemical structure and the chemical shifts match the ones reported in the literature.<sup>[16]</sup> It has to be mentioned that the signal at 1.56 ppm originates from water, which is usually present in the deuterated chloroform.<sup>[162]</sup> Although the integrals and chemical shifts fit to the expected structure, further analysis is necessary as demonstrated in chapter 4.1. Therefore, a  $^1\text{H}$  NMR spectrum of the homocoupling product, which is 1,4-diphenylbuta-1,3-diyne in this case, was recorded (Figure 13, black curve) and compared to the NMR spectrum of the monomer (Figure 13, red curve).

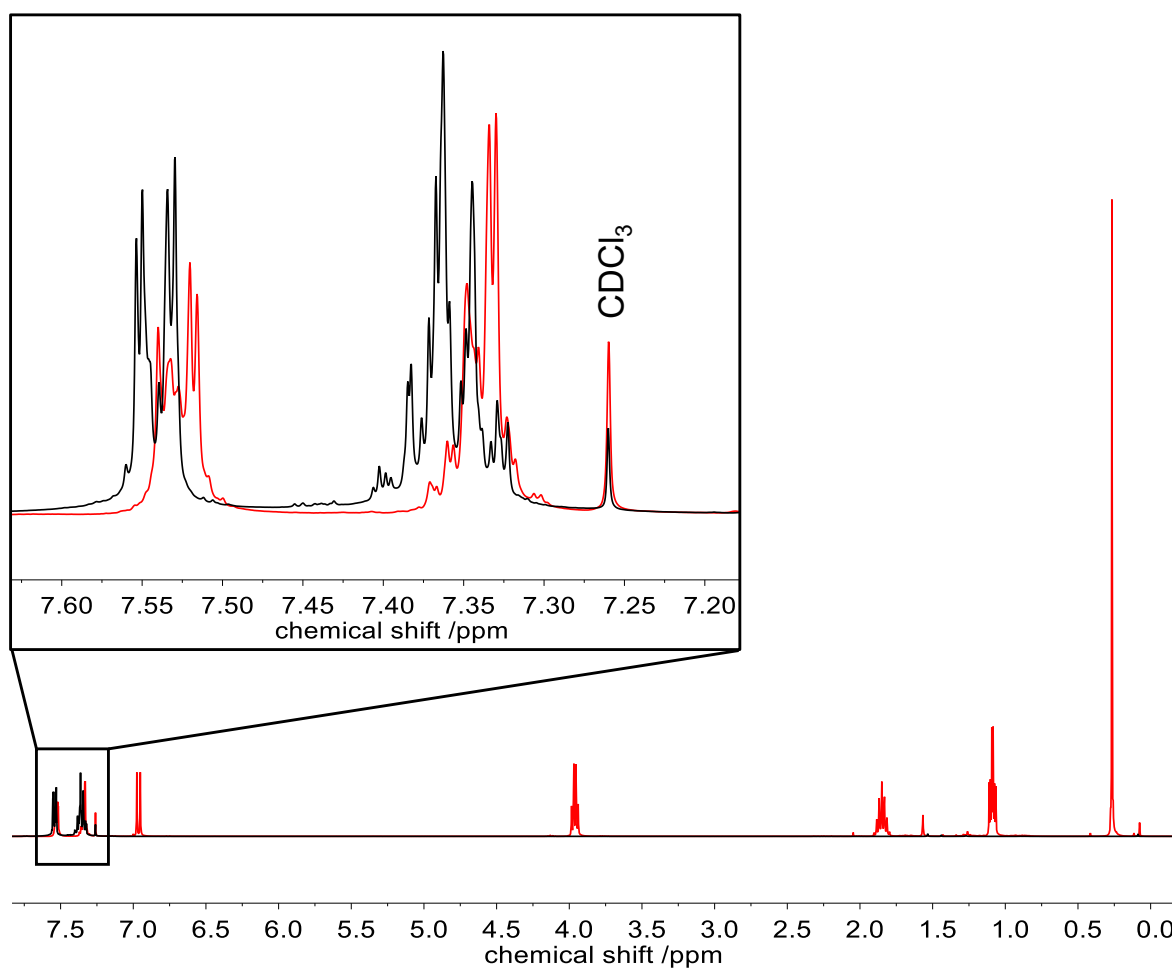


Figure 13: Comparison of the  $^1\text{H}$  NMR spectra of **P1a** (red) and 1,4-diphenylbuta-1,3-diyne (black). The signals in the aromatic region overlap, thus detection of the homocoupling product is not possible using only NMR spectroscopy.

Regarding the  $^1\text{H}$  NMR spectra depicted in Figure 12, the signals of the respective homocoupling product strongly overlap with the signal of the aromatic protons of the phenyl end group. Due to similar chemical shifts of the respective homocoupling product, further analysis *via* SEC is necessary. In Figure 14, the SEC traces of the obtained monomer (red) and the homocoupling product (black) are depicted.

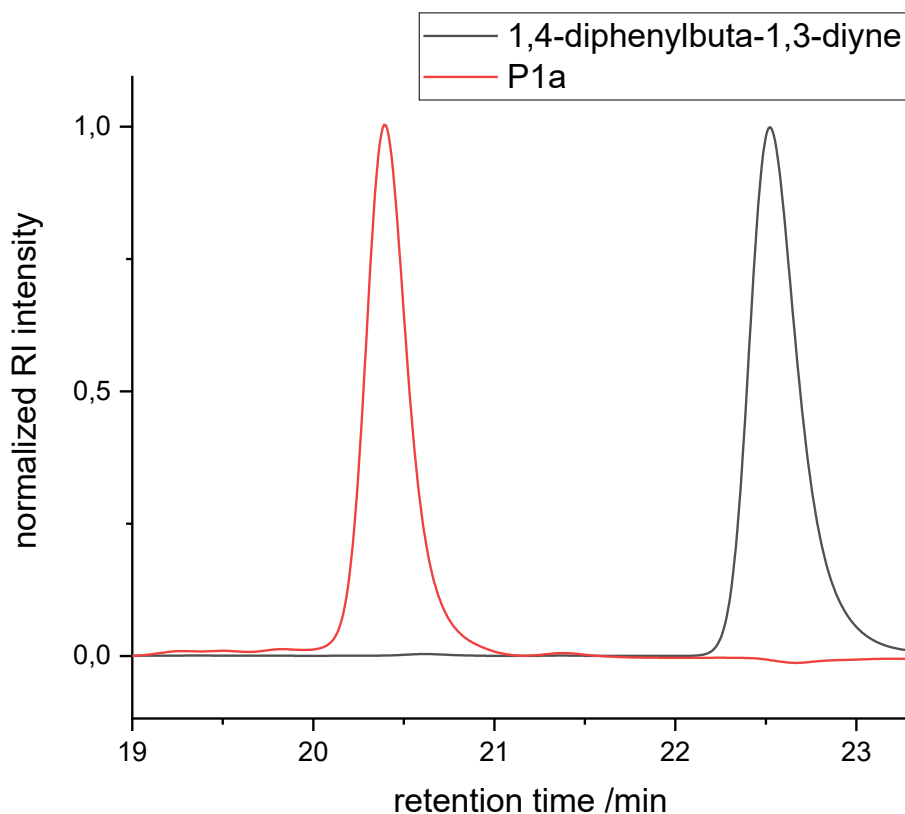
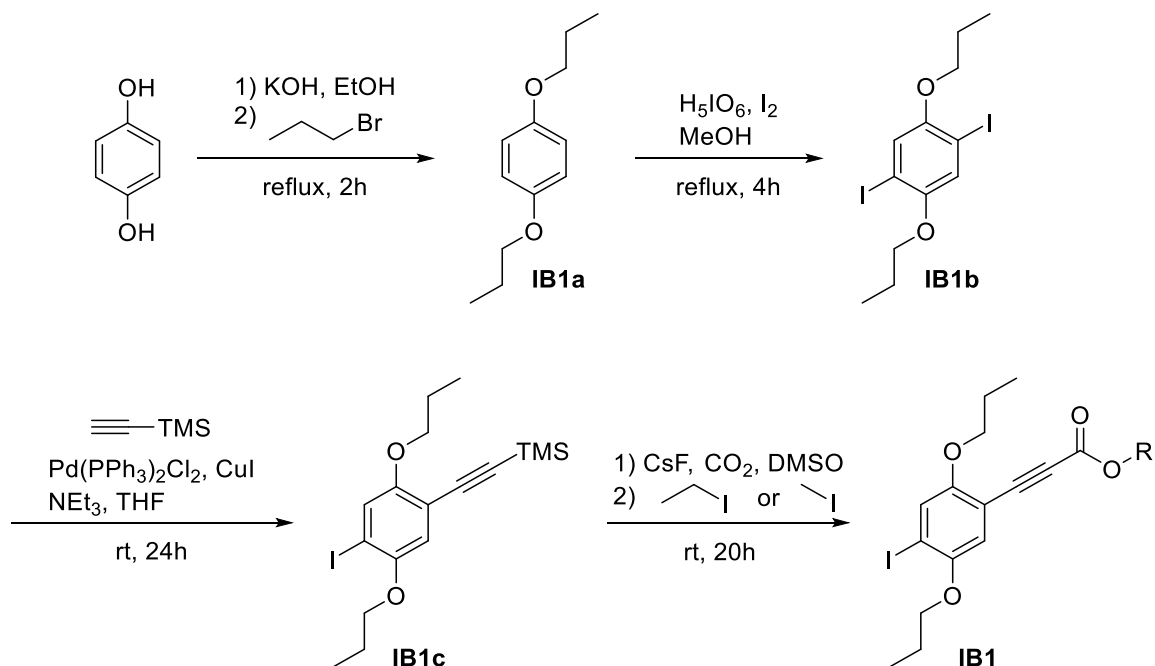


Figure 14: SEC traces of **P1a** (red) and the possible homocoupling product 1,4-diphenylbuta-1,3-diyne (black). After simple purification via silica column chromatography no homocoupling product is observed in the SEC trace of **P1a**.

The monomer **P1a** elutes at 20.4 minutes, whereas the homocoupling product elutes at 22.6 minutes. Simple column chromatography with cyclohexane/ethyl acetate was sufficient to obtain a pure monomer, as confirmed by the narrow distribution of the respective SEC traces. Since no additional peak was observed it was assumed that no homocoupling product was formed, thus the respective oligomer could be eluted faster in column chromatography.

## 4.2.1 Synthesis of building units

The first test reaction demonstrated that indeed the decarboxylative coupling is an alternative for the synthesis of OPEs. In contrast to the predominant Sonogashira coupling, the use of a copper co-catalyst is not necessary, which is advantageous since the Glaser side reaction is avoided. However, the used building unit **IB1c** with a TMS protected triple bond is not applicable anymore. Deprotection leads to the respective terminal triple bond which can be used in the Sonogashira approach but not in decarboxylative coupling. Instead, an alkynyl carboxylic acid is required to continue the synthesis towards OPEs. Thus, the existing building unit **IB1c** was modified by converting the TMS group into an ester protected alkynyl carboxylic acid to allow for further decarboxylative couplings. The reaction procedure towards the respective new building unit **IB1** is depicted in Scheme 35.

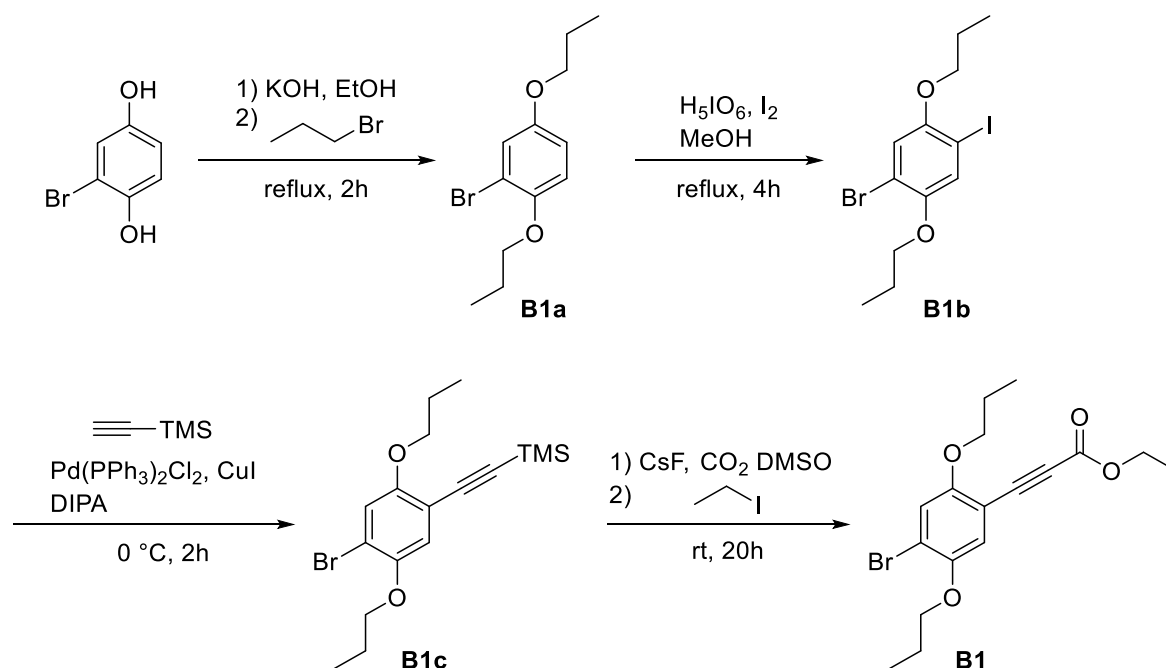


Scheme 35: Synthesis of building unit **IB1** based on hydroquinone. The synthesis towards **IB1c** was adopted from Meier et al. In the final step, the TMS protecting group was converted into ester protected alkynyl carboxylic acid.

The building unit **IB1** is still based on hydroquinone and synthesized in four steps. The first three steps are similar to the building unit, which was used in the Sonogashira coupling. First, a Williamson ether synthesis with 1-bromopropane was performed to introduce solubilizing propoxy side chains. The product, 1,4-dipropoxybenzene **IB1a**, was obtained after filtration through silica with 67% yield. Subsequently, **IB1a** was iodized to 1,4-diodo-2,5-dipropoxybenzene **IB1b** using

periodic acid and iodine. The product was obtained after recrystallization from methanol with 80% yield. The building unit **IB1b** was still symmetric at this point. The iodine moieties are equally accessible in the Sonogashira coupling, but only monofunctionalization is required. Generally, an excess of 1,4-diiodo-2,5-dipropoxybenzene compared to TMS acetylene is applied to achieve monosubstitution. Purification of the monofunctionalized product *via* column chromatography is inevitable, since unreacted starting material remains. Finding the right balance between the equivalents is essential and was investigated in a previous work of our group.<sup>[159]</sup> Working at high dilution and using 1.20 equivalents of TMS acetylene were found best. Apart from the monosubstituted main product **IB1c**, unreacted starting material and the disubstituted side product were detected. After purification *via* column chromatography, the monofunctionalized building unit **IB1c** was obtained with 44% yield. In the last step, the TMS protecting group was converted to an alkynyl carboxylic ester *via* a carboxylation with carbon dioxide, mediated by cesium fluoride in dimethyl sulfoxide and subsequent alkylation with methyl iodide. The final building unit **IB1**, exhibiting an iodine moiety and an alkynyl carboxylic ester, was obtained after four steps with 23% overall yield. Since methyl iodide is highly toxic and suspected to be carcinogenic, it was substituted by ethyl iodide in further building unit syntheses. The conversion from the TMS group to the alkynyl ethyl ester proceeded straightforward with slightly lower yields resulting in 17% overall yield.

Especially the low selectivity in the Sonogashira coupling is a draw back in the described approach above. Not only the yield drops to 44%, but also purification becomes more challenging and time consuming since, three products must be separated. To circumvent the non-selectivity, another approach towards a building unit was investigated. Instead of introducing the asymmetry in the Sonogashira coupling step, an unsymmetric starting compound was selected. The alternative approach is depicted in Scheme 36.



Scheme 36: Synthesis of the building unit **B1** starting from bromohydroquinone. After Williamson ether synthesis, iodination, Sonogashira monocoupling, carboxylation and alkylation **B1** was obtained with 54% overall yield.

Bromo hydroquinone was used as a starting compound, which already introduces the asymmetry. After the four steps of Williamson ether synthesis, iodination, Sonogashira coupling and carboxylation followed by alkylation, the building unit **B1** was obtained in 54% overall yield. The building unit, as well as all intermediates, were thoroughly characterized by proton and carbon NMR spectroscopy, IR spectroscopy, and MS.

Despite the fact that both approaches are very similar and the same synthetic steps are applied, the second approach is superior regarding the overall yield. After iodination, the building unit **B1b** exhibits both, a bromine and an iodine moiety. Both halogens are addressable in the subsequent Sonogashira coupling, however, the iodine moiety is more reactive. By adjusting the reaction temperature to 0 °C, mainly the iodine moiety reacts, while the activation energy for the coupling with the bromine moiety is too low. Still, small amounts of disubstituted by-product were observed and column chromatography was necessary. The yield raised to 80% of the monofunctionalized building unit **B1c** in the Sonogashira coupling step. Purification was still challenging due to the minor amounts of side product, however, since the isolated yield almost doubled it was reasonable to pursue further with the second approach. In Figure 15, the  $^1\text{H}$  NMR spectra of both building units **B1** (top) and **IB1** (bottom) with alkynyl ethyl esters are depicted.

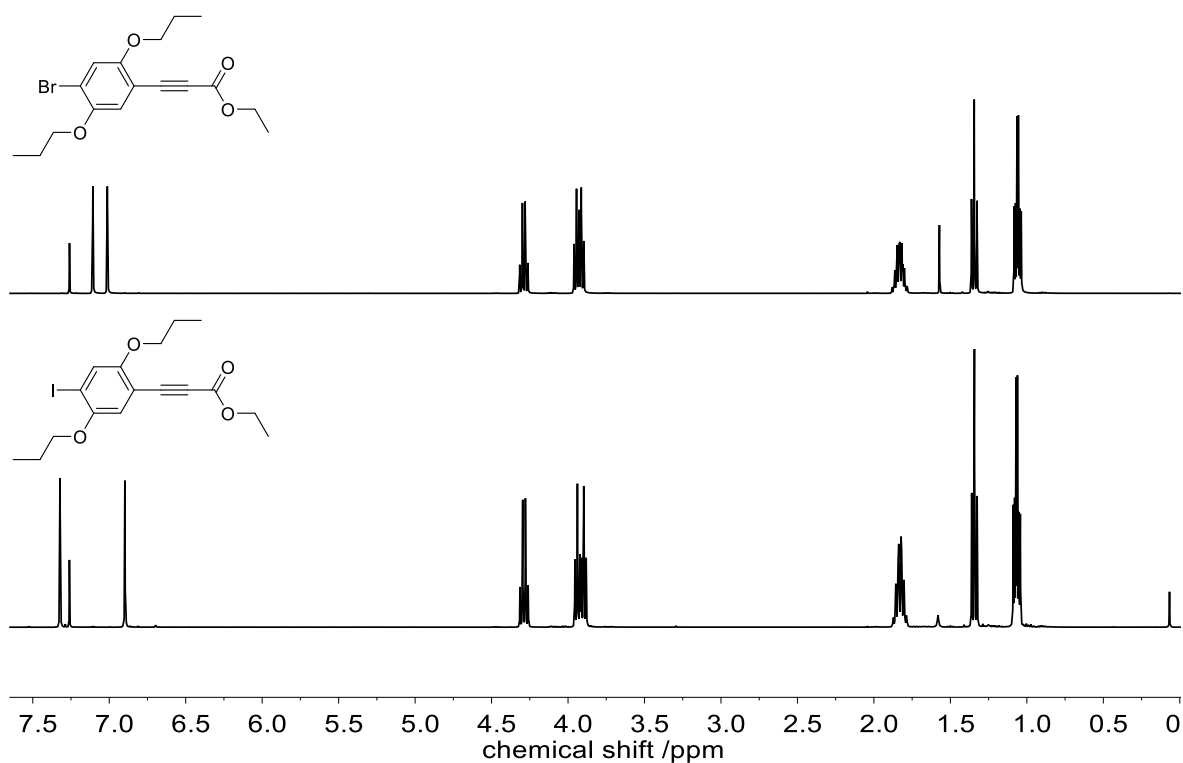


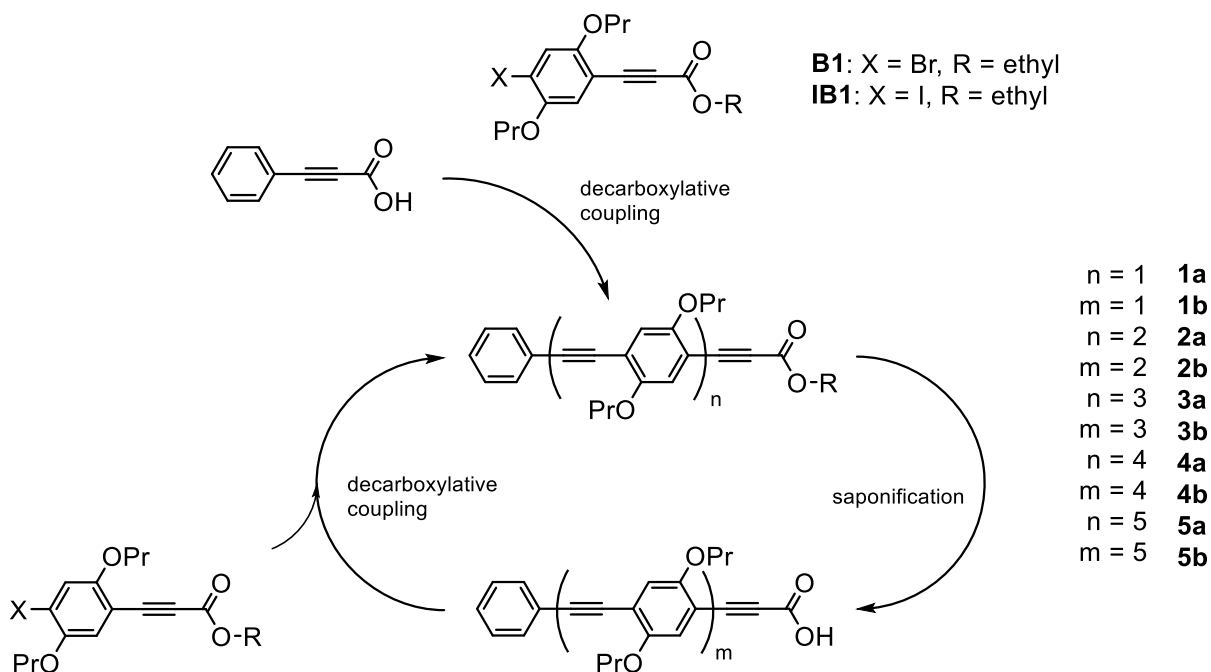
Figure 15:  $^1\text{H}$  NMR spectra of the building units **B1** and **IB1**. Both building units exhibit an ethyl ester protected alkynyl carboxylic acid and a halogen moiety. The different halogens, namely bromine and iodine result in a different shift of the aromatic protons which is observed around 7.00 ppm.

The synthesized building units differ only in the halogen atom. Regarding the  $^1\text{H}$  NMR spectra, this difference is especially visible around 7.0 ppm, where the aromatic signals of the iodine substituted building unit **IB1** split more in contrast to the ones of **B1**. Although the different reactivity of iodine and bromine was exploited in the second approach, both building units should react similar in the decarboxylative coupling, since elevated temperatures are used.

## 4.2.2 Synthesis concept for uniform OPEs

With the new building unit in hand, an iterative synthesis strategy towards OPEs was developed. The new synthesis concept is depicted in Scheme 37. The iterative cycle comprises two steps, which are based on a decarboxylative coupling followed by saponification. Initially, only the building unit **B1** was used to establish the developed synthesis procedure. The respective oligomers were named according to their DP, for instance, **1a** for the ester protected monomer and **1b** for the saponified monomer.

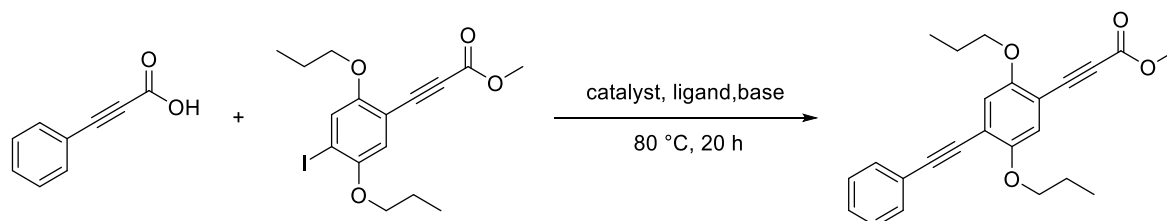
Commercially available phenyl propiolic acid was used as starting compound and reacted in a decarboxylative coupling with the building unit **B1** to obtain the monomer **1a**. Subsequently, the ethyl ester group was saponified with sodium hydroxide in a mixture of THF, methanol and water. The obtained alkynyl carboxylic acid **1b** was further reacted in another decarboxylative coupling with the building unit **B1**. Following the two-step iterative cycle, the oligomers were built up in a linear fashion. The stepwise addition of the building units allows high control over the OPE sequence: hence, varying properties can be adjusted.



Scheme 37: Developed synthesis strategy towards uniform OPEs. The strategy comprises a decarboxylative coupling step and a subsequent saponification.

As described in chapter 4.2.1, the building unit **IB1** was synthesized first and therefore used in the first decarboxylative coupling reactions. The conditions for the decarboxylative coupling of phenyl propiolic acid with various organic iodides were thoroughly studied by Li *et al.*, however, small adjustments were also investigated in this thesis.<sup>[161]</sup> The reaction of phenyl propiolic acid with the building unit **IB1** served as model reaction (Table 3, entry 1).

Table 3: Investigation of reaction conditions.



Entry	Catalyst	Ligand	Base	Solvent	yield
1	Pd(OAc) <sub>2</sub>	XPhos	Cs <sub>2</sub> CO <sub>3</sub>	THF	62%
2	Pd(OAc) <sub>2</sub>	SPhos	Cs <sub>2</sub> CO <sub>3</sub>	THF	74%
3	Pd(OAc) <sub>2</sub>	SPhos	NEt <sub>3</sub>	THF	n.a.
4	Pd(dppf)Cl <sub>2</sub>	SPhos	Cs <sub>2</sub> CO <sub>3</sub>	Toluol/ THF	78%

The results for the model reaction demonstrated that the coupling was successful with the reported conditions. Since XPhos was the most active ligand in the study of Li *et al.*, another dialkylbiaryl phosphine ligand was tested.<sup>[161]</sup> The yield increased to 74% when SPhos was used (Table 3, entry 2). Triethylamine is mainly used in the related Sonogashira coupling as base, however, in the tested decarboxylative coupling, no formation of the coupling product was observed by TLC monitoring (Table 3, entry 3). In a further approach, the palladium source was changed to Pd(dppf)Cl<sub>2</sub> and toluene was added since THF evaporated during the reaction. The solvent system in combination with the catalyst enhanced the yield further to 78% for this model reaction (Table 3, entry 4). Thus, for further reactions, the toluene/THF solvent system, Pd(dppf)Cl<sub>2</sub> as catalyst, SPhos as ligand and Cs<sub>2</sub>CO<sub>3</sub> as base were used.

### 4.2.3 Synthesis of uniform rod-like oligomers

The synthesis towards rod-like oligomers was performed according to the developed concept, which is outlined in Scheme 37. First, the building unit **B1** is converted with phenyl propiolic acid to the respective monomer **1a**. The conversion to monomer **1a** was performed similar to the test reaction. An excess of phenyl propiolic acid (1.25 eq.) was used to assure full conversion of the building unit **B1**, hence forcing a high yield. The reactants were placed in a sealed vial, evacuated, and backfilled with argon three times. Subsequently, the solvents were added, and the mixture stirred at 60 °C under an argon atmosphere. The reaction was monitored by TLC, which indicated full conversion of the building unit after 20 hours. Silica column chromatography was performed with cyclohexane/ethyl acetate to obtain the pure monomer **1a** in a scale of 515 mg and 66% yield. As in the first test reaction, the homocoupling product was avoided and isolation of the product was achieved by simple column chromatography. After the coupling step, saponification was performed using sodium hydroxide in a mixture of THF, methanol and water in a 3:1:1 ratio resulting in alkynyl carboxylic acid **1b** in quantitative yield. The saponification was monitored by TLC as well and the saponified monomer **1b** was sufficiently pure after acidification with hydrochloric acid and simple extraction with dichloromethane. The respective <sup>1</sup>H NMR spectra are depicted in Figure 16 confirming the cleavage of the ethyl ester.

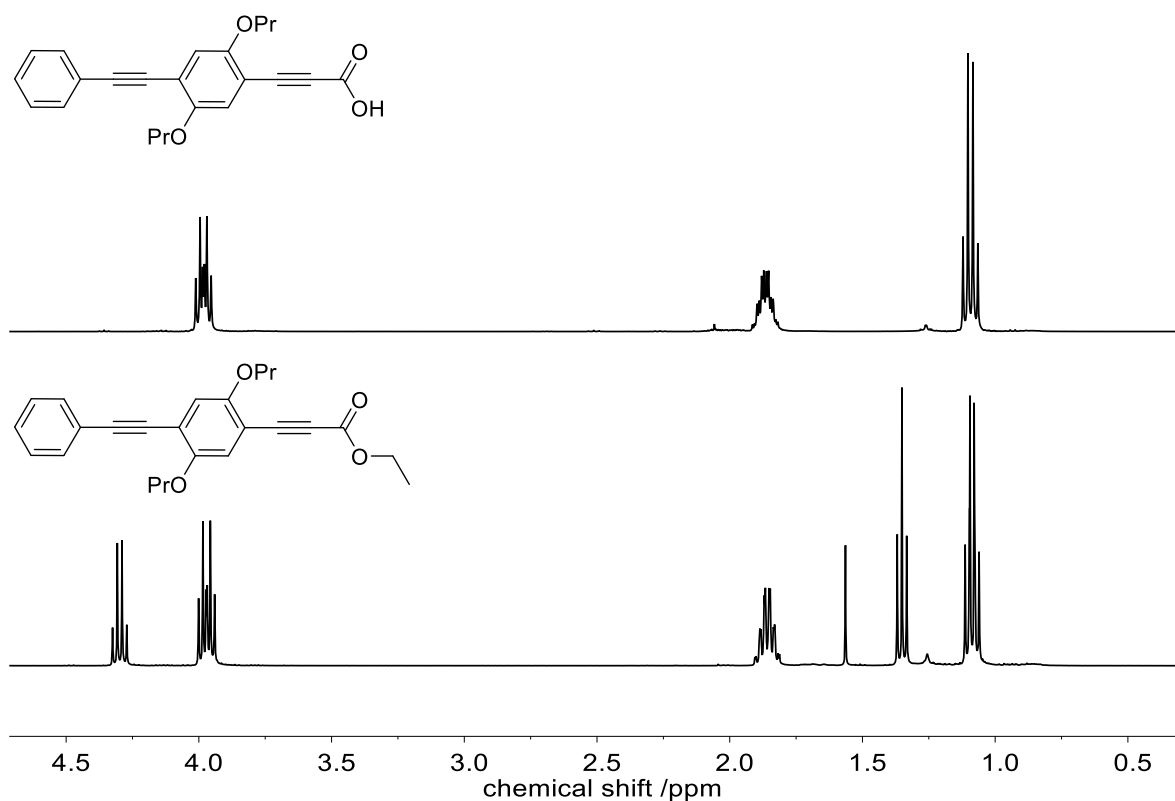


Figure 16: Cutout of the <sup>1</sup>H NMR spectra of the monomer ester **1a** (bottom) and monomer acid **1b** (top). The cleavage of the ethyl ester group is observed at 4.30 ppm and 1.35 ppm.

Since the signals of the ethyl ester are isolated from the signals of the propoxy side chains, the successful cleavage was observed by the disappearance of the quartet at 4.30 ppm and the triplet at 1.35 ppm in the <sup>1</sup>H NMR spectrum of the alkynyl carboxylic acid **1b**. Furthermore, the monomer ester **1a** and the monomer acid **1b** were analyzed by SEC. The corresponding SEC traces are depicted in Figure 17.

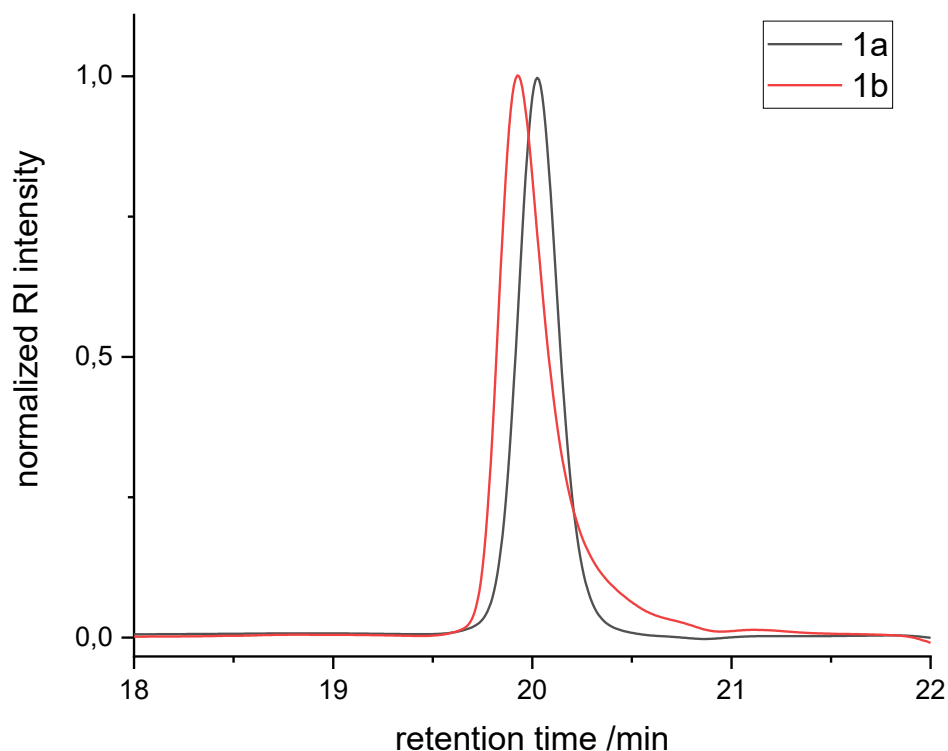


Figure 17: SEC traces of monomer ester **1a** (black) and monomer acid **1b** (red). The narrow peak confirms their uniformity. Tailing of the SEC trace of the monomer acid **1b** was assigned to the free carboxylic acid which might interact with the column material.

A monomodal and narrow peak was observed for the monomer **1a** (Figure 16, black curve), which indicated a high purity and uniformity. However, the SEC trace of the deprotected monomer **1b** (Figure 16, red curve) shows slight tailing towards higher retention times. The tailing was attributed to the free carboxylic acid, possibly interacting with the column material. Interestingly, the retention time of the deprotected monomer acid is shifted towards higher hydrodynamic radii, although the molecular weight is decreased when the ethyl ester is cleaved.

Following the iterative cycle, the deprotected monomer **1b** was reacted with the building unit **B1** to the dimer **2a**. Similar to the Sonogashira approach, the reaction towards the respective dimer is more complex. An excess of the alkynyl carboxylic acid is not desirable anymore, since it is the respective valuable oligomer. Thus, an excess of the building unit **B1** (1.10 eq.) was applied to assure full conversion of alkynyl carboxylic acid **1b**. Purification by silica column chromatography yielded dimer **2a** in a scale of 516 mg and 77% yield. Using a small excess of the building unit was assumed to have a positive effect on the conversion of the alkynyl carboxylic acid and a 10% higher yield was obtained compared to synthesis of the

monomer **1a**. Saponification of the dimer ester **2a** was straightforward and the dimer alkynyl carboxylic acid was obtained in quantitative yield. As for the monomer, dimer acid **2a** was sufficiently pure and further used without any purification. In Figure 18, the SEC traces of the monomer ester **1a** (black) and the monomer acid **1b** (red) as well as the dimer ester **2a** (blue) and the dimer acid **2b** (green) are depicted.

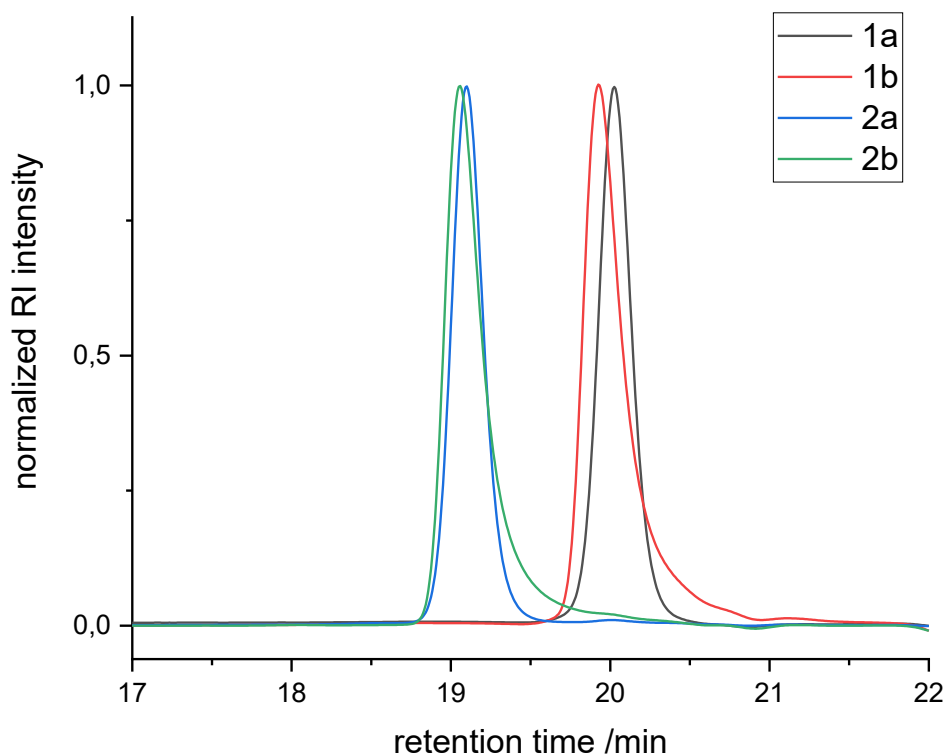


Figure 18: SEC traces of the dimer ester **2a** (blue) and the dimer acid **2b** (green) as well as the respective monomer species (black and red). No homocoupling product is observed after purification via silica column chromatography.

Since 244.33 g/mol are added to the molecular weight in each decarboxylative coupling step, the respective higher DP oligomer elutes at lower retention times. The SEC trace of the dimer ester **2a** (Figure 17, blue curve) also shows a narrow distribution and the respective homocoupling product was not observed. Similar to the SEC trace of the monomer acid **1b**, the peak of the dimer acid **2b** is shifted towards shorter retention times. However, the retention time difference between the peaks of dimer ester **2a** and dimer acid **2b** is smaller since the molecular weight loss relative to the overall molecular weight is smaller.

With the promising results of the first two cycles, the decarboxylative coupling to the trimer ester **3a** proceeded straightforward as well. The small excess of the building

unit **B1** of 1.10 equivalents was maintained. Consistent with the decarboxylative couplings before the homocoupling product was not detected and simple silica column chromatography with cyclohexane/ethyl acetate yielded the pure trimer ester **3a** in a scale of 416 mg and 73% yield. The structures of the obtained monomer, dimer, and trimer esters as well as their corresponding SEC traces are depicted in Figure 19.

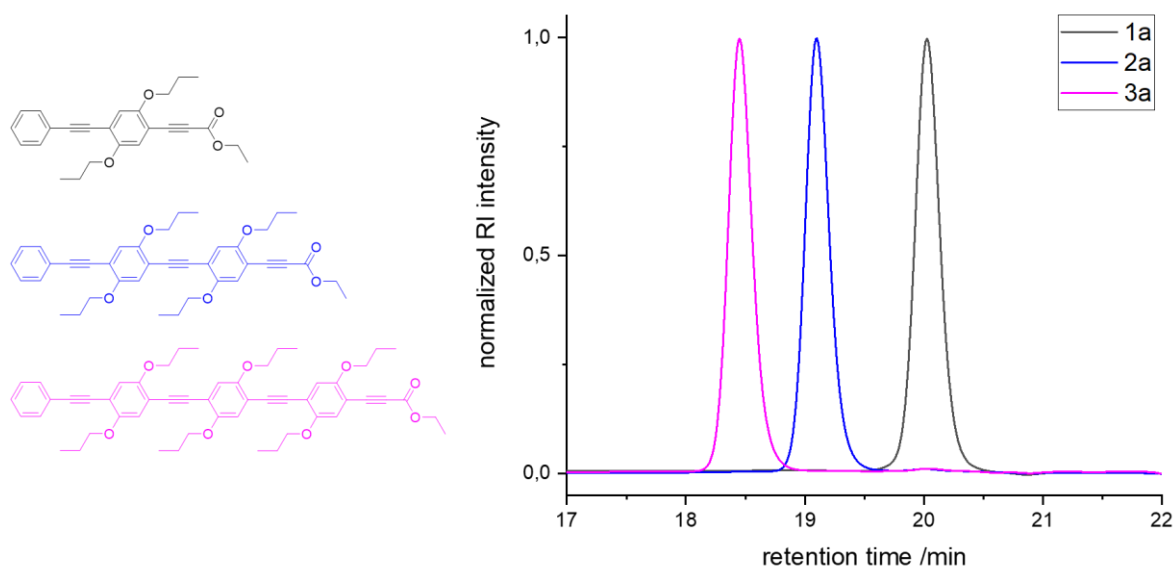


Figure 19: Left: structures of the monomer **1a** (black), dimer **2a** (blue), and trimer **3a** (pink) ester. Right: corresponding SEC traces which confirm uniformity of the obtained OPEs (**1a-3a**).

The obtained oligomers show a monomodal and narrow peak, confirming their high purity and uniformity. As mentioned in chapter 4.1, SEC is the most important analyzing method to assure uniformity. Furthermore, all oligomers were analyzed by NMR spectroscopy and mass spectrometry as well. The SEC trace of the trimer is shifted towards lower retention times which is in accordance with the growing oligomer. Subsequent saponification closed the third cycle and the deprotected trimer acid **3b** was obtained in a scale of 386 mg and 37% overall yield after six steps. Compared to the Sonogashira approach, in which the isolated yields decrease for each coupling step, the yields in the decarboxylative coupling were rather constant around 70%. To assure this trend, the trimer acid **3b** was further reacted towards the respective tetramer **4a**.

The reaction towards the tetramer ester **4a** proved to be very challenging. As for the second and third cycle, a small excess of the building unit **B1** was used. The reaction

was followed by TLC monitoring and the formation of a highly fluorescent product was observed. Indeed, even after purification *via* silica column chromatography, an additional peak was observed in the SEC trace of tetramer ester **4a** which is depicted in Figure 20.

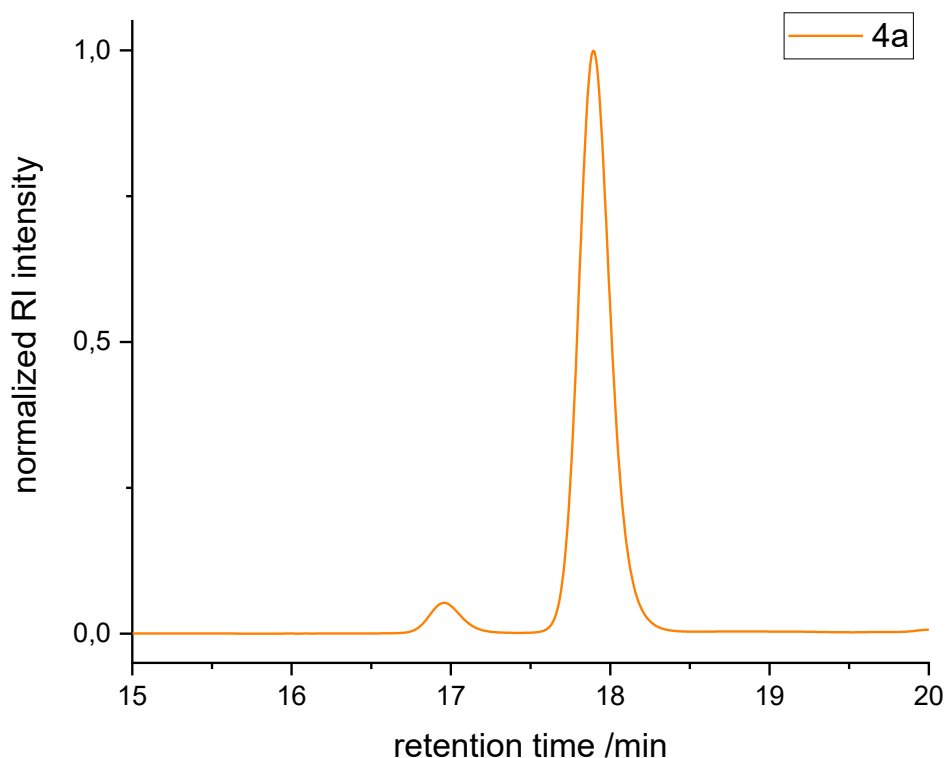


Figure 20: SEC trace of the tetramer **4a** after column chromatography. A second peak is detected at lower retention time. Analysis by ESI-MS revealed the presence of the homocoupling product of **3b**.

Tetramer ester **4a** was purified by column chromatography using a mixture of cyclohexane/ethyl acetate. TLC of the respective fractions visualized only one fluorescent spot on the TLC plate. Analysis by  $^1\text{H}$  NMR spectroscopy also revealed no additional signals; moreover, the integrals fit to the number of protons estimated from the tetramer structure. However, the second peak in the SEC trace revealed that a higher molecular species was still present after column chromatography, which further demonstrated the importance of SEC analysis regarding the detection of impurities (*cf.* chapter 4.1). Since no additional signals were found in the NMR spectrum, it was assumed that the homocoupling product was formed during the reaction. Indeed, the respective mass of the homocoupling product of trimer **3b** was found *via* ESI-MS analysis (see chapter 6.3.3). This was the first time the homocoupling product was observed in the decarboxylative coupling in this work. The reason could be that with growing oligomer length, conjugation of the OPE

backbone is increased, eventually deactivating the acid, and thus leading to a homocoupling process.<sup>[161]</sup> Considering the intensities of the SEC traces, the cross-coupling process was still largely favored and led to the formation of the desired oligomer. However, the very similar retention factors of the tetramer and the homocoupling product as detected by TLC made separation *via* silica column chromatography not possible.

Due to the purification problems, the synthesis strategy had to be adapted. Although the pure tetramer ester **4a** could not be obtained after purification *via* column chromatography, the mixture was used in the subsequent saponification. While the ethyl ester of the tetramer **4a** was saponified, the homocoupling product was not affected. The free carboxylic acid of the deprotected tetramer **4b** resulted in a significantly different retention factor, thus the pure alkynyl carboxylic acid **4b** was obtained after a simple and fast to perform silica filtration column. The corresponding SEC traces are depicted in Figure 21.

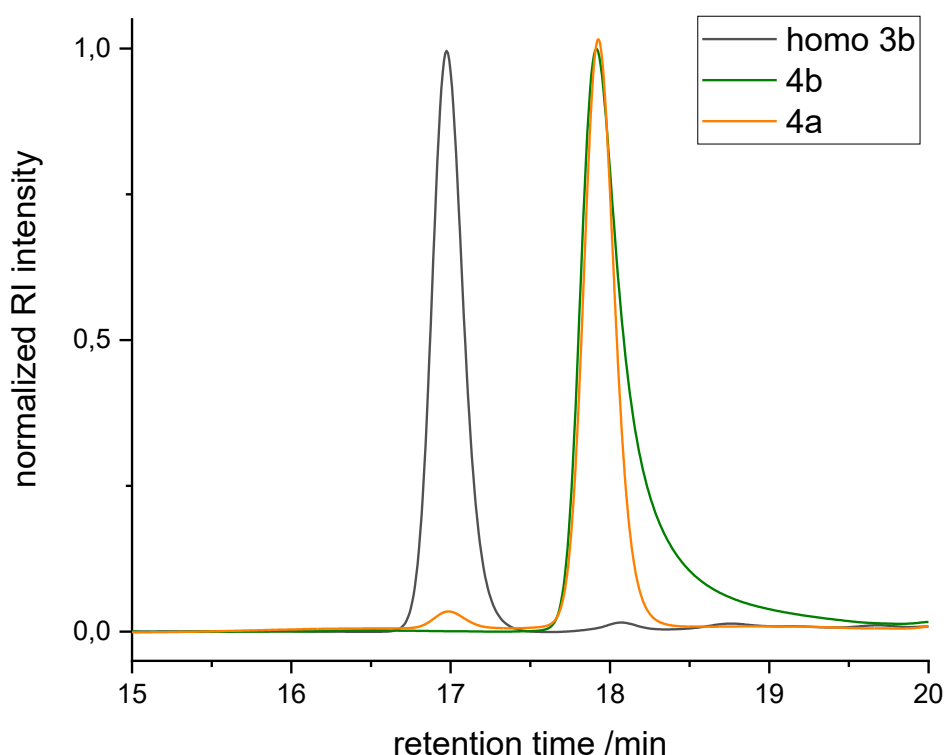


Figure 21: SEC traces of impure tetramer ester **4a** (orange), tetramer acid **4b** (green), and homocoupling product of **3b** (grey). Pure tetramer acid **4b**, was obtained after saponification followed by a silica filtration column.

The SEC traces clearly demonstrate that the modified purification method was successful since the peak at a retention time of 17 minutes vanished. During the

purification, the homocoupling product was eluted first with pure dichloromethane and could be isolated (Figure 20, grey curve). Subsequently, the eluent was switched to a mixture of acetone and methanol with 1% acetic acid to elute pure tetramer acid **4b**.

The synthesis of the pentamer ester **5a** showed the same difficulties as for the tetramer ester **4a**. According to SEC, a second peak towards shorter retention times was observed. Similarly, the  $^1\text{H}$  NMR spectrum showed no additional signals and the respective mass of the homocoupling product of the tetramer **4b** was found in the ESI-MS spectrum (see chapter 6.3.3). The intensity of the by-product relative to the coupling product increased in the SEC chromatogram for the pentamer. The SEC traces of all obtained oligomer ester **1a-5a** are depicted in Figure 22. Homocoupling was avoided until the trimer stage while the decarboxylative coupling towards the tetramer and pentamer ester produced the homocoupling product which was identified by ESI-MS.

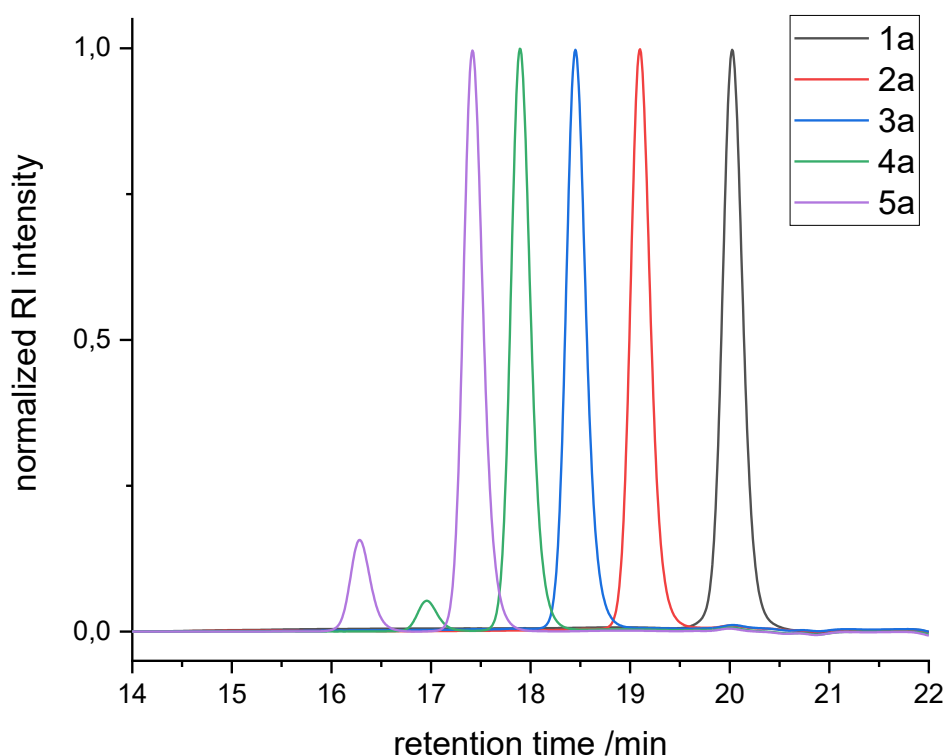


Figure 22: SEC traces of the obtained ethyl ester protected OPEs. Homocoupling was avoided until the trimer stage. For the tetramer **4a** (green) and the pentamer **5a** (purple) a second peak towards shorter retention times arises, which could be assigned to the homocoupling product by ESI-MS.

A mixture of cyclohexane/ethyl acetate was used at any stage for the purification *via* column chromatography. It is mentioned that in the previous PhD thesis of Rebekka Schneider, the separation of homocoupling product and oligomer was achieved by using dichloromethane/cyclohexane as a solvent mixture.<sup>[159]</sup> However, silica column chromatography with a high content of dichloromethane requires significantly more time and purification using a different solvent system than cyclohexane/ethyl acetate was not performed in this thesis. Instead, an alternative purification method for the respective alkynyl carboxylic acid was developed. Saponification of the pentamer ester **5a** followed by purification *via* filtration through a short silica column yielded the pure pentamer acid **5b** in a scale of 73 mg and 75% yield. Figure 23 depicts, all oligomeric alkynyl carboxylic acids **1b-5b**.

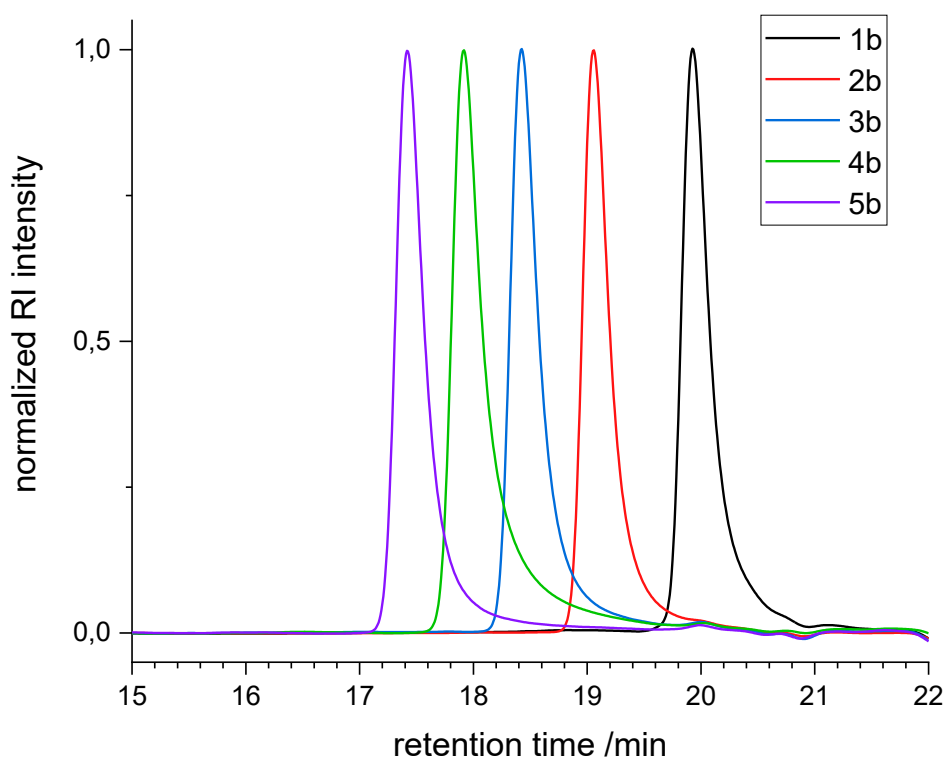


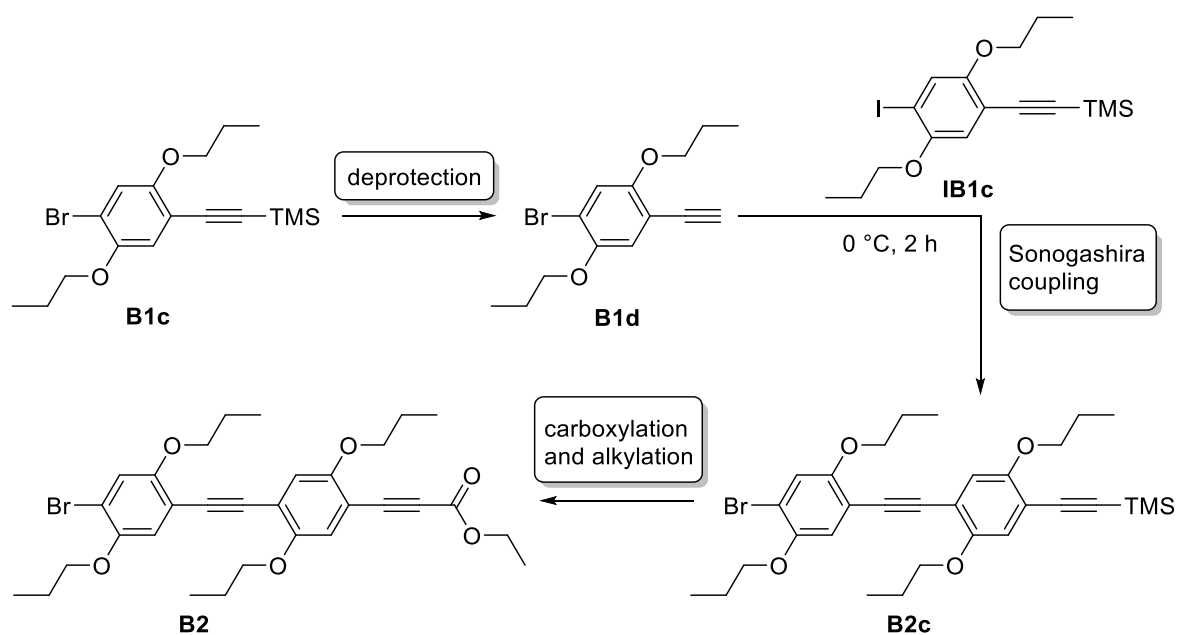
Figure 23: SEC traces of the deprotected uniform OPEs.

As discussed before, the SEC traces of the alkynyl carboxylic acid terminated oligomers show tailing towards higher retention times, while the esterified oligomers were narrow. However, also considering NMR spectroscopy and MS data, it is fair to assume that both series of oligomers (**1a-3a** and **1b-5b**) are pure and uniform.

The results demonstrate that the developed synthesis strategy is capable to produce uniform OPEs. The overall yield of 14% for the deprotected pentamer was

comparable with the overall yield of 18% of the Sonogashira approach. Still, the reactivity of bromine and iodine in coupling reactions is different. Organic iodides often react better and faster than organic bromides. Therefore, the synthesis was repeated using building unit **IB1** which exhibits an iodine instead of a bromine moiety. Since an excess of the building unit seemed to have a positive effect on the yield in the decarboxylative coupling, this was maintained from the monomer stage on. The yield for the monomer increased from 66% to 84% and was constant around 80% for the subsequent coupling reactions (previously 70%). Saponification proceeded with quantitative yield. A uniform trimer ester **3a** was obtained after 5 steps in a scale of 471 mg and 60% overall yield (compared to 37% overall yield of the trimer ester obtained with building unit **B1**). Like for the synthesis with building unit **B1**, no homocoupling product was observed. However, in the following reaction towards the tetramer **4a**, the yield decreased in the decarboxylative coupling and formation of a homocoupling product was observed in the SEC trace.

To confirm that homocoupling begins at the trimer stage and to build up OPEs even faster, an alternative synthesis pathway towards the tetramer **4a** was investigated. Therefore, a double building unit **B2** which is able to introduce two repeating units at once was synthesized. The synthesis concept for the double building unit **B2** is outlined in Scheme 38.



Scheme 38: Synthesis of the double building unit **B2**. The obtained double building unit introduces two repeating units at once.

First, the building units **B1c** and **IB1c** were synthesized according to the described procedure (chapter 4.2.1). Subsequently, building unit **B1c** was deprotected using potassium carbonate in a mixture of dichloromethane and methanol. The obtained deprotected building unit **B1d** exhibited a bromine moiety and a terminal triple bond. The combination of functional groups generally allows polymerization by Sonogashira coupling. However, in this approach, building unit **B1d** was coupled to the building unit **IB1c** exploiting the different reactivity of bromine and iodine. Since the reaction was conducted at 0 °C, building unit **B1d** did not polymerize but was coupled to yield the building unit **IB1c**. After purification *via* silica column chromatography the TMS protected double building unit **B2c** was obtained in a scale of 1.84 g and 94% yield. Subsequent carboxylation and alkylation with ethyl iodide yielded the ester protected building unit **B2** with 86% yield. Column chromatography was necessary to separate the double building unit **B2** from the side product. During the carboxylation the TMS protecting group is cleaved by fluoride ions before reacting with carbon dioxide. Thus, the main side product is the double building unit with an unreacted terminal triple bond.

The double building unit **B2** was then used to build up OPEs using the developed new synthesis concept as well. First, phenyl propiolic acid was reacted with the double building unit **B2** to obtain the dimer **2a** with 58% yield. Saponification of the dimer led to the alkynyl carboxylic acid **2b** which was further reacted with double building unit **B2** towards the tetramer. After silica column chromatography, pure tetramer **4a'** was obtained with 56% yield. Combining all reactions, the tetramer **4a'** was synthesized in three steps with 32% overall yield. The SEC traces are depicted in Figure 22.

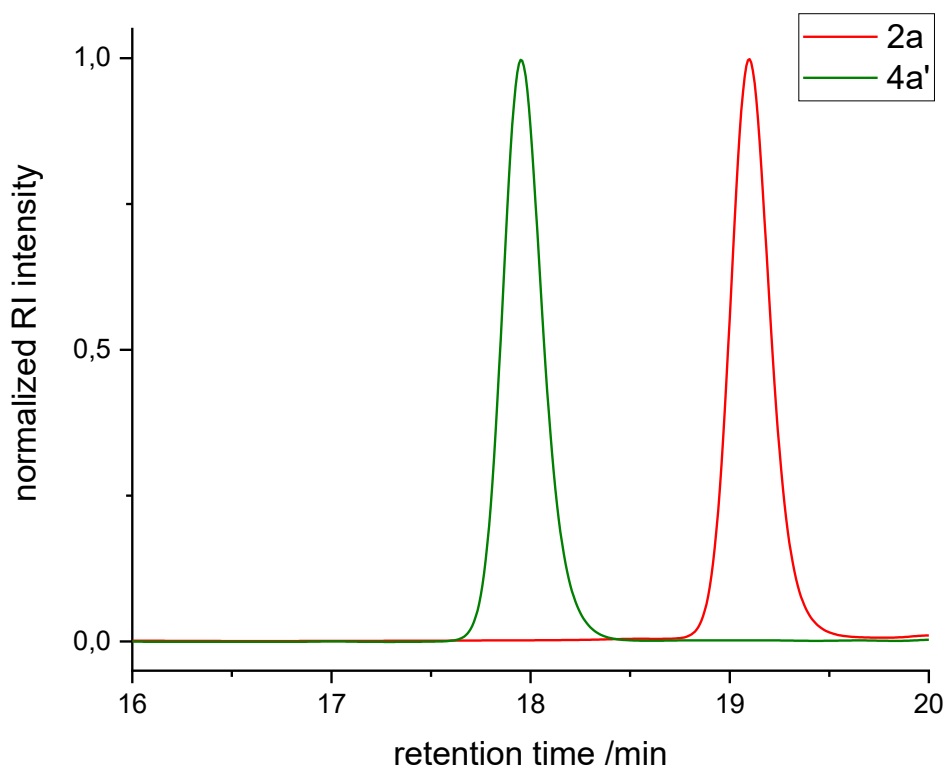


Figure 24: SEC traces of dimer ester **2a** (red) and tetramer ester **4a'** (green). No homocoupling was observed when the tetramer is synthesized from the dimer with the double building unit.

Interestingly, analysis by SEC showed no additional peak towards lower retention times. When the tetramer **4a** was synthesized from the trimer **3b**, homocoupling was observed in the SEC trace. However, in this case, the tetramer **4a'** was synthesized from the dimer **2a**, hence no homocoupling occurred. This result confirms the assumption that homocoupling begins from the trimer stage onwards. Advantageously, the oligomers grow also faster using the double building unit **B2**, but the yield in the decarboxylative coupling decreases as well.

#### 4.2.4 Synthesis of new building units for sequence-defined OPEs

To further increase the scope of the developed synthesis concept for sequence-defined OPEs, three different building units were synthesized. In the following parts of this chapter, the syntheses are briefly discussed. The new building units were synthesized in a related Bachelor thesis under the co-supervision of the author (Daniel Hahn). The respective molecules are marked with footnotes in the experimental section. The coupling of the derived building units towards sequence-defined oligomers was performed by the author himself.

The synthesis concept towards the building units, which were based on a benzene core, was already discussed in chapter 4.2.1 (*cf.* Scheme 23). However, three different core molecules were selected, namely thiophene, biphenyl and anthracene. Commercially available precursors were used and functionalized to exhibit a halide moiety on one side and an ethyl ester protected alkynyl carboxylic acid on the other side.

For the building unit based on thiophene, 2-bromothiophene was used as precursor. The respective building unit **B3** (Figure 25, top) was synthesized in three steps comprising iodination, monofunctionalization with TMS acetylene and carboxylation followed by alkylation with ethyl iodide. Iodination of the 2-bromothiophene was challenging since unreacted starting material remained in the reaction mixture. The product **B3b**, 2-bromo-5-iodothiophene, was obtained in a scale of 1.39 g and 24% yield, after purification *via* column chromatography and vacuum distillation. Subsequently, the **B3b** was reacted with TMS acetylene in a Sonogashira coupling at 0 °C. Double substitution occurred only marginally and the monosubstituted product **B3c** was separated *via* column chromatography in a scale of 550 mg with 61% yield. Carboxylation and alkylation proceeded straightforward and the thiophene building unit **B3** was obtained in a scale of 183 mg and 91% yield (13% overall yield).

The respective building unit **B4** (Figure 25, middle), based on a biphenyl core, was synthesized in two steps. The symmetric 4,4'-dibromobiphenyl served as starting compound, hence, monofunctionalization with TMS acetylene was challenging. Elevated temperatures were needed in the Sonogashira coupling, which also increases side reactions. Two main side products were identified. Since a small excess of TMS acetylene was used, the homocoupling product 1,4-bis(trimethylsilyl)buta-1,3-diyne was observed. Furthermore, double substitution occurred and thus, column chromatography was inevitable. After purification, the monofunctionalized building unit **B4c** bearing a bromine and a TMS protected triple bond was obtained in a scale of 1.83 g and 35% yield. Subsequently, the TMS group was converted into the ethyl ester group in the second step. TLC monitoring showed the formation of a side product which was the building unit bearing a terminal alkynyl due to incomplete carboxylation. However, purification *via* column chromatography

using pure cyclohexane as eluent, yielded the biphenyl building unit **B4** in a scale of 1.26 g with 30% overall yield.

The third selected building unit was based on an anthracene core. Similar to the biphenyl building unit **B4**, the anthracene building unit **B5** (Figure 25, bottom) was synthesized in two steps. Herein, the symmetric 9,10-dibromoanthracene served as starting compound. Introduction of the TMS acetylene remained challenging, since both bromine moieties are equally addressable. In a first try, mainly the disubstituted anthracene was obtained. As a consequence, the equivalents of TMS acetylene were reduced to 0.8 equivalents in a second try leading to the monosubstituted anthracene building unit **B4c**, which was obtained in 41% yield. Further optimization was not pursued; however, the use of even lower equivalents of TMS acetylene is found in the literature.<sup>[163]</sup> As for the building units before, conversion of the TMS group to the ethyl ester protected alkynyl carboxylic ester proceeded straightforwardly. The anthracene building unit **B5** was obtained in a scale of 1.10 g and 23% overall yield. The respective structures of the three mentioned building units as well as a comparison of the <sup>1</sup>H NMR spectra is given in Figure 25.

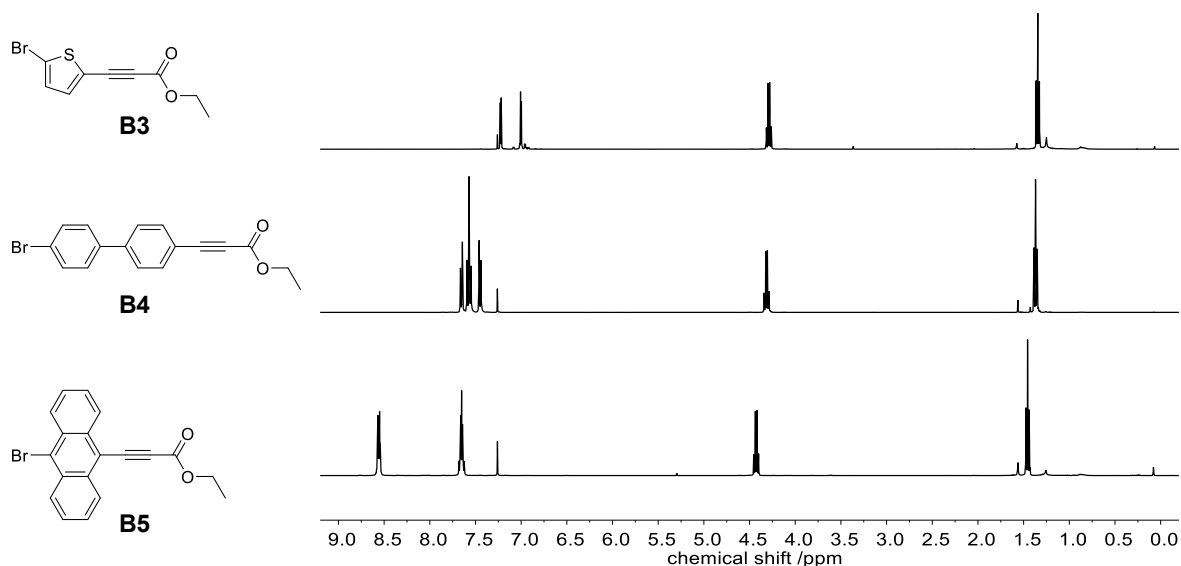


Figure 25: Comparison of the <sup>1</sup>H NMR spectra of the three new building units **B4**, **B5**, **B6**.

In a previous related PhD thesis in our group, also building units with electron accepting properties, like benzothiadiazole, were synthesized and used in the synthesis of OPEs.<sup>[159]</sup> However, conversion of the TMS group of a benzothiadiazole precursor with a bromine moiety and a TMS protected triple bond into the ethyl ester was not successful. Analysis by NMR spectroscopy revealed that only deprotection

of the TMS group occurred. Presumably, carboxylation with carbon dioxide gas is not favored with electron poor triple bonds. Thus, the synthesis of electron accepting building units is challenging, however, was not further investigated in the present thesis.

To test the compatibility of the obtained building units with the decarboxylative coupling approach, first test reactions towards sequence-defined OPEs were performed. The decarboxylative coupling of the biphenyl building unit **B4** with the dimer **2b** was straightforward, and the sequence-defined trimer **BP3a** was obtained after purification *via* column chromatography. The structure and the  $^1\text{H}$  NMR spectrum are depicted in Figure 26

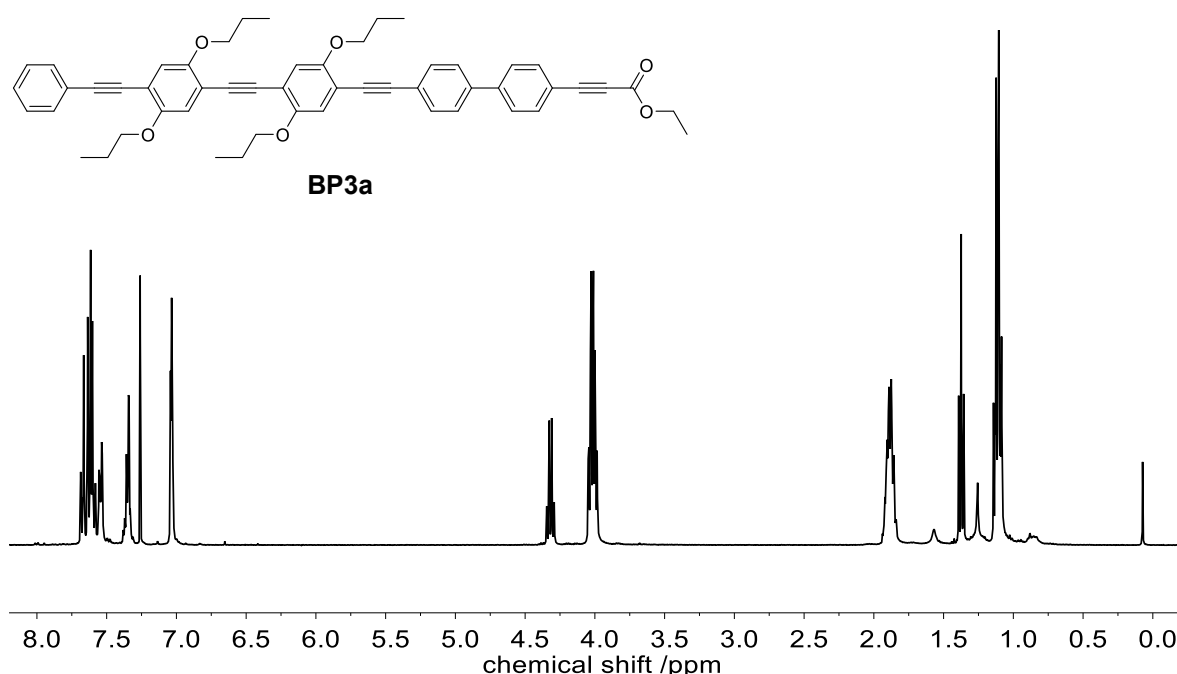


Figure 26:  $^1\text{H}$  NMR spectrum of the sequence-defined trimer **BP3a**.

Furthermore, the anthracene building unit **B5** was reacted with the dimer **2b** as well as phenyl propiolic acid to obtain the sequence-defined trimer **A3a** and monomer **A1a**, respectively. Monitoring by TLC indicated full conversion of the building unit after 16 hours reaction time over night. After purification *via* column chromatography, the respective oligomers **A1a** and **A3a** were obtained as dark red solids. However, while the fractions were collected from column chromatography, a color change of the solution from bright orange to brown was observed, already indicating degradation. The obtained oligomers were analyzed by SEC. The respective SEC traces are depicted in Figure 27.

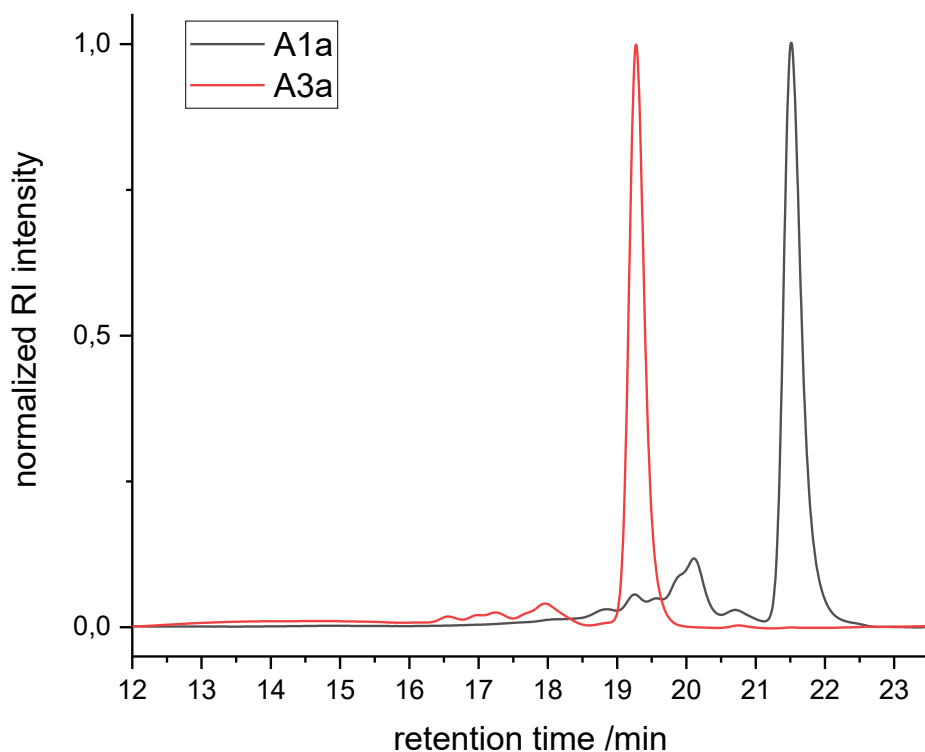


Figure 27: SEC traces of sequence-defined monomer **A1a** (black) and sequence-defined trimer **A3a** (red), in which the anthracene building unit **B6** was incorporated. Additional peaks towards lower retention times indicate the presence of higher molecular weight species.

The SEC traces of both oligomers show additional peaks towards lower retention times. Presumably, the oligomers are prone to undergo Diels-Alder reaction, thus cross-linking to higher molecular weight species. The structure of the oligomer might enhance the possibility of Diels-Alder reaction. Generally, electron rich dienes react with electron deficient dienophiles in a Diels-Alder reaction with a normal electron demand. The electron withdrawing ethyl ester could thus lead to a reactive dienophile. Additionally, the electron donating propoxy side chains enhance the reactivity of the diene (here anthracene). The respective reaction using the Sonogashira coupling and a building unit with a triisopropylsilyl protected triple bond is reported in the literature.<sup>[163]</sup> Thus, sequence-definition employing the anthracene building unit **B5** combined with the decarboxylative coupling approach is challenging.

### 4.2.5 Conclusion

A new synthesis strategy towards OPEs was developed. With the iterative two-step synthesis, a uniform pentamer with propoxy side chains was obtained with 14% overall yield after ten reaction steps. Homocoupling was not observed until the trimer stage. In case of homocoupling, the oligomers were saponified and then purified by a silica filtration column. To demonstrate that homocoupling starts from the trimer stage onwards, a double building unit was synthesized. When the tetramer **4a'** was synthesized from the dimer **2b** with the double building unit, the homocoupling product was not observed. Furthermore, three different building units, based on a thiophene, biphenyl, or anthracene core, were synthesized. Subsequently, the biphenyl building unit **B4** was used to synthesize a sequence-defined trimer. In contrast, coupling of the anthracene building unit **B5** was difficult and analysis by SEC revealed that higher molecular species were present, which could be formed *via* Diels-Alder reaction. Nevertheless, the decarboxylative coupling proved to be a reliable alternative to the Sonogashira coupling, however, to highlight the advantages and disadvantages a thoroughly comparison is described in the following chapter.

### 4.3 Sonogashira versus decarboxylative coupling – a comparison

Parts of this comparative study and the associated parts in the experimental part have been published before:

D. Hahn, R. V. Schneider, E. Foitzik, M. A. R. Meier, *Macromol. Rapid Commun.* **2021**, 2000735.

#### Abstract:

*In this comparative study, the Sonogashira coupling approach and the decarboxylative coupling approach towards uniform sequence-defined OPEs are evaluated regarding time, purification, and yield. The developed decarboxylative coupling approach was superior in terms of overall time which was decreased significantly to one third of a time due to easier and faster purification. The obtained yields (14% decarboxylative coupling approach, 18% Sonogashira coupling approach) are comparable, however, the decarboxylative coupling approach was performed in a much smaller scale.*

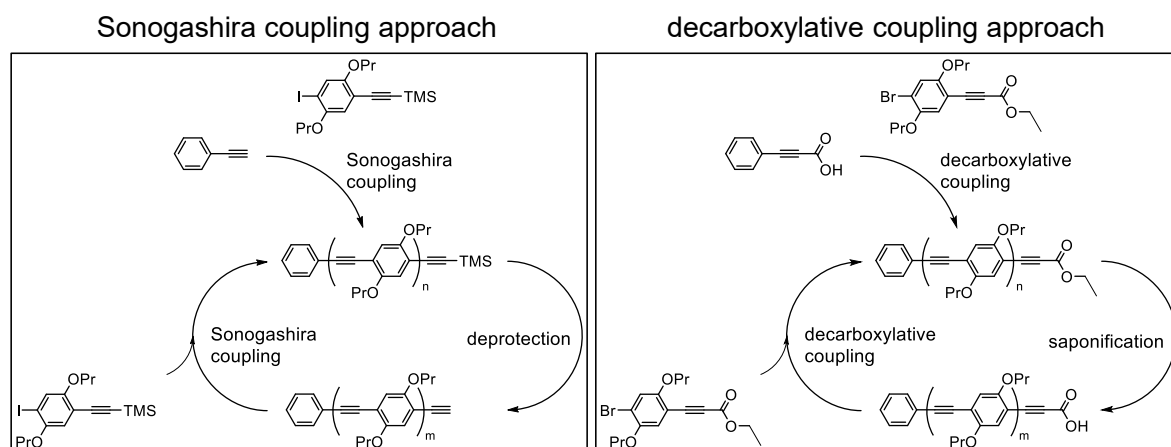


Figure 28: Left: established Sonogashira coupling approach consisting of Sonogashira coupling and subsequent deprotection. Adopted from Meier et al. Right: developed decarboxylative coupling approach based on decarboxylative coupling followed by saponification.

To clearly demonstrate the advantage of the herein described new synthesis strategy towards OPEs using the decarboxylative coupling, a thorough comparison to the reported Sonogashira approach from our group in 2018 was performed in terms of efficiency and working time (*cf.* Figure 28).<sup>[16]</sup> In the reported Sonogashira approach, a uniform pentamer and a sequence-defined pentamer were synthesized with an overall yield of 18% and 3.2%, respectively. However, the major drawback of this well-established procedure is the formation of a homocoupling product *via* Glaser coupling, which complicates the purification. Separation of the OPE from the Glaser side product *via* silica column chromatography required up to two weeks and was highly solvent consuming. Since both approaches lead to uniform OPEs, it is reasonable to compare and evaluate them regarding time, purification, and overall yield for the uniform pentamer.

The reaction setup for both approaches was very similar. All reactants and solvents were added to a Schlenk flask under an argon atmosphere. For the Sonogashira approach it was beneficial to dissolve the acetylene terminated oligomer first and slowly add it last to the reaction mixture to avoid homocoupling. Subsequently, the reaction mixture was stirred for the indicated time. Concerning the reaction temperature, the Sonogashira approach started at ambient temperature for the monomer but required elevated temperatures for the higher oligomers. In contrast, the decarboxylative coupling was conducted at 60 °C for each coupling step. The respective reaction times are summed up in Table 4.

Table 4: Overview of reaction times in the Sonogashira and the decarboxylative coupling approach.

reaction time	Sonogashira approach	decarboxylative coupling
monomer	48 h	16 h
deprotected monomer	12 h	16 h
dimer	72 h	16 h
deprotected dimer	12 h	16 h
trimer	48 h	16 h
deprotected trimer	12 h	16 h
tetramer	48 h	16 h
deprotected tetramer	12 h	16 h
pentamer	72 h	16 h
deprotected pentamer	12 h	16 h
overall	348 h	160 h

For the decarboxylative coupling approach, a reaction time of 16 hours over night was sufficient for any step to reach full conversion of the reactants (TLC). In the Sonogashira approach, a reaction time of 48 or 72 hours was needed for the coupling and 12 hours for the deprotection step. All ten reaction steps combined resulted in a reaction time of 160 hours for the decarboxylative coupling approach compared to 348 hours for the Sonogashira approach.

To obtain uniform oligomers, careful purification is essential after each synthetic step. The work-up for both approaches consist of several washing steps to remove inorganic salts which were formed during the reaction. The crude product was subsequently further purified by silica column chromatography which was inevitable to obtain the uniform OPEs. For oligomers obtained from the decarboxylative coupling approach, significantly faster elution was possible, since no homocoupling was observed until the trimer stage. After saponification, the alkynyl carboxylic acids were sufficiently pure and were used without further purification. From the tetramer stage on, the alkynyl carboxylic acids were purified *via* a fast to perform silica filtration column. However, during the Sonogashira approach, column chromatography was necessary after each coupling and deprotection step. The oligomers had to be eluted very slowly with a eluent mixture of

cyclohexane/dichloromethane to assure good separation from the homocoupling product, which is present from the first stage on. Often a second column was necessary to obtain the uniform oligomers. The deprotected oligomers were obtained after column chromatography as well. In total, 12 steps required purification with column chromatography in the Sonogashira approach. In contrast, in the decarboxylative coupling approach, only seven purification steps with faster column chromatography were necessary to obtain the final product. This saved time as well as large amounts of solvents and less waste was produced as a positive side effect.

Accompanied with the amount of column chromatography is the factor of active working time, which decreases significantly for the decarboxylative coupling approach. Table 5 sums up the required time for purification per cycle for both approaches.

*Table 5: Overview of estimated time needed for purification of the uniform oligomers.*

<b>purification time</b>	Sonogashira approach	Decarboxylative coupling
1st cycle	32 h	12 h
2nd cycle	48 h	12 h
3rd cycle	48 h	12 h
4th cycle	64 h	16 h
5th cycle	64 h	16 h
<b>Overall</b>	<b>256 h</b>	<b>68 h</b>

Column chromatography in the Sonogashira approach required up to ten days for one oligomer and purification for all ten steps took around 256 hours in total. Since less purification steps *via* column chromatography were performed and the oligomers can be eluted much faster in the decarboxylative coupling approach, the time for purification decreases to around 68 hours, which is approximately a quarter of the time and makes the newly developed approach much more time efficient.

An important measure for iterative synthesis strategies is the yield. The results of both approaches are compared in Table 6. The decarboxylative coupling approach shows yields ranging from 68-85% for all coupling steps. The length of the OPE chain does not seem to have a significant influence on the coupling reaction until the trimer stage. However, starting with the tetramer, the formation of the homocoupling product decreases the yield of the desired OPEs marginally. The Sonogashira coupling shows a continuously decreasing yield with a growing OPE chain, since the oligomers are more prone to undergo homocoupling. After 10 steps, a uniform pentamer is obtained with an overall yield of 14% for the decarboxylative coupling approach and 18% for the Sonogashira approach.

Table 6: Overview of the yield for the oligomers at any stage

yield	Sonogashira coupling		decarboxylative coupling	
	scale	yield	scale	yield
monomer	4.63 g	99%	515 mg	66%
deprotected monomer	3.15 g	97%	464 mg	100%
dimer	3.20 g	84%	516 mg	77%
deprotected dimer	2.63 g	100%	426 mg	100%
trimer	2.10 g	68%	416 mg	73%
deprotected trimer	1.74 g	98%	386 mg	100%
tetramer	1.22 g	65%	317 mg	80%
deprotected tetramer	682 mg	99%	226 mg	94%
pentamer	307 mg	53%	125 mg	68%
deprotected pentamer	116 mg	98%	73 mg	75%
overall		18%		14%

In summary, the comparison of the developed decarboxylative coupling approach to the established Sonogashira approach clearly highlights the advantages of the new synthesis concept. All results are summed up in Table 7.

*Table 7: Comparison of the combined results over ten reaction steps.*

---

	Decarboxylative coupling approach	Sonogashira approach
Reaction time	160 h	348 h
Purification	7 × column chromatography	12 × column chromatography
Time for purification	68 h	256 h
Overall yield	14%	18%

---

With the new synthesis concept OPEs were obtained in comparable overall yield. The main advantage is the time needed for the synthesis of the pentamer. Since less purification steps are needed, and the oligomers can be eluted faster the decarboxylative approach is much more time efficient. Still, the reaction conditions of the decarboxylative coupling were not thoroughly investigated and further optimized is possible.

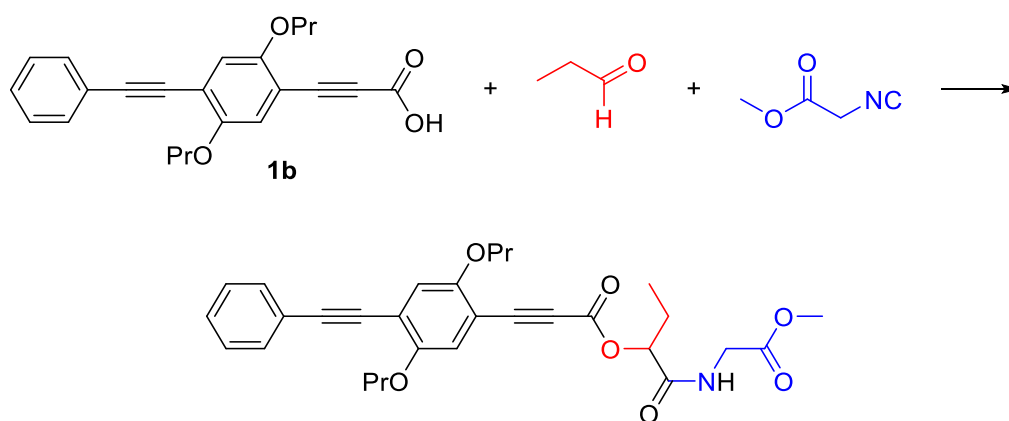
## 4.4 Application of uniform stiff-oligomers in Multicomponent Reactions

**Abstract**

MCRs, like the P-3CR and the U-4CR, are often used to synthesize complex molecules from easily accessible functional groups and simple scaffolds in one step. In here, the deprotected rod-like oligomers, introduced in this thesis, are combined with isocyanide-based MCRs to synthesize molecules with a rigid backbone bearing flexible and solubilizing elongations. First, the monomer **1b** is successfully used in the P-3CR with 99% yield. Furthermore, an iterative synthesis approach is investigated, combining the U-4CR and a Sonogashira coupling.

MCRs offer a wide range of applications. Generally, three or more components are reacted to form one complex molecule.<sup>[164]</sup> The modular character combined with high atom efficiency enables the synthesis of a great variety of molecules in a large scale.<sup>[165]</sup> Two of the most popular isocyanide-based MCRs are the P-3CR and the U-4CR.<sup>[166,167]</sup> In the classic P-3CR, a carboxylic acid is reacted with a carbonyl compound (aldehyde or ketone) and an isocyanide to yield a  $\alpha$ -acyloxyamide.<sup>[167]</sup> In the related U-4CR, an amine is added as a fourth component to the three mentioned reactants, to yield a *bis*-amide.<sup>[166]</sup> Since the oligomers **1b-5b** exhibit a free alkynyl carboxylic acid after saponification, they can be used in both MCRs, which would offer the possibility of further modifications.

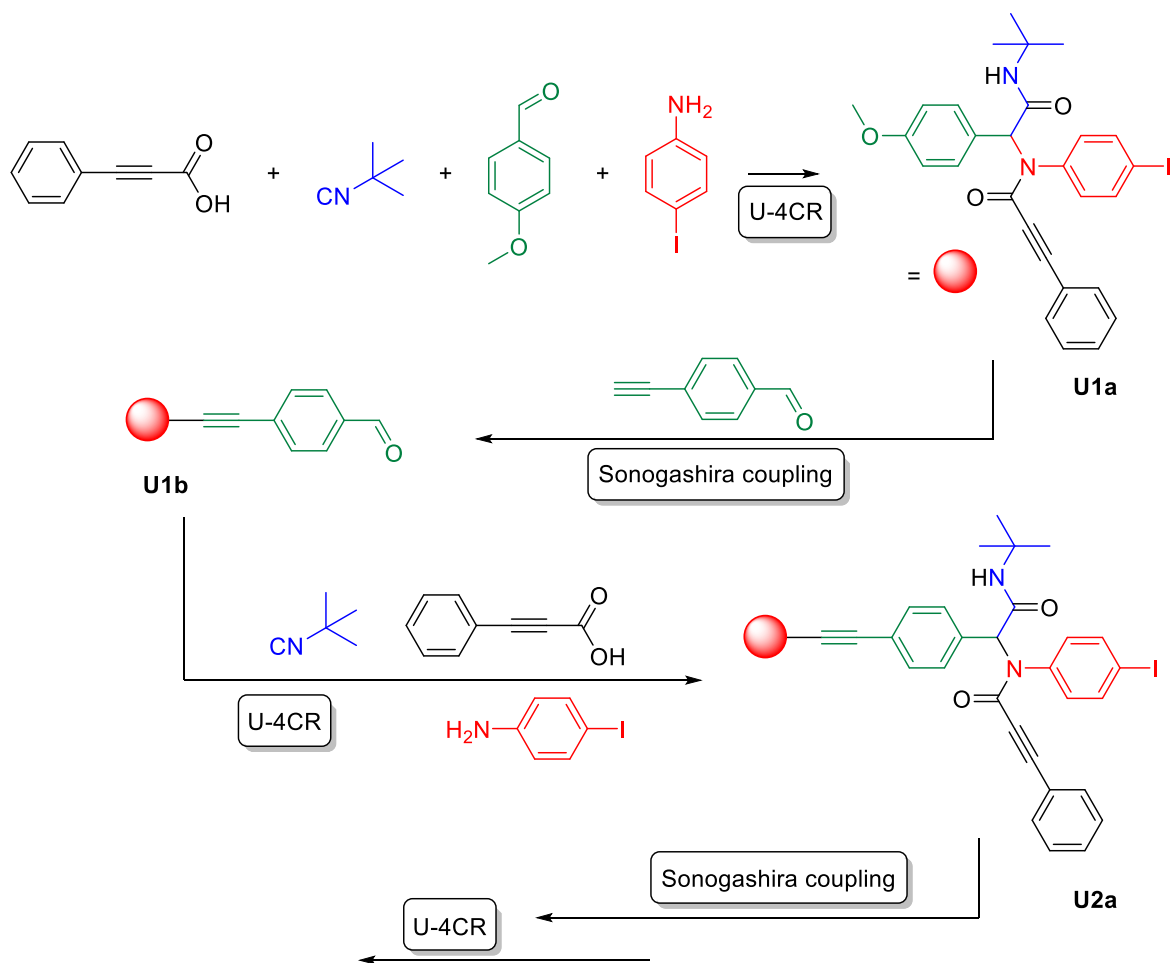
First, the monomer **1b** was used in a P-3CR together with propionaldehyde and methyl isocyanoacetate as a test reaction. The reaction is depicted in Scheme 39.



Scheme 39: Test reaction to incorporation of the monomer **1b** into a more complex molecule using the P-3CR.

Methyl isocyanoacetate was selected as an AB type monomer since further elongation of the flexible side by saponification of the methyl ester after the P-3CR is possibly offered. The product was obtained after purification *via* column chromatography in a scale of 516 mg and 99% yield. This first result indicated that the reactivity of an alkynyl carboxylic acid in a P-3CR is not decreased due to conjugation to an electron-rich aromatic moiety. Subsequently, a saponification was performed, however, since the structure features a second ester, the Passerini product degraded and the signals of the monomer **1b** were again observed while monitoring the reaction *via* <sup>1</sup>H NMR spectroscopy. Nevertheless, the P-3CR offers to opportunity to combine the defined rod-like oligomers, obtained in this thesis, with rather flexible scaffolds. The approach could be extended to the U-4CR reaction. Since a *bis*-amide is generated, degradation of the Ugi backbone could possibly be avoided.

Moreover, another iterative approach was investigated, in which the rod-like oligomers are utilized in a MCR. Typically, an AB type monomer, bearing isocyanide as well as an ester protected carboxylic acid, is used for the chain elongation and the carbonyl compound is varied to achieve sequence-definition.<sup>[134,136–139]</sup> However, to incorporate different carboxylic acid terminated rod-like oligomers into a more complex molecule, a different strategy based on the U-4CR and the Sonogashira coupling was investigated. The investigated concept is outlined in Scheme 40.



Scheme 40: Iterative two-step reaction procedure combining the U-4CR and the Sonogashira coupling. The 4-methoxy benzaldehyde is used as the starting aldehyde. Variation of the carboxylic acid and the isocyanide component would give control of the side groups.

The iterative two-step cycle starts with a U-4CR of phenyl propionic acid, *tert*-butyl isocyanide, 4-methoxy benzaldehyde and 4-iodoaniline. The use of 4-iodoaniline is essential as an iodine moiety is introduced to the Ugi product, which enables a subsequent Sonogashira coupling with 4-ethynyl benzaldehyde. Thus, an aldehyde functionality is introduced which enables a second U-4CR with 4-iodoaniline and so on. In this way, the roles of the components have changed compared to the before-mentioned P-3CR/hydration (chapter 2.2.1, Scheme 23) or U-4CR/thiol-ene approach (chapter 2.2.1): the isocyanide and the carboxylic acid can be varied instead of the amine and the carbonyl compound. Many amine and carbonyl compounds are commercially available and can therefore be varied easily in the synthesis of sequence-defined macromolecules. However, by now also isocyanides can be easily synthesized with a large scope, which could be used in the presented approach.<sup>[168]</sup>

To establish the iterative procedure, phenyl propiolic acid and *tert*-butyl isocyanide were used in the U-4CR and not varied. In the first U-4CR, 4-methoxy benzaldehyde served as carbonyl compound. The respective Ugi monomer **U1a** was obtained in a scale of 2.69 g with 95% yield. Subsequent Sonogashira coupling with 4-ethynyl benzaldehyde led to coupling product **U1b** with 61% yield, which was low compared to typical yields of Sonogashira couplings. Nevertheless, an aldehyde functionality was reintroduced in sufficient yield, and the product used in the next U-4CR with phenyl propiolic acid, *tert*-butyl isocyanide and 4-iodoaniline. The reaction was again straightforward and produced the Ugi dimer **U2a** with 89% yield, proving that this two-step iterative approach can be repeated. All molecules were completely characterized by proton and carbon NMR spectroscopy, IR spectroscopy, MS, and SEC. The respective SEC traces of the obtained products are depicted in Figure 29.

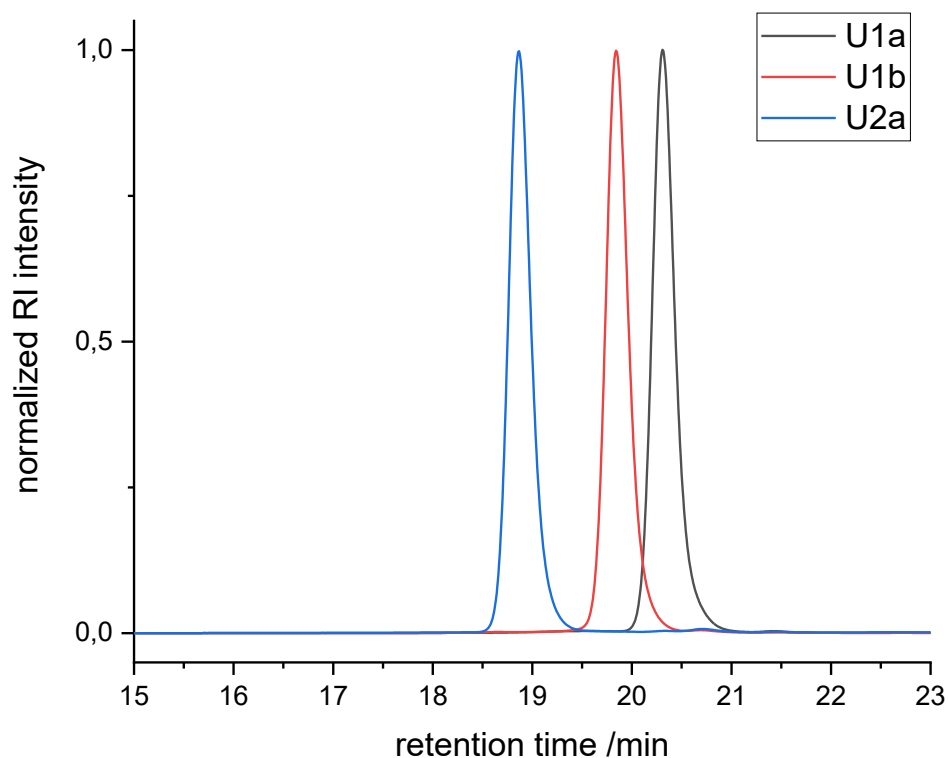


Figure 29: SEC traces after the first U-4CR (black), after the follow-up Sonogashira coupling (red) and after the second U-4CR (blue). The narrow peaks confirm the high purity and uniformity.

With the promising results using phenyl propiolic acid, the monomer **1b** was used in a first U-4CR as carboxylic acid component to evaluate the feasibility of this approach for different rod-like acid components. The respective Ugi product was obtained with 85% yield after simple purification *via* column chromatography. The

incorporated iodine moiety allows for further Sonogashira coupling, which was not performed yet.

In summary, the application of the rod-like oligomers, introduced in this thesis, in MCRs, namely the P-3CR and the U-4CR, was demonstrated. The P-3CR with the monomer acid **1b** proceeded straightforward and the respective Passerini product was obtained in excellent yield of 99%. Furthermore, an iterative two-step reaction cycle combining the U-4CR and the Sonogashira coupling was investigated. While high yields were obtained in the U-4CR, a comparably low yield was observed in the Sonogashira coupling and further investigations are needed. However, the developed synthesis procedure allows for variation of the carboxylic acid and the isocyanide component and incorporation of the rod-like molecules into more complex molecules is enabled.



## 5 Conclusion and Outlook

Conjugated rod-like macromolecules, like OPEs, have been synthesized by various groups for the investigation of their electronic and optical properties as well as antimicrobial activity. Most of the synthesis approaches rely on bidirectional Sonogashira coupling, forming sequence-defined, symmetric structures. Linear iterative approaches towards sequence-defined OPEs are rarely found. This is underlined by the fact that up to this date, only two examples have been reported. These iterative synthesis concepts are based on Sonogashira coupling as well, followed by deprotection of a TMS protected triple bond. However, purification is often complicated due to formation of unavoidable Glaser product. In this thesis, a new strategy towards conjugated rod-like macromolecules based on a decarboxylative coupling and subsequent saponification was developed. In order to identify and characterize products as well as detect potential impurities, a comprehensive investigation of the analytical methods, namely NMR spectroscopy, ESI-MS, and SEC was conducted. Therefore, the detection thresholds of the three different analytical methods were determined first by analyzing a uniform tetramer, which was intentionally contaminated with different ratios of a known impurity up to 15 wt%, *i.e.* the respective uniform trimer. Detection of the impurity was not possible using  $^1\text{H}$  NMR spectroscopy. The signals of the tetramer and trimer arose in the same ppm range and the integral values are in the error margins for NMR spectroscopy. Analysis of the mass spectra was challenging, since the signal of small amounts of impurity interfered with the baseline noise. If the impurity was known, detection of  $\geq 1\%$  was possible by comparison with the pure sample. Impurities higher than 7% were clearly detectable by ESI-MS. Finally, impurities  $\geq 1\%$  were detected *via* SEC. The impurity study revealed the strengths and weaknesses of each analytical method when used solely. To assure the successful synthesis and especially the high purity of the molecules, combination of all three analytical methods is thus indispensable.

To establish the developed iterative two-step synthesis strategy based on decarboxylative coupling followed by saponification, uniform OPEs with propoxy side chains were synthesized up to a DP of five. The deprotected pentamer was obtained after ten steps with an overall yield of 14% in excellent purity. Homocoupling was not observed until the trimer stage. In case of homocoupling for

the tetramer and the pentamer, the superiority of this approach was shown, since the purification was easily performed by saponifying the oligomer mixtures, which allowed fast silica filtration columns as only work-up step to obtain the pure deprotected oligomers (**4a-5a**). All molecules were completely characterized by proton and carbon NMR spectroscopy, IR spectroscopy, MS, and SEC. The results were then compared to the established Sonogashira approach, which was performed by Rebekka Schneider during a previous PhD thesis. With the new synthesis strategy, OPEs can be synthesized in a comparable overall yield within a third of the time (14% in 228 hours compared to 18% in 604 hours, respectively). Less purification steps were needed, and column chromatography was significantly facilitated. The main point of view had to be set on the purification process of this approach due to discussed reasons, therefore it has to be noted that the reaction conditions were only briefly optimized and further investigation is necessary, which would possibly improve the overall yield leading to further advantage over the Sonogashira-based approach.

As proof of concept, for further applications in sequence-definition, three different building units, based on thiophene, biphenyl and anthracene moieties, were synthesized in a related Bachelor Thesis. A sequence-defined trimer with the biphenyl building unit was obtained straightforwardly. Coupling of the anthracene building unit proved to be challenging, since the ethyl ester group assumably activates the triple bond leading to a reactive dienophile which could probably undergo Diels-Alder reaction with the anthracene. Nevertheless, it was shown that tailoring the backbone of the uniform oligomers is possible.

Furthermore, the obtained carboxylic acid bearing oligomers were used in MCRs. Utilization of the monomer **1a** in a P-3CR led to complex molecules with 99% yield. Combination of the rigid, rod-like oligomers with flexible scaffolds could lead to interesting structures regarding self-assembly. Since the oligomers derived from the new approach exhibit a carboxylic acid functionality, various applications seem possible.

The herein established two-step approach can be envisioned to be transferred to a bidirectional synthesis of OPEs. The rod-like structure combined with carboxylic acid terminated ends as well as the modular character of the approach makes them ideal candidates as linker for metal organic frameworks (MOFs). The exact positioning of

building units can lead to sequence-defined linkers for MOFs, which potentially allow fine tuning of the MOF properties.

Furthermore, the obtained OPEs could be connected to molecules with a TADF function. These TADF adducts are interesting compounds for plastic solar cells and thus investigated regarding their photophysical properties.<sup>[160]</sup>



## 6 Experimental Section

### 6.1 Materials

The following chemicals were used as received: acetic acid (96%, Roth), bromo hydroquinone (>90%, TCI), 1-bromopropane (99%, Fluka), 2-bromothiophene (98%, Sigma Aldrich), *tert*-butyl isocyanide (97%, Acros Organics), carbon dioxide (99.99% Air Liquide), cesium carbonate (99%, Sigma Aldrich), cesium fluoride (99.9%, Acros Organics), copper(I) iodide (98%, Sigma Aldrich), 9,10-dibromoanthracene (98%, Sigma Aldrich), 4,4'-dibromobiphenyl (98%, Sigma Aldrich), 2-dicyclohexylphosphin-2',6'-dimethoxybiphenyl (98%, abcr), diisopropyl amine (>99.5, Sigma Aldrich), [1,1'-Bis(diphenylphosphino)ferrocene] dichloropalladium(II) complex with dichloromethane (98%, fluoro chem), 4-ethynyl benzaldehyde (98%, BLD Pharm), hydroquinone ( $\geq 99\%$ , Bayer), iodethane (98+ %, Alfa Aesar), iodine (>98%, TCI), 4-iodoaniline (98%, Sigma Aldrich), methyl isocyanoacetate (95%, Acros Organics), periodic acid (for analysis, Merck), phenylpropionic acid (99%, Sigma Aldrich), potassium hydroxide (for analysis, Bernd Kraft), potassium metabisulfite (97% Acros Organics), propionaldehyde (97%, Sigma Aldrich), sodium hydroxide (for analysis, Bernd Kraft), sodium sulfate (anhydrous, Bernd Kraft), sodium thiosulfate (anhydrous, Sigma Aldrich), triethylamine (>99.5%, Sigma Aldrich), trimethylsilyl acetylene (99%, fluoro chem), bis(triphenylphosphine)palladium(II) dichloride (98%, Acros Organics), ethanol (99.8%, Fisher chemicals), dimethyl sulfoxide ( $\geq 99.9\%$ , Sigma Aldrich), methanol (HPLC grade, VWR chemicals), tetrahydrofuran ( $\geq 99.9\%$ , Sigma Aldrich), toluene (99.85%, Acros Organics), tris(dibenzylideneacetone)dipalladium (>98%, fluoro chem). Solvents like ethyl acetate, cyclohexane, dichloromethane and acetone were used in HPLC grade without further purification. Diethyl ether was used in technical grade. Silica gel (technical grade, pore size 60 Å. 230-400 mesh particle size, 40-63  $\mu\text{m}$  particle size) was purchased from Sigma-Aldrich.

### 6.2 Instrumentation

#### *Nuclear Magnetic Resonance (NMR)*

$^1\text{H}$  and  $^{13}\text{C}$  spectra were recorded at the Karlsruhe Institute of Technology (KIT, Germany) on a Bruker Avance 400 NMR instrument at 400 MHz for  $^1\text{H}$  NMR and 101 MHz for  $^{13}\text{C}$  NMR or on a Bruker AVANCE DRX at 500 MHz for  $^1\text{H}$ -NMR and 126 MHz for  $^{13}\text{C}$  NMR.  $\text{CDCl}_3$  was used as solvent. Chemical shifts are presented in parts per million ( $\delta$ ) relative to the resonance signal at 7.26 ppm ( $^1\text{H}$ ,  $\text{CDCl}_3$ ) and 77.16 ppm ( $^{13}\text{C}$ ,  $\text{CDCl}_3$ ). The spin multiplicity and corresponding signal patterns were abbreviated as follows: s = singlet, d = doublet, t = triplet, q = quartet, quint. = quintet, sext. = sextet, m = multiplet and br = broad signal. Coupling constants ( $J$ ) are reported in Hertz (Hz). All measurements were recorded in a standard fashion at 25 °C unless otherwise stated. Full assignment of structures was aided by 2D NMR analysis (COSY, HSQC and HMBC).

#### *Size Exclusion Chromatography (SEC)*

Measurements were performed on a SHIMADZU Size Exclusion Chromatography (SEC) system equipped with a SHIMADZU isocratic pump (LCYCLO20AD), a SHIMADZU refractive index detector (24 °C) (RID-20A), a SHIMADZU autosampler (SIL-20A) and a VARIAN column oven (510, 50 °C). For separation, a three-column setup was used with one SDV 3  $\mu\text{m}$ , 8×50 mm precolumn and two SDV 3  $\mu\text{m}$ , 1000 Å, 3×300 mm columns supplied by PSS, Germany. Tetrahydrofuran (THF) stabilized with 250 ppm butylated hydroxytoluene (BHT,  $\geq 99.9\%$ ) supplied by SIGMA-ALDRICH was used at a flow rate of 1.0 mL  $\text{min}^{-1}$ . Calibration was carried out by injection of eight narrow polymethylmethacrylate (PMMA) standards ranging from 102 to 58300 kDa.

#### *Orbitrap Electrospray-Ionization Mass Spectrometry (ESI-MS)*

Mass spectra were recorded on a Q Exactive (Orbitrap) mass spectrometer (Thermo Fisher Scientific, San Jose, CA, USA) equipped with an atmospheric pressure ionization source operating in the nebulizer assisted electrospray mode. The instrument was calibrated in the  $m/z$ -range 150-2000 using a standard containing caffeine, Met-Arg-Phe-Ala acetate (MRFA) and a mixture of fluorinated phosphazenes (Ultramark 1621, all from SIGMA-ALDRICH). A constant spray voltage of 3.5 kV, a dimensionless sheath gas of 6, and a sweep gas flow rate of 2 were

applied. The capillary voltage and the S-lens RF level were set to 68.0 V and 320 °C, respectively. For the interpretation of the spectra, molecular peaks  $[M]^+$ , peaks of pseudo molecules  $[M+H]^+$  and  $[M+Na]^+$  characteristic fragment peaks are indicated with their mass to charge ratio ( $m/z$ ) and their intensity in percent, relative to the most intense peak (100%).

#### *Electron ionization (EI)*

Mass spectra were recorded on a Finnigan instrument, model MAT 90 (70 eV). 3-nitrobenzyl alcohol (3-NBA) was used as matrix. For the interpretation of the spectra, molecular peaks  $[M]^+$ , peaks of pseudo molecules  $[M+H]^+$  and characteristic fragment peaks are indicated with their mass to charge ratio ( $m/z$ ) and their intensity in percent, relative to the most intense peak (100%).

#### *Fast atom bombardment (FAB)*

Mass spectra were recorded on a Finnigan MAT 95 instrument. The protonated molecule ion is expressed by the term:  $[M+H]^+$  and  $[M+Na]^+$

#### *Infrared spectra (IR)*

IR were recorded on a Bruker Alpha-p instrument in a frequency range from 3998 to 374  $\text{cm}^{-1}$  applying KBr and Attenuated Total Reflection (ATR) technology. IR (Type of measurement)  $\nu / \text{cm}^{-1}$  = wave number (signal intensity, molecular oscillation assignment).

#### *Thin layer chromatography (TLC)*

All TLC experiments were performed on silica gel coated aluminum foil (silica gel 60 F<sub>254</sub>, SIGMA-ALDRICH). Compounds were visualized first by fluorescence quenching ( $\lambda = 254 \text{ nm}$  and  $365 \text{ nm}$ ), and staining with Seebach-solution (mixture of phosphomolybdic acid hydrate, cerium(IV)-sulfate, sulfuric acid and water).

### 6.3 Experimental Procedures

#### 6.3.1 Analyzing Macromolecules

The molecules were gratefully obtained from Dr. Rebekka Schneider. For experimental details see the corresponding publication:

R. V. Schneider, K. A. Waibel, A. P. Arndt, M. Lang, R. Seim, D. Busko, S. Bräse, U. Lemmer, M. A. R. Meier, *Sci. Rep.* **2018**, *8*, 17483.

*NMR spectroscopy:*

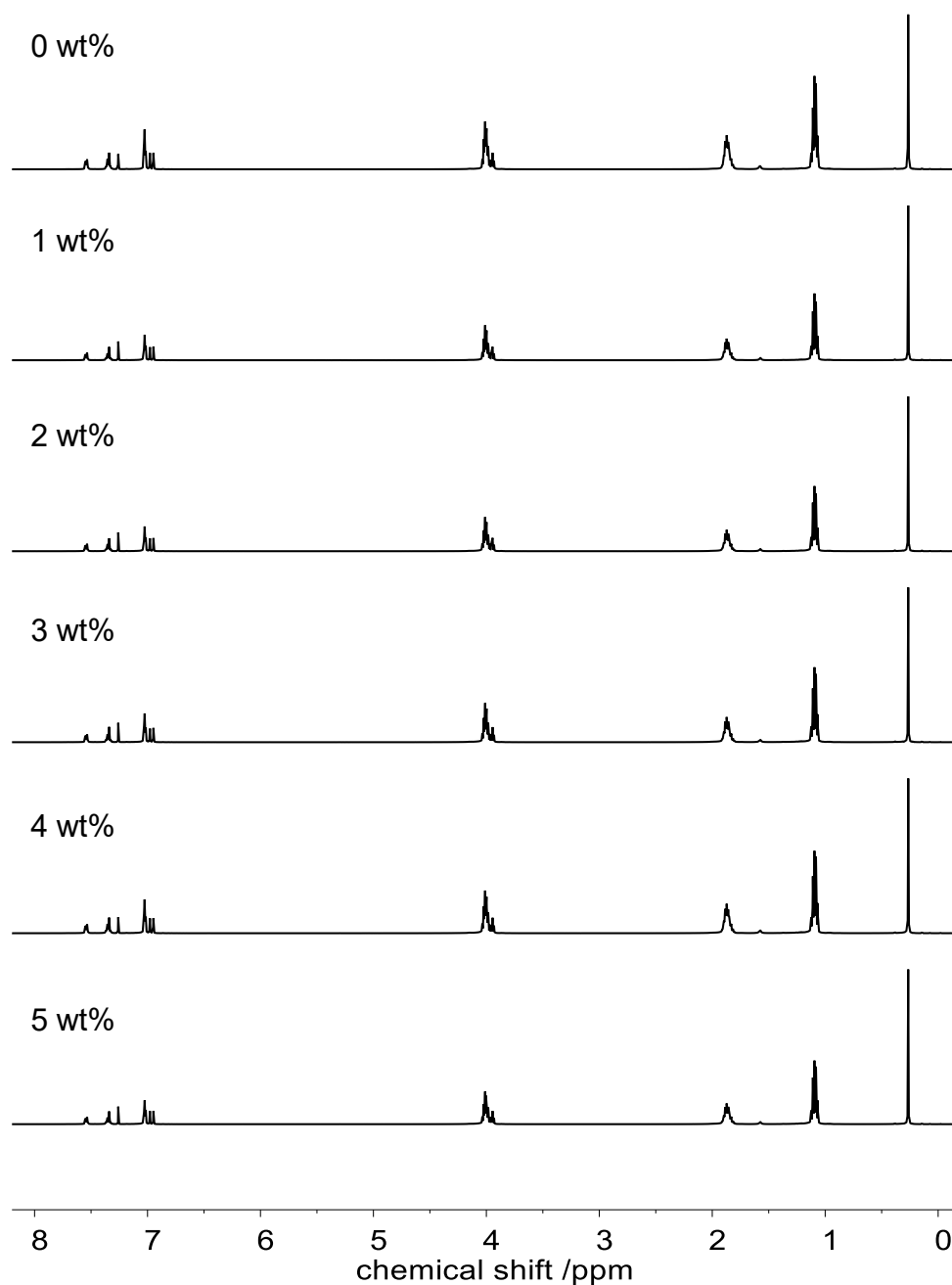


Figure S1: <sup>1</sup>H NMR spectra of the samples with 0-5 wt% impurity.

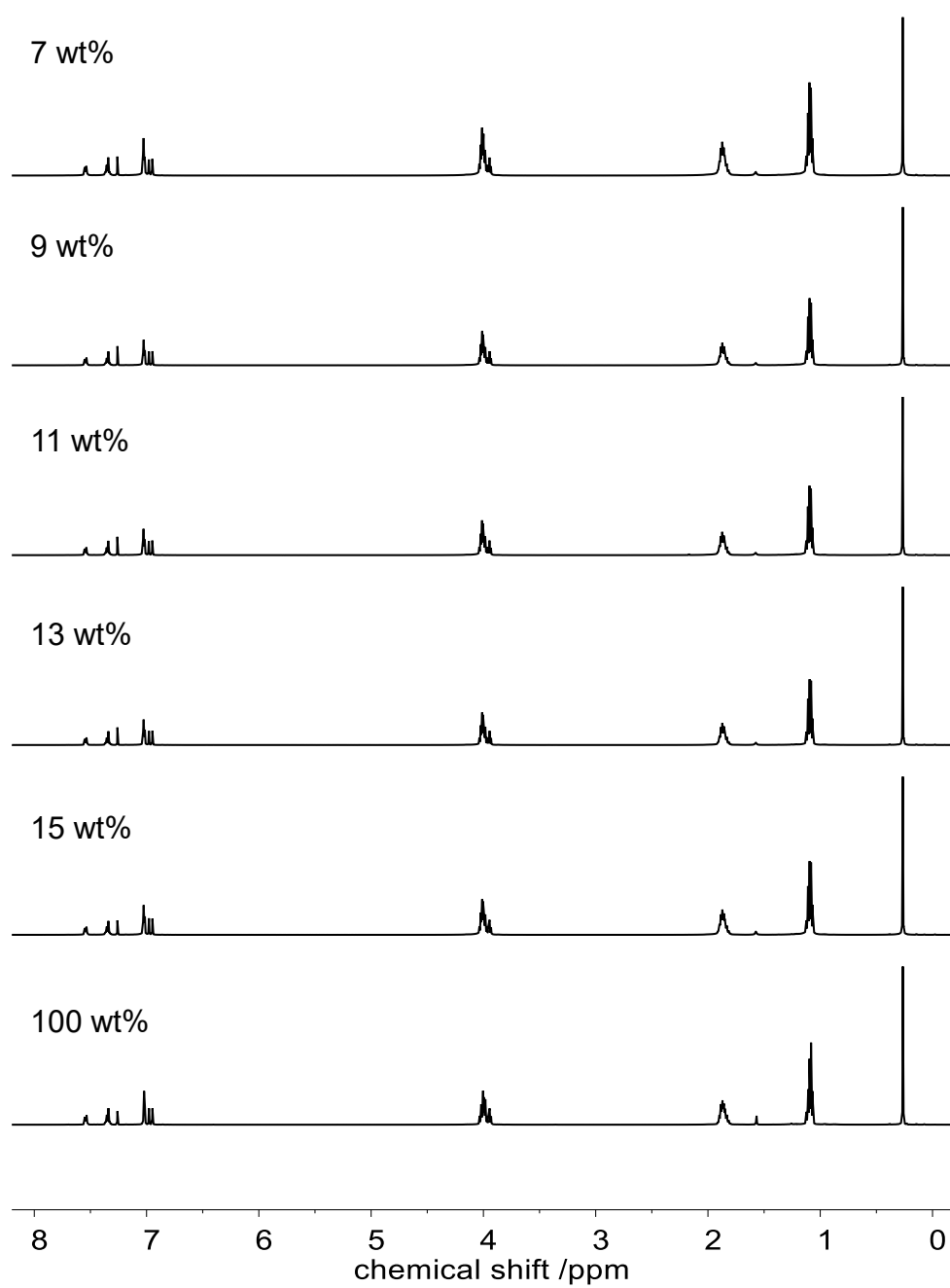


Figure S2:  $^1\text{H}$  NMR spectra of the samples with 7-15 wt% impurity.

Mass spectrometry:

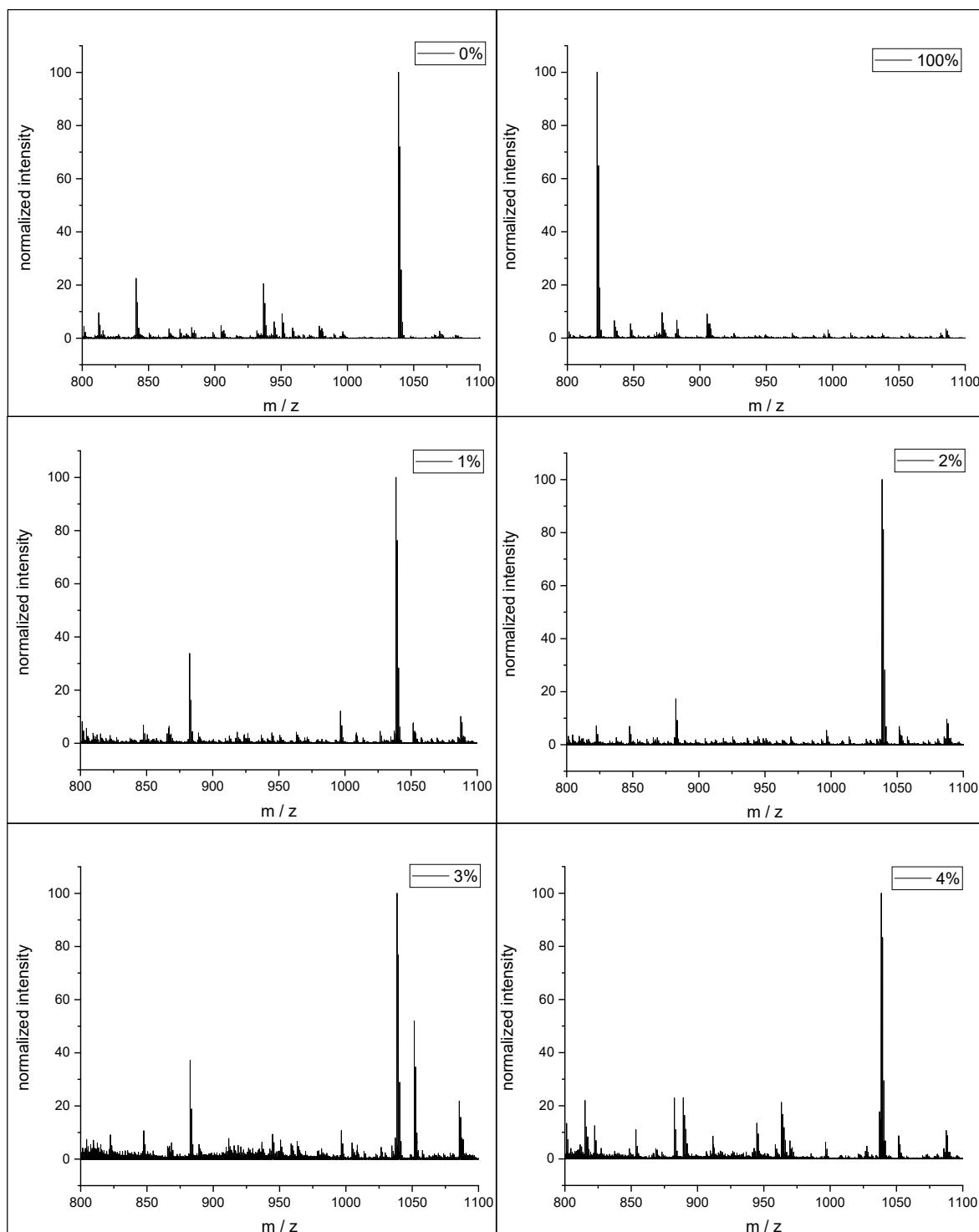


Figure S3: ESI-MS spectra of the impurity study

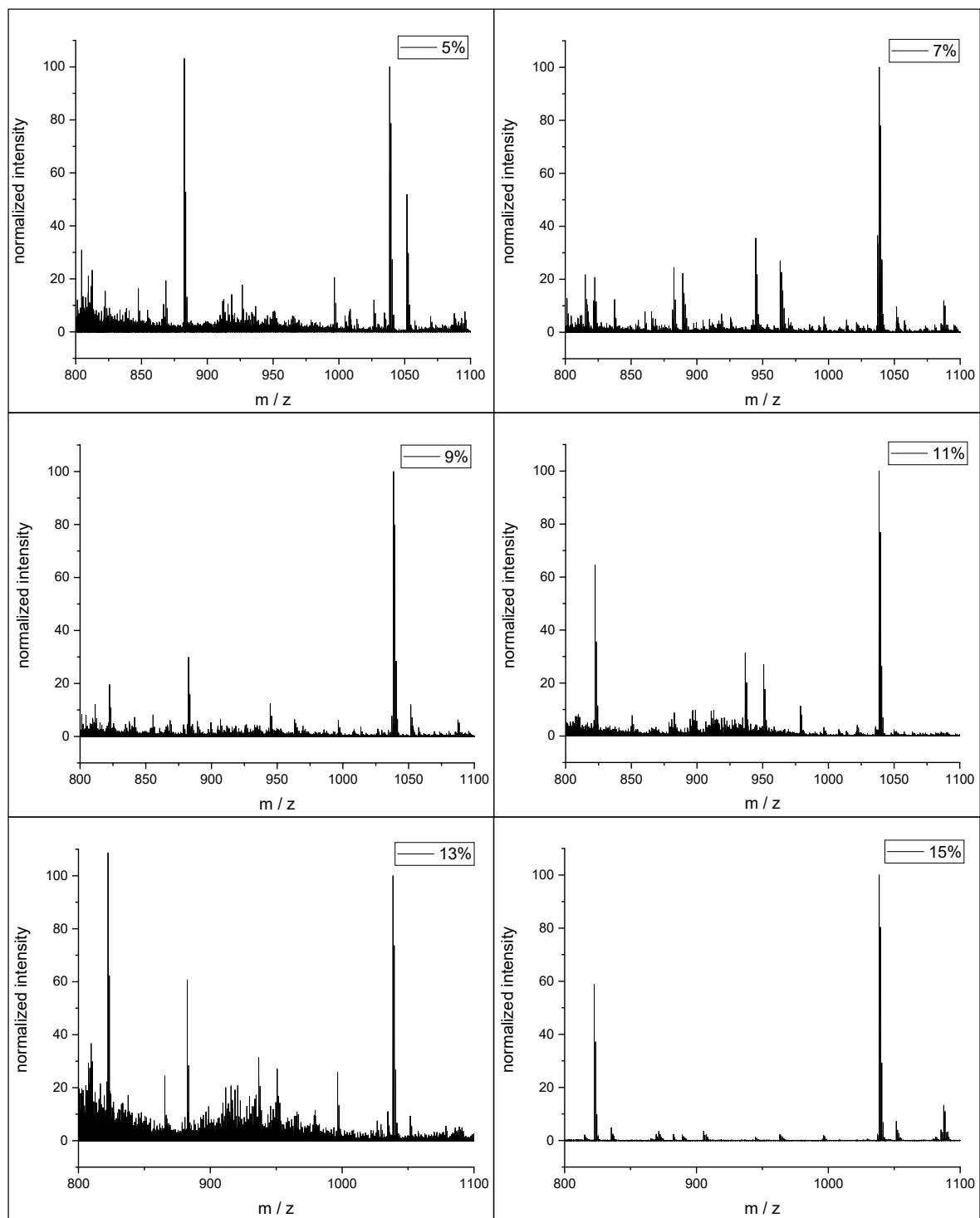


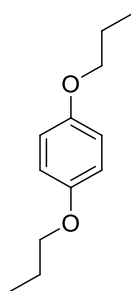
Figure S4: ESI-MS spectra of the impurity study

### 6.3.2 Synthesis of the Building Units

Parts of this chapter have been published before as a part of the supplementary information:

D. Hahn, R. V. Schneider, E. Foitzik, M. A. R. Meier, *Macromol. Rapid Commun.* **2021**, 2000735.

#### *Synthesis of 1,4-dipropoxybenzene (IB1a)*



Hydroquinone (22.0 g, 200 mmol, 1.00 eq.) was dissolved in 200 mL absolute ethanol. Potassium hydroxide (28.0 g, 500 mmol, 2.50 eq.) was added and the mixture was stirred for 30 min under reflux. Subsequently, 1-bromopropane (45.5 mL, 61.5 g, 500 mmol, 2.50 eq.) was slowly added over a 50-minute period and stirred under reflux for another 2 h. Ethanol was removed under reduced pressure and the residue was taken up in dichloromethane. The organic phase was washed with water for three times, once more with saturated NaHCO<sub>3</sub> solution and dried over sodium sulfate. Afterwards the solvent was removed under reduced pressure and the crude product was purified *via* silica filtration column (cyclohexane/ethyl acetate 20:1) to yield a white solid (26.1 g, 135 mmol, 67 %).

R<sub>f</sub> = 0.81 in cyclohexane/ethyl acetate (5:1). Visualized *via* Seebach staining solution.

<sup>1</sup>H NMR (400 MHz, CDCl<sub>3</sub>): δ(ppm) = 6.84 (s, 4H, CH<sub>ar</sub>), 3.87 (t, *J* = 6.6 Hz, 4H, CH<sub>2</sub>), 1.79 (h, *J* = 7.4 Hz, 4H, CH<sub>2</sub>), 1.03 (t, *J* = 7.4 Hz, 6H, CH<sub>3</sub>).

<sup>13</sup>C NMR (101 MHz, CDCl<sub>3</sub>): δ(ppm) = 153.31, 115.51, 70.28, 22.82, 10.66.

IR (ATR): ν / cm<sup>-1</sup> = 2963, 2936, 2875, 1504, 1461, 1392, 1275, 1218, 1115, 1069, 1049, 1026, 1005, 979, 907, 887, 824, 805, 793, 770, 736, 723, 530.

HRMS (ESI) of  $[M]^+$   $[C_{12}H_{18}O_2]^+$ : calc. 195.1379; found 195.1374,  $\Delta = 0.5$  mmu

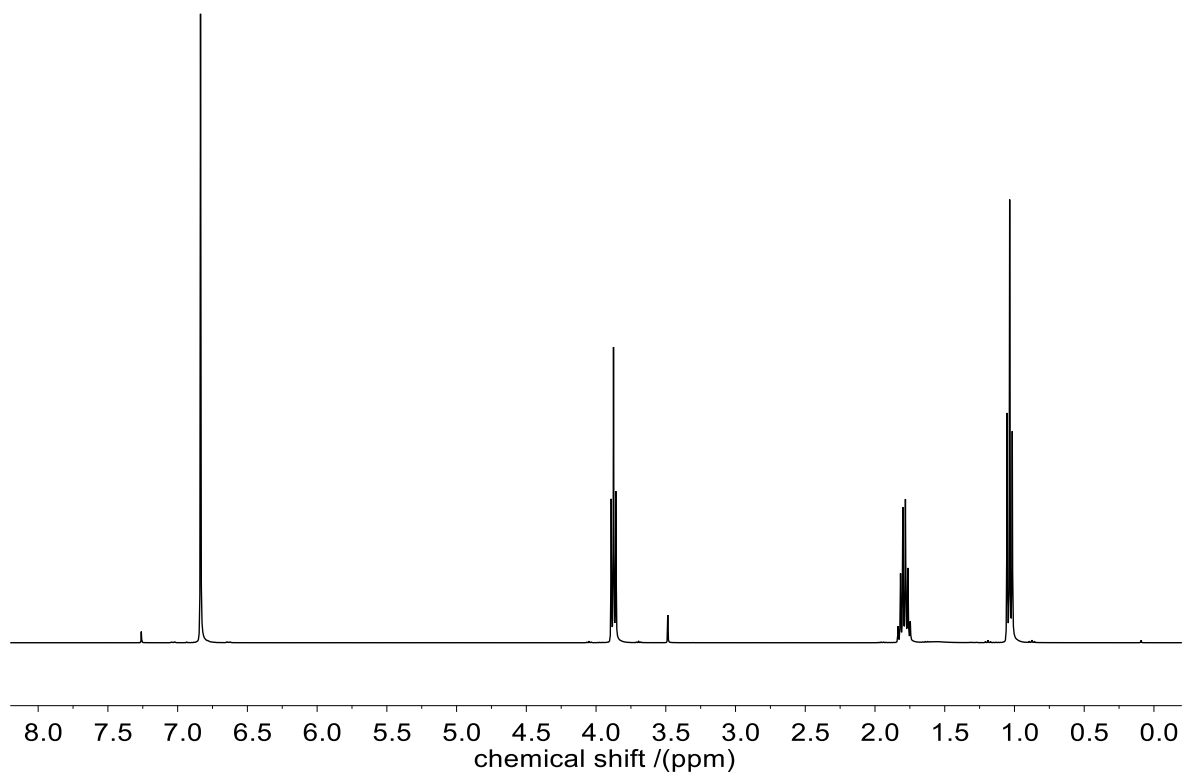
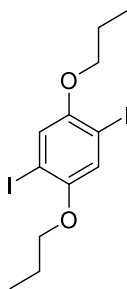


Figure S5:  $^1H$  NMR spectrum of **IB1a** measured in  $CDCl_3$ .

### Synthesis of 1,4-Diiodo-2,5-dipropoxybenzene (**IB1b**)



Periodic acid (12.0 g, 52.4 mmol, 0.68 eq.) was dissolved in 100 mL methanol and stirred for 10 minutes. Subsequently, iodine (26.3 g, 103 mmol, 1.34 eq.) was added and after an additional reaction time of 10 minutes 1,4-dipropoxybenzene (**IB1a**) (15.0 g, 77.2 mmol, 1.00 eq.) was added. The reaction mixture was stirred under reflux for 4 h. The residue was carefully poured into 400 mL water containing potassium metabisulfite (25.7 g, 116 mmol, 1.50 eq.). The precipitate was washed with methanol and dissolved in dichloromethane. The solution was filtered, and the

filtrate was concentrated under reduced pressure. The residue was purified by recrystallization from methanol (250 mL) to yield the product as a white solid (27.4 g, 61.5 mmol, 80%).

$R_f = 0.84$  in cyclohexane/ethyl acetate (5:1). Visualized *via* Seebach staining solution.

$^1\text{H}$  NMR (400 MHz,  $\text{CDCl}_3$ ):  $\delta(\text{ppm}) = 7.17$  (s, 2H,  $\text{CH}_{\text{ar}}$ ), 3.90 (t,  $J = 6.4$  Hz, 4H,  $\text{CH}_2$ ), 1.83 (h,  $J = 7.4$  Hz, 4H,  $\text{CH}_2$ ), 1.07 (t,  $J = 7.4$  Hz, 6H,  $\text{CH}_3$ ).

$^{13}\text{C}$  NMR (101 MHz,  $\text{CDCl}_3$ ):  $\delta(\text{ppm}) = 153.73, 123.71, 87.22, 72.75, 23.52, 11.63$ .

IR (ATR):  $\nu / \text{cm}^{-1} = 3853, 3734, 3648, 3617, 3099, 2958, 2908, 2870, 2342, 2219, 2053, 2017, 1968, 1944, 1682, 1558, 1487, 1463, 1448, 1393, 1376, 1348, 1263, 1244, 1207, 1126, 1054, 1039, 1006, 909, 850, 796, 768, 620, 506, 459, 434, 421$ .

HRMS (EI) of  $[\text{M}]^+$   $[\text{C}_{12}\text{H}_{16}\text{I}_2\text{O}_2]^+$  calc. 445.9240; found 446.9239,  $\Delta = 0.1$  mmu.

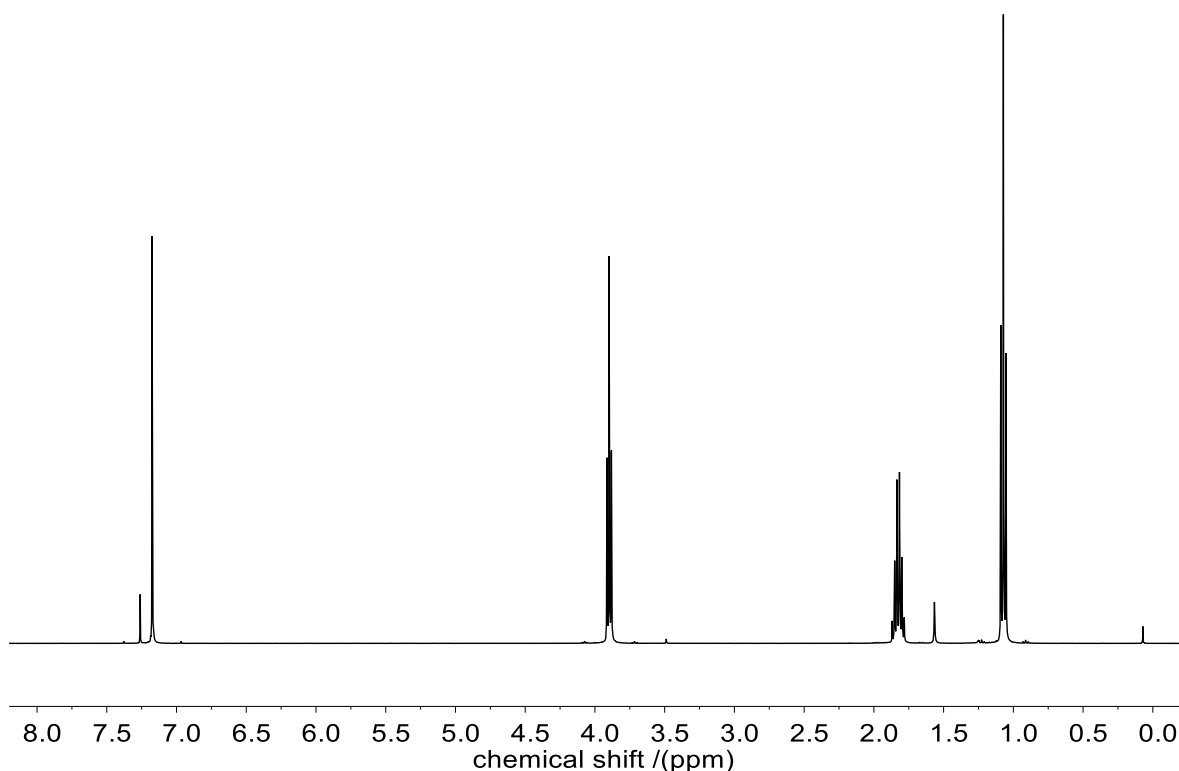
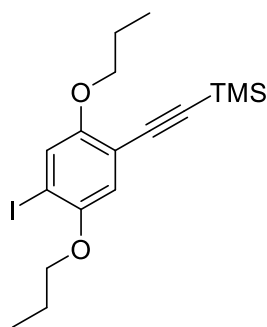


Figure S6:  $^1\text{H}$  NMR spectrum of **IB1b** measured in  $\text{CDCl}_3$ .

Synthesis of 1,4-bis(propyloxy)-2-iodo-5-trimethylsilylacetylenebenzene (**IB1c**)



**IB1b** (10.0 g, 22.4 mmol, 1.00 eq.), 2.5 mol% *bis*(triphenylphosphine)palladium(II) dichloride (393 mg, 560  $\mu$ mol, 0.025 eq.) and 5 mol% copper(I) iodide (214 mg, 1.12 mmol, 0.05 eq.) were placed into a Schlenk flask and degassed. Under continuous argon flow, 400 mL dry THF and 31.1 mL dry triethylamine were added. The mixture was stirred for 10 minutes. Subsequently, 3.41 mL trimethylsilyl acetylene (2.42 g, 24.7 mmol, 1.10 eq.) were added dropwise. The reaction mixture was stirred for 20 hours at ambient temperature. Saturated ammonium chloride solution was added, and the phases separated. The organic phase was washed once more with saturated ammonium chloride solution. The combined aqueous phases were extracted three times with dichloromethane. The combined organic phases were dried over sodium sulfate, filtered and concentrated under reduced pressure. The residue was purified by silica column chromatography (cyclohexane/dichloromethane 9:1) to yield the product as a yellow solid (4.09 g, 9.83 mmol, 44%).

$R_f$  = 0.25 cyclohexane/dichloromethane (9:1). Visualized *via* Seebach staining solution.

$^1\text{H}$  NMR (400 MHz,  $\text{CDCl}_3$ ):  $\delta$ (ppm) = 7.26 (s, 1H,  $\text{CH}_{\text{ar}}$ ), 6.84 (s, 1H,  $\text{CH}_{\text{ar}}$ ), 3.91 (t,  $J$  = 6.3 Hz, 4H,  $\text{CH}_2$ ), 1.88 – 1.77 (m, 4H,  $\text{CH}_2$ ), 1.07 (t,  $J$  = 7.4 Hz, 6H,  $\text{CH}_3$ ), 0.25 (s, 9H,  $\text{CH}_3$ ).

$^{13}\text{C}$  NMR (101 MHz,  $\text{CDCl}_3$ ):  $\delta$ (ppm) = 155.02, 151.84, 124.16, 116.43, 113.67, 100.91, 99.60, 88.03, 71.72, 71.49, 22.83, 22.76, 10.86, 10.62, 0.07.

IR (ATR):  $\nu$  /  $\text{cm}^{-1}$  = 638, 664, 697, 736, 757, 839, 954, 979, 1012, 1047, 1068, 1160, 1214, 1246, 1259, 1267, 1374, 1462, 1493, 2147, 2876, 2935, 2962.

HRMS (FAB) of  $[\text{M}]^+$   $[\text{C}_{17}\text{H}_{25}\text{IO}_2\text{Si}]^+$ : calc. 416.0663; found 416.0661;  $\Delta$  = 0.2 mmu

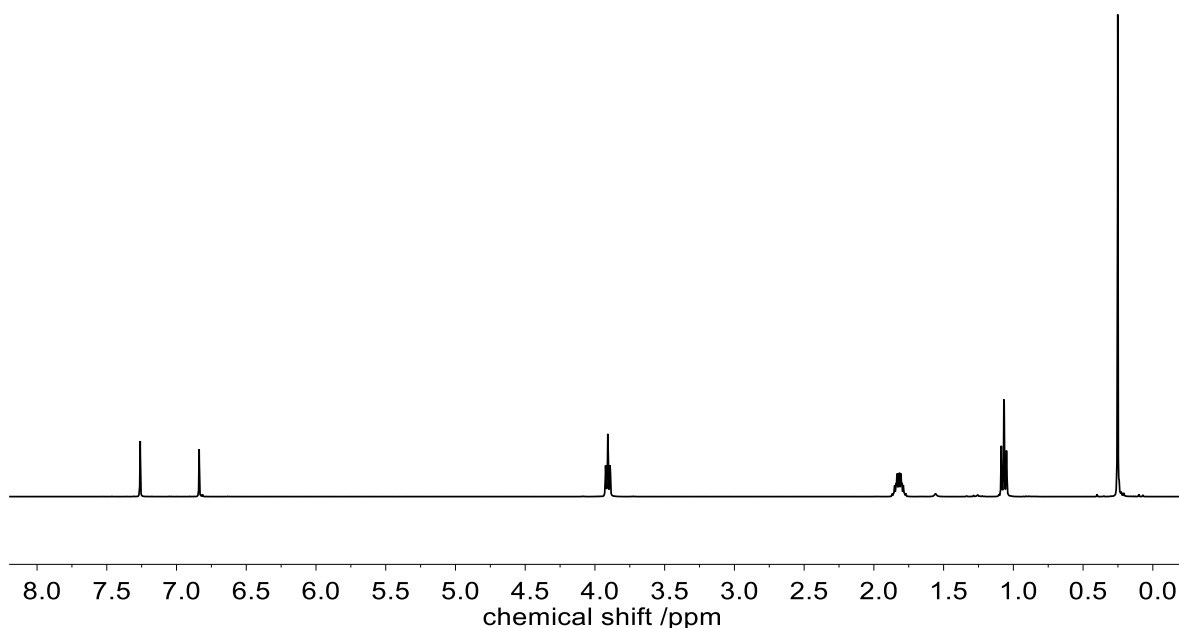
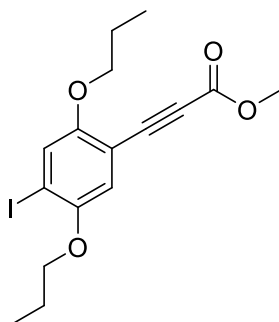


Figure S7:  $^1\text{H}$  NMR spectrum of **IB1c** measured in  $\text{CDCl}_3$ .

#### Synthesis of methyl 3-(4-iodo-2,5-dipropoxyphenyl) propiolate



**IB1c** (5.00 g, 12.0 mmol, 1.00 eq.) and cesium fluoride (2.19 g, 14.4 mmol, 1.20 eq.) were placed into Schlenk flask, degassed, and backfilled with  $\text{CO}_2$  gas. Subsequently, 35 mL DMSO was added, and the resulting solution was stirred for three hours at ambient temperature. Ethyl iodide (1.05 mL, 2.04 g, 14.4 mmol, 1.20 eq.) was added dropwise and the reaction mixture was stirred over night at ambient temperature. The reaction was quenched by addition of 80 mL saturated ammonium chloride solution. The mixture was extracted three times with 150 mL ethyl acetate and the combined organic phases washed once with brine. The solvent was removed under reduced pressure, and the residue purified by column chromatography (cyclohexane/ethyl acetate 40:1 $\rightarrow$ 30:1). The product was isolated as a white solid (4.68 g, 11.6 mmol, 97%).

$R_f = 0.26$  in cyclohexane/ethyl acetate (20:1). Visualized *via* Seebach staining solution.

$^1\text{H}$  NMR (400 MHz,  $\text{CDCl}_3$ ):  $\delta(\text{ppm}) = 7.32$  (s, 1H,  $\text{CH}_{\text{ar}}$ ), 6.89 (s, 1H,  $\text{CH}_{\text{ar}}$ ), 3.94 (t,  $J = 6.5$  Hz, 2H,  $\text{CH}_2$ ), 3.90 (t,  $J = 6.4$  Hz, 2H,  $\text{CH}_2$ ), 3.83 (s, 3H,  $\text{CH}_3$ ), 1.89 – 1.76 (m, 4H,  $\text{CH}_2$ ), 1.07 (t,  $J = 7.3$  Hz, 3H,  $\text{CH}_3$ ), 1.06 (t,  $J = 7.3$  Hz, 3H,  $\text{CH}_3$ ).

$^{13}\text{C}$  NMR (101 MHz,  $\text{CDCl}_3$ ):  $\delta(\text{ppm}) = 155.86, 154.68, 151.86, 124.17, 116.77, 109.69, 91.72, 84.81, 83.28, 71.73, 71.52, 52.90, 22.66, 22.64, 10.82, 10.52$ .

IR (ATR):  $\nu / \text{cm}^{-1} = 621, 652, 743, 767, 790, 817, 845, 868, 909, 950, 985, 1004, 1037, 1070, 1129, 1156, 1195, 1216, 1240, 1265, 1316, 1378, 1436, 1467, 1495, 1557, 1592, 1713, 2211, 2876, 2945, 2962$ .

HRMS (FAB) of  $[\text{M}]^+$   $[\text{C}_{16}\text{H}_{19}\text{IO}_4]^+$ : calc. 402.0323; found 402.0325;  $\Delta = 0.2$  mmu

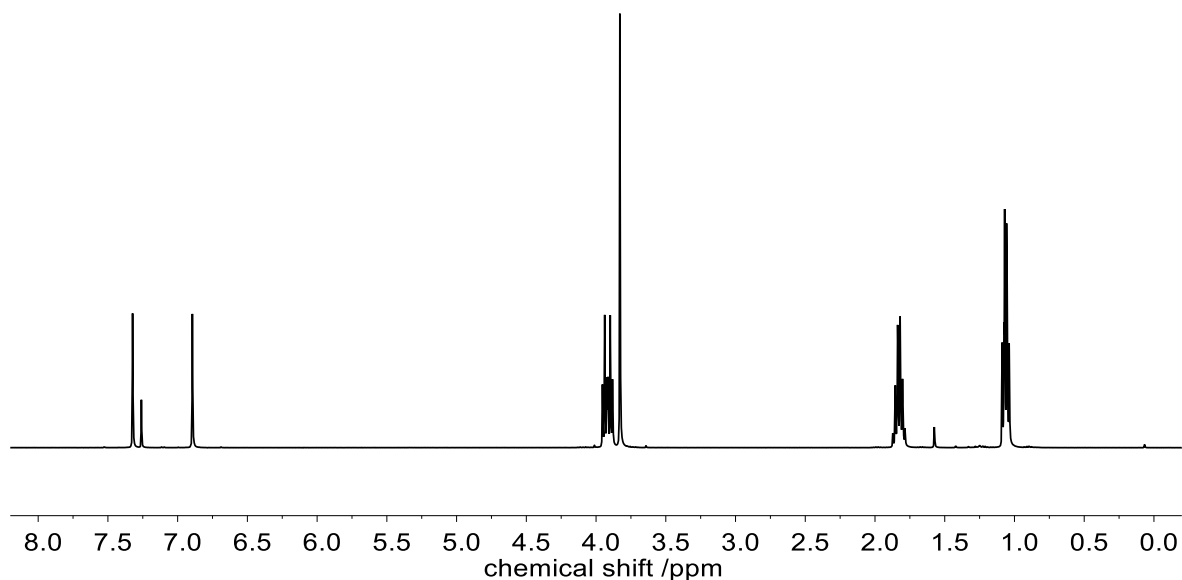
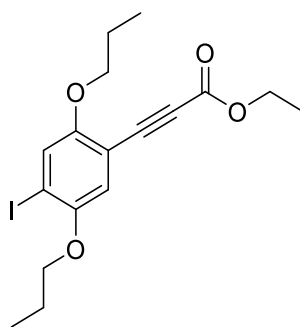


Figure S8:  $^1\text{H}$  NMR spectrum of **IB1** measured in  $\text{CDCl}_3$ .

Synthesis of ethyl 3-(4-iodo-2,5-dipropoxyphenyl) propiolate (**IB1**)

**IB1c** (3.85 g, 9.26 mmol, 1.00 eq.) and cesium fluoride (1.69 g, 11.1 mmol, 1.20 eq.) were placed into Schlenk flask, degassed, and backfilled with CO<sub>2</sub> gas. Subsequently, 30 mL DMSO was added, and the resulting solution was stirred for three hours at ambient temperature. Ethyliodide (893  $\mu$ L, 1.73 g, 11.1 mmol, 1.20 eq.) was added dropwise and the reaction mixture was stirred over night at ambient temperature. The reaction was quenched by addition of 80 mL saturated ammonium chloride solution. The mixture was extracted three times with 100 mL ethyl acetate and the combined organic phases washed once with brine. The solvent was removed under reduced pressure, and the residue purified by column chromatography (cyclohexane/ethyl acetate 40:1 $\rightarrow$ 30:1). The product was isolated as a white solid (2.85 g, 6.84 mmol, 74%).

R<sub>f</sub> = 0.31 in cyclohexane/ethyl acetate (20:1). Visualized *via* Seebach staining solution.

<sup>1</sup>H NMR (400 MHz, CDCl<sub>3</sub>):  $\delta$ (ppm) = 7.32 (s, 1H, CH<sub>ar</sub>), 6.90 (s, 1H, CH<sub>ar</sub>), 4.29 (q,  $J$  = 7.1 Hz, 2H, CH<sub>2</sub>), 3.94 (t,  $J$  = 6.5 Hz, 2H, CH<sub>2</sub>), 3.90 (t,  $J$  = 6.4 Hz, 2H, CH<sub>2</sub>), 1.88 – 1.78 (m, 4H, CH<sub>2</sub>), 1.34 (t,  $J$  = 7.1 Hz, 3H, CH<sub>3</sub>), 1.07 (t,  $J$  = 7.4 Hz, 2H, CH<sub>3</sub>), 1.07 (t,  $J$  = 7.4 Hz, 3H, CH<sub>3</sub>).

<sup>13</sup>C NMR (101 MHz, CDCl<sub>3</sub>):  $\delta$ (ppm) = 155.86, 154.25, 151.86, 124.20, 116.74, 109.85, 91.56, 85.19, 82.80, 71.73, 71.54, 62.15, 22.66, 14.23, 10.82, 10.51.

IR (ATR):  $\nu$  / cm<sup>-1</sup> = 720, 745, 767, 796, 823, 850, 905, 928, 959, 1014, 1031, 1043, 1065, 1094, 1107, 1150, 1170, 1214, 1236, 1265, 1312, 1366, 1380, 1397, 1460, 1481, 1493, 1701, 2215, 2876, 2935, 2966.

HRMS (FAB) of [M]<sup>+</sup> [C<sub>17</sub>H<sub>21</sub>IO<sub>4</sub>]<sup>+</sup>: calc. 416.0479; found 416.0480;  $\Delta$  = 0.1 mmu

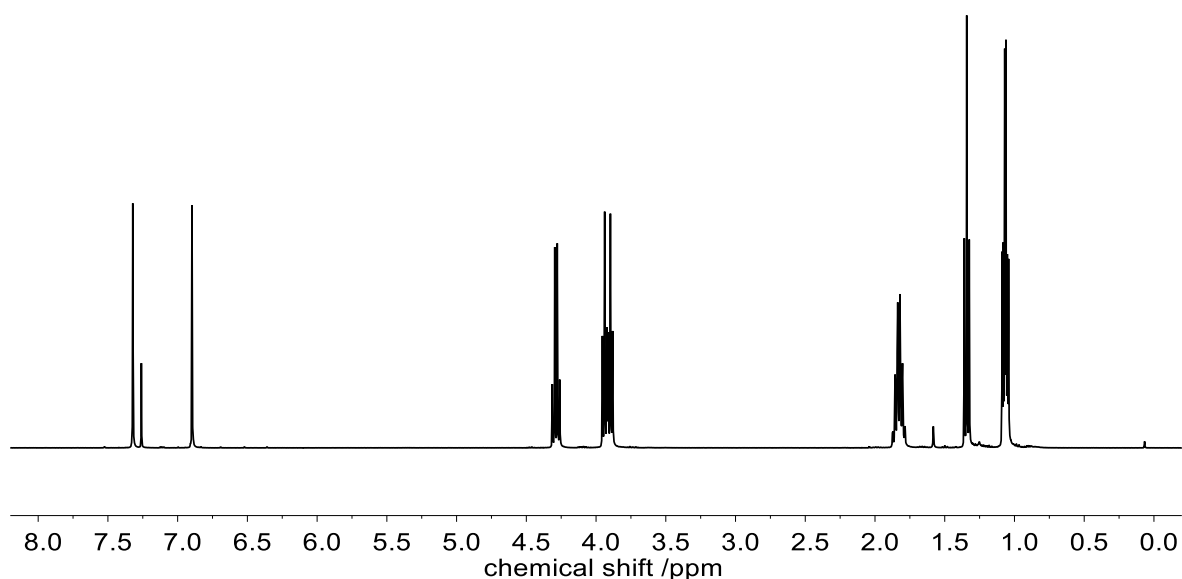
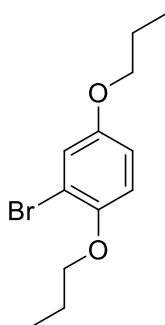


Figure S9:  $^1\text{H}$  NMR spectrum of **IB1** measured in  $\text{CDCl}_3$ .

#### Synthesis of 2-bromo-1,4-dipropoxybenzene (**B1a**)



Bromohydroquinone (10.4 g, 55.0 mmol, 1.00 eq.) was dissolved in 55 mL absolute ethanol. Potassium hydroxide (7.71 g, 138 mmol, 2.50 eq.) was added and the mixture was stirred for 30 min under reflux. Subsequently, 1-bromopropane (12.5 mL, 16.9 g, 138 mmol, 2.50 eq.) was slowly added over a 50-minute period and stirred under reflux for another 2 h. Ethanol was removed under reduced pressure and the residue was taken up in dichloromethane. The organic phase was washed with water for three times, once more with saturated  $\text{NaHCO}_3$  solution and dried over anhydrous sodium sulfate. The solvent was removed under reduced pressure and the crude product was purified *via* column chromatography (cyclohexane/ethyl acetate 40:1) to yield a colorless liquid (12.6 g, 46.0 mmol, 84%).

$R_f = 0.53$  in cyclohexane/ethyl acetate (20:1). Visualized *via* Seebach staining solution.

$^1\text{H}$  NMR (400 MHz,  $\text{CDCl}_3$ ):  $\delta(\text{ppm}) = 7.12$  (d,  $J = 2.7$  Hz, 1H,  $\text{CH}_{\text{ar}}$ ), 6.85 – 6.76 (m, 2H,  $\text{CH}_{\text{ar}}$ ), 3.92 (t,  $J = 6.5$  Hz, 2H,  $\text{OCH}_2$ ), 3.85 (t,  $J = 6.6$  Hz, 2H,  $\text{OCH}_2$ ), 1.88 – 1.72 (m, 4H,  $\text{CH}_2$ ), 1.06 (t,  $J = 7.4$  Hz, 3H,  $\text{CH}_3$ ), 1.02 (t,  $J = 7.4$  Hz, 3H,  $\text{CH}_3$ ).

$^{13}\text{C}$  NMR (101 MHz,  $\text{CDCl}_3$ ):  $\delta(\text{ppm}) = 153.73, 149.90, 119.67, 114.90, 114.56, 112.94, 71.84, 70.48, 22.80, 22.72, 10.70, 10.61$ .

IR (ATR):  $\nu / \text{cm}^{-1} = 2964, 2935, 2878, 1604, 1574, 1491, 1467, 1388, 1269, 1205, 1148, 1135, 1107, 1065, 1049, 1035, 1022, 979, 909, 884, 860, 841, 798, 765, 736, 677. 578, 440$ .

HRMS (FAB) of  $[\text{M}]^+ [\text{C}_{12}\text{H}_{17}\text{O}_2\text{Br}]^+$ : calc. 272.0406; found 272.0408;  $\Delta = 0.2$  mmu

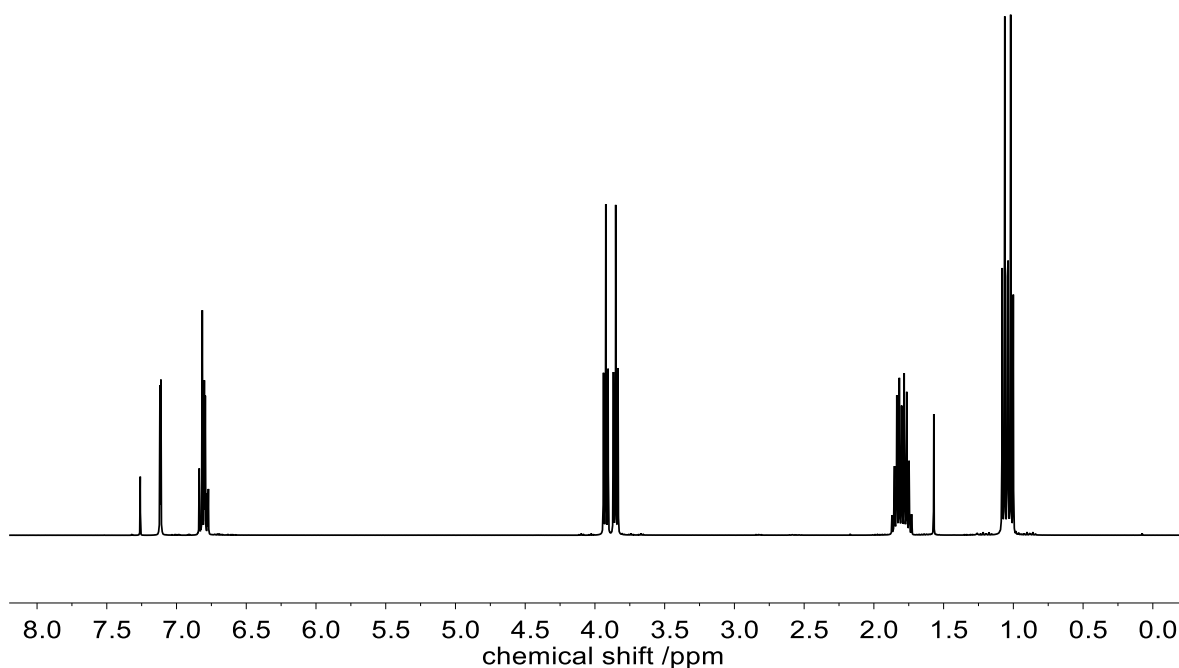
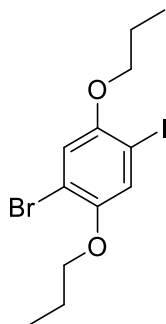


Figure S10:  $^1\text{H}$  NMR spectrum of **B1a** measured in  $\text{CDCl}_3$ .

*Synthesis of 1-Bromo-4-iodo-2,5-dipropoxybenzene (B1b)*

Periodic acid (1.84 g, 8.09 mmol, 0.34 eq.) was dissolved in 15 mL methanol and stirred for 10 minutes. Subsequently, iodine (4.05 g, 15.9 mmol, 0.67 eq.) was added and after an additional reaction time of 10 minutes **B1a** (6.50 g, 23.8 mmol, 1.00 eq.) was added. The reaction mixture was stirred under reflux for 4 h. The residue was carefully poured into 250 mL water containing potassium metabisulfite (10.6 g, 47.8 mmol, 2.00 eq.). The precipitate was washed with methanol and dissolved in dichloromethane. The solution was filtered, and the filtrate was concentrated under reduced pressure. The residue was purified by recrystallization from methanol to yield the product as a white solid (8.55 g, 21.4 mmol, 90%).

$R_f = 0.65$  in cyclohexane/ethyl acetate (20:1). Visualized *via* Seebach staining solution.

$^1\text{H NMR}$  (400 MHz,  $\text{CDCl}_3$ ):  $\delta(\text{ppm}) = 7.28$  (s, 1H,  $\text{CH}_{\text{ar}}$ ), 6.99 (s, 1H,  $\text{CH}_{\text{ar}}$ ), 3.95 – 3.86 (m, 4H,  $\text{OCH}_2$ ), 1.89 – 1.76 (m, 4H,  $\text{CH}_2$ ), 1.08 (t,  $J = 7.3$  Hz, 3H,  $\text{CH}_3$ ), 1.06 (t,  $J = 7.3$  Hz, 3H,  $\text{CH}_3$ ).

$^{13}\text{C NMR}$  (101 MHz,  $\text{CDCl}_3$ ):  $\delta(\text{ppm}) = 152.67, 150.56, 124.45, 117.24, 112.70, 84.93, 71.99, 71.94, 22.72, 10.84, 10.67$ .

IR (ATR):  $\nu / \text{cm}^{-1} = 2962, 2910, 2872, 1490, 1468, 1453, 1394, 1377, 1354, 1266, 1244, 1208, 1127, 1061, 1040, 1008, 910, 851, 801, 772, 629, 437$ .

HRMS (FAB) of  $[\text{M}]^+ [\text{C}_{12}\text{H}_{16}\text{O}_2\text{Br}]^+$ : calc. 397.9373; found 397.9374;  $\Delta = 0.1$  mmu

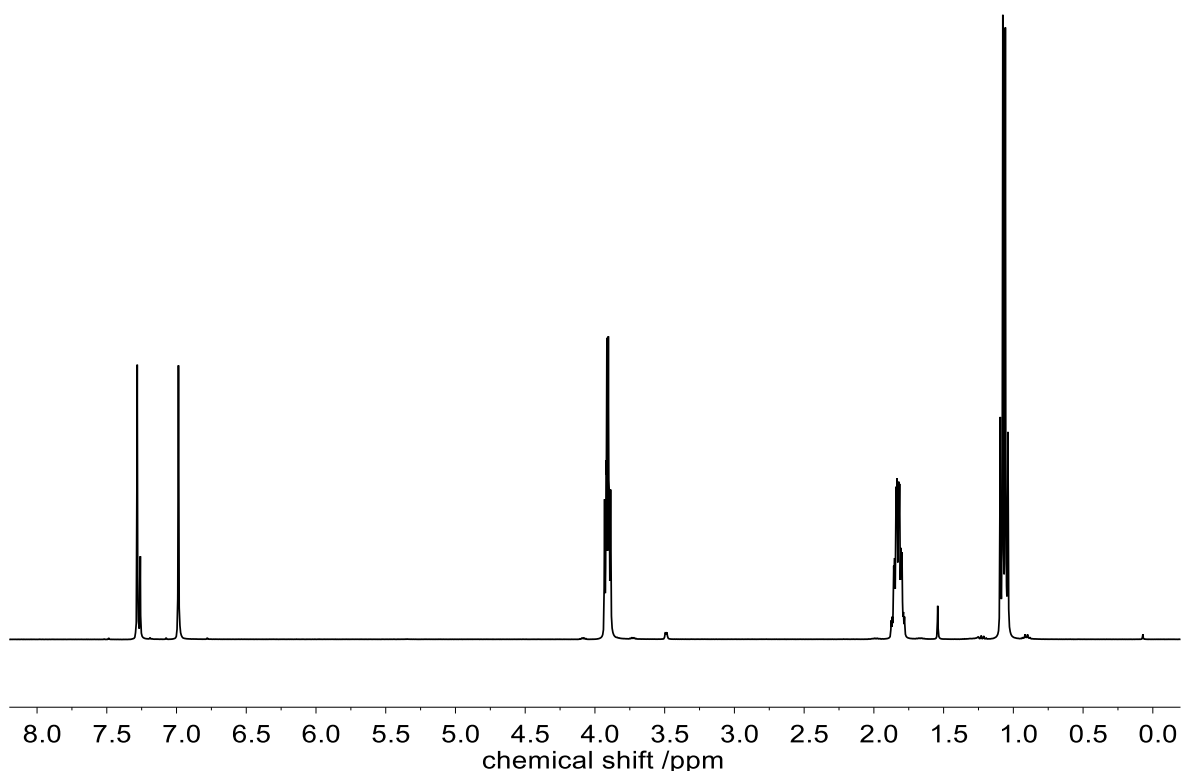
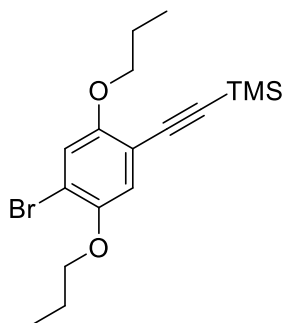


Figure S11:  $^1\text{H}$  NMR spectrum of **B1b** measured in  $\text{CDCl}_3$ .

#### Synthesis of 1,4-bis(propoxy)-2-bromo-5-trimethylsilylacetylenebenzene (**B1c**)



**B1b** (4.00 g, 10.02 mmol, 1.00 eq.), 5 mol% *bis*(triphenylphosphine)palladium(II) dichloride (352 mg, 0.501 mmol, 0.05 eq.) and 10 mol% copper(I) iodide (191 mg, 1.00 mmol, 0.1 eq.) were placed into a Schlenk flask and degassed. Under continuous argon flow, 75 mL diisopropylamine was added and the resulting mixture cooled with an ice bath. Subsequently, trimethylsilyl acetylene (1.43 mL, 985 mg, 10.0 mmol, 1.00 eq.) was added dropwise with a syringe. The reaction mixture was stirred for 30 minutes at 0 °C and one hour at room temperature. The mixture was then filtered through a silica plug and washed with diethyl ether. The solvent was

evaporated, and the residue purified by column chromatography (cyclohexane/DCM 9:1) to yield the product as a light-yellow solid (2.98 g, 8.06 mmol, 80%).

$R_f = 0.63$  in cyclohexane/ethyl acetate (20:1). Visualized *via* Seebach staining solution.

$^1\text{H}$  NMR (400 MHz,  $\text{CDCl}_3$ ):  $\delta(\text{ppm}) = 7.05$  (s, 1H,  $\text{CH}_{\text{ar}}$ ), 6.94 (s, 1H,  $\text{CH}_{\text{ar}}$ ), 3.95 – 3.88 (m, 4H,  $\text{OCH}_2$ ), 1.89 – 1.75 (m, 4H,  $\text{CH}_2$ ), 1.07 (t,  $J = 7.4$  Hz, 3H,  $\text{CH}_3$ ), 1.05 (t,  $J = 7.5$  Hz, 3H,  $\text{CH}_3$ ), 0.25 (s, 9H,  $\text{Si}(\text{CH}_3)_3$ ).

$^{13}\text{C}$  NMR (101 MHz,  $\text{CDCl}_3$ ):  $\delta(\text{ppm}) = 154.87, 149.46, 118.25, 118.06, 113.73, 112.66, 100.73, 99.39, 71.69, 71.43, 22.80, 22.73, 10.68, 10.62, 0.07$ .

IR (ATR):  $\nu / \text{cm}^{-1} = 2958, 2935, 2911, 2900, 2871, 2160, 1504, 1491, 1458, 1397, 1380, 1372, 1292, 1267, 1255, 1244, 1216, 1205, 1166, 1127, 1041, 1033, 1018, 981, 907, 858, 833, 769, 757, 697, 671, 642, 613, 570, 502, 494, 473, 405$ .

HRMS (FAB) of  $[\text{M}]^+$  [ $\text{C}_{17}\text{H}_{25}\text{O}_2\text{BrSi}$ ] $^+$ : calc. 368.0802; found 368.0803;  $\Delta = 0.1$  mmu

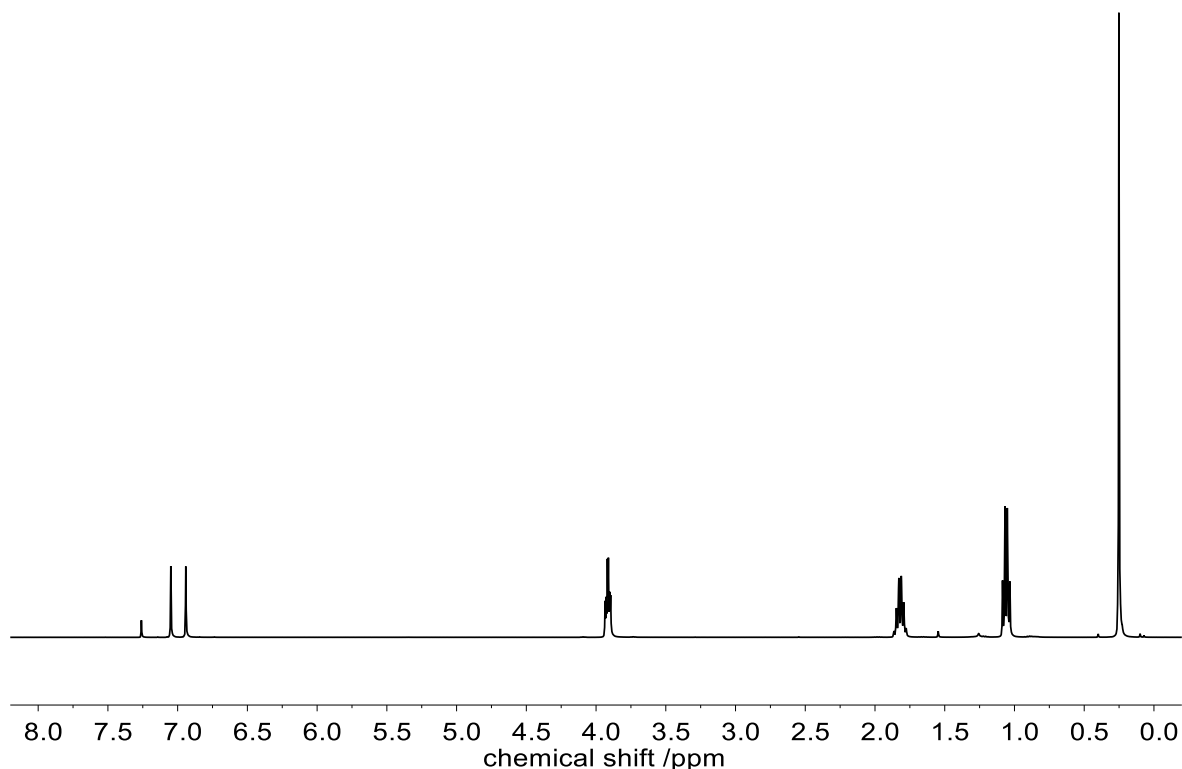
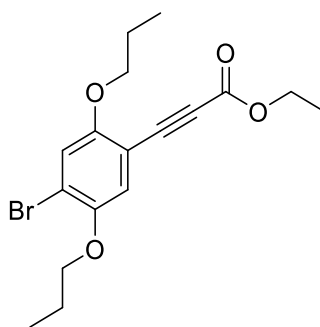


Figure S12:  $^1\text{H}$  NMR spectrum of **B1c** measured in  $\text{CDCl}_3$ .

Synthesis of ethyl 3-(4-bromo-2,5-dipropoxyphenyl) propiolate (**B1**)

**B1c** (2.50 g, 6.77 mmol, 1.00 eq.) and caesium fluoride (1.23 g, 8.12 mmol, 1.20 eq.) were placed into Schlenk flask, degassed, and backfilled with CO<sub>2</sub> gas. Subsequently, 22 mL DMSO was added, and the resulting solution was stirred for three hours at ambient temperature. Ethyliodide (653  $\mu$ L, 1.27 g, 8.12 mmol, 1.20 eq.) was added dropwise and the reaction mixture was stirred over night at ambient temperature. The reaction was quenched by addition of 80 mL saturated ammonium chloride solution. The mixture was extracted three times with 100 mL ethyl acetate and the combined organic phases washed once with brine. The solvent was removed under reduced pressure, and the residue purified by column chromatography (cyclohexane/ethyl acetate 40:1 $\rightarrow$ 30:1). The product was isolated as a white solid (2.26 g, 6.13 mmol, 90%).

R<sub>f</sub> = 0.34 in cyclohexane/ethyl acetate (20:1). Visualized *via* Seebach staining solution.

<sup>1</sup>H NMR (400 MHz, CDCl<sub>3</sub>):  $\delta$ (ppm) = 7.11 (s, 1H, CH<sub>ar</sub>), 7.01 (s, 1H, CH<sub>ar</sub>), 4.29 (q,  $J$  = 7.1 Hz, 2H, CH<sub>2</sub>), 3.94 (t,  $J$  = 6.4 Hz, 2H, OCH<sub>2</sub>), 3.91 (t,  $J$  = 6.4 Hz, 2H, OCH<sub>2</sub>), 1.90 – 1.77 (m, 4H, CH<sub>2</sub>), 1.34 (t,  $J$  = 7.1 Hz, 3H, CH<sub>3</sub>), 1.06 (t,  $J$  = 7.4 Hz, 3H, CH<sub>3</sub>), 1.06 (t,  $J$  = 7.4 Hz, 3H, CH<sub>3</sub>).

<sup>13</sup>C NMR (101 MHz, CDCl<sub>3</sub>):  $\delta$ (ppm) = 155.79, 154.26, 149.53, 118.46, 118.26, 116.76, 108.87, 85.05, 82.63, 71.68, 71.51, 62.16, 22.63, 14.24, 10.64, 10.51.

IR (ATR):  $\nu$  / cm<sup>-1</sup> = 2962, 2939, 2878, 2209, 1701, 1596, 1559, 1497, 1467, 1403, 1382, 1366, 1323, 1304, 1242, 1216, 1195, 1158, 1129, 1117, 1068, 1037, 1016, 989, 975, 965, 907, 850, 829, 796, 767, 745, 736, 652, 570, 557, 424.

HRMS (FAB) of [M]<sup>+</sup> [C<sub>17</sub>H<sub>21</sub>O<sub>4</sub>Br]<sup>+</sup>: calc. 368.0618; found 368.0615;  $\Delta$  = 0.3 mmu

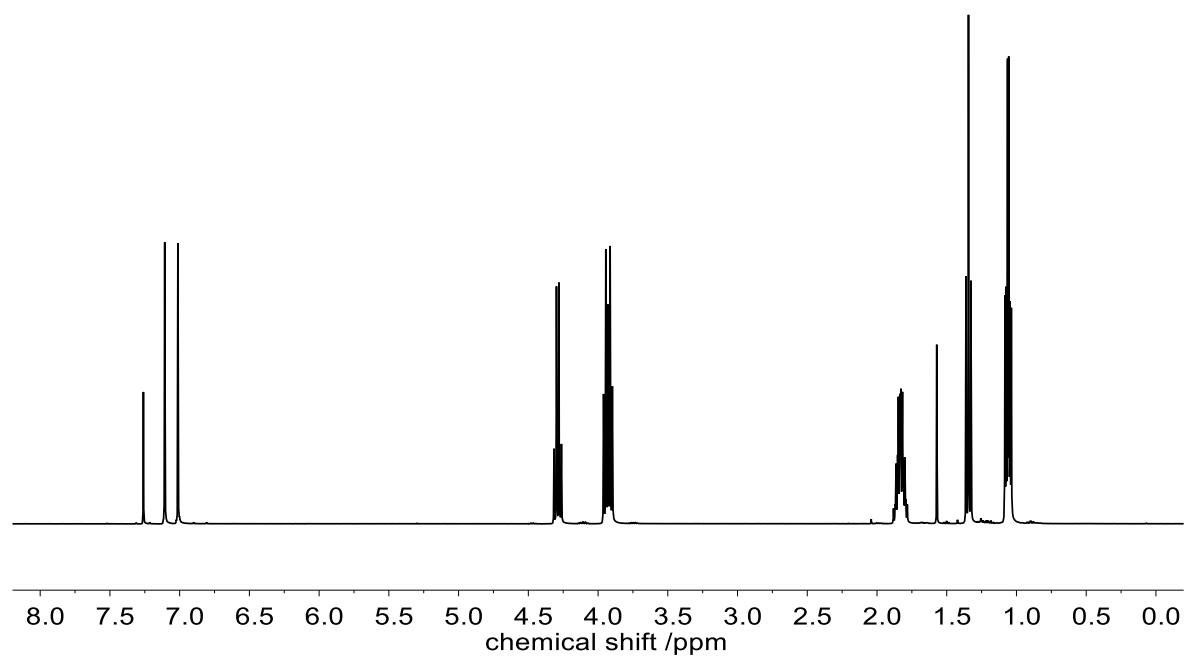


Figure S13:  $^1\text{H}$  NMR spectrum of **B1** measured in  $\text{CDCl}_3$ .

### 6.3.3 Synthesis of uniform OPEs

This chapter has been published before as part of the supplementary information:

D. Hahn, R. V. Schneider, E. Foitzik, M. A. R. Meier, *Macromol. Rapid Commun.* **2021**, 2000735.

#### *General procedure for the decarboxylative coupling reaction (G1)*

Alkynyl carboxylic acid (1.00 eq.), ethyl 3-(4-bromo-2,5-dipropoxyphenyl)propionate (1.10 eq.), SPhos (0.05 eq.), cesium carbonate (1.20 eq.) and 1,1'-Bis(diphenylphosphino)ferrocene-palladium(II)dichloride dichloromethane complex (0.025 eq.) were placed into a 50 mL glass vial and sealed with a cap. The vial was evacuated three times and backfilled with argon. Subsequently, toluene and THF (7/3) was added, and the solution was stirred over night at 60°C under argon atmosphere. The reaction mixture was diluted with THF and washed with water. The aqueous phase was extracted four times with DCM. The combined organic phases were washed with brine, dried over sodium sulfate, filtered, and concentrated under reduced pressure. The residue was purified by silica column chromatography (cyclohexane/ethyl acetate).

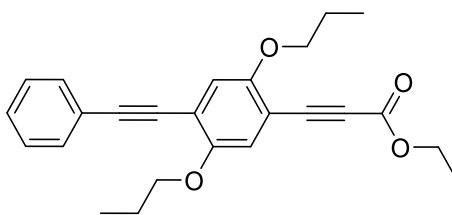
#### *General procedure for saponification (G2)*

The ester protected oligomer (**1a-3a**) was dissolved in a mixture of THF/MeOH/water (3/1/1). Sodium hydroxide (2.00 eq.) was added and the reaction mixture was stirred over night at ambient temperature. After the reaction was finished, the mixture was diluted with DCM and HCl solution (1 M) was added. The phases were separated, and the aqueous phase was extracted three times with DCM. The combined organic phases were dried over sodium sulfate, and the solvent was removed under reduced pressure to yield the alkynyl carboxylic acid, which was further used without any purification for 1b, 2b and 3b. OPE4b and OPE5b were purified by silica filter column (DCM → acetone → acetone/methanol/acetic acid)

#### *General procedure for saponification (G2a)*

The ester protected oligomer (**4a-5a**) was dissolved in a mixture of THF/MeOH/water (3/1/1). Sodium hydroxide (2.00 eq.) was added and the reaction mixture was stirred over night at ambient temperature. After the reaction was

finished, the mixture was diluted with DCM and HCl solution (1 M) was added. The phases were separated, and the aqueous phase was extracted three times with DCM. The combined organic phases were dried over sodium sulfate, and the solvent was removed under reduced pressure. The residue was purified by silica filter column (DCM → acetone → acetone/methanol/acetic acid).

Synthesis of monomer ester (**1a**)

Monomer **1a** was prepared according to general procedure G1. Phenylpropionic acid (365 mg, 2.50 mmol, 1.25 eq.), ethyl 3-(4-bromo-2,5-dipropoxyphenyl)propiolate (739 mg, 2.0 mmol, 1.00 eq.), SPhos (41.0 mg, 100  $\mu$ mol, 0.05 eq.), cesium carbonate (782 mg, 2.40 mmol, 1.20 eq.) and 1,1'-Bis(diphenylphosphino)ferrocene palladium(II)dichloride dichloromethane complex (36.6 mg, 50.0  $\mu$ mol, 0.025 eq.) were used. Purification by silica column chromatography (cyclohexane/ethyl acetate 50:1 $\rightarrow$ 40:1) yielded the product as a yellow solid (515 mg, 1.32 mmol, 66%).

$R_f$  = 0.36 in cyclohexane/ethyl acetate (10:1). Visualized *via* Seebach staining solution.

$^1\text{H}$  NMR (400 MHz,  $\text{CDCl}_3$ ):  $\delta$ (ppm) = 7.57 – 7.50 (m, 2H,  $\text{CH}_{\text{ar}}$ ), 7.38 – 7.32 (m, 3H,  $\text{CH}_{\text{ar}}$ ), 7.02 (s, 1H,  $\text{CH}_{\text{ar}}$ ), 7.01 (s, 1H,  $\text{CH}_{\text{ar}}$ ), 4.30 (q,  $J$  = 7.1 Hz, 2H,  $\text{OCH}_2$ ), 3.98 (t,  $J$  = 6.5 Hz, 2H,  $\text{OCH}_2$ ), 3.96 (t,  $J$  = 6.5 Hz, 2H,  $\text{CH}_2$ ), 1.86 (h,  $J$  = 7.4 Hz, 2H,  $\text{CH}_2$ ), 1.86 (h,  $J$  = 7.4 Hz, 2H,  $\text{CH}_2$ ), 1.35 (t,  $J$  = 7.1 Hz, 3H,  $\text{CH}_3$ ), 1.10 (t,  $J$  = 7.4 Hz, 3H,  $\text{CH}_3$ ), 1.08 (t,  $J$  = 7.4 Hz, 3H,  $\text{CH}_3$ ).

$^{13}\text{C}$  NMR (101 MHz,  $\text{CDCl}_3$ ):  $\delta$ (ppm) = 155.36, 154.28, 153.46, 131.77, 128.68, 128.51, 123.27, 118.02, 117.12, 117.07, 109.96, 85.57, 83.15, 71.28, 71.23, 62.12, 22.77, 22.67, 14.23, 10.64, 10.53.

IR (ATR):  $\nu$  /  $\text{cm}^{-1}$  = 2964, 2931, 2876, 2855, 2209, 1699, 1602, 1504, 1487, 1465, 1442, 1413, 1386, 1368, 1339, 1267, 1218, 1152, 1103, 1065, 1014, 983, 917, 860, 847, 798, 757, 745, 689, 660, 529.

HRMS (FAB) of  $[\text{M}]^+$   $[\text{C}_{25}\text{H}_{26}\text{O}_4]^+$ : calc. 390.1831; found 390.1831;  $\Delta$  = 0.0 mmu

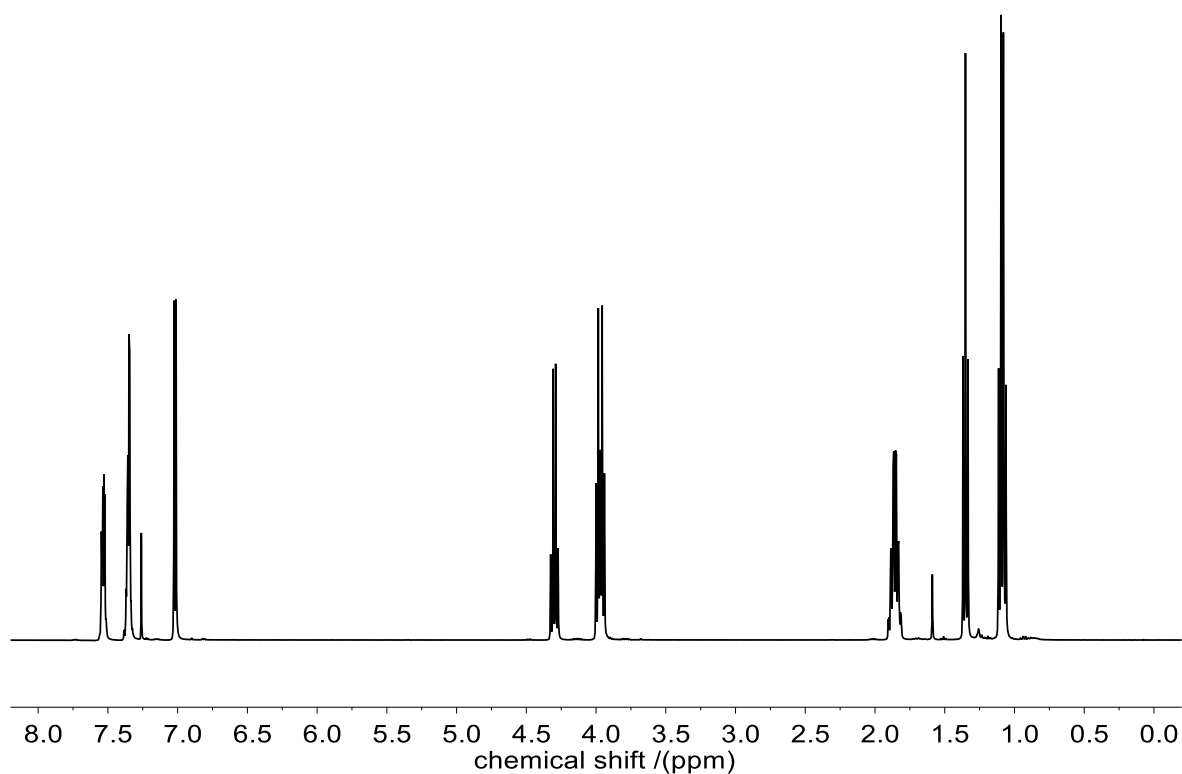
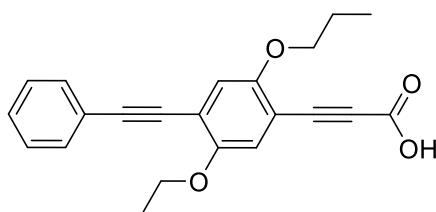


Figure S14:  $^1\text{H}$  NMR spectrum of **1a** measured in  $\text{CDCl}_3$ .

### Synthesis of monomer acid **1b**



Monomer acid **1b** was prepared according to general procedure G2. **1a** (500 mg, 1.28 mmol, 1.00 eq.) and NaOH (102 mg, 2.56 mmol, 2.00 eq.) were used. **1b** was obtained as a yellow solid (464 mg, 1.28 mmol, quant.)

$R_f = 0.00$  in cyclohexane/ethyl acetate (10:1). Visualized *via* Seebach staining solution.

$^1\text{H}$  NMR (400 MHz,  $\text{CDCl}_3$ ):  $\delta$ (ppm) = 7.57 – 7.52 (m, 2H,  $\text{CH}_{\text{ar}}$ ), 7.38 – 7.33 (m, 3H,  $\text{CH}_{\text{ar}}$ ), 7.04 (s, 1H,  $\text{CH}_{\text{ar}}$ ), 7.02 (s, 1H,  $\text{CH}_{\text{ar}}$ ), 4.00 (t,  $J = 6.5$  Hz, 2H,  $\text{OCH}_2$ ), 3.97 (t,  $J = 6.4$  Hz, 2H,  $\text{OCH}_2$ ), 1.87 (h,  $J = 7.4$  Hz, 4H,  $\text{CH}_2$ ), 1.86 (h,  $J = 7.3$  Hz, 4H,  $\text{CH}_2$ ), 1.10 (t,  $J = 7.4$  Hz, 3H,  $\text{CH}_3$ ), 1.08 (t,  $J = 7.4$  Hz, 3H,  $\text{CH}_3$ ).

## Experimental Section

---

$^{13}\text{C}$  NMR (101 MHz,  $\text{CDCl}_3$ ):  $\delta(\text{ppm}) = 158.45, 155.70, 153.45, 131.82, 128.77, 128.54, 123.21, 118.13, 117.82, 117.04, 109.31, 96.56, 86.17, 85.52, 84.92, 71.30, 71.28, 22.77, 22.68, 10.66, 10.56.$

IR (ATR):  $\nu / \text{cm}^{-1} = 2966, 2925, 2876, 2853, 2213, 1676, 1604, 1506, 1489, 1469, 1425, 1407, 1386, 1288, 1277, 1238, 1214, 1191, 1168, 1065, 1016, 985, 907, 858, 843, 751, 685, 654, 607, 529.$

HRMS (FAB) of  $[\text{M}]^+ [\text{C}_{23}\text{H}_{22}\text{O}_4]^+$ : calc. 362.1518; found 362.1517;  $\Delta = 0.1 \text{ mmu}$

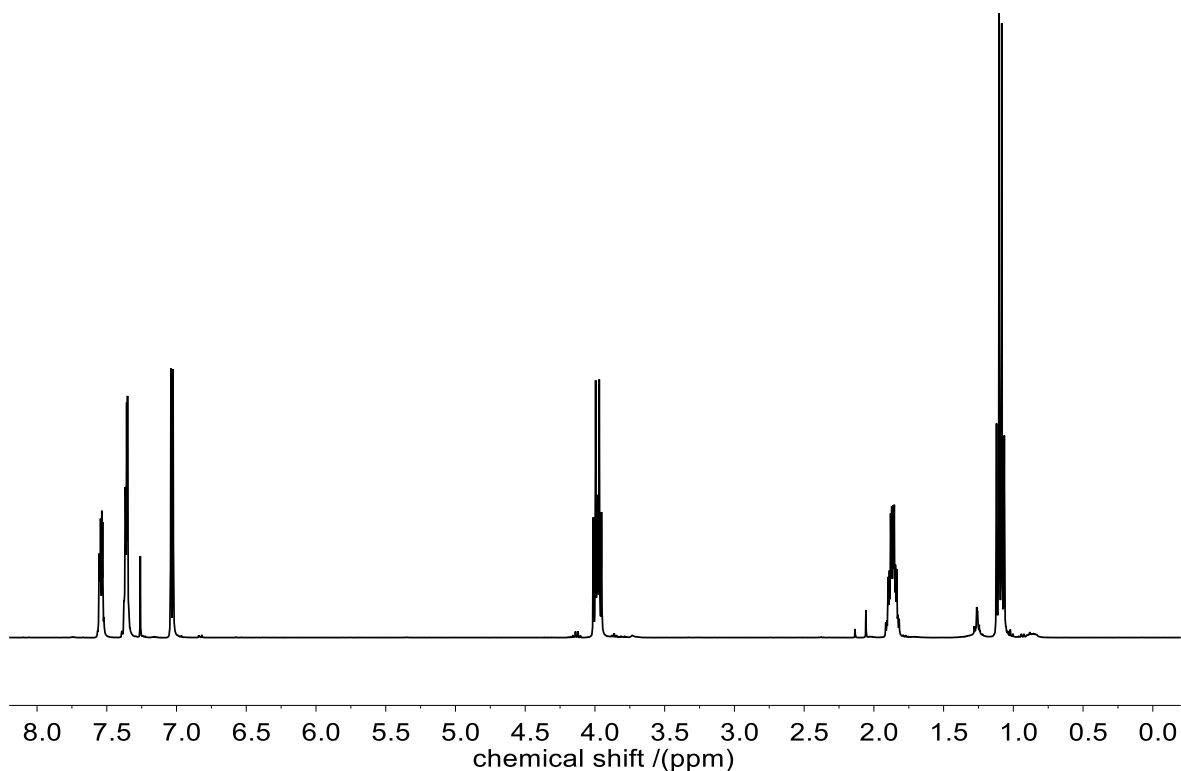
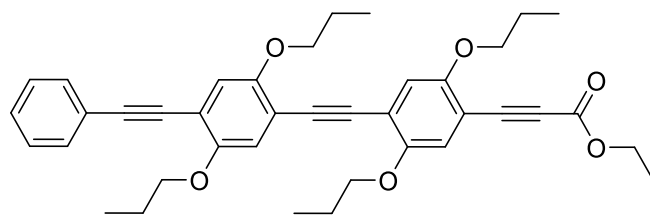


Figure S15:  $^1\text{H}$  NMR spectrum of **1b** measured in  $\text{CDCl}_3$ .

Synthesis of dimer ester (**2a**)

Dimer ester **2a** was prepared according to general procedure G1. **1b** (400 mg, 1.10 mmol, 1.00 eq.), ethyl 3-(4-bromo-2,5-dipropoxyphenyl)propiolate (448 mg, 1.21 mmol, 1.10 eq.), SPhos (22.7 mg, 55.2  $\mu\text{mol}$ , 0.05 eq.), cesium carbonate (432 mg, 1.32 mmol, 1.20 eq.) and 1,1'-Bis(diphenylphosphino)ferrocene-palladium(II)dichloride dichloromethane complex (20.2 mg, 27.6  $\mu\text{mol}$ , 0.025 eq.) were used. Purification by silica column chromatography (cyclohexane/ethyl acetate 25:1 $\rightarrow$ 20:1) yielded **2a** as a yellow solid (516 mg, 850  $\mu\text{mol}$ , 82%).

$R_f$  = 0.28 in cyclohexane/ethyl acetate (10:1). Visualized *via* Seebach staining solution.

$^1\text{H}$  NMR (400 MHz,  $\text{CDCl}_3$ ):  $\delta$ (ppm) = 7.58 – 7.50 (m, 2H,  $\text{CH}_{\text{ar}}$ ), 7.39 – 7.30 (m, 3H,  $\text{CH}_{\text{ar}}$ ), 7.04 – 6.99 (m, 4H,  $\text{CH}_2$ ), 4.30 (q,  $J$  = 7.1 Hz, 2H,  $\text{CH}_2$ ), 4.04 – 3.94 (m, 8H,  $\text{OCH}_2$ ), 1.94 – 1.79 (m, 8H,  $\text{CH}_2$ ), 1.35 (t,  $J$  = 7.1 Hz, 3H,  $\text{CH}_3$ ), 1.14 – 1.04 (m, 12H,  $\text{CH}_3$ ).

$^{13}\text{C}$  NMR (101 MHz,  $\text{CDCl}_3$ ):  $\delta$ (ppm) = 155.34, 154.31, 153.73, 153.28, 131.72, 128.48, 128.44, 123.57, 118.15, 117.45, 117.38, 117.27, 114.63, 113.98, 109.94, 95.20, 92.88, 91.00, 86.02, 85.62, 83.20, 76.84, 71.30, 71.25, 71.22, 62.14, 22.86, 22.80, 22.71, 22.67, 14.25, 10.69, 10.64, 10.53.

IR (ATR):  $\nu$  /  $\text{cm}^{-1}$  = 2964, 2933, 2873, 2209, 1701, 1598, 1508, 1465, 1421, 1388, 1366, 1345, 1314, 1277, 1242, 1209, 1172, 1146, 1117, 1063, 1045, 1014, 985, 971, 909, 882, 850, 753, 726, 689, 654, 621, 562, 527, 463.

HRMS (ESI) of  $[\text{M}]^+$   $[\text{C}_{39}\text{H}_{42}\text{O}_6]^+$ : calc. 606.2981; found 606.2972;  $\Delta$  = 0.9 mmu

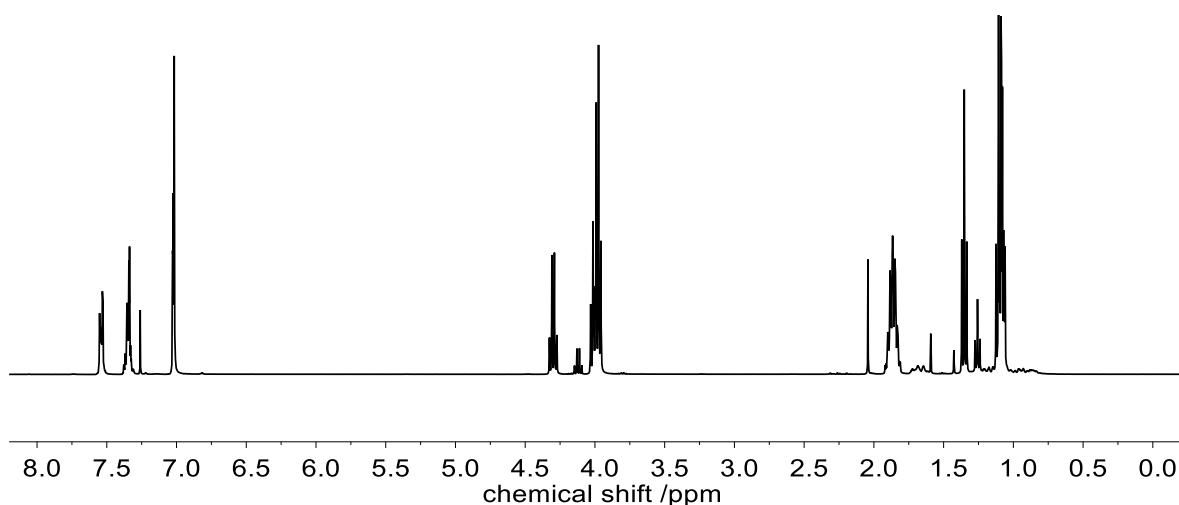
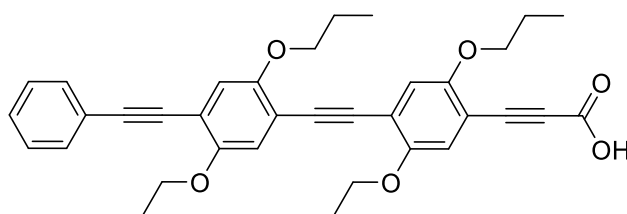


Figure S16:  $^1\text{H}$  NMR spectrum of **2a** measured in  $\text{CDCl}_3$ .

### Synthesis of dimer acid (**2b**)



Dimer acid **2b** was prepared according to general procedure G2. **2a** (457 mg, 753  $\mu\text{mol}$ , 1.00 eq.) and NaOH (60.3 mg, 1.51 mmol, 2.00 eq.) were used. **2b** was obtained as a yellow solid (436 mg, 753  $\mu\text{mol}$ , quant.).

$R_f$  = 0.00 in cyclohexane/ethyl acetate (10:1). Visualized *via* Seebach staining solution.

$^1\text{H}$  NMR (400 MHz,  $\text{CDCl}_3$ ):  $\delta$ (ppm) = 7.57 – 7.52 (m, 2H,  $\text{CH}_{\text{ar}}$ ), 7.41 – 7.30 (m, 3H,  $\text{CH}_{\text{ar}}$ ), 7.06 – 7.00 (m, 4H,  $\text{CH}_{\text{ar}}$ ), 4.05 – 3.95 (m, 8H,  $\text{OCH}_2$ ), 1.94 – 1.80 (m, 8H,  $\text{CH}_2$ ), 1.14 – 1.04 (m, 12H,  $\text{CH}_3$ ).

$^{13}\text{C}$  NMR (101 MHz,  $\text{CDCl}_3$ ):  $\delta$ (ppm) = 157.73, 155.66, 153.77, 153.73, 153.28, 131.73, 128.49, 123.56, 118.27, 118.07, 117.49, 117.29, 117.23, 114.76, 113.91, 109.32, 95.27, 93.24, 90.95, 86.12, 86.01, 84.88, 71.34, 71.32, 71.29, 71.24, 22.87, 22.81, 22.71, 22.67, 10.70, 10.65, 10.55.

IR (ATR):  $\nu / \text{cm}^{-1} = 2964, 2933, 2873, 2209, 1687, 1664, 1596, 1508, 1489, 1465, 1440, 1421, 1388, 1318, 1279, 1255, 1209, 1164, 1129, 1117, 1063, 1045, 1016, 983, 971, 921, 911, 860, 850, 765, 749, 716, 689, 681, 601.$

HRMS (FAB) of  $[\text{M}]^+ [\text{C}_{37}\text{H}_{38}\text{O}_6]^+$ : calc. 578.2668; found 578.2667;  $\Delta = 0.1\text{mmu}.$

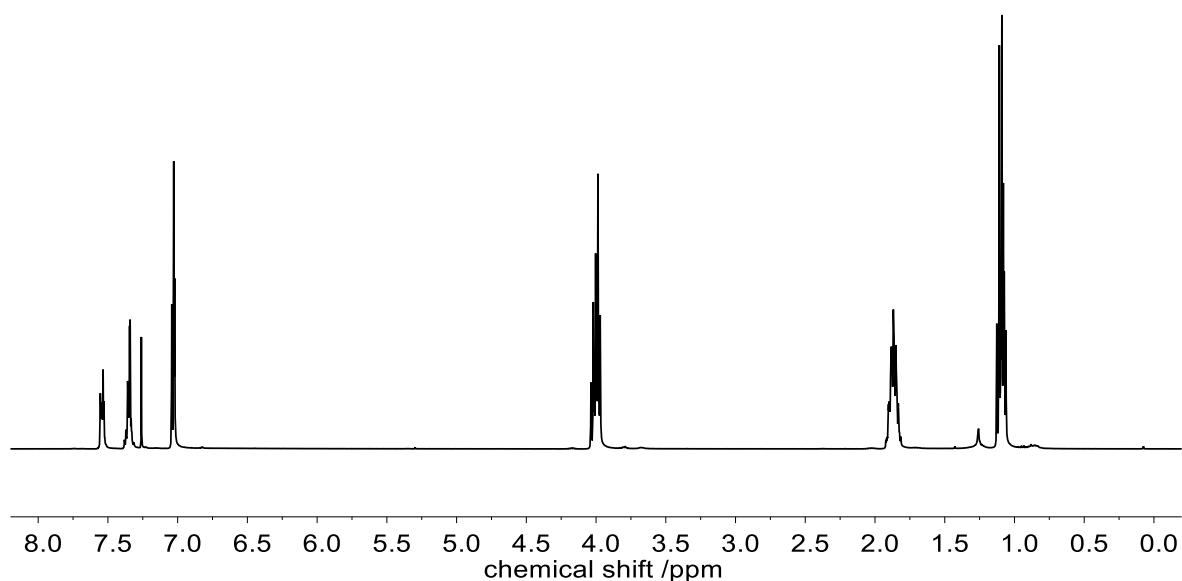
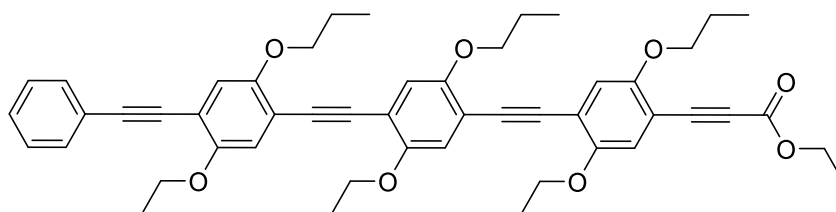


Figure S17:  $^1\text{H}$  NMR spectrum of **2b** measured in  $\text{CDCl}_3$ .

### Synthesis of trimer ester (**3a**)



Trimer ester **3a** was prepared according to general procedure G1. **2b** (400 mg, 691  $\mu\text{mol}$ , 1.00 eq.), ethyl 3-(4-bromo-2,5-dipropoxyphenyl)propiolate (281 mg, 760  $\mu\text{mol}$ , 1.10 eq.), SPhos (14.2 mg, 34.6  $\mu\text{mol}$ , 0.05 eq.), cesium carbonate (270 mg, 829  $\mu\text{mol}$ , 1.20 eq.) and 1,1'-Bis(diphenylphosphino)ferrocene-palladium(II)dichloride dichloromethane complex (12.6 mg, 17.3  $\mu\text{mol}$ , 0.025 eq.)

were used. Purification by silica column chromatography (cyclohexane/ethyl acetate 20:1→16:1) yielded **3a** as a yellow solid (417 mg, 506  $\mu\text{mol}$ , 78%).

$R_f = 0.21$  in cyclohexane/ethyl acetate (10:1). Visualized *via* Seebach staining solution.

$^1\text{H}$  NMR (400 MHz,  $\text{CDCl}_3$ ):  $\delta(\text{ppm}) = 7.57 - 7.51$  (m, 2H,  $\text{CH}_{\text{ar}}$ ),  $7.39 - 7.31$  (m, 3H,  $\text{CH}_{\text{ar}}$ ),  $7.06 - 6.99$  (m, 6H,  $\text{CH}_{\text{ar}}$ ),  $4.30$  (q,  $J = 7.1$  Hz, 2H,  $\text{CH}_2$ ),  $4.06 - 3.94$  (m, 12H,  $\text{OCH}_2$ ),  $1.94 - 1.80$  (m, 12H,  $\text{CH}_2$ ),  $1.35$  (t,  $J = 7.1$  Hz, 3H,  $\text{CH}_3$ ),  $1.14 - 1.05$  (m, 18H,  $\text{CH}_3$ ).

$^{13}\text{C}$  NMR (101 MHz,  $\text{CDCl}_3$ ):  $\delta(\text{ppm}) = 155.34, 154.32, 153.74, 153.69, 153.64, 153.55, 153.28, 131.71, 128.47, 128.40, 123.61, 118.14, 117.57, 117.46, 117.42, 117.38, 117.31, 117.23, 114.90, 114.36, 114.28, 113.99, 109.93, 95.06, 92.94, 91.86, 91.54, 91.06, 86.09, 85.62, 83.22, 71.33, 71.32, 71.29, 71.24, 71.22, 62.15, 22.86, 22.82, 22.79, 22.78, 22.71, 22.67, 14.25, 10.70, 10.68, 10.65, 10.53$ .

IR (ATR):  $\nu / \text{cm}^{-1} = 2966, 2937, 2876, 2211, 1703, 1596, 1512, 1497, 1473, 1421, 1390, 1366, 1273, 1249, 1214, 1156, 1094, 1061, 1043, 1024, 1014, 969, 909, 893, 860, 771, 751, 724, 697, 689$ .

HRMS (FAB) of  $[\text{M}]^+ [\text{C}_{53}\text{H}_{58}\text{O}_8]^+$ : calc. 822.4132; found 822.4130;  $\Delta = 0.2$  mmu.

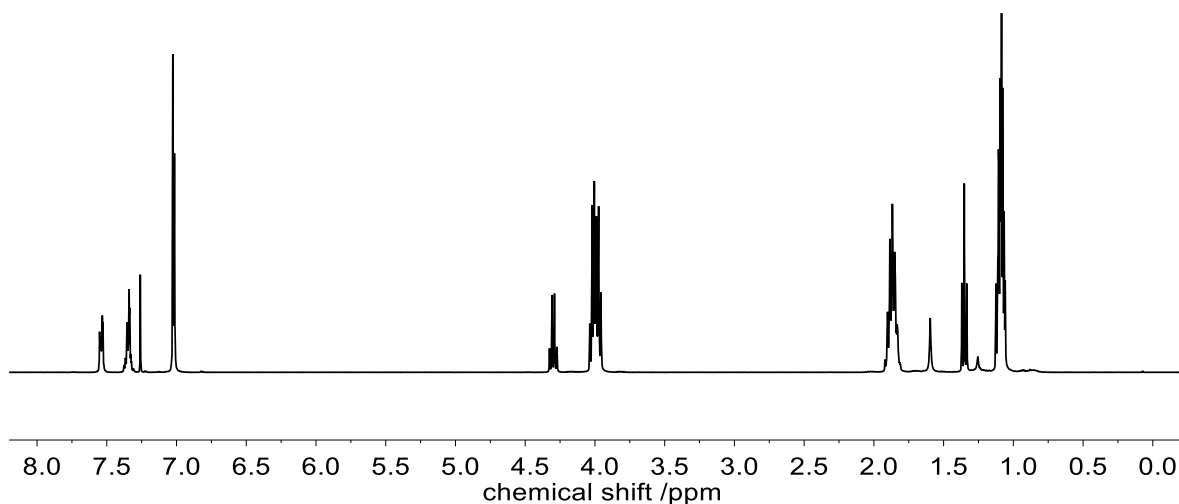
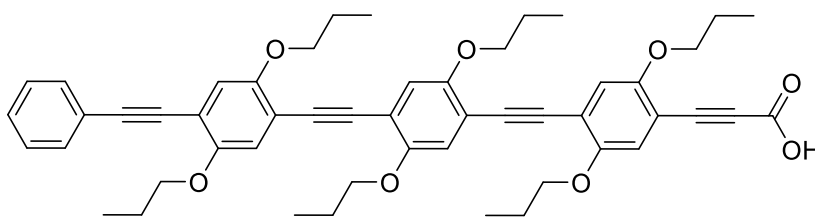


Figure S 18:  $^1\text{H}$  NMR spectrum of **3a** measured in  $\text{CDCl}_3$ .

*Synthesis of trimer acid (3b)*

Trimer acid **3b** was prepared according to general procedure G2. **3a** (400 mg, 486  $\mu\text{mol}$ , 1.00 eq.) and NaOH (38.9 mg, 972  $\mu\text{mol}$ , 2.00 eq.) were used. **3b** was obtained as a yellow solid (386 mg, 486  $\mu\text{mol}$ , quant.).

$R_f$  = 0.00 in cyclohexane/ethyl acetate (10:1). Visualized *via* Seebach staining solution.

$^1\text{H}$  NMR (400 MHz,  $\text{CDCl}_3$ ):  $\delta$ (ppm) = 7.57 – 7.52 (m, 2H,  $\text{CH}_{\text{ar}}$ ), 7.39 – 7.32 (m, 3H,  $\text{CH}_{\text{ar}}$ ), 7.05 – 7.01 (m, 6H,  $\text{CH}_{\text{ar}}$ ), 4.05 – 3.96 (m, 12H,  $\text{CH}_2$ ), 1.94 – 1.81 (m, 12H,  $\text{CH}_2$ ), 1.14 – 1.05 (m, 18H,  $\text{CH}_3$ ).

$^{13}\text{C}$  NMR (101 MHz,  $\text{CDCl}_3$ ):  $\delta$ (ppm) = 157.28, 155.60, 153.75, 153.73, 153.64, 153.55, 153.28, 131.72, 128.48, 128.41, 123.61, 118.25, 118.02, 117.60, 117.46, 117.44, 117.33, 117.21, 115.01, 114.35, 114.32, 113.90, 109.33, 95.08, 93.28, 91.92, 91.53, 91.00, 86.09, 85.95, 84.89, 71.34, 71.25, 22.87, 22.82, 22.80, 22.78, 22.71, 22.66, 10.71, 10.68, 10.66, 10.54.

IR (ATR):  $\nu / \text{cm}^{-1}$  = 2964, 2933, 2906, 2871, 2211, 1670, 1602, 1512, 1497, 1473, 1462, 1421, 1388, 1273, 1216, 1164, 1125, 1096, 1041, 1022, 921, 907, 891, 858, 773, 755, 718, 689, 675, 605, 527.

HRMS (FAB) of  $[\text{M}]^+$   $[\text{C}_{51}\text{H}_{54}\text{O}_8]^+$ : calc. 794.3813; found 794.3815;  $\Delta$  = 0.2 mmu.

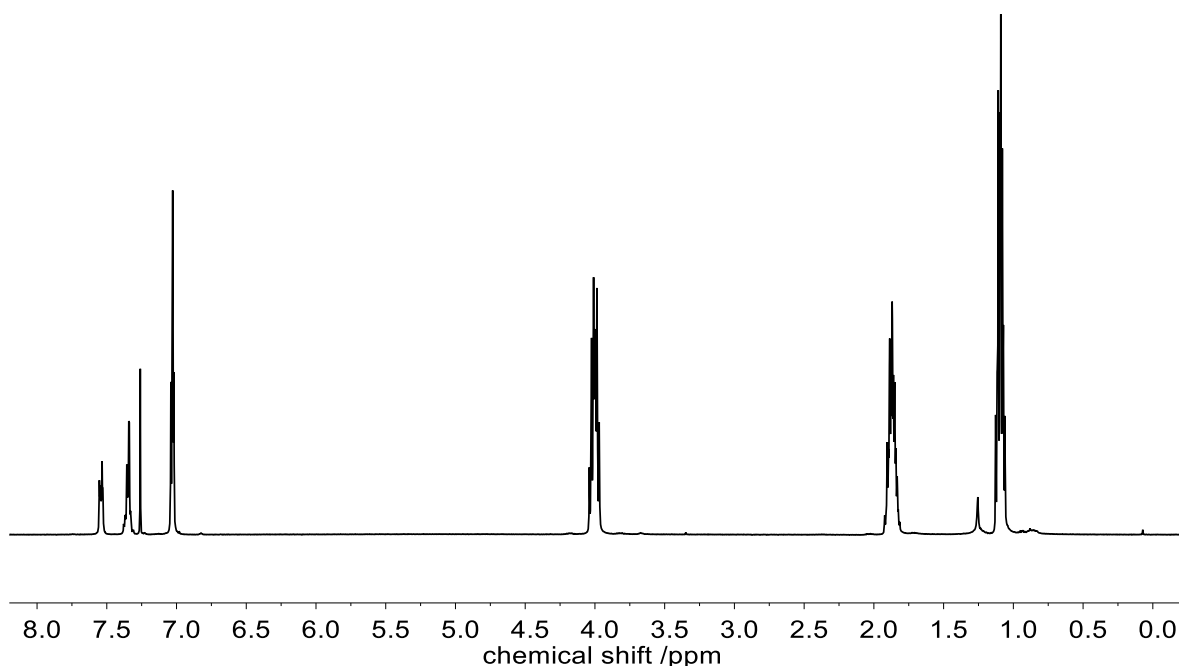
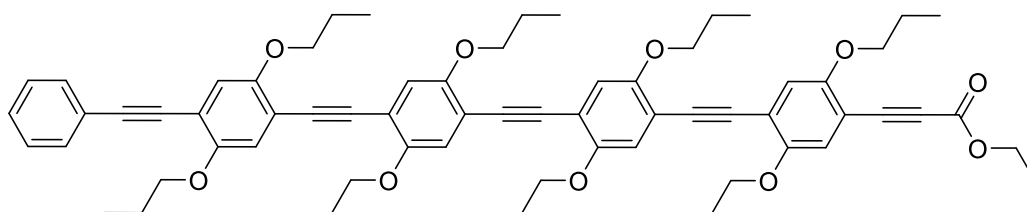


Figure S19:  $^1\text{H}$  NMR spectrum of **3b** measured in  $\text{CDCl}_3$ .

#### Synthesis of tetramer ester (**4a**)



Tetramer ester **4a** was prepared according to general procedure G1. **3b** (300 mg, 377  $\mu\text{mol}$ , 1.00 eq.), ethyl 3-(4-bromo-2,5-dipropoxyphenyl)propiolate (153 mg, 415  $\mu\text{mol}$ , 1.10 eq.), SPhos (7.75 mg, 18.9  $\mu\text{mol}$ , 0.05 eq.), cesium carbonate (148 mg, 453  $\mu\text{mol}$ , 1.20 eq.) and 1,1'-Bis(diphenylphosphino)ferrocene-palladium(II)dichloride dichloromethane complex (6.90 mg, 9.4  $\mu\text{mol}$ , 0.025 eq.) were used. Purification by silica column chromatography (cyclohexane/ethyl acetate 15:1) yielded **4a** as a yellow solid (317 mg, 305  $\mu\text{mol}$ , 80%)

$R_f$  = 0.17 in cyclohexane/ethyl acetate (10:1). Visualized *via* Seebach staining solution.

$^1\text{H}$  NMR (400 MHz,  $\text{CDCl}_3$ ):  $\delta$ (ppm) = 7.58 – 7.51 (m, 2H,  $\text{CH}_{\text{ar}}$ ), 7.39 – 7.31 (m, 3H,  $\text{CH}_{\text{ar}}$ ), 7.05 – 6.99 (m, 8H,  $\text{CH}_{\text{ar}}$ ), 4.30 (q,  $J = 7.1$  Hz, 2H,  $\text{CH}_2$ ), 4.06 – 3.95 (m, 16H,  $\text{OCH}_2$ ), 1.93 – 1.80 (m, 16H,  $\text{CH}_2$ ), 1.35 (t,  $J = 7.1$  Hz, 3H,  $\text{CH}_3$ ), 1.14 – 1.05 (m, 24H,  $\text{CH}_3$ ).

$^{13}\text{C}$  NMR (101 MHz,  $\text{CDCl}_3$ ):  $\delta$ (ppm) = 155.34, 154.30, 153.76, 153.70, 153.60, 153.29, 131.70, 128.46, 128.39, 123.63, 118.16, 117.56, 117.47, 117.44, 117.35, 117.25, 114.93, 114.58, 114.45, 114.40, 114.25, 114.01, 109.95, 95.03, 92.94, 91.92, 91.71, 91.63, 91.61, 91.07, 86.11, 85.62, 83.22, 71.32, 71.25, 62.14, 22.86, 22.82, 22.80, 22.71, 22.66, 14.24, 10.68, 10.65, 10.52.

IR (ATR):  $\nu / \text{cm}^{-1} = 2960, 2927, 2911, 2871, 2855, 2213, 1703, 1596, 1510, 1471, 1462, 1425, 1388, 1273, 1251, 1207, 1158, 1129, 1105, 1061, 1041, 1016, 975, 940, 907, 895, 860, 769, 759, 747, 718, 691$ .

HRMS (ESI) of  $[\text{M}]^+$   $[\text{C}_{67}\text{H}_{74}\text{O}_{10}]^+$ : calc. 1038.5282; found 1038.5275;  $\Delta = 0.7$  mmu

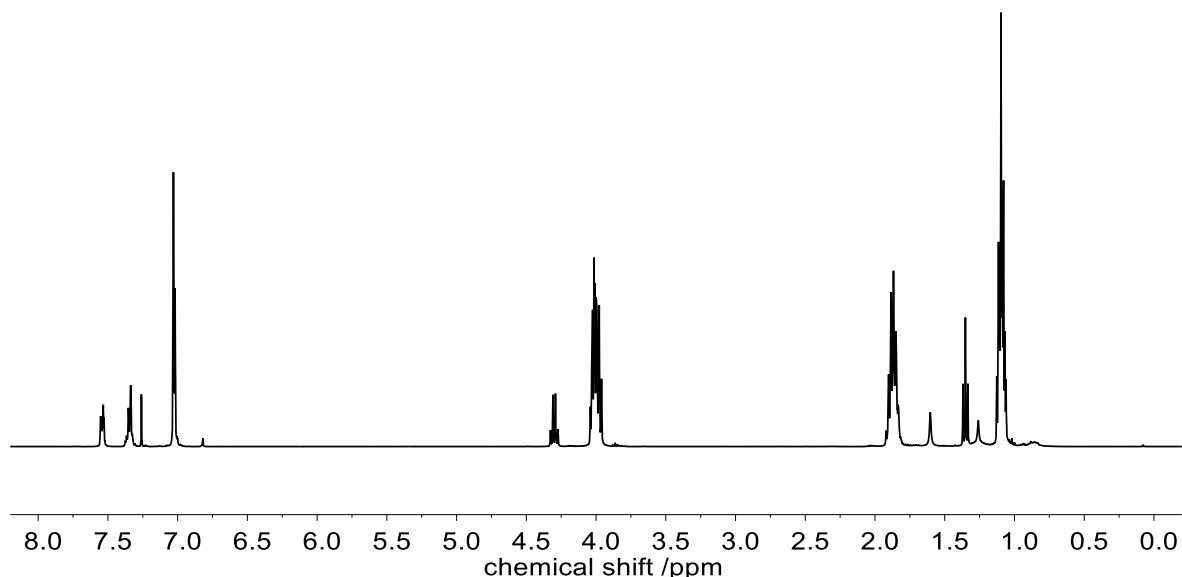
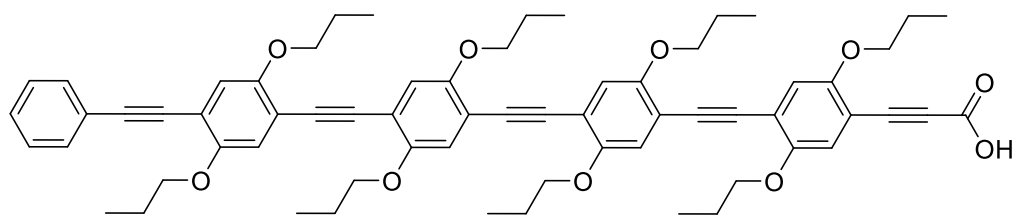


Figure S20:  $^1\text{H}$  NMR spectrum of **4a** measured in  $\text{CDCl}_3$ .

Synthesis of tetramer acid (**4b**)

Tetramer acid **4b** was prepared according to general procedure G2a. **4a** (250 mg, 241  $\mu\text{mol}$ , 1.00 eq.) and NaOH (19.2 mg, 481  $\mu\text{mol}$ , 2.00 eq.) were used. **4b** was obtained after filter column chromatography (dichloromethane $\rightarrow$ acetone $\rightarrow$ acetone/methanol 19:1 + 1%acetic acid) as a yellow solid (226 mg, 223  $\mu\text{mol}$ , 93%).

$R_f = 0.00$  in cyclohexane/ethyl acetate (10:1). Visualized *via* Seebach staining solution.

$^1\text{H}$  NMR (400 MHz,  $\text{CDCl}_3$ ):  $\delta(\text{ppm}) = 7.56 - 7.52$  (m, 2H,  $\text{CH}_{\text{ar}}$ ),  $7.38 - 7.32$  (m, 3H,  $\text{CH}_{\text{ar}}$ ),  $7.05 - 7.01$  (m, 8H,  $\text{CH}_{\text{ar}}$ ),  $4.05 - 3.96$  (m, 16H,  $\text{CH}_2$ ),  $1.93 - 1.82$  (m, 16H,  $\text{CH}_2$ ),  $1.14 - 1.05$  (m, 24H,  $\text{CH}_3$ ).

$^{13}\text{C}$  NMR (101 MHz,  $\text{CDCl}_3$ ):  $\delta(\text{ppm}) = 157.03, 155.53, 153.76, 153.73, 153.63, 153.62, 153.59, 153.57, 153.29, 131.71, 128.47, 128.39, 123.63, 118.26, 117.87, 117.60, 117.57, 117.54, 117.47, 117.44, 117.35, 117.23, 115.00, 114.59, 114.45, 114.39, 114.25, 113.94, 109.52, 95.04, 93.20, 91.96, 91.72, 91.63, 91.60, 91.03, 86.11, 85.43, 85.13, 71.36, 71.33, 71.30, 71.26, 22.87, 22.83, 22.80, 22.78, 22.71, 22.66, 10.71, 10.69, 10.65, 10.55$ .

IR (ATR):  $\nu / \text{cm}^{-1} = 2958, 2929, 2906, 2873, 2207, 1672, 1598, 1510, 1469, 1456, 1425, 1386, 1273, 1236, 1207, 1162, 1105, 1063, 1041, 1020, 981, 907, 862, 767, 755, 689$ .

HRMS (FAB) of  $[\text{M}]^+ [\text{C}_{65}\text{H}_{70}\text{O}_{10}]^+$ : calc. 1010.4964; found 1010.4962;  $\Delta = 0.2$  mmu.

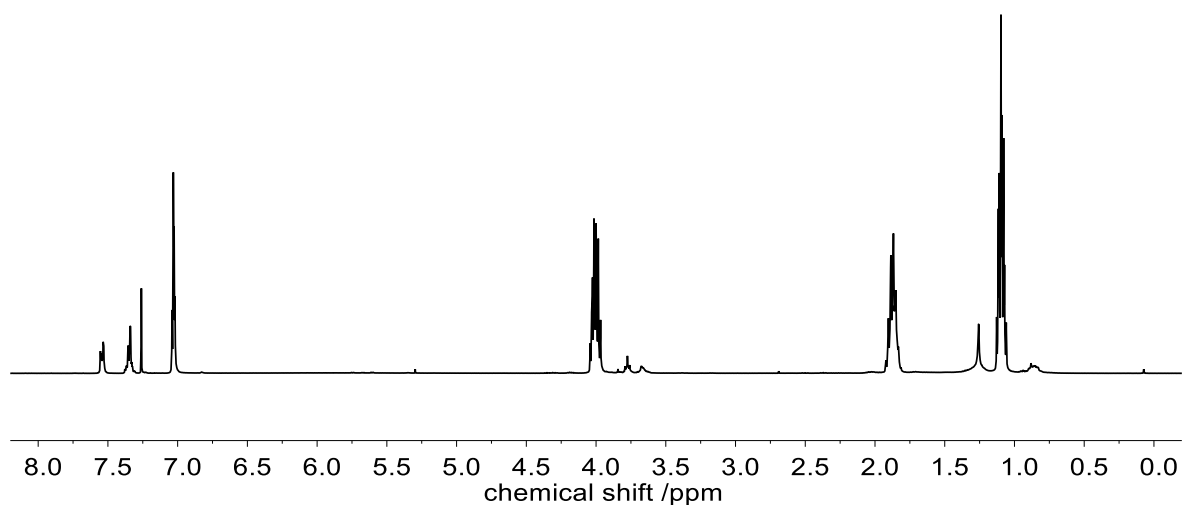
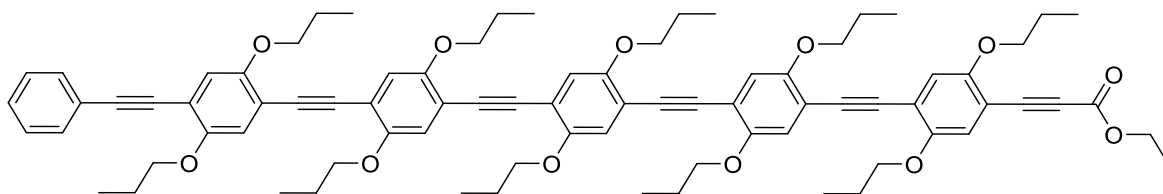


Figure S21:  $^1\text{H}$  NMR spectrum of **4b** measured in  $\text{CDCl}_3$ .

#### Synthesis of pentamer ester (**5a**)



Pentamer ester **5a** was prepared according to general procedure G1. **4b** (150 mg, 148  $\mu\text{mol}$ , 1.00 eq.), ethyl 3-(4-bromo-2,5-dipropoxyphenyl)propiolate (60.2 mg, 163  $\mu\text{mol}$ , 1.10 eq.), SPhos (6.1 mg, 15.0  $\mu\text{mol}$ , 0.1 eq.), cesium carbonate (58.0 mg, 178  $\mu\text{mol}$ , 1.20 eq.) and 1,1'-Bis(diphenylphosphino)ferrocene-palladium(II)dichloride dichloromethane complex (5.4 mg, 7.4  $\mu\text{mol}$ , 0.05 eq.) were used. Purification by silica column chromatography (cyclohexane/ethyl acetate 15:1 $\rightarrow$ 10:1) yielded **5a** as a yellow solid (123 mg, 98.0  $\mu\text{mol}$ , 68%).

$R_f$  = 0.53 in cyclohexane/ethyl acetate (5:1). Visualized *via* Seebach staining solution.

$^1\text{H}$  NMR (400 MHz,  $\text{CDCl}_3$ ):  $\delta$ (ppm) = 7.59 – 7.48 (m, 2H,  $\text{CH}_{\text{ar}}$ ), 7.39 – 7.30 (m, 3H,  $\text{CH}_{\text{ar}}$ ), 7.07 – 6.97 (m, 10H,  $\text{CH}_{\text{ar}}$ ), 4.30 (q,  $J$  = 7.1 Hz, 2H,  $\text{CH}_2$ ), 4.06 – 3.95 (m, 20H,  $\text{CH}_2$ ), 1.94 – 1.80 (m, 20H,  $\text{CH}_2$ ), 1.35 (t,  $J$  = 7.1 Hz, 3H,  $\text{CH}_3$ ), 1.14 – 1.04 (m, 30H,  $\text{CH}_3$ ).

$^{13}\text{C}$  NMR (101 MHz,  $\text{CDCl}_3$ ):  $\delta(\text{ppm}) = 155.34, 154.32, 153.75, 153.70, 153.63, 153.59, 153.56, 153.28, 131.71, 128.47, 123.63, 118.15, 117.53, 117.46, 117.42, 117.33, 117.23, 114.92, 114.57, 114.50, 114.46, 114.39, 114.21, 113.99, 109.94, 95.02, 92.95, 91.93, 91.68, 91.07, 86.12, 85.62, 83.21, 71.35, 71.30, 71.24, 62.15, 22.87, 22.81, 22.72, 22.67, 14.25, 10.69, 10.54.$

IR (ATR):  $\nu / \text{cm}^{-1} = 2960, 2933, 2904, 2876, 2215, 1707, 1596, 1512, 1471, 1425, 1386, 1275, 1236, 1207, 1152, 1107, 1063, 1041, 1020, 981, 905, 862, 757, 718, 689.$

HRMS (ESI) of  $[\text{M}]^+ [\text{C}_{81}\text{H}_{90}\text{O}_{12}]^+$ : calc. 1254.6432; found 1254.6428;  $\Delta = 0.4$  mmu

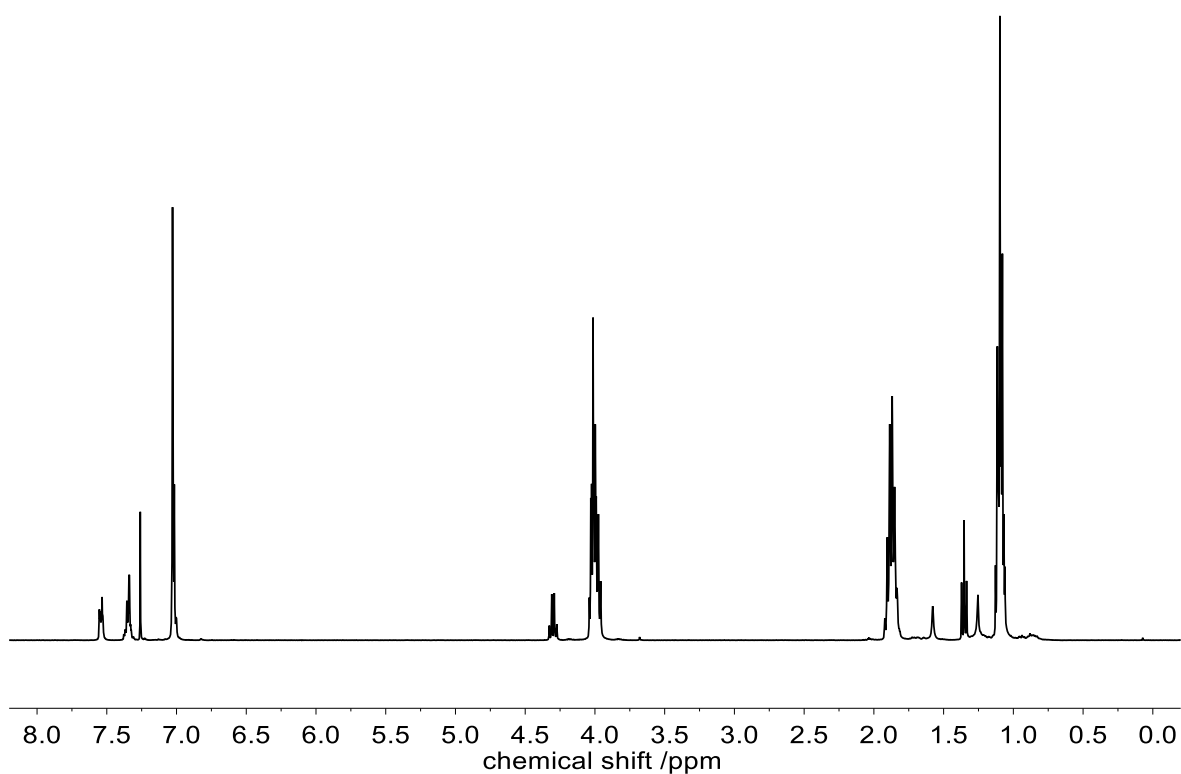
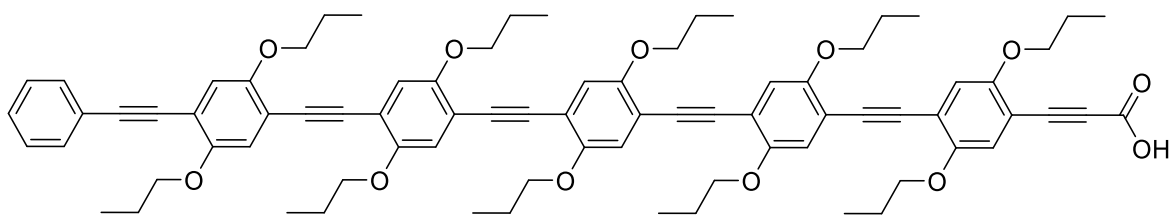


Figure S22:  $^1\text{H}$  NMR spectrum of **5a** measured in  $\text{CDCl}_3$ .

*Synthesis of pentamer acid (5b)*

Pentamer acid **5b** was prepared according to general procedure G2a. **5a** (100 mg, 79.6  $\mu\text{mol}$ , 1.00 eq.) and NaOH (6.4 mg, 159  $\mu\text{mol}$ , 2.00 eq.) were used. **5b** was obtained after filter column chromatography (dichloromethane $\rightarrow$ acetone $\rightarrow$ acetone/methanol 19:1 + 1%acetic acid) as a yellow solid (72.9 mg, 59.4  $\mu\text{mol}$ , 75%).

$R_f$  = 0.00 in cyclohexane/ethyl acetate (10:1). Visualized *via* Seebach staining solution.

$^1\text{H}$  NMR (400 MHz,  $\text{CDCl}_3$ ):  $\delta$ (ppm) = 7.57 – 7.51 (m, 2H,  $\text{CH}_{\text{ar}}$ ), 7.39 – 7.30 (m, 3H,  $\text{CH}_{\text{ar}}$ ), 7.06 – 6.99 (m, 10H,  $\text{CH}_{\text{ar}}$ ), 4.06 – 3.94 (m, 20H,  $\text{CH}_2$ ), 1.96 – 1.76 (m, 20H,  $\text{CH}_2$ ), 1.15 – 1.03 (m, 30H,  $\text{CH}_3$ ).

$^{13}\text{C}$  NMR (101 MHz,  $\text{CDCl}_3$ ):  $\delta$ (ppm) = 154.26, 153.76, 153.63, 153.60, 131.71, 128.47, 123.63, 118.19, 117.55, 117.44, 117.35, 117.29, 114.61, 114.47, 114.22, 112.73, 95.03, 91.74, 91.68, 91.35, 86.12, 71.36, 71.31, 71.25, 71.20, 22.87, 22.81, 22.68, 10.69, 10.58.

IR (ATR):  $\nu / \text{cm}^{-1}$  = 2964, 2937, 2876, 2203, 1711, 1668, 1600, 1510, 1467, 1423, 1384, 1273, 1203, 1105, 1061, 1041, 1014, 981, 909, 860, 852, 753, 689, 638, 605, 527.

HRMS (ESI) of  $[\text{M}]^+$   $[\text{C}_{79}\text{H}_{86}\text{O}_{12}]^+$ : calc. 1226.6119; found 1226.6113;  $\Delta$  = 0.6 mmu

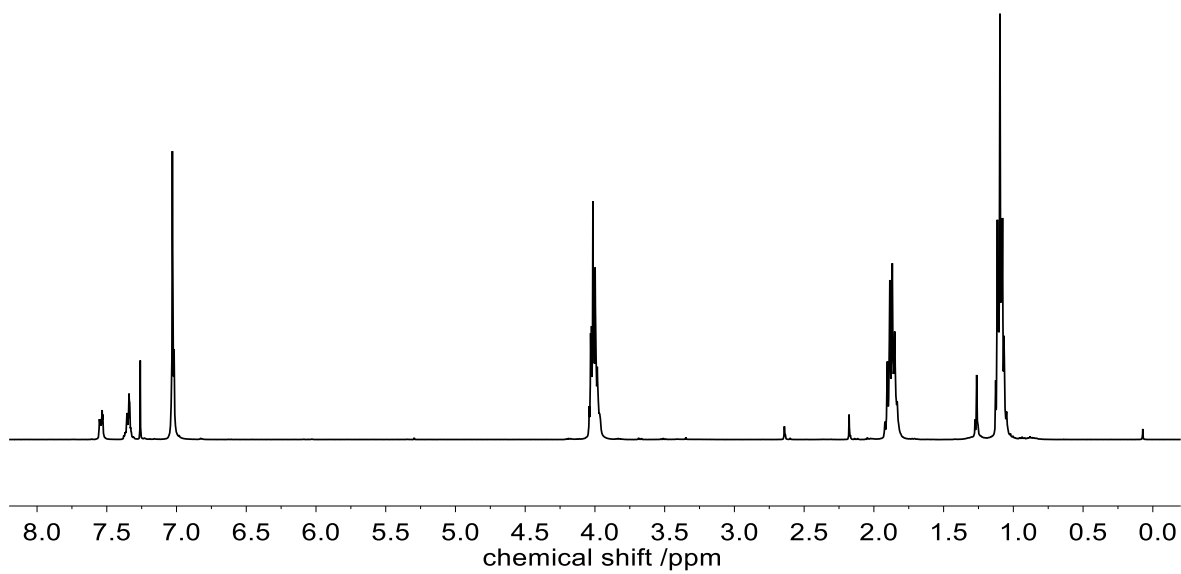
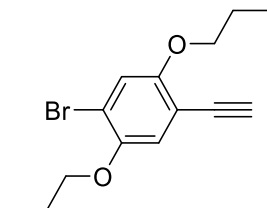


Figure S23:  $^1\text{H}$  NMR spectrum of **5b** measured in  $\text{CDCl}_3$ .

## 6.3.4 Synthesis of the double building unit

This chapter has been published before as a part of the supplementary information:

D. Hahn, R. V. Schneider, E. Foitzik, M. A. R. Meier, *Macromol. Rapid Commun.* **2021**, 2000735.

*Synthesis of 1-bromo-4-ethynyl-2,5-dipropoxybenzene (B1d)*

**B1c** (2.00 g, 5.41 mmol, 1.00 eq.) was dissolved in 50 mL Methanol and 50 mL THF. Subsequently, potassium carbonate (1.50 g, 10.8 mmol, 2.00 eq.) was added and the mixture stirred for two hours at ambient temperature. and quenched with distilled water. The aqueous phase was extracted three times with dichloromethane, dried over Na<sub>2</sub>SO<sub>4</sub>, filtered, and concentrated under reduced pressure to yield the product as a yellow solid (1.54 g, 5.18 mmol, 96 %).

R<sub>f</sub> = 0.53 in cyclohexane/ethyl acetate (20:1). Visualized *via* Seebach staining solution.

<sup>1</sup>H NMR (400 MHz, CDCl<sub>3</sub>): δ(ppm) = 7.08 (s, 1H, CH<sub>ar</sub>), 6.97 (s, 1H, CH<sub>ar</sub>), 3.94 (t, *J* = 6.6 Hz, 2H, OCH<sub>2</sub>), 3.92 (t, *J* = 6.4 Hz, 2H, OCH<sub>2</sub>), 3.29 (s, 1H, CCH), 1.88 – 1.76 (m, 4H, CH<sub>2</sub>), 1.05 (t, *J* = 7.4 Hz, 3H, CH<sub>3</sub>), 1.05 (t, *J* = 7.4 Hz, 3H, CH<sub>3</sub>).

<sup>13</sup>C NMR (101 MHz, CDCl<sub>3</sub>): δ(ppm) = 154.82, 149.45, 118.53, 118.12, 114.11, 111.44, 81.73, 79.63, 71.70, 71.44, 22.70, 22.64, 10.67, 10.56.

IR (ATR): ν / cm<sup>-1</sup> = 3275, 2956, 2911, 2871, 1489, 1458, 1444, 1372, 1267, 1212, 1193, 1039, 1016, 969, 907, 858, 827, 769, 726, 685, 662, 650, 444, 424.

HRMS (FAB) of [M]<sup>+</sup> [C<sub>14</sub>H<sub>17</sub>O<sub>2</sub>Br]<sup>+</sup>: calc. 296.0406; found 296.0408; Δ = 0.2 mmu

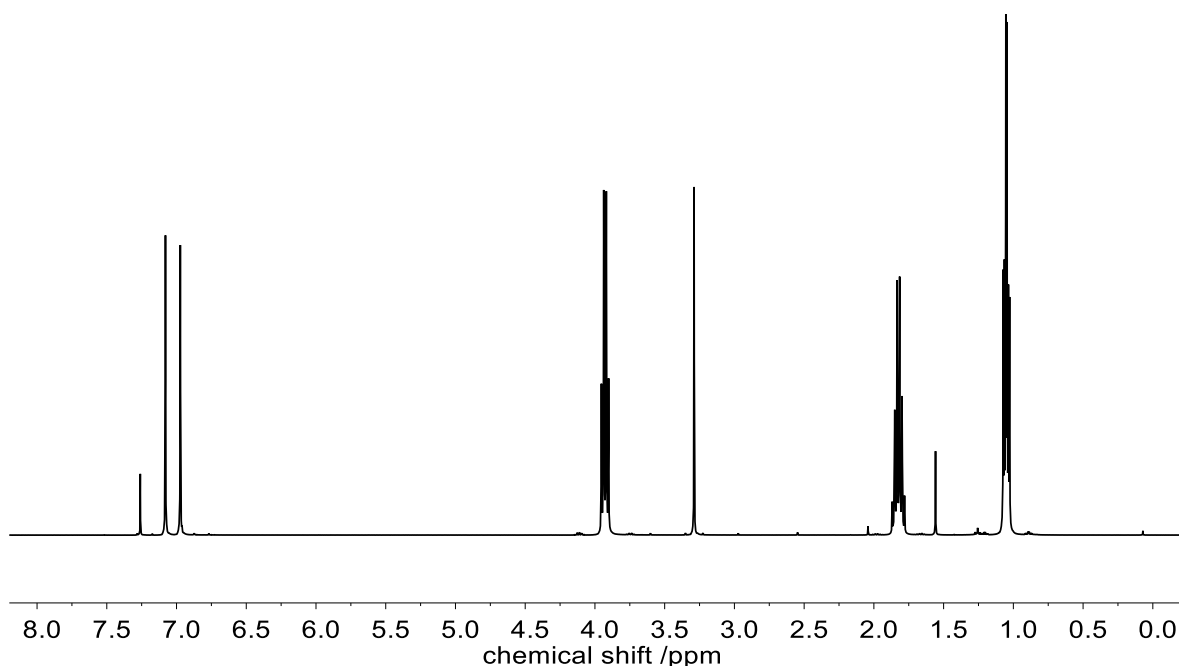
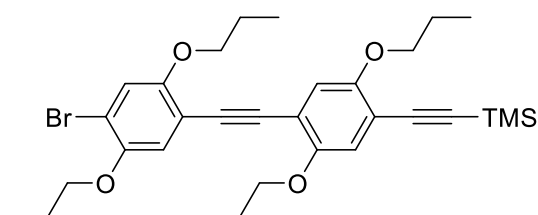


Figure S24:  $^1\text{H}$  NMR spectrum of **B1d** measured in  $\text{CDCl}_3$ .

### Synthesis of

((4-((4-bromo-2,5-dipropoxyphenyl)ethynyl)-2,5-dipropoxyphenyl)ethynyl)trimethylsilane (**B2c**).



**B1d** (1.00 g, 3.36 mmol, 1.00 eq.), **IB1c** (1.40 g, 3.36 mmol, 1.00 eq.), bis(triphenylphosphin)palladium(II) dichlorid (33.8 mg, 0.067 mmol, 0.02 eq.) and copper(I)iodid (9.61 mg, 0.05 mmol, 0.01 eq.) were placed in a sealed vial, degassed and backfilled with argon for three times. Subsequently, the vial was wrapped with aluminium foil and cooled to  $0^\circ\text{C}$  in an ice bath before 14 mL dry triethylamine was added and stirred for one hour. The reaction was diluted with DCM and quenched by addition of ammonium chloride solution. Phases were separated and the aqueous phase extracted three times with DCM. The combined organic

phases were dried over  $\text{Na}_2\text{SO}_4$ , and the solvent evaporated under reduced pressure. The residue was purified by silica column chromatography (cyclohexane/ethyl acetate 100:1  $\rightarrow$  50:1). The product was isolated as a light brown solid (1.84 g, 3.15 mmol, 94%).

$R_f = 0.51$  in cyclohexane/ethyl acetate (20:1). Visualized *via* Seebach staining solution.

$^1\text{H}$  NMR (400 MHz,  $\text{CDCl}_3$ ):  $\delta(\text{ppm}) = 7.09$  (s, 1H,  $\text{CH}_{\text{ar}}$ ), 7.01 (s, 1H,  $\text{CH}_{\text{ar}}$ ), 6.96 (s, 1H,  $\text{CH}_{\text{ar}}$ ), 6.94 (s, 1H,  $\text{CH}_{\text{ar}}$ ), 4.01 – 3.90 (m, 8H,  $\text{OCH}_2$ ), 1.91 – 1.76 (m, 8H,  $\text{CH}_2$ ), 1.11 – 1.02 (m, 12H,  $\text{CH}_3$ ), 0.26 (s, 9H,  $\text{SiCH}_3$ ).

$^{13}\text{C}$  NMR (101 MHz,  $\text{CDCl}_3$ ):  $\delta(\text{ppm}) = 154.29, 154.11, 153.43, 149.56, 118.37, 117.95, 117.57, 117.35, 114.62, 113.92, 113.45, 113.06, 101.27, 100.26, 90.97, 90.60, 71.65, 71.56, 71.26, 71.14, 22.84, 22.79, 22.74, 22.72, 10.68, 10.65, 0.09$ .

IR (ATR):  $\nu / \text{cm}^{-1} = 2962, 2937, 2908, 2876, 2152, 1502, 1469, 1417, 1390, 1378, 1271, 1246, 1214, 1162, 1045, 1024, 1018, 911, 880, 839, 773, 757, 747, 693, 648, 629$ .

HRMS (FAB) of  $[\text{M}]^+ [\text{C}_{31}\text{H}_{41}\text{O}_4\text{BrSi}]^+$ : calc. 584.1952; found 584.1951;  $\Delta = 0.1$  mmu

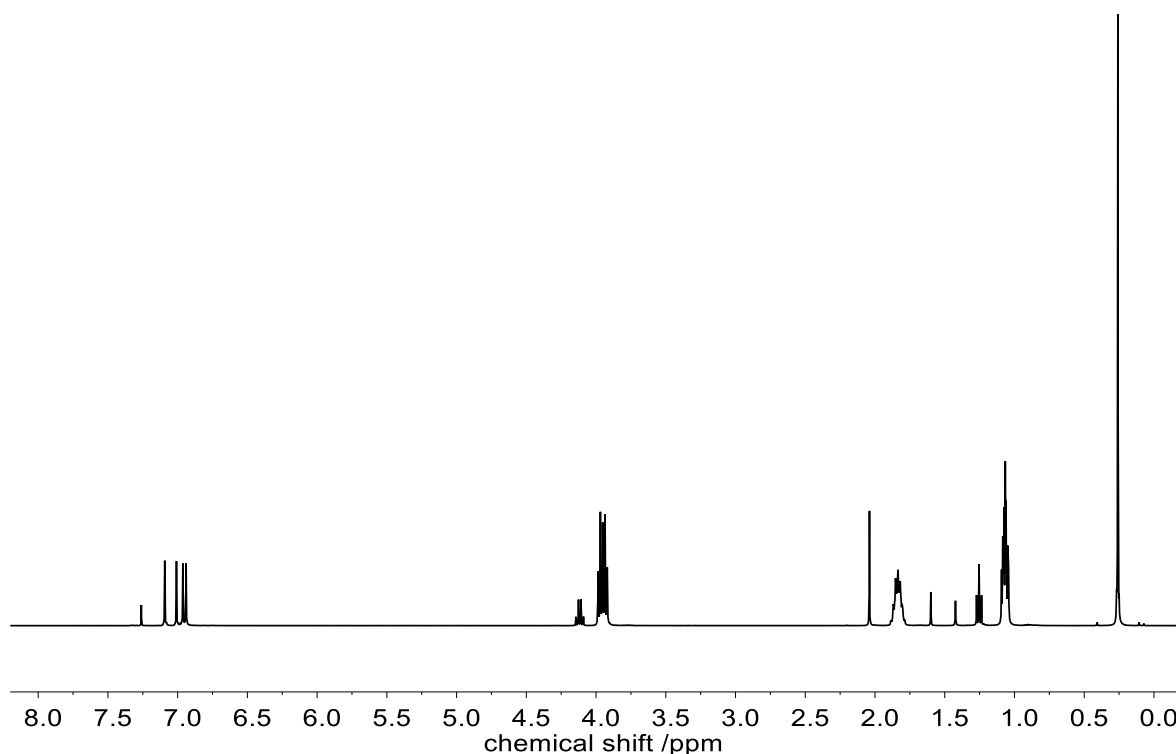
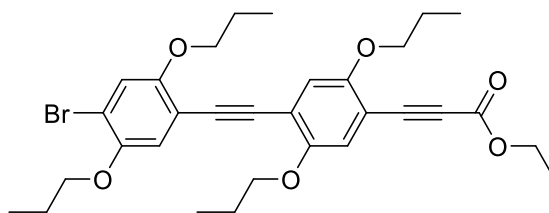


Figure S25:  $^1\text{H}$  NMR spectrum of **B2c** measured in  $\text{CDCl}_3$ .

## Synthesis of

ethyl 3-(4-((4-bromo-2,5-dipropoxyphenyl)ethynyl)-2,5-dipropoxyphenyl)propiolate  
(B2)

**B2c** (1.60 g, 2.73 mmol, 1.00 eq.) and cesium fluoride (498 mg, 3.28 mmol, 1.20 eq.) were placed into Schlenk flask, degassed, and backfilled with CO<sub>2</sub> gas. Subsequently, 30 mL DMSO was added and the resulting solution was stirred for three hours at ambient temperature. Ethyliodide (264  $\mu$ L, 511 mg, 3.28 mmol, 1.20 eq.) was added dropwise and the reaction mixture was stirred over night at ambient temperature. The reaction was quenched by addition of 80 mL saturated ammonium chloride solution. The mixture was extracted three times with 100 mL ethyl acetate and the combined organic phases washed once with brine. The solvent was removed under reduced pressure, and the residue purified by column chromatography (cyclohexane/ethyl acetate 40:1 $\rightarrow$ 30:1). The product was isolated as a yellow solid (1.38 g, 2.35 mmol, 86%).

R<sub>f</sub> = 0.81 in cyclohexane/ethyl acetate (5:1). Visualized *via* Seebach staining solution.

<sup>1</sup>H NMR (400 MHz, CDCl<sub>3</sub>):  $\delta$ (ppm) = 7.10 (s, 1H, CH<sub>ar</sub>), 7.05 – 6.98 (m, 3H, CH<sub>ar</sub>), 4.29 (q, *J* = 7.1 Hz, 2H, CH<sub>2</sub>), 4.01 – 3.88 (m, 8H, OCH<sub>2</sub>), 1.90 – 1.79 (m, 8H, CH<sub>2</sub>), 1.35 (t, *J* = 7.1 Hz, 3H, CH<sub>3</sub>), 1.11 – 1.02 (m, 12H, CH<sub>3</sub>).

<sup>13</sup>C NMR (101 MHz, CDCl<sub>3</sub>):  $\delta$ (ppm) = 155.32, 154.28, 154.21, 153.24, 149.57, 118.32, 118.12, 117.95, 117.26, 117.18, 113.89, 112.66, 109.95, 92.23, 90.14, 85.60, 83.14, 71.66, 71.50, 71.25, 71.21, 62.14, 22.73, 22.70, 22.66, 14.24, 10.66, 10.64, 10.52.

IR (ATR):  $\nu$  / cm<sup>-1</sup> = 2964, 2935, 2873, 2209, 1711, 1600, 1506, 1465, 1419, 1386, 1366, 1275, 1244, 1222, 1205, 1154, 1107, 1096, 1065, 1022, 1010, 983, 956, 930, 854, 835, 782, 745, 720, 675.

HRMS (FAB) of [M]<sup>+</sup> [C<sub>31</sub>H<sub>37</sub>O<sub>6</sub>Br]<sup>+</sup>: calc. 584.1768; found 584.1769;  $\Delta$  = 0.1 mmu

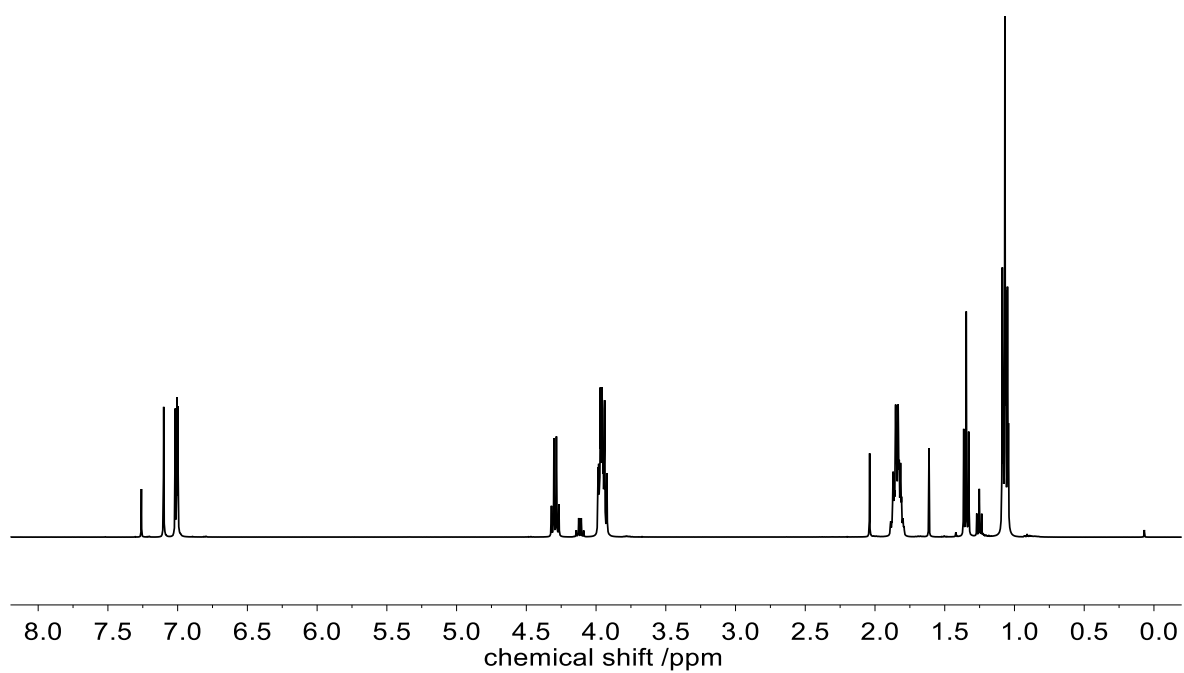
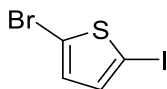


Figure S26:  $^1\text{H}$  NMR spectrum of **B2** measured in  $\text{CDCl}_3$

### 6.3.5 Synthesis of new building units

#### Synthesis of 2-bromo-5-iodothiophene (**B3b**)<sup>i</sup>



2-Bromothiophene (3.26 g, 20.0 mmol, 1.00 eq.) was dissolved in 50 ml DCM. After cooling to 0 °C iodine (2.79 g, 11.0 mmol, 0.55 eq.) and (diacetoxyiodo)benzene (3.87 g, 12.0 mmol, 0.60 eq.) were added at 0 °C and the mixture was stirred for 5 hours at room temperature. Na<sub>2</sub>S<sub>2</sub>O<sub>3</sub> solution (10%) was added, and the mixture was extracted three times with diethylether. The combined organic phases were dried over sodium sulfate and the solvent was removed under reduced pressure. The crude product was purified *via* column chromatography (cyclohexane) followed by vacuum distillation (1 mbar, 70 °C) to obtain the product as a brown liquid (1.39 g, 4.83 mmol, 24%).

R<sub>f</sub> = 1.00 in cyclohexane. Visualized *via* Seebach staining solution.

<sup>1</sup>H NMR (400 MHz, CDCl<sub>3</sub>): δ(ppm) = 6.96 (d, *J* = 3.8 Hz, 1H, CH<sub>ar</sub>), 6.68 (d, *J* = 3.8 Hz, 1H, CH<sub>ar</sub>).

<sup>13</sup>C NMR (101 MHz, CDCl<sub>3</sub>): δ(ppm) = 137.48, 131.69, 115.21, 72.26.

IR (ATR): ν / cm<sup>-1</sup> = 459, 697, 728, 780, 930, 967, 1201, 1397, 1508.

HRMS (FAB) of [M]<sup>+</sup>[C<sub>4</sub>H<sub>2</sub>BrIS]<sup>+</sup>: calc. 287.8105; found 278.8102; Δ = 0.3 mmu

---

<sup>i</sup> The synthesis was carried out by Till Rohde in the Bachelor Thesis "New Building Blocks for Sequence-Defined Stiff Oligomers" under the laboratory supervision of Daniel Hahn.<sup>[169]</sup>

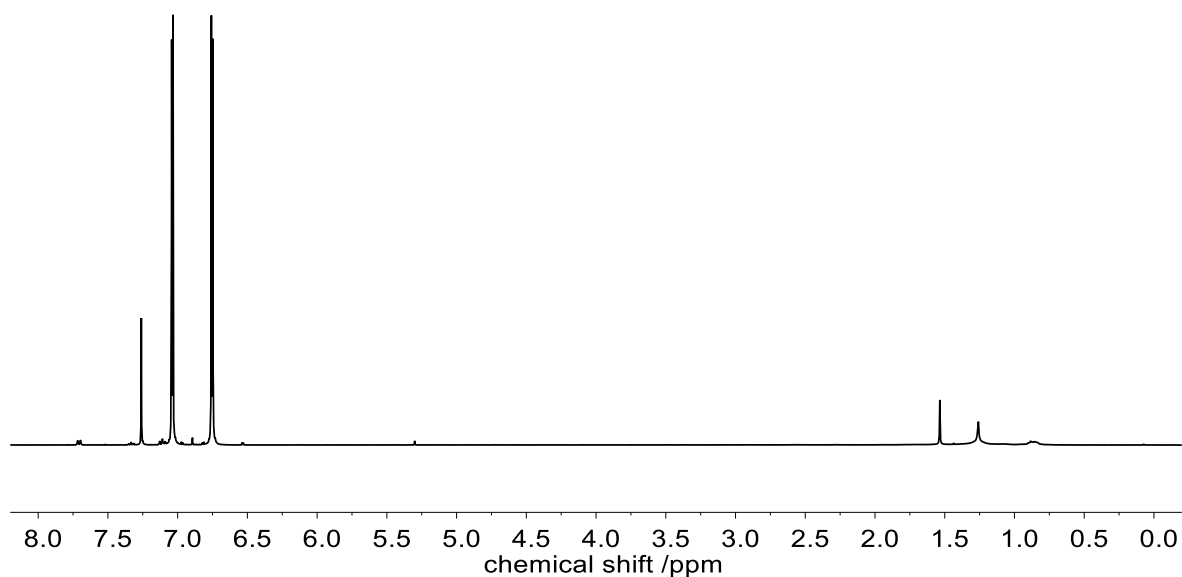
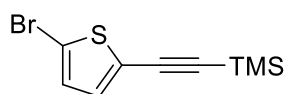


Figure S27:  $^1\text{H}$  NMR spectrum of **B3b** measured in  $\text{CDCl}_3$ .

#### Synthesis of ((5-bromothiophen-2-yl)ethynyl)trimethylsilane (**B3c**)<sup>ii</sup>



2-Bromo-5-Iodothiophene (1.00 g, 3.46 mmol, 1.00 eq.) was dissolved in 13 ml diisopropylamine and purged with argon for 10 minutes. Copper(I) iodide (65.9 mg, 346  $\mu\text{mol}$ , 0.10 eq.) and *bis*(triphenylphosphine)palladium(II) dichloride (121 mg, 173  $\mu\text{mol}$ , 0.05 eq.) were added and the mixture was purged again with argon for 10 minutes. The mixture was cooled to 0 °C and trimethylsilyl acetylene (897mg, 3.46 mmol, 1.00 eq.) was added dropwise. The mixture was stirred 30 minutes at 0 °C and then 1.5 hours at room temperature. The mixture was filtered through silica and Celite® and washed with diethyl ether. The solvent was removed under reduced pressure and the crude mixture was purified *via* column chromatography (n-hexane) to yield the product as a brown oil (550 mg, 2.12 mmol, 61%).

$R_f$  = 0.69 in n-hexane. Visualized *via* Seebach staining solution.

<sup>ii</sup> The synthesis was carried out by Till Rohde in the Bachelor Thesis "New Building Blocks for Sequence-Defined Stiff Oligomers" under the laboratory supervision of Daniel Hahn.<sup>[169]</sup>

$^1\text{H}$  NMR (400 MHz,  $\text{CDCl}_3$ ):  $\delta$ (ppm) = 6.99 (d,  $J$  = 3.9 Hz, 1H,  $\text{CH}_{\text{ar}}$ ), 6.92 (d,  $J$  = 3.9 Hz, 1H,  $\text{CH}_{\text{ar}}$ ), 0.26 (s, 9H,  $\text{CH}_3$ ).

$^{13}\text{C}$  NMR (101 MHz,  $\text{CDCl}_3$ ):  $\delta$ (ppm) = 133.11, 130.08, 125.26, 113.34, 100.34, 96.62.

IR (ATR):  $\nu$  /  $\text{cm}^{-1}$  = 492, 512, 559, 646, 699, 722, 745, 757, 790, 837, 967, 1051, 1158, 1249, 1419, 1520, 2145, 2958.

HRMS (FAB) of  $[\text{M}]^+$  [ $\text{C}_9\text{H}_{11}\text{BrSSi}$ ] $^+$ : calc. 257.9529; found 257.9531;  $\Delta$  = 0.2 mmu.

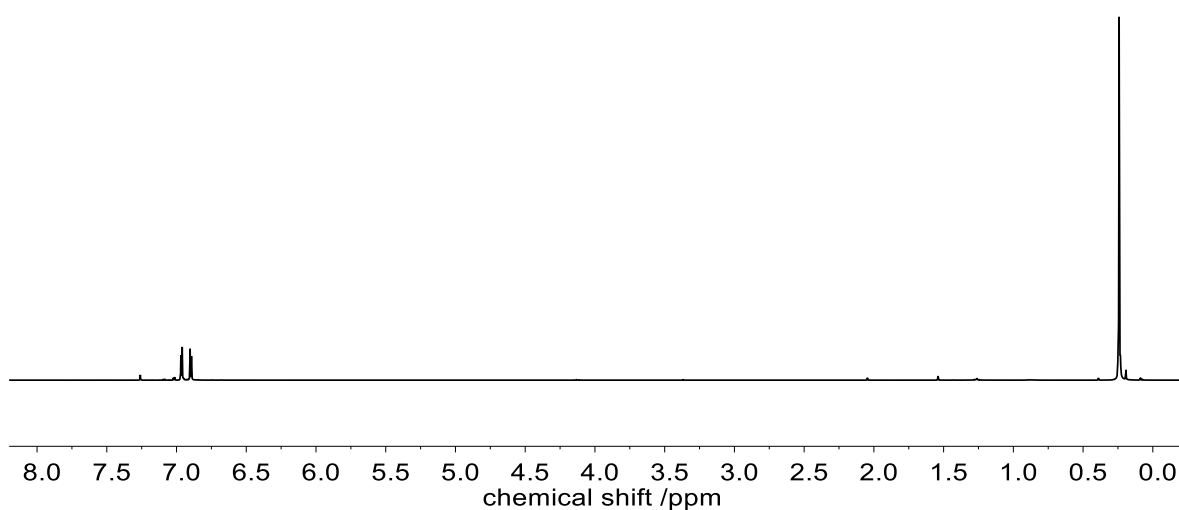
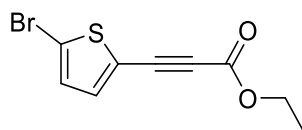


Figure S28:  $^1\text{H}$  NMR spectrum of **B3c** measured in  $\text{CDCl}_3$ .

### Synthesis of ethyl 3-(5-bromothiophen-2-yl)propiolate (**B3**)<sup>iii</sup>



((5-bromothiophen-2-yl)ethynyl)trimethylsilane (200 mg, 772  $\mu\text{mol}$ , 1.00 eq.) and cesium fluoride (141 mg, 926  $\mu\text{mol}$ , 1.20 eq.) were placed into Schlenk flask, degassed, and backfilled with  $\text{CO}_2$  gas. Subsequently, 2.5 mL DMSO were added and the resulting solution was stirred for three hours at ambient temperature. Ethyl iodide (74.4  $\mu\text{L}$ , 144 mg, 926  $\mu\text{mol}$ , 1.20 eq.) was added dropwise and the

---

<sup>iii</sup> The synthesis was carried out by Till Rohde in the Bachelor Thesis "New Building Blocks for Sequence-Defined Stiff Oligomers" under the laboratory supervision of Daniel Hahn.<sup>[169]</sup>

reaction mixture was stirred over night at ambient temperature. The reaction was quenched by addition of 80 mL saturated ammonium chloride solution. The mixture was extracted three times with 100 mL ethyl acetate and the combined organic phases washed once with brine. The solvent was removed under reduced pressure, and the residue purified by column chromatography (cyclohexane/ethyl acetate 10:1). The product was isolated as a brown oil (184 mg, 709  $\mu\text{mol}$ , 92%).

$R_f = 0.44$  in cyclohexane/ethyl acetate (10:1). Visualized *via* Seebach staining solution.

$^1\text{H}$  NMR (400 MHz,  $\text{CDCl}_3$ ):  $\delta(\text{ppm}) = 7.16$  (d,  $J = 4.0$  Hz, 1H, CH), 6.94 (d,  $J = 3.8$  Hz, 1H, CH), 4.23 (q,  $J = 7.1$  Hz, 2H,  $\text{CH}_2$ ), 1.28 (t,  $J = 7.1$  Hz, 3H,  $\text{CH}_3$ ).

$^{13}\text{C}$  NMR (101 MHz,  $\text{CDCl}_3$ ):  $\delta(\text{ppm}) = 153.71, 136.90, 130.60, 121.15, 117.68, 85.63, 78.69, 62.27, 14.09$ .

IR (ATR):  $\nu / \text{cm}^{-1} = 512, 559, 701, 743, 794, 858, 971, 1016, 1055, 1094, 1113, 1150, 1203, 1244, 1298, 1327, 1366, 1388, 1419, 1444, 1520, 1701, 2205, 2925, 2980$ .

HRMS (FAB) of  $[\text{M}]^+ [\text{C}_9\text{H}_7\text{BrO}_2\text{S}]^+$ : calc. 257.9345; found 257.9344;  $\Delta = 0.1$  mmu

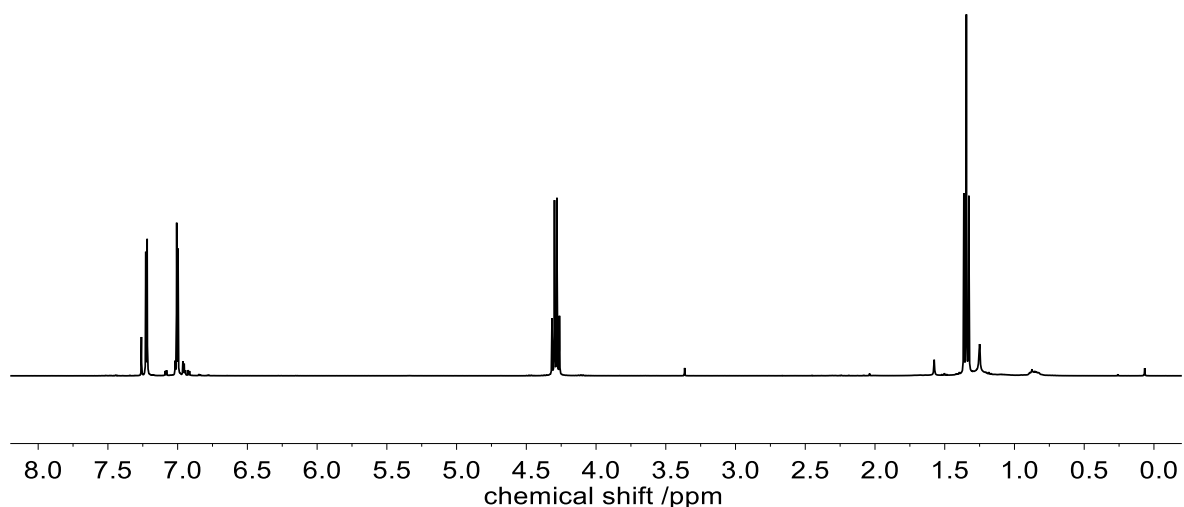
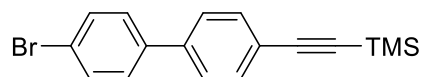


Figure S29:  $^1\text{H}$  NMR spectrum of **B3** measured in  $\text{CDCl}_3$ .

Synthesis of ((4'-bromo-[1,1'-biphenyl]-4-yl)ethynyl)trimethylsilane (**B4c**)<sup>iv</sup>

4,4'-Dibromobiphenyl (5.00 g, 16.0 mmol, 1.00 eq.), 10 mol% *bis*(triphenylphosphine) palladium(II) dichloride (1.12 g, 1.60 mmol, 0.10 eq.) and 10 mol% copper(I) iodide (305 mg, 1.60 mmol, 0.1 eq.) were placed into a Schlenk flask and degassed. Under continuous argon flow, 42 mL THF and 72 mL diisopropylamine were added. Subsequently, trimethylsilyl acetylene (2.51 mL, 1.73 g, 17.6 mmol, 1.10 eq.) was added dropwise with a syringe. The reaction mixture was stirred for 12 hours at 60 °C and one hour at room temperature. Saturated ammonium chloride solution was added, and the phases separated. The organic phase was washed once more with saturated ammonium chloride solution. The combined aqueous phases were extracted three times with dichloromethane. The combined organic phases were dried over sodium sulfate, filtered, and concentrated under reduced pressure. The residue was purified by silica column chromatography (cyclohexane) to yield the product as a white solid (1.83 g, 5.57 mmol, 35%).

$R_f = 0.49$  in cyclohexane. Visualized *via* Seebach staining solution.

<sup>1</sup>H NMR (400 MHz, CDCl<sub>3</sub>):  $\delta$ (ppm) = 7.50 – 7.28 (m, 8H, CH<sub>ar</sub>), 0.15 (s, 9H, CH<sub>3</sub>).

<sup>13</sup>C NMR (101 MHz, CDCl<sub>3</sub>):  $\delta$ (ppm) = 139.92, 139.25, 132.53, 131.99, 128.61, 126.67, 122.49, 121.98, 104.76, 95.28, 0.00.

IR (ATR):  $\nu / \text{cm}^{-1} = 455, 508, 553, 648, 699, 736, 759, 810, 837, 1000, 1078, 1197, 1230, 1244, 1253, 1386, 1454, 1479, 1586, 2158, 2956$ .

HRMS (FAB) of [M]<sup>+</sup> [C<sub>17</sub>H<sub>17</sub>BrSi]<sup>+</sup>: calc. 328.0277; found 328.0279;  $\Delta = 0.2$  mmu.

<sup>iv</sup> The synthesis was carried out by Till Rohde in the Bachelor Thesis "New Building Blocks for Sequence-Defined Stiff Oligomers" under the laboratory supervision of Daniel Hahn.<sup>[169]</sup>

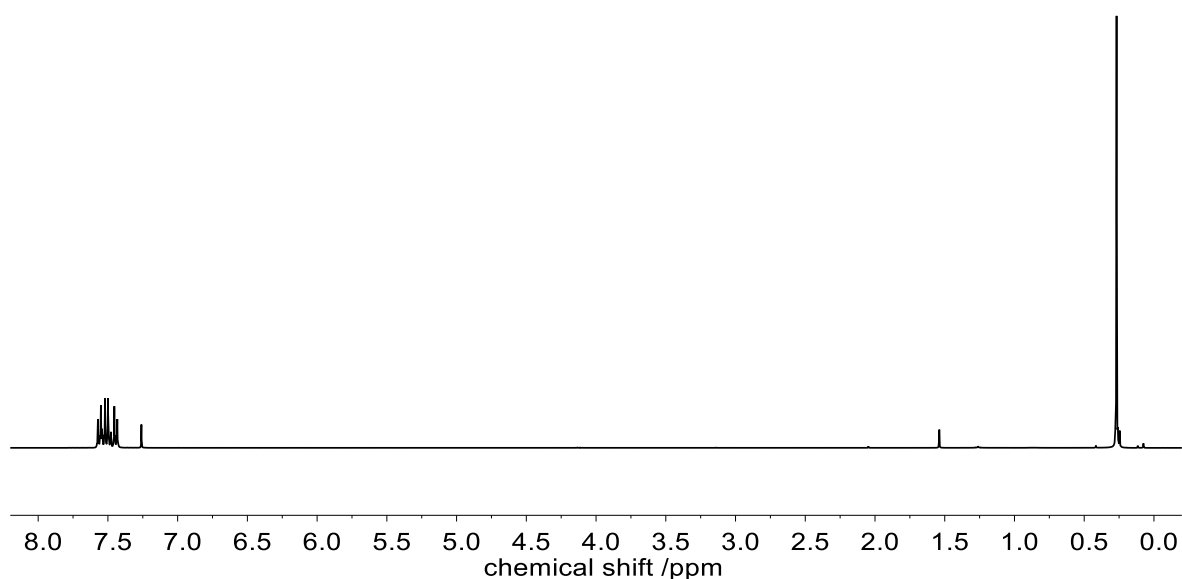
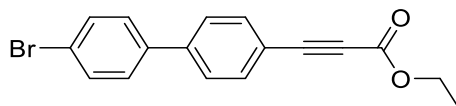


Figure S30:  $^1\text{H}$  NMR spectrum of **B4c** measured in  $\text{CDCl}_3$ .

#### Synthesis of ethyl 3-(4'-bromo-[1,1'-biphenyl]-4-yl)propiolate (**B4**)<sup>v</sup>



**B4c** (1.50 g, 4.55 mmol, 1.00 eq.) and cesium fluoride (830 mg, 5.47 mmol, 1.20 eq.) were placed into Schlenk flask, degassed, and backfilled with  $\text{CO}_2$  gas. Subsequently, 12.5 mL DMSO was added, and the resulting solution was stirred for three hours at ambient temperature. Ethyliodide (439  $\mu\text{L}$ , 853 mg, 5.47 mmol, 1.20 eq.) was added dropwise and the reaction mixture was stirred over night at ambient temperature. The reaction was quenched by addition of 80 mL saturated ammonium chloride solution. The mixture was extracted three times with 100 mL ethyl acetate and the combined organic phases washed once with brine. The solvent was removed under reduced pressure, and the residue purified by column chromatography (cyclohexane/ethyl acetate 50:1 $\rightarrow$ 30:1). The product was isolated as a yellow solid (1.26 g, 3.83 mmol, 85%).

<sup>v</sup> The synthesis was carried out by Till Rohde in the Bachelor Thesis "New Building Blocks for Sequence-Defined Stiff Oligomers" under the laboratory supervision of Daniel Hahn.<sup>[169]</sup>

## Experimental Section

---

$R_f = 0.45$  in cyclohexane/ethyl acetate (50:1). Visualized *via* Seebach staining solution.

$^1\text{H}$  NMR (400 MHz,  $\text{CDCl}_3$ ):  $\delta(\text{ppm}) = 7.58$  (d,  $J = 8.4$  Hz, 2H,  $\text{CH}_{\text{ar}}$ ), 7.55 – 7.43 (m, 4H,  $\text{CH}_{\text{ar}}$ ), 7.38 (d,  $J = 8.5$  Hz, 2H,  $\text{CH}_{\text{ar}}$ ), 4.24 (q,  $J = 7.1$  Hz, 2H,  $\text{CH}_2$ ), 1.30 (t,  $J = 7.1$  Hz, 3H,  $\text{CH}_3$ ).

$^{13}\text{C}$  NMR (101 MHz,  $\text{CDCl}_3$ ):  $\delta(\text{ppm}) = 154.05, 142.13, 138.72, 133.58, 132.12, 128.69, 127.03, 122.56, 118.82, 85.79, 81.49, 62.17, 14.12$ .

IR (ATR):  $\nu / \text{cm}^{-1} = 500, 520, 562, 625, 734, 749, 775, 812, 852, 928, 1000, 1012, 1072, 1092, 1117, 1179, 1197, 1286, 1366, 1386, 1446, 1479, 1586, 1600, 1701, 2205, 2230$ .

HRMS (FAB) of  $[\text{M}]^+ [\text{C}_{17}\text{H}_{13}\text{BrO}_2]^+$ : calc. 329.0172; found 329.0174;  $\Delta = 0.2$  mmu

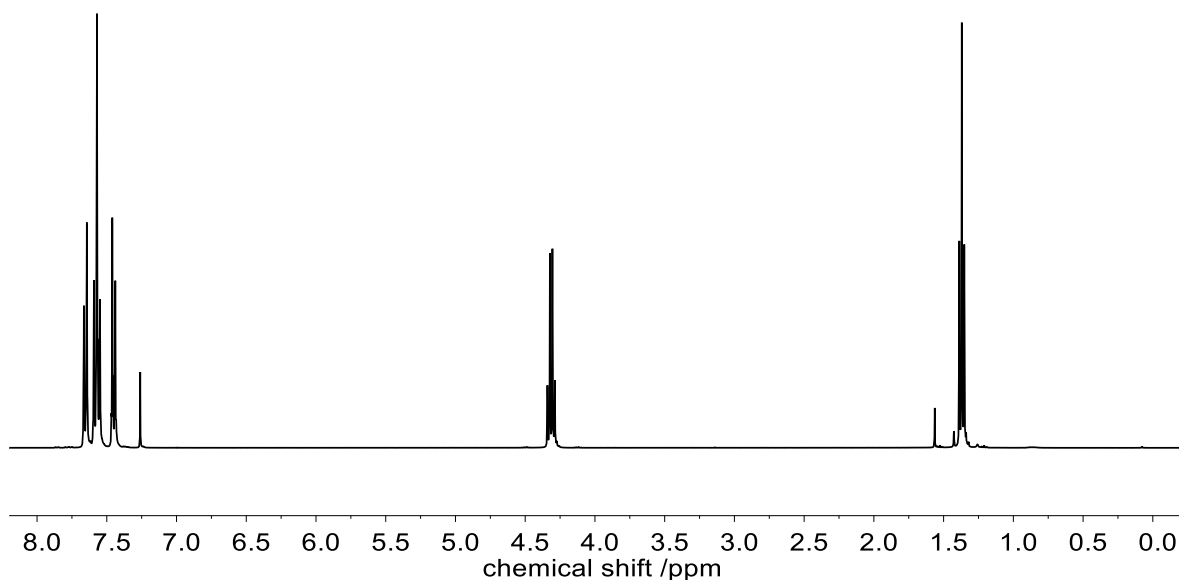
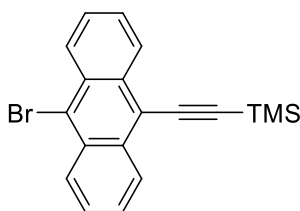


Figure S31:  $^1\text{H}$  NMR spectrum of **B4** measured in  $\text{CDCl}_3$ .

*Synthesis of ((10-bromoanthracen-9-yl)ethynyl)trimethylsilane (B5c)<sup>vi</sup>*

9,10-Dibromanthracene (5.00 g, 14.9 mmol, 1.00 eq.), tris(dibenzylideneacetone) dipalladium(0) (82.5 mg, 90.1  $\mu\text{mol}$ , 0.01 eq.), triphenylphosphine (115.2 mg, 439  $\mu\text{mol}$ , 0.03 eq.), and copper(I) iodide (77.8 mg, 409  $\mu\text{mol}$ , 0.03 eq.) were placed into a Schlenk flask and degassed. Under continuous argon flow, 100 mL toluene and 25 mL triethylamine were added. Subsequently, trimethylsilyl acetylene (1.67 mL, 1.16 g, 11.8 mmol, 0.80 eq.) was added dropwise with a syringe. The reaction mixture was stirred for 20 hours at 65 °C. The reaction mixture was filtered, and the filtrate concentrated under reduced pressure. The residue was purified by silica column chromatography (cyclohexane) to yield the product as an orange solid (2.19 g, 6.19 mmol, 42%).

$R_f = 0.29$  in cyclohexane/ethyl acetate (35:1). Visualized *via* Seebach staining solution.

$^1\text{H}$  NMR (400 MHz,  $\text{CDCl}_3$ ):  $\delta(\text{ppm}) = 8.46 - 8.40$  (m, 2H,  $\text{CH}_{\text{ar}}$ ), 8.39 – 8.35 (m, 2H,  $\text{CH}_{\text{ar}}$ ), 7.49 – 7.41 (m, 4H,  $\text{CH}_{\text{ar}}$ ), 0.26 (s, 9H,  $\text{CH}_3$ ).

$^{13}\text{C}$  NMR (101 MHz,  $\text{CDCl}_3$ ):  $\delta(\text{ppm}) = 133.93, 133.10, 130.88, 129.98, 128.11, 128.00, 127.29, 127.22, 127.09, 126.72, 117.90, 107.44, 100.92$ .

IR (ATR):  $\nu / \text{cm}^{-1} = 457, 578, 603, 625, 646, 662, 675, 701, 749, 841, 907, 926, 1026, 1047, 1059, 1249, 1304, 1327, 1436, 1623, 2139, 2919, 2960$ .

HRMS (FAB) of  $[\text{M}]^+$   $[\text{C}_{19}\text{H}_{17}\text{BrSi}]^+$ : calc. 352.0277; found 352.0275;  $\Delta = 0.2$  mmu.

<sup>vi</sup> The synthesis was carried out by Till Rohde in the Bachelor Thesis “New Building Blocks for Sequence-Defined Stiff Oligomers” under the laboratory supervision of Daniel Hahn.<sup>[169]</sup>

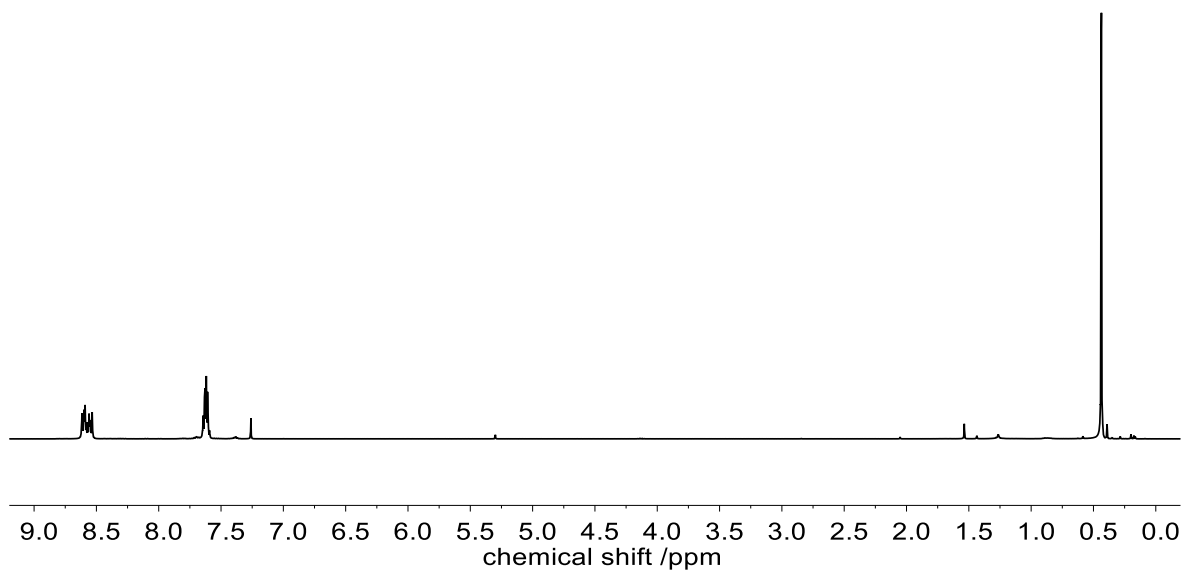
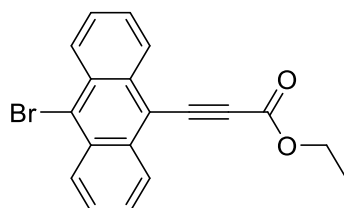


Figure S32:  $^1\text{H}$  NMR spectrum of **B5c** measured in  $\text{CDCl}_3$ .

**Synthesis of the anthracene building unit (B5)<sup>vii</sup>**



**B5c** (1.50 g, 4.25 mmol, 1.00 eq.) and cesium fluoride (774 mg, 5.09 mmol, 1.20 eq.) were placed into Schlenk flask, degassed, and backfilled with  $\text{CO}_2$  gas. Subsequently, 12.5 mL DMSO was added, and the resulting solution was stirred for three hours at ambient temperature. Ethyl iodide (409  $\mu\text{L}$ , 795 mg, 5.09 mmol, 1.20 eq.) was added dropwise and the reaction mixture was stirred over night at ambient temperature. The reaction was quenched by addition of 80 mL saturated ammonium chloride solution. The mixture was extracted three times with 100 mL ethyl acetate and the combined organic phases washed once with brine. The solvent was removed under reduced pressure, and the residue purified by column chromatography (cyclohexane/ethyl acetate 50:1). The product was isolated as an orange solid (1.10 g, 3.10 mmol, 73%).

<sup>vii</sup> The synthesis was carried out by Till Rohde in the Bachelor Thesis "New Building Blocks for Sequence-Defined Stiff Oligomers" under the laboratory supervision of Daniel Hahn.<sup>[169]</sup>

$R_f = 0.51$  in cyclohexane. Visualized *via* Seebach staining solution.

$^1\text{H}$  NMR (400 MHz,  $\text{CDCl}_3$ ):  $\delta(\text{ppm}) = 8.52$  (m, 3H,  $\text{CH}_{\text{ar}}$ ), 7.65 – 7.55 (m, 3H,  $\text{CH}_{\text{ar}}$ ), 7.19 (s, 2H,  $\text{CH}_{\text{ar}}$ ), 4.35 (q,  $J = 7.2$  Hz, 2H,  $\text{CH}_2$ ), 1.38 (t,  $J = 7.1$  Hz, 3H,  $\text{CH}_3$ ).

$^{13}\text{C}$  NMR (101 MHz,  $\text{CDCl}_3$ ):  $\delta(\text{ppm}) = 154.28, 134.36, 130.33, 130.17, 128.50, 128.00, 127.76, 126.73, 113.90, 92.36, 82.65, 62.31, 14.24$ .

IR (ATR):  $\nu / \text{cm}^{-1} = 453, 555, 576, 603, 619, 634, 743, 749, 765, 845, 860, 887, 921, 961, 1020, 1076, 1090, 1115, 1150, 1166, 1177, 1236, 1263, 1286, 1339, 1362, 1413, 1438, 1450, 1465, 1477, 1621, 1699, 2201, 2921, 2993$ .

HRMS (FAB) of  $[\text{M}]^+$   $[\text{C}_{19}\text{H}_{13}\text{BrO}_2]^+$ : calc. 352.0093; found 352.0092;  $\Delta = 0.1$  mmu.

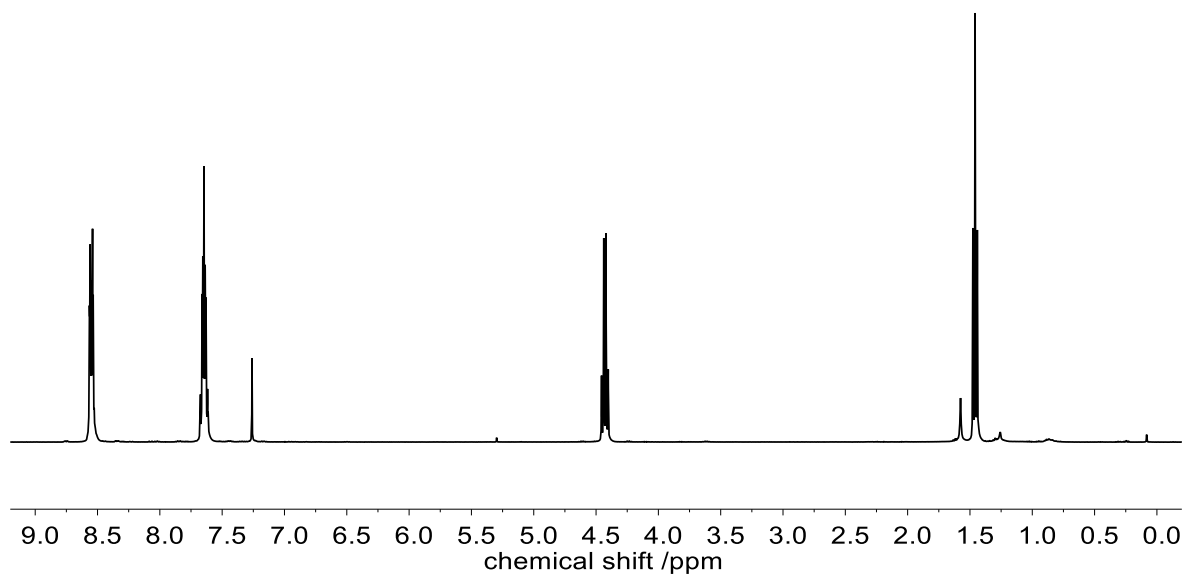
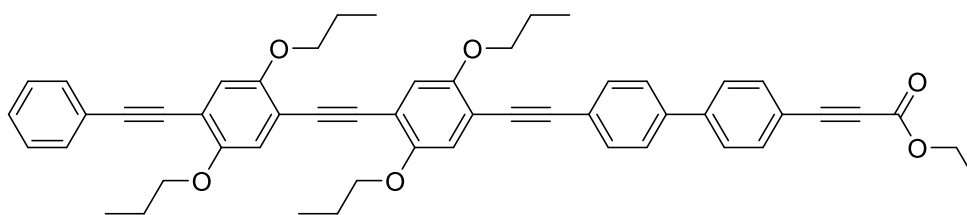


Figure S33:  $^1\text{H}$  NMR spectrum of **B5** measured in  $\text{CDCl}_3$ .

Synthesis of sequence-defined trimer (**BP3a**)

Sequence-defined trimer ester was prepared according to general procedure G1. **2b** (200 mg, 114  $\mu\text{mol}$ , 1.00 eq.), **B5** (60.2 mg, 163  $\mu\text{mol}$ , 1.10 eq.), SPhos (14.2 mg, 34.6  $\mu\text{mol}$ , 0.1 eq.), cesium carbonate (135 mg, 415  $\mu\text{mol}$ , 1.20 eq.) and 1,1'-Bis(diphenylphosphino)ferrocene-palladium(II)dichloride dichloromethane complex (14.1 mg, 17.3  $\mu\text{mol}$ , 0.05 eq.) were used. Purification by silica column chromatography (cyclohexane/ethyl acetate 10:1) yielded **BP3a** as a yellow solid (100 mg, 128  $\mu\text{mol}$ , 37%).

$R_f$  = 0.08 in cyclohexane/ethyl acetate (20:1). Visualized *via* Seebach staining solution.

$^1\text{H}$  NMR (400 MHz,  $\text{CDCl}_3$ ):  $\delta$ (ppm) = 7.52 (m, 10H,  $\text{CH}_{\text{ar}}$ ), 7.39 – 7.31 (m, 3H,  $\text{CH}_{\text{ar}}$ ), 7.06 – 7.01 (m, 4H,  $\text{CH}_{\text{ar}}$ ), 4.32 (q,  $J$  = 7.1 Hz, 2H,  $\text{CH}_2$ ), 4.06 – 3.97 (m, 8H,  $\text{CH}_2$ ), 1.96 – 1.80 (m, 8H,  $\text{CH}_2$ ), 1.37 (t,  $J$  = 7.1 Hz, 3H,  $\text{CH}_3$ ), 1.16 – 1.06 (m, 12H,  $\text{CH}_3$ ).

$^{13}\text{C}$  NMR (101 MHz,  $\text{CDCl}_3$ ):  $\delta$ (ppm) = 154.22, 153.83, 153.77, 153.65, 142.64, 139.53, 133.70, 132.28, 131.72, 128.48, 128.44, 127.21, 127.16, 123.64, 123.56, 118.87, 117.45, 117.39, 117.35, 114.73, 114.43, 114.29, 113.98, 95.05, 94.66, 91.78, 91.57, 87.53, 86.12, 86.08, 81.65, 71.39, 71.37, 71.27, 71.23, 62.29, 22.88, 22.84, 14.26, 10.72.

IR (ATR):  $\nu$  /  $\text{cm}^{-1}$  = 529, 541, 640, 687, 720, 745, 755, 784, 825, 837, 858, 891, 915, 985, 1002, 1014, 1059, 1105, 1113, 1177, 1199, 1220, 1273, 1290, 1366, 1384, 1423, 1442, 1462, 1489, 1508, 1707, 2205, 2867, 2925, 2962.

HRMS (FAB) of  $[\text{M}]^+$   $[\text{C}_{53}\text{H}_{50}\text{O}_6]^+$ : calc.: 782.3602; found: 782.3604;  $\Delta$  = 0.2 mmu.

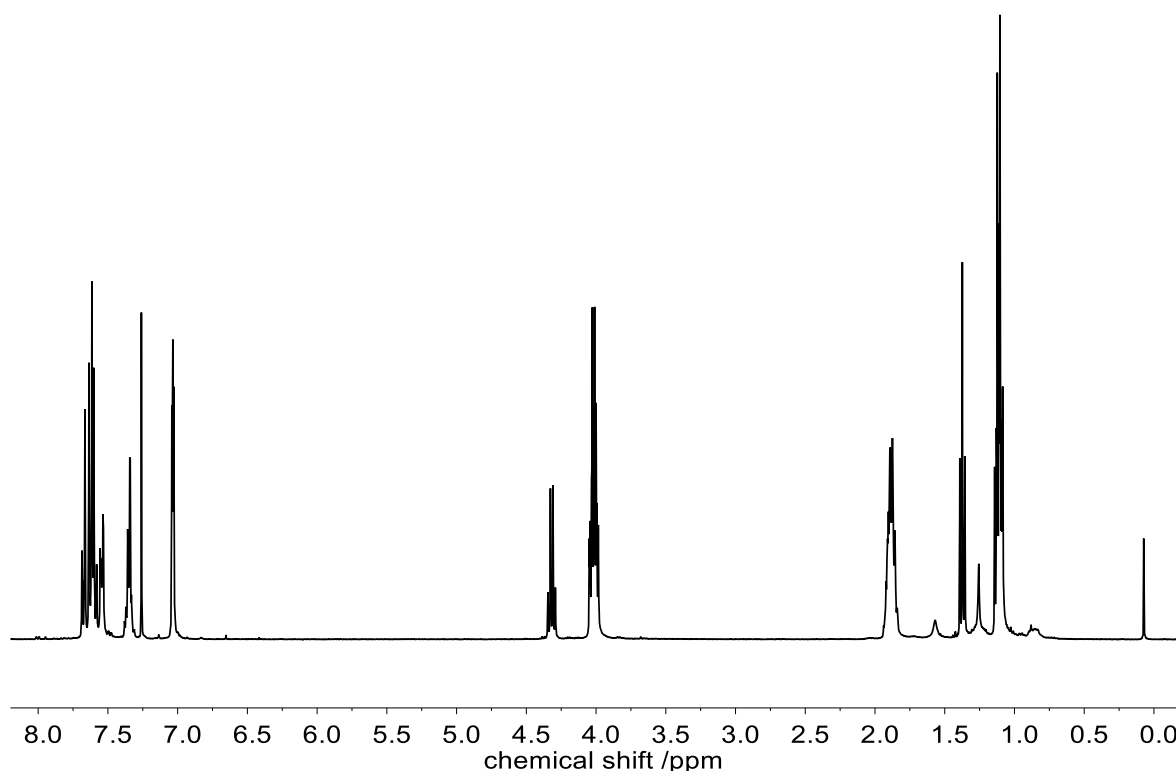
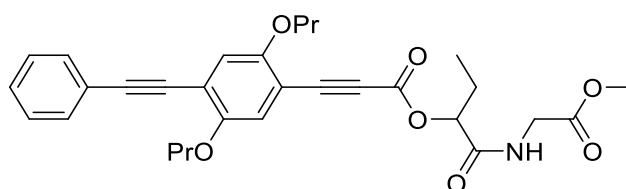


Figure S34:  $^1\text{H}$  NMR spectrum of **BP3a** measured in  $\text{CDCl}_3$ .

### 6.3.6 Applications of OPEs in MCRs

#### *Passerini reaction*



Monomer **1a** (362 mg, 1.00 mmol, 1.00 eq.) was stirred in 1.00 mL DCM. Subsequently, propionaldehyde (108  $\mu\text{L}$ , 87.1 mg, 1.50 mmol, 1.50 eq.) and methyl isocyanoacetate (138  $\mu\text{L}$ , 150 mg, 1.50 mmol, 1.50 eq.) were added. The resulting reaction mixture was stirred at ambient temperature for 24 hours. Afterwards, the mixture was diluted with DCM and washed with brine. Phases were separated and the aqueous phase extracted three times with DCM. The combined organic phases were dried over  $\text{Na}_2\text{SO}_4$ , and the solvent evaporated under reduced pressure. The residue was purified by silica column chromatography (cyclohexane/ethyl acetate 3:1  $\rightarrow$  2:1). The product was isolated as a light-yellow solid (516 mg, 993  $\mu\text{mol}$ , 99%).

$R_f = 0.60$  in cyclohexane/ethyl acetate (1:1). Visualized *via* Seebach staining solution.

$^1\text{H}$  NMR (400 MHz,  $\text{CDCl}_3$ ):  $\delta(\text{ppm}) = 7.57 - 7.50$  (m, 2H,  $\text{CH}_{\text{ar}}$ ),  $7.38 - 7.32$  (m, 3H,  $\text{CH}_{\text{ar}}$ ),  $7.05$  (s, 1H,  $\text{CH}_{\text{ar}}$ ),  $7.03$  (s, 1H,  $\text{CH}_{\text{ar}}$ ),  $6.70$  (t,  $J = 5.5$  Hz, 1H, NH),  $5.36$  (t,  $J = 5.3$  Hz, 1H),  $4.23 - 3.93$  (m, 6H,  $\text{CH}_2$ ),  $3.77$  (s, 3H,  $\text{CH}_3$ ),  $2.07 - 1.93$  (m, 2H,  $\text{CH}_2$ ),  $1.87$  (m, 4H,  $\text{CH}_2$ ),  $1.10$  (t,  $J = 7.4$  Hz, 3H,  $\text{CH}_3$ ),  $1.08$  (t,  $J = 7.4$  Hz, 3H,  $\text{CH}_3$ ),  $1.01$  (t,  $J = 7.4$  Hz, 3H,  $\text{CH}_3$ ).

$^{13}\text{C}$  NMR (101 MHz,  $\text{CDCl}_3$ ):  $\delta(\text{ppm}) = 169.99, 169.54, 155.63, 153.48, 152.68, 131.80, 128.79, 128.54, 123.17, 117.97, 117.73, 116.98, 109.27, 96.57, 85.51, 85.47, 84.67, 76.25, 71.27, 71.20, 52.56, 40.99, 25.28, 22.77, 22.67, 10.67, 10.57, 8.92$ .

IR (ATR):  $\nu / \text{cm}^{-1} = 500, 533, 664, 679, 693, 710, 738, 761, 862, 919, 969, 1018, 1041, 1063, 1088, 1105, 1129, 1158, 1189, 1216, 1261, 1279, 1339, 1347, 1388, 1413, 1436, 1442, 1460, 1471, 1489, 1506, 1567, 1664, 1713, 1746, 2217, 2878, 2939, 2964, 3089, 3272$ .

HRMS (FAB) of  $[\text{M}]^+$   $[\text{C}_{30}\text{H}_{33}\text{O}_7\text{N}]^+$ : calc. 519.2252; found 519.2250;  $\Delta = 0.2$  mmu

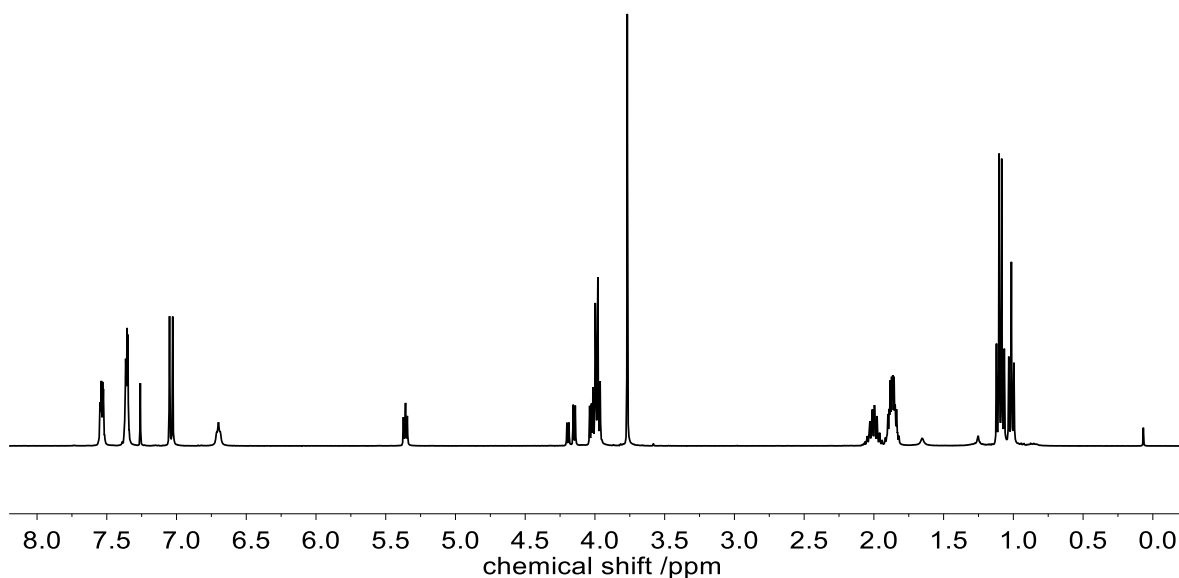
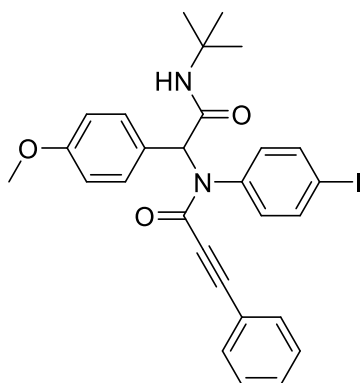


Figure S35:  $^1\text{H}$  NMR spectrum of the Passerini product measured in  $\text{CDCl}_3$ .

### Synthesis of the Ugi monomer (**U1a**)



4-Iodoaniline (1.10 g, 5.00 mmol, 1.00 eq.) and 4-methoxy benzaldehyde (608  $\mu\text{L}$ , 681 mg, 5.00 mmol, 1.00 eq.) were stirred in 10 mL methanol. Subsequently, phenyl propionic acid (731 mg, 5.00 mmol, 1.00 eq.) and *tert* butyl isocyanide (566  $\mu\text{L}$ , 416 mg, 5.00 mmol, 1.00 eq.) were added. The resulting mixture was stirred at ambient temperature for 24 hours. Afterwards, the mixture was diluted with DCM and washed with brine. The aqueous phase was extracted with DCM. The combined organic phases were dried over  $\text{Na}_2\text{SO}_4$ , filtered, and concentrated under reduced pressure. The residue was purified *via* silica column chromatography (cyclohexane/ethyl acetate 3:1  $\rightarrow$  7:3  $\rightarrow$  13:7  $\rightarrow$  1:1) to yield the Ugi product as a white solid (2.69 g, 4.75 mmol, 95%).

$R_f = 0.72$  in cyclohexane/ethyl acetate (1:1). Visualized *via* Seebach staining solution.

$^1\text{H}$  NMR (400 MHz,  $\text{CDCl}_3$ ):  $\delta$ (ppm) = 7.61 – 7.51 (m, 2H,  $\text{CH}_{\text{ar}}$ ), 7.37 – 7.20 (m, 3H,  $\text{CH}_{\text{ar}}$ ), 7.12 – 6.94 (m, 6H,  $\text{CH}_{\text{ar}}$ ), 6.79 – 6.71 (m, 2H,  $\text{CH}_{\text{ar}}$ ), 6.00 (s, 1H, CH), 5.51 (s, 1H, NH), 3.77 (s, 3H,  $\text{CH}_3$ ), 1.34 (s, 9H,  $\text{CH}_3$ ).

$^{13}\text{C}$  NMR (101 MHz,  $\text{CDCl}_3$ ):  $\delta$ (ppm) = 168.33, 159.86, 154.76, 154.37, 153.28, 139.53, 137.64, 133.31, 131.75, 128.58, 128.47, 126.06, 123.33, 117.90, 116.90, 116.42, 114.07, 114.07, 110.58, 95.87, 94.04, 89.70, 87.21, 85.65, 77.48, 77.16, 76.84, 71.07, 64.29, 55.36, 51.87, 28.78, 22.77, 22.53, 10.76, 10.61.

IR (ATR):  $\nu / \text{cm}^{-1} = 442, 494, 525, 547, 597, 634, 642, 689, 718, 728, 740, 759, 784, 800, 812, 847, 1010, 1028, 1177, 1183, 1218, 1230, 1251, 1294, 1308, 1358, 1390, 1444, 1454, 1481, 1514, 1541, 1580, 1621, 1683, 2207, 2954, 2972, 3336$ .

HRMS (FAB) of  $[\text{M}]^+$   $[\text{C}_{28}\text{H}_{28}\text{O}_3\text{N}_2]^+$ : calc. 567.1139; found 567.1141;  $\Delta = 0.2$  mmu

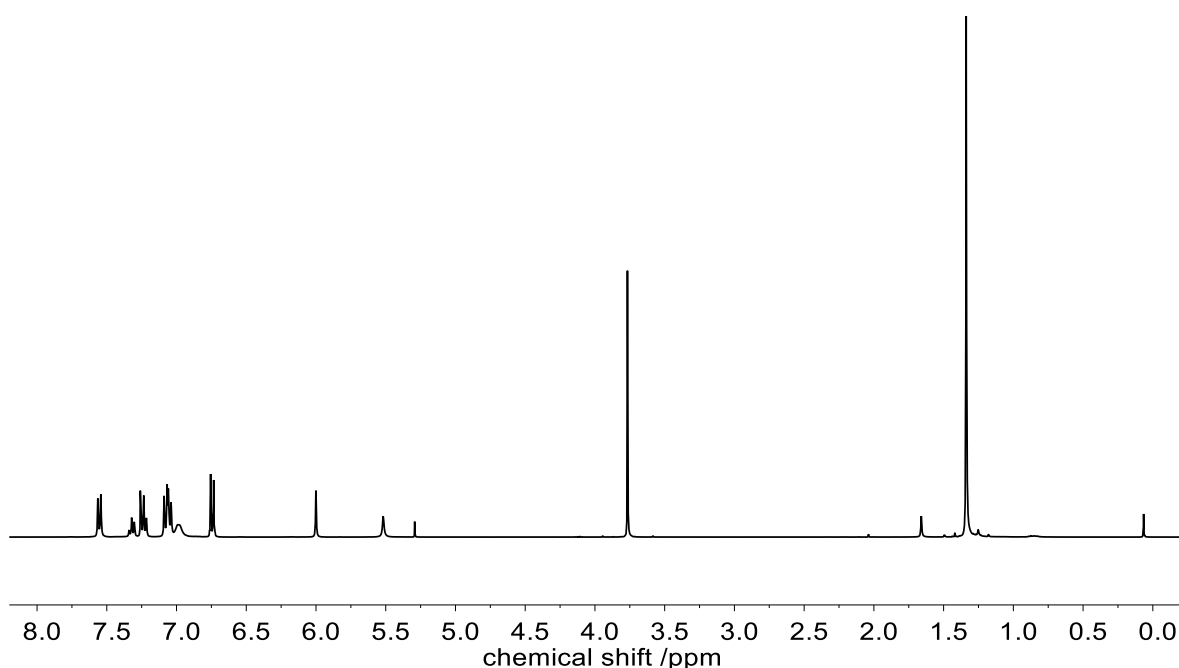
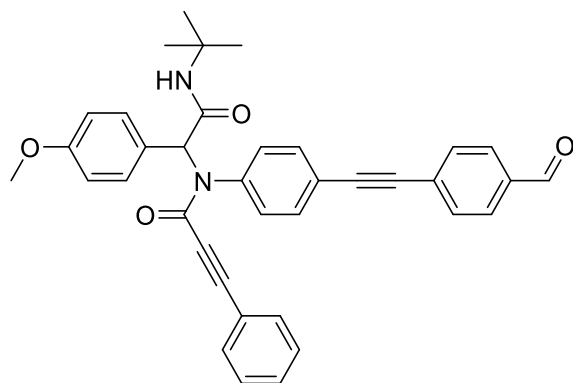


Figure S36:  $^1\text{H}$  NMR spectrum of **U1a** measured in  $\text{CDCl}_3$ .

### Synthesis of the functionalized Ugi monomer (**U1b**)



**U1a** (870 mg, 1.54 mmol, 1.00 eq.), 4-ethynyl benzaldehyde (200 mg, 1.54 mmol, 1.00 eq.), bis(triphenylphosphine) palladium chloride (27.0 mg, 38.4  $\mu\text{mol}$ , 0.03 eq.), copper (I) iodide (14.6 mg, 76.8  $\mu\text{mol}$ , 0.05 eq.) were placed in a vial and sealed with a cap. The vial was evacuated and backfilled with argon for three times. Subsequently, 10 mL THF and triethylamine (2.14 mL, 1.56 mg, 15.4 mmol, 10.0 eq.) were added. The reaction mixture was stirred for 3 hours at ambient temperature. The reaction mixture was diluted with DCM and washed with saturated

ammonium chloride solution. The aqueous phase was extracted three times with DCM. The combined organic phases were dried over Na<sub>2</sub>SO<sub>4</sub>, filtered, and concentrated under reduced pressure. The residue was purified *via* silica column chromatography (cyclohexane/ethyl acetate 3:1 → 7:3) and the product **U1b** was obtained as a brown solid (538 mg, 946 μmol, 61%)

R<sub>f</sub> = 0.66 in cyclohexane/ethyl acetate (1:1). Visualized *via* Seebach staining solution.

<sup>1</sup>H NMR (400 MHz, CDCl<sub>3</sub>): δ(ppm) = 10.02 (s, 1H, CHO), 7.95 – 7.80 (m, 2H, CH<sub>ar</sub>), 7.71 – 7.60 (m, 2H, CH<sub>ar</sub>), 7.46 – 7.38 (m, 2H, CH<sub>ar</sub>), 7.36 – 7.16 (m, 5H, CH<sub>ar</sub>), 7.15 – 7.06 (m, 4H, CH<sub>ar</sub>), 6.78 – 6.70 (m, 2H, CH<sub>ar</sub>), 6.01 (s, 1H, CH), 5.57 (s, 1H, NH), 3.76 (s, 3H, CH<sub>3</sub>), 1.36 (s, 9H, CH<sub>3</sub>).

<sup>13</sup>C NMR (101 MHz, CDCl<sub>3</sub>): δ(ppm) = 191.48, 168.34, 159.88, 154.76, 140.25, 135.69, 132.59, 132.25, 131.89, 131.75, 131.51, 130.17, 129.74, 129.37, 128.48, 125.95, 122.47, 120.35, 114.09, 92.88, 92.45, 89.62, 82.58, 64.50, 55.34, 51.94, 28.79.

IR (ATR): ν / cm<sup>-1</sup> = 436, 483, 516, 533, 553, 613, 631, 642, 658, 687, 712, 743, 761, 784, 796, 808, 825, 847, 1033, 1100, 1115, 1137, 1174, 1189, 1205, 1222, 1249, 1284, 1302, 1329, 1345, 1376, 1444, 1467, 1491, 1512, 1543, 1561, 1594, 1617, 1683, 1703, 2205, 2927, 2964, 3324.

HRMS (FAB) of [M]<sup>+</sup> [C<sub>37</sub>H<sub>33</sub>O<sub>4</sub>N<sub>2</sub>]<sup>+</sup>: calc. 569.2435; found 569.2437; Δ = 0.2 mmu

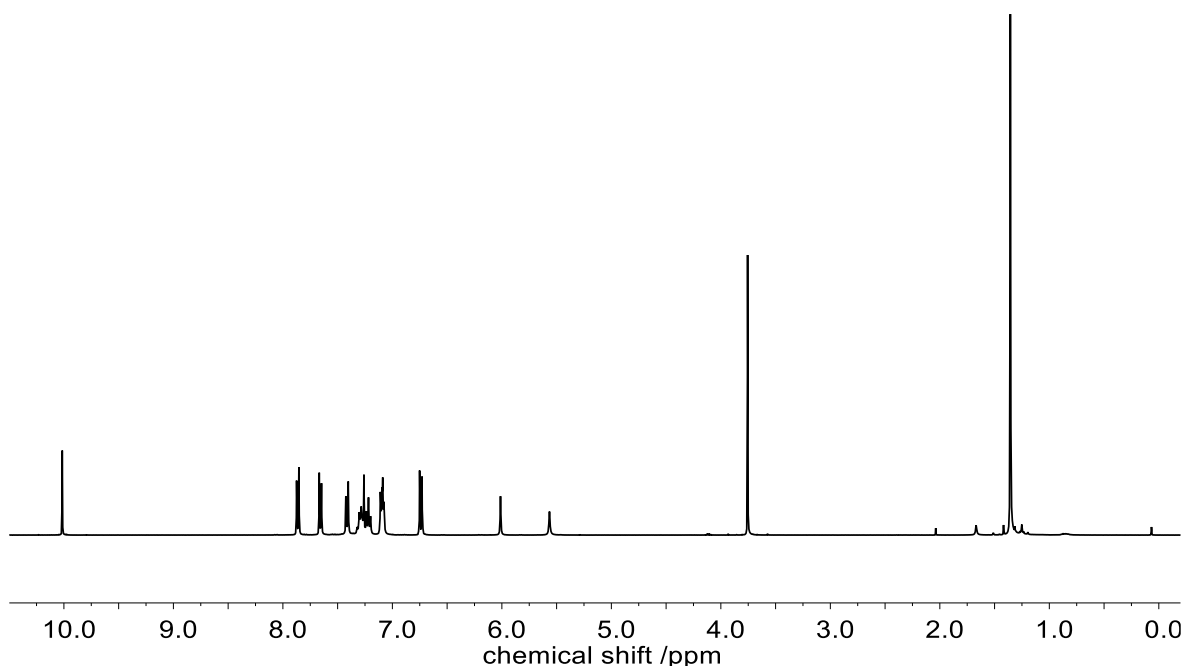
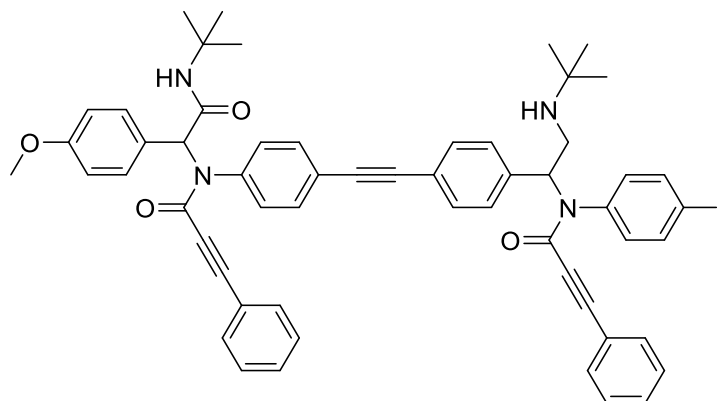


Figure S37:  $^1\text{H}$  NMR spectrum of **U1b** measured in  $\text{CDCl}_3$ .

### Synthesis of the Ugi dimer (**U2a**)



4-Iodoaniline (193 mg, 879  $\mu\text{mol}$ , 1.00 eq.) and **U1b** (500 mg, 879  $\mu\text{mol}$ , 1.00 eq.) were stirred in 15 mL methanol. Subsequently, phenyl propiolic acid (129 mg, 879  $\mu\text{mol}$ , 1.00 eq.) and *tert*-butyl isocyanide (99.5  $\mu\text{L}$ , 73.1 mg, 879  $\mu\text{mol}$ , 1.00 eq.) were added. The resulting mixture was stirred at ambient temperature for 24 hours. Afterwards, the mixture was diluted with DCM and washed with brine. The aqueous phase was extracted with DCM. The combined organic phases were dried over  $\text{Na}_2\text{SO}_4$ , filtered, and concentrated under reduced pressure. The residue was

purified *via* silica column chromatography (cyclohexane/ethyl acetate 7:3) to yield the Ugi product as a white solid (784 mg, 785  $\mu$ mol, 89%).

$R_f$  = 0.59 in cyclohexane/ethyl acetate (1:1). Visualized *via* Seebach staining solution.

$^1\text{H}$  NMR (400 MHz,  $\text{CDCl}_3$ ):  $\delta$ (ppm) = 7.62 – 7.53 (m, 2H,  $\text{CH}_{\text{ar}}$ ), 7.43 – 6.93 (m, 22H,  $\text{CH}_{\text{ar}}$ ), 6.78 – 6.69 (m, 2H,  $\text{CH}_{\text{ar}}$ ), 6.03 (s, 1H, CH), 6.00 (s, 1H, CH), 5.61 (s, 1H, NH), 5.57 (s, 1H, NH), 3.75 (s, 3H,  $\text{CH}_3$ ), 1.35 (s, 18H,  $\text{CH}_3$ ).

$^{13}\text{C}$  NMR (101 MHz,  $\text{CDCl}_3$ ):  $\delta$ (ppm) = 168.36, 167.69, 159.84, 154.90, 154.81, 139.82, 139.32, 137.83, 134.24, 133.24, 132.67, 132.60, 131.92, 131.75, 131.72, 131.39, 130.45, 130.36, 130.15, 128.55, 128.47, 125.94, 123.63, 122.85, 120.35, 120.12, 114.05, 94.37, 93.01, 92.41, 90.19, 89.71, 82.57, 82.34, 64.51, 64.40, 55.33, 52.09, 51.92, 28.78, 28.75.

IR (ATR):  $\nu / \text{cm}^{-1}$  = 436, 444, 457, 487, 522, 545, 611, 646, 687, 714, 728, 743, 757, 796, 835, 845, 989, 1010, 1028, 1063, 1100, 1111, 1177, 1220, 1249, 1325, 1362, 1378, 1454, 1485, 1512, 1539, 1596, 1619, 1683, 2213, 2927, 2962, 3312.

HRMS (FAB) of  $[\text{M}]^+$   $[\text{C}_{57}\text{H}_{52}\text{O}_5\text{N}_4]^+$ : calc. 999.2977; found 999.2979;  $\Delta$  = 0.2 mmu

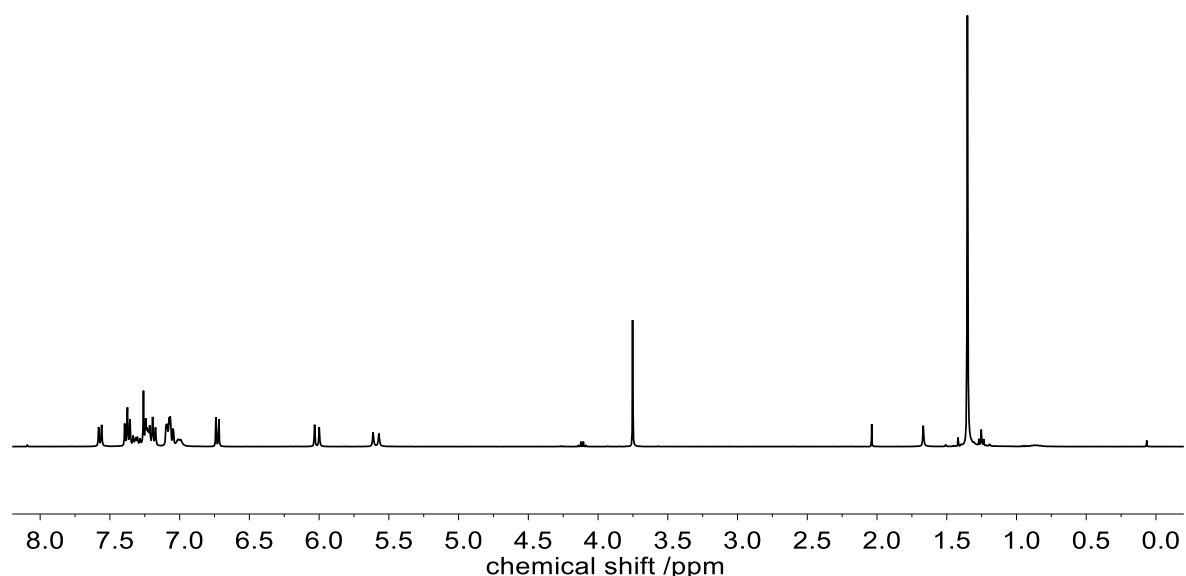
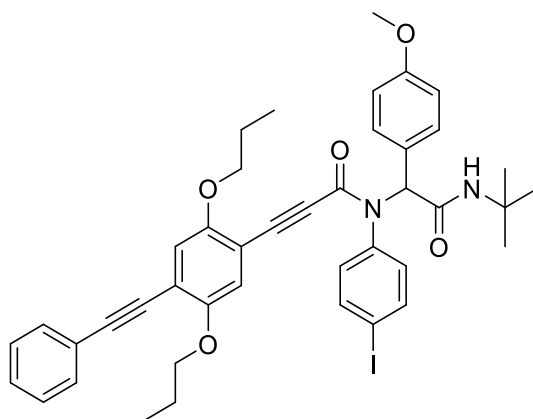


Figure S38:  $^1\text{H}$  NMR spectrum of **U2a** measured in  $\text{CDCl}_3$ .

Synthesis of the Ugi monomer with **1b**

4-Iodoaniline (121 mg, 552  $\mu\text{mol}$ , 1.00 eq.) and 4-methoxy benzaldehyde (67.1  $\mu\text{L}$ , 75.1 mg, 552  $\mu\text{mol}$ , 1.00 eq.) were stirred in 10 mL methanol. Subsequently, the monomer acid **1b** (200 mg, 552  $\mu\text{mol}$ , 1.00 eq.) and *tert*-butyl isocyanide (62.4  $\mu\text{L}$ , 45.9 mg, 552  $\mu\text{mol}$ , 1.00 eq.) were added. The resulting mixture was stirred at ambient temperature for 24 hours. Afterwards, the mixture was diluted with DCM and washed with brine. The aqueous phase was extracted with DCM. The combined organic phases were dried over  $\text{Na}_2\text{SO}_4$ , filtered, and concentrated under reduced pressure. The residue was purified *via* silica column chromatography (cyclohexane/ethyl acetate 3:1) to yield the Ugi product as a white solid (368 mg, 470  $\mu\text{mol}$ , 85%).

$R_f$  = 0.81 in cyclohexane/ethyl acetate (1:1). Visualized *via* Seebach staining solution

$^1\text{H}$  NMR (400 MHz,  $\text{CDCl}_3$ ):  $\delta$ (ppm) = 7.57 – 7.46 (m, 4H,  $\text{CH}_{\text{ar}}$ ), 7.39 – 7.28 (m, 3H,  $\text{CH}_{\text{ar}}$ ), 7.12 – 7.05 (m, 2H,  $\text{CH}_{\text{ar}}$ ), 7.03 – 6.95 (m, 2H,  $\text{CH}_{\text{ar}}$ ), 6.87 (s, 1H,  $\text{CH}_{\text{ar}}$ ), 6.78 – 6.71 (m, 2H,  $\text{CH}_{\text{ar}}$ ), 6.47 (s, 1H,  $\text{CH}_{\text{ar}}$ ), 5.98 (s, 1H, CH), 5.55 (s, 1H, NH), 3.86 (t,  $J$  = 6.3 Hz, 2H,  $\text{CH}_2$ ), 3.81 (t,  $J$  = 6.7 Hz, 2H,  $\text{CH}_2$ ), 3.77 (s, 3H,  $\text{CH}_3$ ), 1.84 (h,  $J$  = 7.0 Hz, 2H,  $\text{CH}_2$ ), 1.69 (h,  $J$  = 7.2 Hz, 2H,  $\text{CH}_2$ ), 1.34 (s, 9H,  $\text{CH}_3$ ), 1.09 (t,  $J$  = 7.4 Hz, 3H,  $\text{CH}_3$ ), 0.98 (t,  $J$  = 7.4 Hz, 3H,  $\text{CH}_3$ ).

$^{13}\text{C}$  NMR (101 MHz,  $\text{CDCl}_3$ ):  $\delta$ (ppm) = 168.33, 159.86, 154.76, 154.37, 153.28, 139.53, 137.64, 133.31, 131.75, 131.72, 128.58, 128.47, 126.06, 123.33, 117.90, 116.90, 116.42, 114.07, 110.58, 95.87, 94.04, 89.70, 87.21, 85.65, 71.08, 64.29, 55.36, 51.88, 28.78, 22.77, 22.53, 10.76, 10.61.

IR (ATR):  $\nu / \text{cm}^{-1}$  = 438, 481, 498, 510, 531, 543, 642, 685, 708, 730, 753, 786, 806, 839, 868, 959, 977, 1010, 1035, 1057, 1100, 1111, 1148, 1174, 1220, 1244, 170

1279, 1302, 1314, 1343, 1360, 1384, 1415, 1442, 1465, 1483, 1510, 1539, 1580, 1619, 1683, 2211, 2874, 2929, 2964, 3354.

HRMS (FAB) of  $[M]^+$   $[C_{42}H_{44}O_5N_2]^+$ : calc. 783.2290; found 783.2287;  $\Delta = 0.3$  mmu

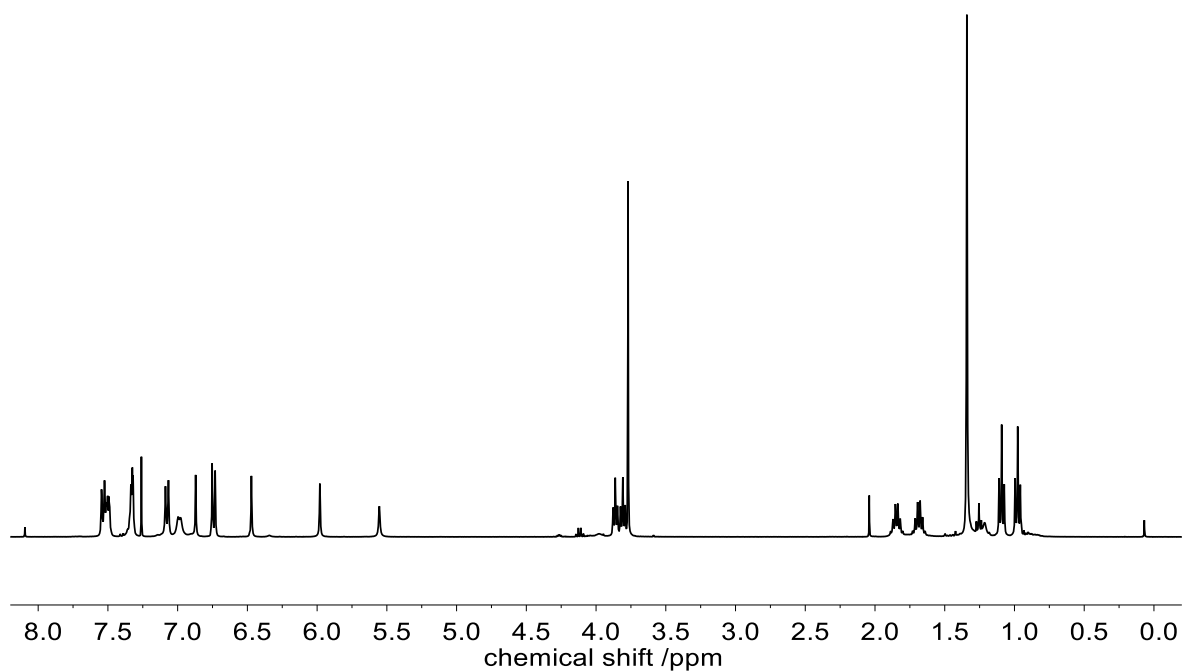


Figure S39:  $^1H$  NMR spectrum of **U1a** measured in  $CDCl_3$ .



## 7 Abbreviations

### 7.1 List of abbreviation

Ar	Aromatic
ADMET	Acyclic diene metathesis
ATRP	Atom transfer radical polymerization
Bn	Benzyl
CDCl <sub>3</sub>	Deuterated chloroform
DBU	1,8-Diazabicyclo[5.4.0]undec-7-en
DCM	Dichloromethane
DIBAL-H	Diisobutylaluminium hydride
DP	Degree of polymerization
CuAAC	Copper-assisted azide-alkyne cycloaddition
DNA	Deoxyribonucleic acid
ESI-MS	Electrospray ionization mass spectrometry
e.g.	exempli gratia, Lat: for example
eq.	Equivalent
et al.	et alii/aliae/alia. lat.: and others
FG	Functional group
HRMS	High resolution mass spectrometry
HWE	Horner-Wadsworth-Emmons
IEG	Iterative exponential growth
i.e.	id est Lat.: that is
in situ	Lat: on site, locally without isolation
IOC	Institute of organic chemistry
IUPAC	International union of pure and applied chemistry
IR	Infrared spectroscopy
KIT	Karlsruher Institut für Technologie
MALDI-ToF	Matrix-assisted laser desorption/ionization time of flight
MCR	Multicomponent reaction
MS	Mass spectroscopy

## Abbreviations

---

NHC	N-heterocyclic carbene
NICAL	nitrile imine-carboxylic acid ligation
NMR	Nuclear magnetic resonance spectroscopy
OAE	Oligo(arylene ethynylene)
OPE	Oligo(phenylene ethynylene)
OPV	Oligo(phenylene vinylene)
P-3CR	Passerini-three component reaction
PEG	Poly(ethylene glycol)s
PG	Protecting group
PPV	Poly(phenylene vinylene)
RNA	Ribonucleic acid
RT	Room temperature
SEC	Size exclusion chromatography
SPPS	Solid phase peptide synthesis
SPOS	Solid phase organic synthesis
TAD	1,2,4-triazoline-3,5-dione
TADF	thermally activated delayed fluorescence
TEMPO	2,2,6,6-Tetramethylpiperidinyloxy
THF	Tetrahydrofuran
THP	Tetrahydropyran-1-yl acetal
TLC	Thin layer chromatography
TMS	Trimethyl silyl
UV/VIS	ultra violet/visible
<i>via</i>	Lat: By way of, using

## 7.2 List of symbols

°C	Degrees Celsius
h	Hours
Hz	Hertz
MHz	Megahertz
g	Gram
mg	Milligram
µg	Microgram
mL	Milliliter
µL	Mikroliter
mol	Mol
mmol	Millimol
µmol	Micromol
mmu	Milli mass unit
ppm	Parts Per Million
m / z	Mass-to-charge ratio
δ	Chemical Shift in NMR spectroscopy
s	singlet
d	doublet
t	triplet
m	multiplet
h	sextet
v	Wavenumber
R <sub>f</sub>	Retention factor



## 8 List of Figures, Schemes and Tables

### 8.1 List of Figures

Figure 1: a) Wurtz reaction. <sup>[29]</sup> b) Wurtz-Fittig reaction. ....	4
Figure 2: a) Cadiot-Chodkiewicz reaction. <sup>[39,40]</sup> b) Castro-Stephens reaction. <sup>[41]</sup> ....	6
Figure 3: Reactivity of different vinyl and aryl halides and triflates in the Sonogashira coupling, respectively. <sup>[64]</sup> .....	15
Figure 4: Possibilities of the decarboxylative coupling. ....	24
Figure 5: Classification of polymers regarding different degrees of control. <sup>[101]</sup> ....	29
Figure 6: Characterization of the sequence-defined tetramer <b>IO4</b> . a) chemical structure of the sequence-defined tetramer <b>IO4</b> . b) SEC traces of the pure trimer <b>IO3</b> (black) and tetramer <b>IO4</b> (red). c) Overlay of the calculated isotopic pattern (red) and the measured isotopic pattern (black) obtained from ESI-MS measurement of <b>IO4</b> . ....	55
Figure 7: Comparison of the <sup>1</sup> H NMR spectra of <b>IO3</b> (top) and <b>IO4</b> (bottom). ....	56
Figure 8: Comparison of the <sup>1</sup> H NMR spectra of the pure <b>IO4</b> (top) and the sample with 15% impurity (bottom). All signals arise in the same ppm range and the integrals are not changing. ....	59
Figure 9: Mass spectrum of the sample with 1 wt% impurity. Subjectively, no impurity is detected. Zoom-in on the respective area reveals the presence of the impurity ( <b>IO3</b> ) with the respective mass of 822.4317 m/z. ....	60
Figure 10: Comparison of the mass spectra of the sample with 1 wt% (left) and 4 wt% (right) impurity. ....	61
Figure 11: Comparison of the SEC traces of the tetramer <b>IO4</b> containing different wt% amounts of impurity. ....	62
Figure 12: <sup>1</sup> H NMR spectrum of the monomer <b>P1a</b> . The observed chemical shifts are in accordance with the literature. <sup>[16]</sup> .....	67
Figure 13: Comparison of the <sup>1</sup> H NMR spectra of <b>P1a</b> (red) and 1,4-diphenylbuta-1,3-diyne (black). The signals in the aromatic region overlap, thus detection of the homocoupling product is not possible using only NMR spectroscopy. ....	68
Figure 14: SEC traces of <b>P1a</b> (red) and the possible homocoupling product 1,4-diphenylbuta-1,3-diyne (black). After simple purification via silica column chromatography no homocoupling product is observed in the SEC trace of <b>P1a</b> . ....	69

Figure 15: $^1\text{H}$ NMR spectra of the building units <b>B1</b> and <b>IB1</b> . Both building units exhibit an ethyl ester protected alkynyl carboxylic acid and a halogen moiety. The different halogens, namely bromine and iodine result in a different shift of the aromatic protons which is observed around 7.00 ppm. ....	73
Figure 16: Cutout of the $^1\text{H}$ NMR spectra of the monomer ester <b>1a</b> (bottom) and monomer acid <b>1b</b> (top). The cleavage of the ethyl ester group is observed at 4.30 ppm and 1.35 ppm. ....	77
Figure 17: SEC traces of monomer ester <b>1a</b> (black) and monomer acid <b>1b</b> (red). The narrow peak confirms their uniformity. Tailing of the SEC trace of the monomer acid <b>1b</b> was assigned to the free carboxylic acid which might interact with the column material.....	78
Figure 18: SEC traces of the dimer ester <b>2a</b> (blue) and the dimer acid <b>2b</b> (green) as well as the respective monomer species (black and red). No homocoupling product is observed after purification via silica column chromatography.....	79
Figure 19: Left: structures of the monomer <b>1a</b> (black), dimer <b>2a</b> (blue), and trimer <b>3a</b> (pink) ester. Right: corresponding SEC traces which confirm uniformity of the obtained OPEs ( <b>1a-3a</b> ).....	80
Figure 20: SEC trace of the tetramer <b>4a</b> after column chromatography. A second peak is detected at lower retention time. Analysis by ESI-MS revealed the presence of the homocoupling product of <b>3b</b> . ....	81
Figure 21: SEC traces of impure tetramer ester <b>4a</b> (orange), tetramer acid <b>4b</b> (green), and homocoupling product of <b>3b</b> (grey). Pure tetramer acid <b>4b</b> , was obtained after saponification followed by a silica filtration column.....	82
Figure 22: SEC traces of the obtained ethyl ester protected OPEs. Homocoupling was avoided until the trimer stage. For the tetramer <b>4a</b> (green) and the pentamer <b>5a</b> (purple) a second peak towards shorter retention times arises, which could be assigned to the homocoupling product by ESI-MS.....	83
Figure 23: SEC traces of the deprotected uniform OPEs. ....	84
Figure 24: SEC traces of dimer ester <b>2a</b> (red) and tetramer ester <b>4a'</b> (green). No homocoupling was observed when the tetramer is synthesized from the dimer with the double building unit. ....	87
Figure 25: Comparison of the $^1\text{H}$ NMR spectra of the three new building units <b>B4</b> , <b>B5</b> , <b>B6</b> . ....	89
Figure 26: $^1\text{H}$ NMR spectrum of the sequence-defined trimer <b>BP3a</b> . ....	90

Figure 27: SEC traces of sequence-defined monomer <b>A1a</b> (black) and sequence-defined trimer <b>A3a</b> (red), in which the anthracene building unit <b>B6</b> was incorporated. Additional peaks towards lower retention times indicate the presence of higher molecular weight species.....	91
Figure 28: Left: established Sonogashira coupling approach consisting of Sonogashira coupling and subsequent deprotection. Adopted from Meier et al. Right: developed decarboxylative coupling approach based on decarboxylative coupling followed by saponification. ....	93
Figure 29: SEC traces after the first U-4CR (black), after the follow-up Sonogashira coupling (red) and after the second U-4CR (blue). The narrow peaks confirm the high purity and uniformity.....	102

## 8.2 List of Supporting Figures

Figure S1: <sup>1</sup> H NMR spectra of the samples with 0-5 wt% impurity. ....	112
Figure S2: <sup>1</sup> H NMR spectra of the samples with 7-15 wt% impurity. ....	113
Figure S3: ESI-MS spectra of the impurity study .....	114
Figure S4: ESI-MS spectra of the impurity study .....	115
Figure S5: <sup>1</sup> H NMR spectrum of <b>IB1a</b> measured in CDCl <sub>3</sub> . ....	117
Figure S6: <sup>1</sup> H NMR spectrum of <b>IB1b</b> measured in CDCl <sub>3</sub> . ....	118
Figure S7: <sup>1</sup> H NMR spectrum of <b>IB1c</b> measured in CDCl <sub>3</sub> . ....	120
Figure S8: <sup>1</sup> H NMR spectrum of <b>IB1</b> measured in CDCl <sub>3</sub> . ....	121
Figure S9: <sup>1</sup> H NMR spectrum of <b>IB1</b> measured in CDCl <sub>3</sub> . ....	123
Figure S10: <sup>1</sup> H NMR spectrum of <b>B1a</b> measured in CDCl <sub>3</sub> . ....	124
Figure S11: <sup>1</sup> H NMR spectrum of <b>B1b</b> measured in CDCl <sub>3</sub> . ....	126
Figure S12: <sup>1</sup> H NMR spectrum of <b>B1c</b> measured in CDCl <sub>3</sub> .....	127
Figure S13: <sup>1</sup> H NMR spectrum of <b>B1</b> measured in CDCl <sub>3</sub> . ....	129
Figure S14: <sup>1</sup> H NMR spectrum of <b>1a</b> measured in CDCl <sub>3</sub> .....	133
Figure S15: <sup>1</sup> H NMR spectrum of <b>1b</b> measured in CDCl <sub>3</sub> .....	134
Figure S16: <sup>1</sup> H NMR spectrum of <b>2a</b> measured in CDCl <sub>3</sub> .....	136
Figure S17: <sup>1</sup> H NMR spectrum of <b>2b</b> measured in CDCl <sub>3</sub> .....	137
Figure S 18: <sup>1</sup> H NMR spectrum of <b>3a</b> measured in CDCl <sub>3</sub> .....	138
Figure S19: <sup>1</sup> H NMR spectrum of <b>3b</b> measured in CDCl <sub>3</sub> .....	140
Figure S20: <sup>1</sup> H NMR spectrum of <b>4a</b> measured in CDCl <sub>3</sub> .....	141
Figure S21: <sup>1</sup> H NMR spectrum of <b>4b</b> measured in CDCl <sub>3</sub> .....	143

Figure S22: <sup>1</sup> H NMR spectrum of <b>5a</b> measured in CDCl <sub>3</sub> .....	144
Figure S23: <sup>1</sup> H NMR spectrum of <b>5b</b> measured in CDCl <sub>3</sub> . ....	146
Figure S24: <sup>1</sup> H NMR spectrum of <b>B1d</b> measured in CDCl <sub>3</sub> .....	148
Figure S25: <sup>1</sup> H NMR spectrum of <b>B2c</b> measured in CDCl <sub>3</sub> . ....	149
Figure S26: <sup>1</sup> H NMR spectrum of <b>B2</b> measured in CDCl <sub>3</sub> .....	151
Figure S27: <sup>1</sup> H NMR spectrum of <b>B3b</b> measured in CDCl <sub>3</sub> .....	153
Figure S28: <sup>1</sup> H NMR spectrum of <b>B3c</b> measured in CDCl <sub>3</sub> . ....	154
Figure S29: <sup>1</sup> H NMR spectrum of <b>B3</b> measured in CDCl <sub>3</sub> . ....	155
Figure S30: <sup>1</sup> H NMR spectrum of <b>B4c</b> measured in CDCl <sub>3</sub> . ....	157
Figure S31: <sup>1</sup> H NMR spectrum of <b>B4</b> measured in CDCl <sub>3</sub> . ....	158
Figure S32: <sup>1</sup> H NMR spectrum of <b>B5c</b> measured in CDCl <sub>3</sub> . ....	160
Figure S33: <sup>1</sup> H NMR spectrum of <b>B5</b> measured in CDCl <sub>3</sub> . ....	161
Figure S34: <sup>1</sup> H NMR spectrum of <b>BP3a</b> measured in CDCl <sub>3</sub> .....	163
Figure S35: <sup>1</sup> H NMR spectrum of the Passerini product measured in CDCl <sub>3</sub> . ....	164
Figure S36: <sup>1</sup> H NMR spectrum of <b>U1a</b> measured in CDCl <sub>3</sub> . ....	166
Figure S37: <sup>1</sup> H NMR spectrum of <b>U1b</b> measured in CDCl <sub>3</sub> . ....	168
Figure S38: <sup>1</sup> H NMR spectrum of <b>U2a</b> measured in CDCl <sub>3</sub> . ....	169
Figure S39: <sup>1</sup> H NMR spectrum of <b>U1a</b> measured in CDCl <sub>3</sub> . ....	171

### 8.3 List of Schemes

Scheme 1: Generally accepted catalytic cycle for cross-couplings. <sup>[28]</sup> .....	3
Scheme 2: Catalytic cycle of the Mizoroki-Heck coupling consisting oxidative addition, migratory insertion, β-hydride elimination and reductive elimination. <sup>[46]</sup> ...	7
Scheme 3: Four-step approach towards oligo(diacetylene)s by Wudl and Bitler. Two cross-couplings, the Negishi and the Kumada coupling are employed. <sup>[58]</sup> .....	10
Scheme 4: Orthogonal approach from Yu et al. towards OPVs. <sup>[59]</sup> .....	11
Scheme 5: a) Synthesis of oligo(paraphenylene)s based on Schlüter et al. <sup>[60]</sup> b)Synthesis of oligo(flourene)s based on Geng et al. <sup>[61]</sup> .....	13
Scheme 6: First reported Sonogashira coupling (top) and a typical Sonogashira reaction (bottom). <sup>[47,63]</sup> .....	14
Scheme 7: Proposed catalytic cycles of the Sonogashira coupling. <sup>[66]</sup> .....	16
Scheme 8: A common side reaction in the Sonogashira coupling: the copper catalysed Glaser coupling. <sup>[33,34]</sup> .....	17

Scheme 9: Application of the Sonogashira reaction in the synthesis of pharmaceuticals Terbinafine (top) and Altinicline (bottom). <sup>[70,71]</sup> .....	19
Scheme 10: Two-step approach for the synthesis of oligo(diacetylene)s based on the Sonogashira coupling and subsequent deprotection by Zuilhof and Sudhölter. <sup>[72]</sup> .....	20
Scheme 11: Commonly used two-step strategy for the synthesis of OPEs from Dixneuf et al. <sup>[76]</sup> .....	20
Scheme 12: Application of the Sonogashira coupling in polymerization by Tomita et al. <sup>[77]</sup> .....	21
Scheme 13: Top: First decarboxylative coupling reported by Nilsson. <sup>[78]</sup> Bottom: Decarboxylative Heck-type coupling from Myers. <sup>[79]</sup> .....	23
Scheme 14: Proposed bimetallic catalytic cycle for the decarboxylative coupling towards biaryls. <sup>[80]</sup> .....	25
Scheme 15: One-pot synthesis of biaryls reported by Lee et al. consisting of a Sonogashira coupling and a subsequent decarboxylative coupling. <sup>[57]</sup> .....	25
Scheme 16: Two possible reaction pathways of the decarboxylative coupling of alkynyl carboxylic acids. <sup>[90]</sup> .....	26
Scheme 17: Proposed catalytic cycle for the monometallic copper catalyzed decarboxylative coupling. <sup>[85]</sup> .....	27
Scheme 18: Decarboxylative coupling with tosylates and arene diazonium salts. PEPPSI <sup>TM</sup> stands for Pyridine-Enhanced Precatalyst Preparation Stabilization and Initiation. <sup>[93–95]</sup> .....	28
Scheme 19: Iterative cycle for the SSPS by Merrifield. <sup>[106]</sup> .....	31
Scheme 20: Three frequently used approaches towards sequence-defined macromolecules. <sup>[18]</sup> .....	33
Scheme 21: Iterative solid-supported synthesis of an information containing macromolecule. <sup>[127]</sup> The binary code is introduced by different sidechains. Cleavage from the solid support (3.) enabled sequential read-out via tandem MS (4.)......	36
Scheme 22: Iterative two-step reaction cycle to build up sequence-defined oligomers on solid phase using thiolactone chemistry. <sup>[143]</sup> .....	37
Scheme 23: Iterative two-step reaction cycle comprising the P-3CR and a deprotection step. A monoprotected isocyanide is used as an AB monomer and aldehydes are varied which introduces a sequence. <sup>[134]</sup> .....	39

Scheme 24: Iterative two-step reaction cycle which combines the P-3CR and the TAD “click” reaction. Three different aldehydes were used to build up a sequence. The reaction was performed in solution as well as on solid phase and the results were compared. <sup>[141]</sup> .....	41
Scheme 25: Bidirectional synthesis towards positively charged sequence-defined oligomers. The positively charged quaternary ammonium group in the backbone enables purification by precipitation and centrifugation. <sup>[148]</sup> .....	42
Scheme 26: Iterative synthesis concept towards sequence-defined oligomers. Three different heterocycles are generated by varying the reaction conditions in each cycle to achieve sequence-definition. <sup>[21]</sup> .....	44
Scheme 27: Left: Iterative two-step reaction cycle towards sequence-defined OPVs. The HWE reaction is combined with a deprotection. Right: monomers based on stilbene core which were used to synthesize the first sequence-defined OPV. <sup>[151,152]</sup> .....	45
Scheme 28: Left: Iterative two-step reaction cycle towards sequence-defined OPVs using the HWE reaction and subsequent reduction of a nitrile. Right: monomers which were used for the synthesis of sequence-defined OPVs by Meyer et al. <sup>[153–155]</sup> .....	46
Scheme 29: IEG approach towards OPEs. Orthogonal deprotection and subsequent combination yielded a fast growing OPE. <sup>[156]</sup> .....	47
Scheme 30: Top: two-step synthesis of the building unit bearing an iodine moiety and a TMS protected triple bond. Bottom: Iterative synthesis towards a sequence-defined OPE based on Sonogashira coupling and subsequent deprotection. <sup>[75]</sup> ..	48
Scheme 31: Iterative two-step reaction cycle towards sequence-defined OAEs. The synthesis was performed on a soluble polymer support. <sup>[158]</sup> .....	49
Scheme 32: Iterative two-step synthesis based on Sonogashira coupling and subsequent deprotection. The strategy was established using the same building unit. Then, five different building units were used to synthesise a sequence-defined pentamer. <sup>[16,159]</sup> .....	50
Scheme 33: Iterative two-step approach consisting of Sonogashira coupling and subsequent deprotection of a TMS protected triple bond. <sup>[16]</sup> .....	54
Scheme 34: First test reaction towards OPEs. The commonly used building unit <b>IB1c</b> is reacted with phenyl propiolic acid in a decarboxylative coupling to obtain the monomer <b>P1a</b> .....	66

Scheme 35: Synthesis of building unit <b>IB1</b> based on hydroquinone. The synthesis towards <b>IB1c</b> was adopted from Meier et al. In the final step, the TMS protecting group was converted into ester protected alkynyl carboxylic acid. ....	70
Scheme 36: Synthesis of the building unit <b>B1</b> starting from bromohydroquinon. After Williamson ether synthesis, iodination, Sonogashira monocoupling, carboxylation and alkylation <b>B1</b> was obtained with 54% overall yield.....	72
Scheme 37: Developed synthesis strategy towards uniform OPEs. The strategy comprises a decarboxylative coupling step and a subsequent saponification. ....	74
Scheme 38: Synthesis of the double building unit <b>B2</b> . The obtained double building unit introduces two repeating units at once.....	85
Scheme 39: Test reaction to incorporation of the monomer <b>1b</b> into a more complex molecule using the P-3CR.....	99
Scheme 40: Iterative two-step reaction procedure combining the U-4CR and the Sonogashira coupling. The 4-methoxy benzaldehyde is used as the starting aldehyde. Variation of the carboxylic acid and the isocyanide component would give control of the side groups. ....	101

#### 8.4 List of Tables

Table 1: Overview of coupling and cross-coupling reactions.....	9
Table 2: Summary of the results of the impurity study.....	58
Table 3: Investigation of reaction conditions.....	75
Table 4: Overview of reaction times in the Sonogashira and the decarboxylative coupling approach. ....	95
Table 5: Overview of estimated time needed for purification of the uniform oligomers.....	96
Table 6: Overview of the yield for the oligomers at any stage .....	97
Table 7: Comparison of the combined results over ten reaction steps. ....	98



## 9 Publication List

- D. Hahn, R. V. Schneider, E. Foitzik, M. A. R. Meier, *Macromol. Rapid Commun.* **2021**, 2000735.
- O. Franco, M. Jakoby, R. V. Schneider, F. Hundemer, D. Hahn, B. S. Richards, S. Bräse, M. A. R. Meier, U. Lemmer, I. A. Howard, *Front. Chem.* **2020**, 8, 126.



## 10 References

- [1] a) D. G. Whitten, Y. Tang, Z. Zhou, J. Yang, Y. Wang, E. H. Hill, H. C. Pappas, P. L. Donabedian, E. Y. Chi, *Langmuir* **2019**, *35*, 307; b) A. Krywko-Cendrowska, D. Szweda, R. Szweda, *Processes* **2020**, *8*, 539.
- [2] a) H. Hoppe, D. A. M. Egbe, D. Mühlbacher, N. S. Sariciftci, *J. Mater. Chem.* **2004**, *14*, 3462; b) J. K. Mwaura, M. R. Pinto, D. Witker, N. Ananthakrishnan, K. S. Schanze, J. R. Reynolds, *Langmuir* **2005**, *21*, 10119.
- [3] C. Schmitz, P. Pösch, M. Thelakkat, H.-W. Schmidt, A. Montali, K. Feldman, P. Smith, C. Weder, *Adv. Funct. Mater.* **2001**, *11*, 41.
- [4] P. T. Mathew, F. Fang, *Engineering* **2018**, *4*, 760.
- [5] K. Liu, X. Wang, F. Wang, *ACS nano* **2008**, *2*, 2315.
- [6] R. Kitouni, P. Selvanathan, O. Galangau, L. Norel, B. Ouarda, S. Rigaut, *Synth. Commun.* **2018**, *48*, 1052.
- [7] L. Jones, J. S. Schumm, J. M. Tour, *J. Org. Chem.* **1997**, *62*, 1388.
- [8] a) U. Ziener, A. Godt, *J. Org. Chem.* **1997**, *62*, 6137; b) A. Montali, C. Bastiaansen, P. Smith, C. Weder, *Nature* **1998**, *392*, 261; c) C. Weder, M. S. Wrighton, *Macromolecules* **1996**, *29*, 5157; d) C. Weder, M. S. Wrighton, R. Spreiter, C. Bosshard, P. Günter, *J. Phys. Chem.* **1996**, *100*, 18931; e) G. Yu, J. Gao, J. C. Hummelen, F. Wudl, A. J. Heeger, *Science* **1995**, *270*, 1789; f) Q. Zhou, T. M. Swager, *J. Am. Chem. Soc.* **1995**, *117*, 12593; g) J. S. Schumm, D. L. Pearson, L. Jones, R. Hara, J. M. Tour, *Nanotechnology* **1996**, *7*, 430; h) H. Shirakawa, E. J. Louis, A. G. MacDiarmid, C. K. Chiang, A. J. Heeger, *J. Chem. Soc., Chem. Commun.* **1977**, *0*, 578; i) P. Galda, M. Rehahn, *Synthesis* **1996**, *1996*, 614.
- [9] R. E. Martin, F. Diederich, *Angew. Chem. Int. Ed.* **1999**, *38*, 1350.
- [10] K. Müllen, G. Wegner, *Electronic Materials: The Oligomer Approach. The oligomer approach*, Wiley, Weinheim, New-York, **1998**.
- [11] J. M. Tour, *Chem. Rev.* **1996**, *96*, 537.
- [12] K. Müllen, *Pure Appl. Chemistry* **1993**, *65*, 89.
- [13] B. Genabeek, B. A. G. Lamers, C. J. Hawker, E. W. Meijer, W. R. Gutekunst, B. V. K. J. Schmidt, *J. Polym. Sci.* **2021**, *59*, 373.
- [14] A. D. Jenkins, P. Kratochvíl, R. F. T. Stepto, U. W. Suter, *Pure Appl. Chemistry* **1996**, *68*, 2287.

- [15] a) S. Tarkuç, R. Eelkema, F. C. Grozema, *Tetrahedron* **2017**, *73*, 4994; b) L. Liang, J.-T. Wang, X. Xiang, J. Ling, F.-G. Zhao, W.-S. Li, *J. Mater. Chem. A* **2014**, *2*, 15396.
- [16] R. V. Schneider, K. A. Waibel, A. P. Arndt, M. Lang, R. Seim, D. Busko, S. Bräse, U. Lemmer, M. A. R. Meier, *Sci. Rep. (Scientific Reports)* **2018**, *8*, 17483.
- [17] J.-F. Lutz, *Macromol. Rapid. Commun.* **2017**, *38*, 1700582.
- [18] S. C. Solleder, R. V. Schneider, K. S. Wetzel, A. C. Boukis, M. A. R. Meier, *Macromol. Rapid. Commun.* **2017**, *38*.
- [19] K. Takizawa, C. Tang, C. J. Hawker, *J. Am. Chem. Soc.* **2008**, *130*, 1718.
- [20] M. R. Bryce, *J. Mater. Chem. C* **2021**, *9*, 10524.
- [21] H. Yu, S. Li, K. E. Schwieter, Y. Liu, B. Sun, J. S. Moore, C. M. Schroeder, *J. Am. Chem. Soc.* **2020**, *142*, 4852.
- [22] V. Kaliginedi, P. Moreno-García, H. Valkenier, W. Hong, V. M. García-Suárez, P. Buitter, J. L. H. Otten, J. C. Hummelen, C. J. Lambert, T. Wandlowski, *J. Am. Chem. Soc.* **2012**, *134*, 5262.
- [23] a) G. Cuniberti, K. Richter, G. Fagas (Eds.) *Lecture Notes Phys., Vol. 680*, Springer Berlin Heidelberg, **2006**; b) A. Aviram, M. A. Ratner (Eds.) *Annals of the New York Academy of Sciences, Vol. 852*, New York Acad. of Sciences, New York, NY, **1998**; c) J. Jortner, M. A. Ratner, *Molecular electronics*, Blackwell Science Oxford, **1997**.
- [24] R. Brückner, *Reaktionsmechanismen: organische Reaktionen, Stereochemie, moderne Synthesemethoden*, Springer-Verlag, **2014**.
- [25] "The Nobel Prize in Chemistry 2010", can be found under [https://www.nobelprize.org/nobel\\_prizes/chemistry/laureates/2010/](https://www.nobelprize.org/nobel_prizes/chemistry/laureates/2010/).
- [26] a) "Thieme RÖMPP", can be found under <https://roempp.thieme.de/roempp4.0/do/data/RD-11-02791>; b) "Cross-coupling reactions - Latest research and news | Nature", can be found under <https://www.nature.com/subjects/cross-coupling-reactions>.
- [27] S. L. Buchwald, *Acc. Chem. Res.* **2008**, *41*, 1439.
- [28] J. F. Hartwig, *Organotransition metal chemistry. From bonding to catalysis*, University Science Books, Mill Valley, California, **2010**.
- [29] A. Wurtz, *Ann. Chem. Pharm.* **1855**, *96*, 364.
- [30] B. Tollens, R. Fittig, *Ann. Chem. Pharm.* **1864**, *131*, 303.
- [31] R. Fittig, J. König, *Ann. Chem. Pharm.* **1867**, *144*, 277.

- [32] a) T. Laue, A. Plagens, *Namen- und Schlagwort-Reaktionen der Organischen Chemie*, Vieweg+Teubner Verlag, Wiesbaden, **2004**; b) M. B. Smith, J. March, *March's advanced organic chemistry. Reactions, mechanisms, and structure*, Wiley, Hoboken, NJ, **2007**.
- [33] C. Glaser, *Ber. Dtsch. Chem. Ges.* **1869**, 2, 422.
- [34] C. Glaser, *Ann. Chem. Pharm.* **1870**, 154, 137.
- [35] A. Baeyer, *Ber. Dtsch. Chem. Ges.* **1882**, 15, 775.
- [36] F. Ullmann, J. Bielecki, *Ber. Dtsch. Chem. Ges.* **1901**, 34, 2174.
- [37] G. M. Bennett, E. E. Turner, *J. Chem. Soc., Trans.* **1914**, 105, 1057.
- [38] M. S. Kharasch, E. K. Fields, *J. Am. Chem. Soc.* **1941**, 63, 2316.
- [39] W. Chodkiewicz, P. Cadiot, *CR Hebd. Sceances. Acad. Sci* **1955**, 241, 1055.
- [40] W. Chodkiewicz, *Ann. Chim.(Paris)* **1957**, 2, 819.
- [41] R. D. Stephens, C. E. Castro, *J. Org. Chem.* **1963**, 28, 3313.
- [42] C. C. C. Johansson Seechurn, M. O. Kitching, T. J. Colacot, V. Snieckus, *Angew. Chem. Int. Ed.* **2012**, 51, 5062.
- [43] a) K. Tamao, K. Sumitani, M. Kumada, *J. Am. Chem. Soc.* **1972**, 94, 4374; b) R. J. P. Corriu, J. P. Masse, *J. Chem. Soc., Chem. Commun.* **1972**, 144a.
- [44] a) T. Mizoroki, K. Mori, A. Ozaki, *Bull. Chem. Soc. Jpn.* **1971**, 44, 581; b) R. F. Heck, J. P. Nolley, *J. Org. Chem.* **1972**, 37, 2320.
- [45] J. Smidt, W. Hafner, R. Jira, J. Sedlmeier, R. Sieber, R. Rüttinger, H. Kojer, *Angew. Chem.* **1959**, 71, 176.
- [46] P. Surawatanawong, Y. Fan, M. B. Hall, *J. Org. Chem.* **2008**, 693, 1552.
- [47] K. Sonogashira, Y. Tohda, N. Hagihara, *Tetrahedron Lett.* **1975**, 16, 4467.
- [48] L. Cassar, *J. Organomet. Chem.* **1975**, 93, 253.
- [49] H. A. Dieck, F. R. Heck, *J. Organomet. Chem.* **1975**, 93, 259.
- [50] a) E. Negishi, A. O. King, N. Okukado, *J. Org. Chem.* **1977**, 42, 1821; b) A. O. King, E. Negishi, F. J. Villani Jr, A. Silveira Jr, *J. Org. Chem.* **1978**, 43, 358.
- [51] J. F. Fauvarque, A. Jutand, *J. Organomet. Chem.* **1977**, 132, C17-C19.
- [52] E. Negishi, S. Baba, *J. Chem. Soc., Chem. Commun.* **1976**, 0, 596b-597b.
- [53] D. Milstein, J. K. Stille, *J. Am. Chem. Soc.* **1978**, 100, 3636.
- [54] N. Miyaoura, K. Yamada, A. Suzuki, *Tetrahedron Lett.* **1979**, 20, 3437.
- [55] Y. Hatanaka, T. Hiyama, *J. Org. Chem.* **1988**, 53, 918.
- [56] A. S. Guram, R. A. Rennels, S. L. Buchwald, *Angew. Chem. Int. Ed.* **1995**, 34, 1348.

- [57] J. Moon, M. Jeong, H. Nam, J. Ju, J. H. Moon, H. M. Jung, S. Lee, *Org. Lett.* **2008**, *10*, 945.
- [58] F. Wudl, S. P. Bitler, *J. Am. Chem. Soc.* **1986**, *108*, 4685.
- [59] T. Maddux, W. Li, L. Yu, *J. Am. Chem. Soc.* **1997**, *119*, 844.
- [60] P. Liess, V. Hensel, A.-D. Schlüter, *Liebigs Ann. Chem.* **1996**, *1996*, 1037.
- [61] Q. Wang, Y. Qu, H. Tian, Y. Geng, F. Wang, *Macromolecules* **2011**, *44*, 1256.
- [62] M. J. Buskes, M.-J. Blanco, *Molecules* **2020**, *25*, 3493.
- [63] K. Sonogashira, *J. Organomet. Chem.* **2002**, *653*, 46.
- [64] R. Chinchilla, C. Nájera, *Chem. Rev.* **2007**, *107*, 874.
- [65] a) S. Cacchi, E. Morera, G. Ortar, *Synthesis* **1986**, *1986*, 320; b) A. Arcadi, S. Cacchi, F. Marinelli, *Tetrahedron Lett.* **1989**, *30*, 2581.
- [66] R. Chinchilla, C. Nájera, *Chem. Soc. Rev.* **2011**, *40*, 5084.
- [67] C. Amatore, A. Jutand, *Acc. Chem. Res.* **2000**, *33*, 314.
- [68] M. García-Melchor, A. A. C. Braga, A. Lledós, G. Ujaque, F. Maseras, *Acc. Chem. Res.* **2013**, *46*, 2626.
- [69] a) J.-H. Li, X.-D. Zhang, Y.-X. Xie, *Ann. Chem. Pharm.* **2005**, *2005*, 4256; b) B. Liang, M. Dai, J. Chen, Z. Yang, *J. Org. Chem.* **2005**, *70*, 391; c) D. Méry, K. Heuzé, D. Astruc, *Chem. Commun.* **2003**, *50*, 1934; d) V. P. W. Böhm, W. A. Herrmann, *Eur. J. Org. Chem.* **2000**, *2000*, 3679.
- [70] U. Beutler, C. Fleury, P. C. Fünfschilling, G. Penn, T. Ryser, B. Schenkel in *Studies in Surface Science and Catalysis*, Elsevier, **1997**, pp. 31–35.
- [71] L. S. Bleicher, N. D. P. Cosford, A. Herbaut, J. S. McCallum, I. A. McDonald, *J. Org. Chem.* **1998**, *63*, 1109.
- [72] M. Polhuis, C. C. Hendrikx, H. Zuilhof, E. J. Sudhölter, *Tetrahedron Lett.* **2003**, *44*, 899.
- [73] C. Kosinski, A. Hirsch, F. W. Heinemann, F. Hampel, *Ann. Chem. Pharm.* **2001**, *2001*, 3879.
- [74] Y. Takayama, C. Delas, K. Muraoka, M. Uemura, F. Sato, *J. Am. Chem. Soc.* **2003**, *125*, 14163.
- [75] J.-J. Hwang, J. M. Tour, *Tetrahedron* **2002**, *58*, 10387.
- [76] O. Lavastre, L. Ollivier, P. H. Dixneuf, S. Sibandhit, *Tetrahedron* **1996**, *52*, 5495.
- [77] A. Tanudjaja, S. Inagi, F. Kitamura, T. Takata, I. Tomita, *Dalton Trans.* **2021**, *50*, 3037.

- [78] M. Nilson, *Acta Chem. Scand.* **1966**, *20*, 423.
- [79] A. G. Myers, D. Tanaka, M. R. Mannion, *J. Am. Chem. Soc.* **2002**, *124*, 11250.
- [80] L. J. Goossen, G. Deng, L. M. Levy, *Science* **2006**, *313*, 662.
- [81] a) R. Shang, L. Liu, *Sci. China Chem.* **2011**, *54*, 1670; b) N. Rodríguez, L. J. Goossen, *Chem. Soc. Rev.* **2011**, *40*, 5030; c) M. A. Idris, S. Lee, *Synthesis* **2020**, *52*, 2277.
- [82] L. J. Goossen, F. Rudolphi, C. Ooppel, N. Rodríguez, *Angew. Chem. Int. Ed.* **2008**, *47*, 3043.
- [83] R. Shang, Y. Fu, J.-B. Li, S.-L. Zhang, Q.-X. Guo, L. Liu, *J. Am. Chem. Soc.* **2009**, *131*, 5738.
- [84] a) Z. Fu, S. Huang, W. Su, M. Hong, *Org. Lett.* **2010**, *12*, 4992; b) L. J. Goossen, B. Zimmermann, T. Knauber, *Beilstein J. Org. Chem.* **2010**, *6*, 43; c) J. Wang, Z. Cui, Y. Zhang, H. Li, L.-M. Wu, Z. Liu, *Org. Biomol. Chem.* **2011**, *9*, 663.
- [85] D. Zhao, C. Gao, X. Su, Y. He, J. You, Y. Xue, *Chem. Commun.* **2010**, *46*, 9049.
- [86] J. Moon, M. Jang, S. Lee, *J. Org. Chem.* **2009**, *74*, 1403.
- [87] W. Jia, N. Jiao, *Org. Lett.* **2010**, *12*, 2000.
- [88] Z. Duan, S. Ranjit, P. Zhang, X. Liu, *Chem. Eur. J.* **2009**, *15*, 3666.
- [89] J. Hu, N. Zhao, B. Yang, G. Wang, L.-N. Guo, Y.-M. Liang, S.-D. Yang, *Chem. Eur. J.* **2011**, *17*, 5516.
- [90] A. Pyo, Y. H. Kim, K. Park, G. C. Kim, H. C. Choi, S. Lee, *Appl. Organometal. Chem.* **2012**, *26*, 650.
- [91] A. Gómez-Herrera, F. Nahra, J. Wu, F. Izquierdo, M. Brill, C. S. J. Cazin, S. P. Nolan, *ChemistrySelect* **2019**, *4*, 5.
- [92] X. Li, F. Yang, Y. Wu, *J. Org. Chem.* **2013**, *78*, 4543.
- [93] T. Fujino, T. Hinoue, Y. Usuki, T. Satoh, *Org. Lett.* **2016**, *18*, 5688.
- [94] J.-H. Lee, G. C. E. Raja, S. Yu, J. Lee, K. H. Song, S. Lee, *ACS omega* **2017**, *2*, 6259.
- [95] J. M. Bhojane, V. G. Jadhav, J. M. Nagarkar, *New J. Chem.* **2017**, *41*, 6775.
- [96] X. Xu, E. V. van der Eycken, H. Feng, *Chin. J. Chem.* **2020**, *38*, 1780.
- [97] J.-F. Lutz, M. Ouchi, D. R. Liu, M. Sawamoto, *Science* **2013**, *341*, 1238149.
- [98] F. Crick, *J. Mol. Biol.* **1968**, *38*, 367.

- [99] M. W. G. de Bolster, *Pure Appl. Chemistry* **1997**, *69*, 1251.
- [100] N. Badi, J.-F. Lutz, *Chem. Soc. Rev.* **2009**, *38*, 3383.
- [101] J.-F. Lutz, *ACS Macro Lett.* **2014**, *3*, 1020.
- [102] J.-F. Lutz (Ed.) *ACS Symp. Ser., Vol. 1170*, American Chemical Soc, Washington, DC, **2014**.
- [103] L. Yu, L.-H. Wang, Z.-T. Hu, Y.-Z. You, D.-C. Wu, C.-Y. Hong, *Polym. Chem.* **2015**, *6*, 1527.
- [104] a) V. Bedian, *Int. J. Quantum Chem.* **1984**, *26*, 87; b) A. Ambrogelly, S. Palioura, D. Söll, *Nat. Chem. Biol. (Nature Chemical Biology)* **2007**, *3*, 29.
- [105] J. D. Watson, F. H. C. Crick, *Nature* **1953**, *171*, 737.
- [106] R. B. Merrifield, *J. Am. Chem. Soc.* **1963**, *85*, 2149.
- [107] a) B. Merrifield, *Biosci. Rep. (Bioscience Reports)* **1985**, *5*, 353; b) S. L. Beaucage, R. P. Iyer, *Tetrahedron* **1992**, *48*, 2223.
- [108] R. J. Simon, R. S. Kania, R. N. Zuckermann, V. D. Huebner, D. A. Jewell, S. Banville, S. Ng, L. Wang, S. Rosenberg, C. K. Marlowe, *Proc. Nat. Acad. Sci. U.S.A.* **1992**, *89*, 9367.
- [109] R. B. Merrifield, J. M. Stewart, N. Jernberg, *Anal. Chem.* **1966**, *38*, 1905.
- [110] M. Amblard, J.-A. Fehrentz, J. Martinez, G. Subra, *Mol. Biotechnol.* **2006**, *33*, 239.
- [111] a) A. Marglin, R. B. Merrifield, *J. Am. Chem. Soc.* **1966**, *88*, 5051; b) B. Gutte, R. B. Merrifield, *J. Biol. Chem.* **1971**, *246*, 1922.
- [112] W. Müller-Esterl, *Biochemie. Eine Einführung für Mediziner und Naturwissenschaftler - Unter Mitarbeit von Ulrich Brandt, Oliver Anderka, Stefan Kerscher, Stefan Kieß und Katrin Ridinger*, Springer Berlin Heidelberg, Berlin, Heidelberg, **2018**.
- [113] R. N. Zuckermann, J. M. Kerr, S. B. H. Kent, W. H. Moos, *J. Am. Chem. Soc.* **1992**, *114*, 10646.
- [114] J. Sun, R. N. Zuckermann, *ACS nano* **2013**, *7*, 4715.
- [115] a) R. N. Zuckermann, *Biopolymers* **2011**, *96*, 545; b) J. E. Murphy, T. Uno, J. D. Hamer, F. E. Cohen, V. Dwarki, R. N. Zuckermann, *Proc. Nat. Acad. Sci. U.S.A.* **1998**, *95*, 1517; c) A. S. Culf, R. J. Ouellette, *Molecules* **2010**, *15*, 5282.
- [116] a) P. H. Hermkens, H. C. Ottenheijm, D. Rees, *Tetrahedron* **1996**, *52*, 4527; b) N. Cankařová, E. Schütznerová, V. Krchňák, *Chem. Rev.* **2019**, *119*, 12089.

- [117] P. Espeel, L. L. G. Carrette, K. Bury, S. Capenberghs, J. C. Martins, F. E. Du Prez, A. Madder, *Angew. Chem. Int. Ed.* **2013**, *52*, 13261.
- [118] a) J. Zhang, J. S. Moore, Z. Xu, R. A. Aguirre, *J. Am. Chem. Soc.* **1992**, *114*, 2273; b) J. K. Young, J. C. Nelson, J. S. Moore, *J. Am. Chem. Soc.* **1994**, *116*, 10841; c) J. C. Nelson, J. K. Young, J. S. Moore, *J. Org. Chem.* **1996**, *61*, 8160.
- [119] M. A. R. Meier, C. Barner-Kowollik, *Adv. Mater.* **2019**, *31*, e1806027.
- [120] S. Binauld, D. Dameron, L. A. Connal, C. J. Hawker, E. Drockenmuller, *Macromol. Rapid Commun.* **2011**, *32*, 147.
- [121] E. M. D. Keegstra, J. W. Zwikker, M. R. Roest, L. W. Jenneskens, *J. Org. Chem.* **1992**, *57*, 6678.
- [122] F. A. Loiseau, K. K. Hii, A. M. Hill, *J. Org. Chem.* **2004**, *69*, 639.
- [123] A. C. French, A. L. Thompson, B. G. Davis, *Angew. Chem. Int. Ed.* **2009**, *48*, 1248.
- [124] a) G. Székely, M. Schaepertoens, P. R. J. Gaffney, A. G. Livingston, *Chem. Eur. J.* **2014**, *20*, 10038; b) G. Székely, M. Schaepertoens, P. R. J. Gaffney, A. G. Livingston, *Polym. Chem.* **2014**, *5*, 694.
- [125] R. Dong, R. Liu, P. R. J. Gaffney, M. Schaepertoens, P. Marchetti, C. M. Williams, R. Chen, A. G. Livingston, *Nature Chem. (Nature Chemistry)* **2019**, *11*, 136.
- [126] P. Bohn, M. A. R. Meier, *Polym. J. (Polymer Journal)* **2020**, *52*, 165.
- [127] R. K. Roy, A. Meszynska, C. Laure, L. Charles, C. Verchin, J.-F. Lutz, *Nat. Commun. (Nature Communications)* **2015**, *6*, 7237.
- [128] a) A. Al Ouahabi, L. Charles, J.-F. Lutz, *J. Am. Chem. Soc.* **2015**, *137*, 5629; b) E. Laurent, J.-A. Amalian, M. Parmentier, L. Oswald, A. Al Ouahabi, F. Dufour, K. Launay, J.-L. Clément, D. Gigmes, M.-A. Delsuc et al., *Macromolecules* **2020**, *53*, 4022.
- [129] G. Cavallo, S. Poyer, J.-A. Amalian, F. Dufour, A. Burel, C. Carapito, L. Charles, J.-F. Lutz, *Angew. Chem. Int. Ed.* **2018**, *57*, 6266.
- [130] J.-A. Amalian, G. Cavallo, A. Al Ouahabi, J.-F. Lutz, L. Charles, *Anal. Chem.* **2019**, *91*, 7266.
- [131] a) A. Al Ouahabi, J.-A. Amalian, L. Charles, J.-F. Lutz, *Nat. Commun.* **2017**, *8*, 967; b) J.-F. Lutz, *Macromolecules* **2015**, *48*, 4759; c) H. Mutlu, J.-F. Lutz, *Angew. Chem. Int. Ed.* **2014**, *53*, 13010.
- [132] S. C. Solleder, M. A. R. Meier, *Angew. Chem. Int. Ed.* **2014**, *53*, 711.

- [133] S. C. Solleder, K. S. Wetzel, M. A. R. Meier, *Polym. Chem.* **2015**, *6*, 3201.
- [134] S. C. Solleder, D. Zengel, K. S. Wetzel, M. A. R. Meier, *Angew. Chem. Int. Ed.* **2016**, *55*, 1204.
- [135] S. C. Solleder, S. Martens, P. Espeel, F. Du Prez, M. A. R. Meier, *Chem. Eur. J.* **2017**, *23*, 13906.
- [136] A. C. Boukis, M. A. Meier, *Eur. Polym. J.* **2018**, *104*, 32.
- [137] A. C. Boukis, K. Reiter, M. Frölich, D. Hofheinz, M. A. R. Meier, *Nat. Commun.* **2018**, *9*, 1439.
- [138] M. Frölich, D. Hofheinz, M. A. R. Meier, *Commun. Chem.* **2020**, *3*.
- [139] K. S. Wetzel, M. Frölich, S. C. Solleder, R. Nickisch, P. Treu, M. A. R. Meier, *Commun. Chem.* **2020**, *3*.
- [140] a) S. Martens, J. O. Holloway, F. E. Du Prez, *Macromol. Rapid Commun.* **2017**, *38*, 1700469; b) S. Martens, A. Landuyt, P. Espeel, B. Devreese, P. Dawyndt, F. Du Prez, *Nat. Commun.* **2018**, *9*, 4451; c) M. Soete, C. Mertens, R. Aksakal, N. Badi, F. Du Prez, *ACS Macro Lett.* **2021**, *10*, 616.
- [141] J. O. Holloway, K. S. Wetzel, S. Martens, F. E. Du Prez, M. A. R. Meier, *Polym. Chem.* **2019**, *10*, 3859.
- [142] J. O. Holloway, F. van Lijsebetten, N. Badi, H. A. Houck, F. E. Du Prez, *Adv. Sci.* **2020**, *7*, 1903698.
- [143] S. Martens, J. van den Begin, A. Madder, F. E. Du Prez, P. Espeel, *J. Am. Chem. Soc.* **2016**, *138*, 14182.
- [144] N. Zydziak, F. Feist, B. Huber, J. O. Mueller, C. Barner-Kowollik, *Chem. Commun.* **2015**, *51*, 1799.
- [145] W. Konrad, C. Fengler, S. Putwa, C. Barner-Kowollik, *Angew. Chem. Int. Ed.* **2019**, *58*, 7133.
- [146] a) Y.-H. Wu, J. Zhang, F.-S. Du, Z.-C. Li, *ACS Macro Lett.* **2017**, *6*, 1398; b) C. Li, L. Han, H. Ma, H. Shen, L. Yang, P. Liu, X. Hao, Y. Li, *Polym. Chem.* **2019**, *10*, 2758; c) M. B. Koo, S. W. Lee, J. M. Lee, K. T. Kim, *J. Am. Chem. Soc.* **2020**, *142*, 14028.
- [147] W. Konrad, F. R. Bloesser, K. S. Wetzel, A. C. Boukis, M. A. R. Meier, C. Barner-Kowollik, *Chem. Eur. J.* **2018**, *24*, 3413.
- [148] B. Zhao, Z. Gao, Y. Zheng, C. Gao, *J. Am. Chem. Soc.* **2019**, *141*, 4541.
- [149] a) E. Keles, Y. Song, D. Du, W.-J. Dong, Y. Lin, *Biomater. Sci.* **2016**, *4*, 1291; b) Y. Yang, Z. Cai, Z. Huang, X. Tang, X. Zhang, *Polym. J.* **2018**, *50*, 33.

- [150] B. N. Norris, T. Pan, T. Y. Meyer, *Org. Lett.* **2010**, *12*, 5514.
- [151] M. Jørgensen, F. C. Krebs, *J. Org. Chem.* **2004**, *69*, 6688.
- [152] M. Jørgensen, F. C. Krebs, *J. Org. Chem.* **2005**, *70*, 6004.
- [153] B. N. Norris, S. Zhang, C. M. Campbell, J. T. Auletta, P. Calvo-Marzal, G. R. Hutchison, T. Y. Meyer, *Macromolecules* **2013**, *46*, 1384.
- [154] S. Zhang, G. R. Hutchison, T. Y. Meyer, *Macromol. Rapid Commun.* **2016**, *37*, 882.
- [155] S. Zhang, N. E. Bauer, I. Y. Kanal, W. You, G. R. Hutchison, T. Y. Meyer, *Macromolecules* **2017**, *50*, 151.
- [156] J. S. Schumm, D. L. Pearson, J. M. Tour, *Angew. Chem. Int. Ed.* **1994**, *33*, 1360.
- [157] S. Huang, J. M. Tour, *Tetrahedron Lett.* **1999**, *40*, 3447.
- [158] R. Szweda, C. Chendo, L. Charles, P. N. W. Baxter, J.-F. Lutz, *Chem. Commun.* **2017**, *53*, 8312.
- [159] R. V. Schneider, Karlsruhe Institut of Technology, Karlsruhe, **2018**.
- [160] O. Franco, M. Jakoby, R. V. Schneider, F. Hundemer, D. Hahn, B. S. Richards, S. Bräse, M. A. R. Meier, U. Lemmer, I. A. Howard, *Front. Chem.* **2020**, *8*, 126.
- [161] W.-W. Zhang, X.-G. Zhang, J.-H. Li, *J. Org. Chem.* **2010**, *75*, 5259.
- [162] a) H. E. Gottlieb, V. Kotlyar, A. Nudelman, *J. Org. Chem.* **1997**, *62*, 7512; b) G. R. Fulmer, A. J. M. Miller, N. H. Sherden, H. E. Gottlieb, A. Nudelman, B. M. Stoltz, J. E. Bercaw, K. I. Goldberg, *Organometallics* **2010**, *29*, 2176.
- [163] D. Nilsson, S. Watcharinyanon, M. Eng, L. Li, E. Moons, L. S. O. Johansson, M. Zharnikov, A. Shaporenko, B. Albinsson, J. Mårtensson, *Langmuir* **2007**, *23*, 6170.
- [164] A. Dömling, I. Ugi, *Angew. Chem. Int. Ed.* **2000**, *39*, 3168.
- [165] a) I. Ugi, A. Dömling, W. Hörl, *Endeavour* **1994**, *18*, 115; b) A. Dömling, *Chem. Rev.* **2006**, *106*, 17.
- [166] I. Ugi, *Angew. Chem. Int. Ed.* **1959**, *71*, 386.
- [167] M. Passerini, *Gazz. Chim. Ital* **1921**, *51*, 181.
- [168] a) P. Patil, M. Ahmadian-Moghaddam, A. Dömling, *Green Chem.* **2020**, *22*, 6902; b) K. A. Waibel, R. Nickisch, N. Möhl, R. Seim, M. A. R. Meier, *Green Chem.* **2020**, *22*, 933.
- [169] Till Rohde, Karlsruhe Institut of Technology, Karlsruhe, **2021**.